Remote Sensing and Avian Biodiversity Patterns in the United States

By

Patrick Davis Culbert

A dissertation submitted in partial fulfillment

of the requirements for the degree of

DOCTOR OF PHILOSOPHY

(Forestry)

at the

UNIVERSITY OF WISCONSIN – MADISON

2012

Date of final oral examination: 6/11/2012

The dissertation is approved by the following members of the Final Oral Committee:
Volker C. Radeloff, Associate Professor, Forest and Wildlife Ecology
Anna M. Pidgeon, Assistant Professor, Forest and Wildlife Ecology
Murray K. Clayton, Professor, Statistics
Claudio Gratton, Associate Professor, Entomology
Phil A. Townsend, Professor, Forest and Wildlife Ecology

Acknowledgements

I owe thanks to numerous people and organizations that have helped me during my time as a graduate student. First and foremost is my advisor Volker Radeloff. Volker has been a great mentor since I first got to know him when I was an undergraduate. In my time as a graduate student, Volker has been extremely available to give guidance and assistance, whether thoughtful comments on a manuscript, career advice, or hunting tips. In addition to research, I have a strong interest in teaching, and Volker was very accommodating by allowing me to take teaching courses as well as giving me valuable experience and feedback in assisting with his forest biometry and forestry field camp courses. Volker is a fantastic scientist, teacher, and mentor, and I aspire to eventually rise to that level in my own career.

In addition to Volker, the other members of my committee, Anna Pidgeon, Claudio Gratton, Murray Clayton, and Phil Townsend have helped make my dissertation possible through helpful advice and feedback. In particular, Anna Pidgeon has given me extremely helpful suggestions and feedback throughout all stages of my time as a graduate student. I am particularly grateful for the assistance in furthering my understanding of avian ecology, which has grown substantially in the past six years.

Many members of the Silvis lab have assisted me over the years and certainly helped to make my experience a fun one. Todd Hawbaker has been a good friend and mentor since my senior thesis as an undergraduate. Later in my graduate career, I had the opportunity to work with three post-docs, Tom Albright, Chad Rittenhouse, and Fred Beaudry. The close work with three post-doctoral researchers gave me a good idea of what was ahead of me in my career. Fred and Chad helped me improve my understanding of wildlife (birds and otherwise), and Tom was a

great role model, office-mate, and friend. Dave Helmers and Nick Keuler provided technical assistance many times. Véronique St-Louis provided substantial assistance to my understanding and processing of image texture. Adrian Lesak and Eric Wood turned me into a bit of a birder, though my skills are nowhere near theirs. Rather than trying to list all the other lab members that I've known over the past six years, I'll just say that this lab has been a great family and a fun, supportive environment, and everyone has made a contribution.

Silvis is a very collaborative lab with numerous contacts and visitors from other institutions. Nicholas Coops, Josef Kellndorfer, and Curt Flather have been particularly helpful with my dissertation by sharing data, ideas, and suggestions.

I would have been unable to complete this degree without the substantial amount of financial support I received. NASA has been my primary patron, with support from the NASA Biodiversity Program and the Earth and Space Sciences Fellowship. I loved science and space as a child, and while I never knew at the time then that NASA supported biological science on earth, the 10-year-old in me is thrilled to have a NASA connection in my work.

My family probably deserves the strongest thanks. My parents always fostered (and indulged) my scientific curiosity and believed strongly in the value of education. My wife Alex deserves special thanks, especially for her willingness to move from Southern California to the cold of Wisconsin for unknown adventure. I love her immensely, and her love and support over the last six years has been crucial to my success.

Table of Contents

Overview

Global avian biodiversity is under great threat, primarily due to human-caused habitat conversion (Gaston et al. 2003). Conservation of biodiversity is therefore of critical importance. Understanding the causes of spatial heterogeneity in biodiversity remains one of the most pressing challenges for ecologists (Gaston 2000). One shortcoming of the current pool of biodiversity studies is that most explore only one or two types of explanatory factors in isolation. A broader perspective of the drivers of biodiversity is needed. MacArthur (1972) hypothesized that biodiversity is a function of productivity, climatic stability, and habitat structure. Even though MacArthur's framework has existed for 40 years, few studies have considered these three factors jointly. Measures of productivity and climatic stability are amenable to remote sensing, and therefore relatively easy to quantify over broad extents. Habitat structure, in contrast, has thus far been measured primarily with labor-intensive field-based techniques. In order to consider the influence of habitat structure on nationwide patterns of avian biodiversity, improved remotely sensed methods for quantifying habitat structure are needed.

Even with a better theoretical understanding of the factors influencing avian biodiversity patterns, the resulting information must be presented in a form useful to resource managers and decision-makers in order to make a practical difference in conservation. With limited resources for habitat conservation, the accurate identification of high-value bird habitat is crucial (Turner et al. 2003). Few national maps of biodiversity exist, and those that do are of relatively coarse resolution (e.g., Dobson et al. 1997). A nationwide, fine-resolution map of avian biodiversity is therefore needed to inform conservation decision-making.

The overarching goal of my dissertation was to explain and predict geographic patterns of avian species richness across the contiguous United States. My objectives were to evaluate methods of characterizing habitat structure over broad extents from remotely sensed data, to determine the relative roles that productivity, climatic stability, and habitat structure play in influencing nationwide patterns of avian species richness, and to produce fine-resolution, nationwide maps of predicted avian species richness.

I explored the relationships of avian species richness to measures of productivity, climatic stability, and habitat structure, and I investigated the relative importance of each. Because of the broad-extent of my work, I extensively used remotely sensed data. Remotely sensed measures of habitat structure are relatively few and untested, therefore a substantial portion of my dissertation involved the evaluation of these measures, in particular image texture. I also compared remotely sensed measures of vertical and horizontal habitat structure, and evaluated the relative contribution of each in explaining avian species richness patterns. Lastly, and most importantly I modeled nationwide patterns of avian species richness as a function of productivity, climatic stability, and habitat structure. I conducted two separate analyses as part of this modeling process. In the first, my goal was to examine the importance and relationship between these three categories of measures and avian species richness. In the second analysis my goal was to produce nationwide, fine-scale maps of species richness for several avian guilds.

Chapter Summaries

The performance of image texture measures for the quantification of habitat structure was one major focus of my dissertation. Because my study area was nationwide, it was apparent that

I would be unable to acquire satellite imagery at the same phenological stage nationwide. Therefore, in **Chapter 1**, I investigated the effect of phenological variability on measures of image texture. The study area for this chapter included three Landsat footprints selected to include contrasting biomes. The first footprint was an area composed primarily of desert scrub along the border of New Mexico, Texas, and Mexico. The second footprint was primarily in southwestern Ontario, extending slightly over the border of Minnesota, consisting of boreal forest. The third footprint was in the Appalachian Mountains including portions of western Maryland, eastern West Virginia, and Virginia. Landcover included deciduous forests on mountain slopes and agricultural areas.

For each study site, I selected three to four scenes spanning the growing season. For each image, I calculated a suite of first- and second-order image texture measures. For each texture measure, I calculated the coefficient of variation for each pixel across all images for each of the three sites. All study sites showed substantial seasonal variation in measures of both first- and second-order textures. Among the three study sites, first-order measures were consistently ranked in their robustness to phenological variation, with mean and entropy being the most robust, followed by variance then skew. In contrast, no clear pattern of robustness emerged in second-order measures because robustness ranking was not consistent among study sites, although homogeneity, entropy, and dissimilarity appeared to be more robust than other measures. I also analyzed whether texture measures calculated with certain window sizes, or of certain bands, were more robust to phenological variation. Phenological variability did not show strong differences among bands. There appeared to be a slight reduction in variability with increasing window size, but the affect was not strong.

My overall finding in this chapter was that phenological variation does indeed strongly influence measures of texture calculated from Landsat imagery. Some measures of texture appeared to be more robust to phenological variation than others, but the difference was relatively small. My findings suggest that, in studies considering measures of image texture, images should be acquired at similar phenological stages if possible. If this is not possible, texture measures may still be useful, but phenological variation will introduce noise into the measures.

Measures of image texture, as a method to quantify habitat structure, have been successfully used to explain patterns of avian distribution and species richness. However, these studies were carried out over limited spatial extents and included only a limited range of landcover types (St-Louis et al. 2006, Wood et al. 2012). In order to determine whether image texture measures can be useful in nationwide models of biodiversity including diverse ecosystems, a more substantial analysis was needed. In **Chapter 2**, I evaluated the ability of image texture measures to explain patterns of avian species richness over the Midwestern United States. The study area covered 1,498,000 km^2, including habitats ranging from grassland to forest. I calculated a suite of image texture measures from 114 Landsat TM scenes, and I used those measures to model avian species richness for forest birds, grassland birds, and shrubland birds, as well as Neotropical migrants, permanent residents, and short-distance migrants. As a benchmark for comparison, I also calculated measures of landscape composition from the National Landcover Dataset (NLCD). Models of avian species richness for each guild were fitted using texture measures alone, landscape composition measures alone, and both together. Models were fitted for the entire study area, as well as for each of the three ecoregion provinces comprising the study area (Laurentian Mixed Forest, Eastern Broadleaf Forest, and Prairie Parkland).

At the study-wide level and for the Eastern Broadleaf Forest and Prairie Parkland Ecosystems, landscape composition measures explained slightly more of the variability in avian species richness than image texture measures, with both types of models explaining roughly one-third of the variability in species richness. When both types of measures were considered simultaneously, model adjusted R^2 values showed modest improvement. However, in the Laurentian Mixed forest, the outcome was notably different. There, texture measures explained 24% of species richness variability while landscape composition metrics explained only 18%. When both types were combined, they explained 33% of the variability.

My results indicated that while measures of image texture were not universally superior to measures of landscape composition, the approach was still valuable. In the Laurentian mixed forest, texture measures demonstrated superior performance and there was a large increase in adjusted R^2 when both types of measures were considered. These results indicate that, in this heavily forested ecoregion, measures of image texture were capturing information that was not present in landscape composition metrics. It may be that in the Prairie Parkland and Eastern Broadleaf Forest, between-class heterogeneity, which landscape metrics capture well, was a driving factor of species richness patterns, while in the Laurentian mixed forest, within-class heterogeneity, which landscape composition does not capture but texture does, was more important. The complementarity of landscape composition metrics and image texture measures that I found in the Laurentian Mixed Forest indicates that the two approaches should be used in conjunction when possible, and in areas where landcover classifications are not available, image texture measures can characterize habitat structure over broad extents.

In addition to texture, other options exist for characterizing habitat structure over broad scales. Considering that bird habitat is three-dimensional by nature, I was especially interested in vertical habitat structure. A well-recognized relationship exists between avian species richness and measures of vertical structure, such as foliage height diversity (MacArthur and MacArthur 1961). The problem is that these labor-intensive field measurements are completely unfeasible over broad scales. Light detection and ranging (LiDAR) has shown the ability to characterize vertical habitat structure, but existing data sets are available only at local to state scales. Consequently, other approaches are needed. In **Chapter 3**, I evaluated the effectiveness of several measures of horizontal and vertical habitat structure for explaining nationwide patterns of avian species richness. The study area for this chapter included the entire contiguous United States. As in Chapter 2, I modeled avian species richness, derived from the Breeding Bird Survey (BBS), as a function of measures of habitat structure from the area surrounding each BBS route. A key focus of this chapter was canopy height and biomass measures from the National Biomass and Carbon Dataset 2000 (NBCD) as represention s of vertical habitat structure. I included measures of landscape composition and configuration derived from the NLCD as representations of horizontal structure. Landscape configuration metrics were calculated using morphological spatial pattern analysis (MSPA) and included area of core and edge forest, grassland, and shrubland. I fitted models of species richness for seven avian guilds as a function of habitat structure nationwide and for three ecoregions: the Central Appalachian Broadleaf Forest, Eastern Broadleaf Forest, and Great Plains. To quantify the explanatory contribution of variables, I first used best subset selection and ranked variables by the number of times they were included in top models. In addition, I used hierarchical partitioning on the top-ranked variables (as determined by best subsets) to establish the independent contribution of each variable in the context of the others.

Avian species richness was strongly related to at least some measures from each of the explanatory variable groups (canopy height and biomass from the NBCD as well as NLCD-derived measures of landcover composition and configuration). Mean canopy height exhibited particularly strong relationships and explained 55% of the nationwide variability of forest bird species richness. The combination of both horizontal and vertical habitat structure measures was most powerful, and nationwide multivariate models of forest and grassland bird species richness yielded adjusted R^2 values of 0.70 and 0.48 respectively. Models developed at the scale of individual ecoregion provinces had slightly weaker performance but still showed strong relationships between species richness and measures of both vertical and horizontal structure. In the nationwide models, measures of both vertical and horizontal habitat structure ranked high in independent contribution (from hierarchical partitioning) and inclusion in top-models (from best subsets selection).

My study showed that measures of vertical structure, as characterized by estimates of biomass and canopy height from the NBCD, capture information not present in measures of horizontal structure. As expected, methods characterizing horizontal habitat structure, such as proportion of landcover class, also contributed to explanation of species richness patterns. The high independent contribution values of both horizontal and vertical measures of habitat structure in the hierarchical partitioning analysis indicate that these measures are complementary, rather than redundant, in their explanation of species richness patterns. For this reason, I recommend that future studies of broad scale avian biodiversity include measures of both vertical and horizontal structure.

The focus of Chapters 1-3 was evaluating potential remotely sensed measures of habitat structure. In **Chapter 4**, I returned to MacArthur's framework of productivity, climatic stability, and habitat structure as primary factors influencing biodiversity. My aim was to determine which groups of measures (and specifically which variables) had the most predictive power and whether there was complementarity between these three groups. I modeled nationwide patterns of avian species richness using measures of habitat structure from Chapters 2 and 3, as well as additional measures of productivity and climatic stability. As in Chapter 3, I modeled nationwide patterns of species richness, derived from the BBS, of seven avian guilds. Measures of productivity included annual sum and annual minimum fraction of photosynthetically active radiation (fPAR), a measure strongly related to vegetative productivity. Seasonal variation of fPAR, and ecoregion province were used as measures of climatic stability. Image texture measures, canopy height, biomass, and landcover composition metrics were used to represent habitat structure. I included more measures of habitat structure than productivity or climatic stability because I modeled species richness at the scale of a BBS route, and local variation in species richness is more strongly influenced by habitat structure (Mackey and Lindenmayer 2001, Pearson and Dawson 2003). In order to evaluate the explanatory power of individual variables as well as measures of productivity, climatic stability, and habitat structure as groups, I again employed best subset selection and hierarchical partitioning.

As expected, all three categories made some contribution to explaining avian species richness patterns, and habitat structure measures were the strongest overall. For five of seven guilds (all birds, forest birds, shrubland birds, Neotropical migrants, and short-distance migrants), measures of habitat structure contributed the bulk of explanatory power followed by a moderate contribution from productivity measures and a small contribution from measures of climatic stability. In the remaining guilds, a different pattern was observed. For grassland birds, habitat structure measures were again dominant, but to a lesser extent, and productivity and climatic stability made moderately strong contributions. For permanent residents, the contribution of different variable groups was roughly split three ways, with productivity explaining the most, followed by climatic stability, then habitat structure. Though habitat structure measures were dominant on the whole, the top-performing individual variables included measures from all three categories. In fact, the strongest performing variable overall was mean annual sum of fPAR (productivity).

While I expected these three factors to exhibit complementarity in explaining patterns of avian species richness, my results did not always support that prediction. The ranking of the top individual variables seemed to indicate complementarity, but comparison of adjusted R^2 values provided mixed evidence. For the all bird, forest bird, shrubland bird, Neotropical migrant, and short-distance migrant guilds, models yielded adjusted R^2 values comparable to the habitat structure-only models from Chapter 3. This would seem to indicate little complementarity, however, in this chapter, canopy height (one of the strongest performing variables in Chapter 3) was not included in final models because it was highly correlated with mean annual sum of fPAR (the strongest performing variable in chapter 4). The grassland bird and permanent resident species richness models showed notable improvement in adjusted R^2, showing that for these guilds there was complementarity between measures of productivity, climatic stability, and habitat structure.

In order to create a final data product that would be of use to planners and resource managers, in **Chapter 5**, I produced nationwide, fine-scale maps of predicted avian species richness. As in Chapter 4, this analysis considered explanatory variables representing productivity, climatic stability, and habitat structure. In contrast to Chapter 4, the goal was to produce accurate maps of predicted avian species richness, rather than developing explanatory models to evaluate drivers of species richness patterns. The statistical analysis, therefore, was quite different. I used two different machine learning approaches to develop the predictive models: random forests and support vector regression. Analysis of mean squared error of both approaches, as well as visual inspection of resulting predictive maps, showed the random forest models to be superior. I therefore used the random forest models to produce maps of nationwide avian species richness for all birds, forest birds, shrubland birds, grassland birds, Neotropical migrants, short-distance migrants, and permanent residents. The maps were of 1-km resolution, with each cell indicating the expected number of species present on a hypothetical BBS route centered at that location.

The nationwide maps showed patterns of species richness that matched expectations. For example, forest birds and Neotropical migrants had highest species richness in the eastern half of the United States and in forested areas in the western half of the country, and grassland bird species richness was heavily concentrated in the Great Plains. I also visually evaluated the predicted maps of species richness for the state of Wisconsin. Again, predicted patterns of richness followed known patterns, such as high Neotropical migrant species richness in northern forests, and highest grassland bird species richness in heavily agricultural areas.

Significance

My dissertation focused on explaining and predicting patterns of avian species richness, and makes technical, theoretical, and applied contributions. The technical contributions are primarily related to the use of image texture. In Chapter 1, I showed that changes in vegetation phenology significantly influence measures of texture, and that close attention should be paid to the phenological stage of imagery when performing multi-image texture analysis. In Chapters 2 and 4, I show that it is feasible (though challenging) to use texture analysis over a very broad extent, and measures of image texture are useful in explaining avian species richness over numerous ecosystem types. In Chapter 5, I evaluated two relatively new and novel machine learning techniques, support vector regression and random forests, in a biodiversity modeling context and found that random forests were very effective. Though best subset selection and hierarchical partitioning are not new techniques, I showed that in tandem, they are useful approaches in evaluating the contribution of explanatory variables, particularly in the context of other variables.

The main theoretical contributions in my dissertation are Chapters 3 and 4. In Chapter 3, I showed that measures of both horizontal and vertical habitat structure were important and complementary in explaining avian species richness patterns nationwide. In Chapter 4, I tested numerous hypotheses regarding the importance and interaction of productivity, climatic stability, and habitat structure with regard to their influence of patterns of species richness for several avian guilds. For example, I found that for most avian guilds, measures of habitat structure made the strongest contribution to explaining species richness at the BBS route level. Permanent resident birds were the exception: in that case, measures of productivity made the largest contribution to explaining patterns of species richness.

Lastly, with Chapter 5, I made a significant contribution to applied conservation science by using my theoretical findings to produce a concrete product, nationwide maps of predicted species richness for several avian guilds. These maps are of a scale appropriate to inform conservation planners and managers about geographic patterns of avian species richness and perhaps highlight areas worthy of further field investigation. By producing maps for several guilds, I intended to convey a significant amount of information in an easily understandable manner. Although the maps are primarily intended for resource managers, I hope they inspire others to take theoretical findings and use them to produce a useable product. In fact, I hope others also undertake broad-extent predictive biodiversity modeling similar to my study, perhaps improving upon my methods and results. Along those lines, some of the technical contributions of my dissertation have an applied aspect as well. The steps and analysis I undertook to produce my maps provide technical advancement to the field of habitat modeling, and I hope my techniques will be applied to other taxa and other regions of the world.

References

Dobson A. P., J. P. Rodriguez, W. M. Roberts, and D. S. Wilcove. 1997. Geographic Distribution of Endangered Species in the United States. Science 275:550-553.

Gaston K. J., T. M. Blackburn, and K. K. Goldewijk. 2003. Habitat conversion and global avian biodiversity loss. Proceedings of the Royal Society B: Biological Sciences 270:1293-1300.

Gaston K. J. 2000. Global patterns in biodiversity. Nature 405:220-227.

MacArthur R. H. 1972. Geographical Ecology: Patterns in the Distribution of Species. Harper & Row.

MacArthur R. H., J. W. MacArthur. 1961. On Bird Species Diversity. Ecology 42:594-598.

Mackey B., D. Lindenmayer. 2001. Towards a hierarchical framework for modelling the spatial distribution of animals. Journal of Biogeography 28:1147-1166.

Pearson R., T. Dawson. 2003. Predicting the impacts of climate change on the distribution of species: are bioclimate envelope models useful? Global Ecology and Biogeography 12:361-371.

St-Louis V., A. M. Pidgeon, V. C. Radeloff, T. J. Hawbaker, and M. K. Clayton. 2006. High-resolution image texture as a predictor of bird species richness. Remote Sensing of Environment 105:299-312.

Turner W., S. Spector, N. Gardiner, M. Fladeland, E. Sterling, and M. Steininger. 2003. Remote sensing for biodiversity science and conservation. Trends in Ecology & Evolution 18:306-314.

Wood E. M., A. M. Pidgeon, V. C. Radeloff, and N. S. Keuler. 2012. Image texture as a remotely sensed measure of vegetation structure. Remote Sensing of Environment 121:516-526.

Chapter 1

The Impact of Phenological Variation on Texture Measures of Remotely Sensed Imagery

Abstract

Measures of image texture derived from remotely sensed imagery have proven useful in many applications. However, when using multi-temporal imagery or multiple images to cover a large study area, it is important to understand how image texture measures are affected by surface phenology. Our goal was to characterize the robustness to phenological variation of common first- and second-order texture measures of satellite imagery. Three North American study sites were chosen to represent different biomes. At each site, a suite of image textures were calculated for three to four dates across the growing season. Texture measures were compared among dates to quantify their stability, and the stability of measures was also compared between biomes. Interseasonal variability of texture measures was high overall (mean interseasonal coefficient of variation = 0.79), indicating that care must be taken when using measures of texture at different phenological stages. Certain texture measures, such as first-order mean and entropy, as well as second-order homogeneity, entropy, and dissimilarity, were more robust to phenological change than other measures.

Introduction

Remotely sensed images are composed of both tone (spectral variation) and texture (spatial variation) (Haralick 1979, Baraldi and Parmiggiani 1995). While spectral information is relatively easy to quantify, texture is more difficult to quantify because it involves measurements of pattern variability, shape, and size (Coburn and Roberts 2004). Because of the difficulties in measurement and interpretation, texture has been less utilized in remote sensing than spectral analysis. This is unfortunate, because pixel-wise spectral analyses ignore the large amount of information present in image texture. The use of texture measures has been recognized as an important method for quantifying spatial heterogeneity and its use has recently increased in studies of land cover classification (Coburn and Roberts 2004, Franklin et al. 2000, Franklin et al. 2001a), habitat modeling (Hepinstall and Sader 1997, Tuttle et al. 2006, Estes et al. 2008), and measurement of vegetation structure (Estes et al. 2008, Kayitakire et al. 2006, Wunderle et al. 2007).

The most commonly used measures of texture are divided into two groups: first-order (occurrence) and second-order (co-occurrence) (Haralick et al. 1973). First-order measures are statistics calculated from the spectral values of pixels in a defined neighborhood, typically implemented as a moving window. Common first-order measures include minimum, maximum, range, mean, standard deviation, skewness, and kurtosis. Of these measures, standard deviation (or variance) is the most commonly used (Coburn and Roberts 2004, Hepinstall and Sader 1997, Tuttle et al. 2006, Tuominen and Pekkarinen 2005). First-order measures are limited in power because they quantify variation in spectral information without regard to the spatial arrangement within the moving window. However, first-order measures are computationally simple and can be quickly calculated over large spatial extents.

Second-order texture measures take into account the spatial distribution of spectral values (Coburn and Roberts 2004). These measures are derived from the gray-level co-occurrence matrix (GLCM) [11]. The GLCM is a symmetric n-by-n matrix, where n is the number of possible gray-tone values. Entries Pij in the matrix, represent the relative frequency of pixels with tone levels i and j co-occurring at a user specified distance and direction (Haralick et al. 1973). There are four commonly used directions, 0° (horizontal), 45° (right diagonal), 90° (vertical), and 135° (left diagonal). The distance parameter, d, is typically set to 1, thus comparing adjacent pixels (Musick and Grover 1991). In multispectral imagery, a separate GLCM is computed for each band of interest.

The GLCM assumes that the texture information of an image can be represented in adjacency relationships between specific gray tones (Haralick et al. 1973, Tso and Mather 2001)(Haralick et al. 1973). Similar to first-order measures, the GLCM is calculated for a neighborhood, typically a moving window. Haralick (1973) originally proposed 14 texture measures derived from the GLCM: angular second moment, contrast, correlation, difference entropy, difference variance, entropy, information measures of correlation (2 different features), inverse difference moment (now more commonly referred to as homogeneity), maximal correlation coefficient, sum average, sum entropy, sum of squares variance, and sum variance. Many of these original second-order measures have been found to be highly correlated, and a subset of six measures is considered most useful for remote sensing analysis: angular second moment (ASM), contrast, correlation, homogeneity, variance, and entropy, with the first three being the least correlated (Baraldi and Parmiggiani 1995, Kayitakire et al. 2006).

Several types of remote sensing data analyses benefit from the inclusion of textural measures. Texture measures are frequently included as additional (or sole) inputs in image classifications. The use of texture measures is especially helpful in classifications of areas such as forests, where species may have similar spectral characteristics but different spatial patterns (Coburn and Roberts 2004, Franklin et al. 2000, Franklin et al. 2001a). Measures of texture are also well-suited to quantify vegetation structure (Kayitakire et al. 2006, Johansen et al. 2007), including forest structure (Kayitakire et al. 2006), forest age class (Franklin et al. 2001b)(Hudak and Wessman 1998), woody plant encroachment (Hudak and Wessman 1998)(Wulder et al. 1998), and leaf area index (Wulder et al. 1998). More recently, habitat modeling studies have incorporated texture measures. For animals such as birds, vegetation structure is an important cue for habitat selection (MacArthur and MacArthur 1961, Cody 1981). Texture measures derived from remotely sensed imagery have proven useful in bird species presence/absence models (Hepinstall and Sader 1997), relating vegetation structure to habitat preference (Tuttle et al. 2006, Bellis et al. 2008), and modeling avian species richness (St-Louis et al. 2006, St-Louis et al. 2009).

However, while the utilization of texture measures in remote sensing analyses is increasing, there is a significant issue that has thus far been mostly overlooked. Any texture analysis involving images of different areas or multi-temporal images of the same area must take into account factors that may severely affect texture measures. Absolute texture comparisons between images are confounded by factors such as light angle, atmospheric effects (Hudak and

Wessman 1998), and vegetation phenology (Vega-Garcia and Chuvieco 2006). In particular, the effect of phenology could significantly affect multi-temporal analyses. Even though these factors can introduce substantial problems to analyses, thus far only a few studies have mentioned the possible effects of phenology on texture measures (Vega-Garcia and Chuvieco 2006, Peroni et al. 2000), and none of these studies explicitly examined the effect.

At the same time, the potential upside of phenological variation in image texture is that texture differences among multi-temporal images could contain important information. The analysis of temporal variation in image texture could thus yield insight into phenological processes and help distinguish different vegetation types. Texture measures derived from certain phenological stages will likely be better suited to specific purposes, such as plant species identification, and specific texture signatures related to a process or feature of interest may be more pronounced at specific phenological stages. To exploit these relationships, more understanding is needed on the behavior of specific texture measures in different biomes over the growing season and which parts of the growing season yield the best texture measures to be related to specific processes.

As computing power increases, so does the ability to carry out analyses over large spatial extents. The historical archive of remotely sensed imagery is growing, and data are becoming more freely available (as with the free release of the USGS Landsat archive). All of these factors will contribute to increases in multi-temporal and large-spatial-extent analyses that utilize texture measures. Thus, both positive and negative implications of the effects of phenology on measures of image texture need more study.

The primary goal of our research was to determine how first- and second-order texture measures respond to changes in phenology. We were interested in finding the degree to which measures of image texture are robust to phenological change. In addition, we were interested in understanding how phenology-related variability in texture measures differs across different biomes, window sizes, and spectral bands.

We expected that image texture measures that are invariant to linear transformations of the digital numbers (e.g., angular second moment and entropy (Haralick et al. 1973)) would be the most robust to phenological change. We also expected that measures of texture would vary the most in biomes with high seasonal variation in vegetation. Strong fine-scale variation in vegetation would lead to high spectral variation, which we expected would translate into higher variation of texture measures.

Texture measures are influenced by window size since the scale of the spatial patterns measured is dependent on window size, but we did not expect different window sizes to substantially differ in their response to phenological change. However, since a larger window contains a larger sample size, we predicted a slight reduction in variance. Lastly, we expected that variance of texture measures would not be uniform across spectral bands. In particular, we believed that Landsat TM band 4 would have higher interseasonal variability in texture measures because near-infrared reflectance is strongly correlated with vegetative vigor (Tucker 1979), which varies substantially across growing seasons.

Methods

We calculated a suite of texture measures for three study sites representing different biomes, and for images acquired at different points in the growing season. The resulting texture measures were compared among image dates to determine which measures were most robust to change in surface phenology and whether ranking in terms of robustness was consistent among different biomes. We used several window sizes and spectral bands in order to analyze their effect on texture measure robustness to phenological variation.

Three study sites were chosen, representing contrasting biomes: a desert scrub region in New Mexico, a mix of deciduous and evergreen forests in Ontario, Canada, and an area of deciduous forest and agriculture in Virginia. These sites correspond to Landsat TM path 33 row 38, path 27 row 26, and path 16 row 33, respectively (Figure 2-1).

The New Mexico site was centered near Las Cruces, New Mexico, and includes areas of New Mexico, Texas, and Chihuahua, Mexico. The area was primarily desert scrubland of the Chihuahuan Desert Province (Bailey 1995), with relatively flat basins as well as mountainous areas. The Rio Grande River was a prominent feature in the scene, with a swath of agriculture approximately 5 miles wide running along the river. The metropolitan area of El Paso, Texas and Ciudad Juárez, Mexico (population approximately 2.2 million) was included in the scene.

The Ontario study site covered mostly southwestern Ontario with a small area of northern Minnesota also included. The scene was in the Boreal Shield ecozone (Wiken 1986). This area had a very low human population and was composed almost entirely of forests and small lakes. The forests were primarily evergreen or mixed evergreen/deciduous. Heavy forest harvesting was apparent in parts of the imagery.

The Virginia site included portions of western Maryland, eastern West Virginia, and Virginia. The West Virginia portion of the image was dominated by deciduous forests on slopes of the Appalachian Mountains, with some agriculture in the valleys. Agriculture dominated most of the Virginia portion of the image, with some mountainous deciduous forest, including nearly all of Shenandoah National Park. The area was primarily in the Central Appalachian Broadleaf Forest-Coniferous Forest-Meadow Province with a small section of Southeastern Mixed Forest Province (Bailey 1995).

For each study site, a collection of Landsat images was assembled with the goal of having mostly cloud free images spanning the growing season within a 1-3 year period (Table 2-1, Figure 2-2). For the Ontario study site, approximately 15% of the 09/12/2000 image was affected by clouds and about 25% of the 04/29/2000 image was contaminated by smoke. In the Virginia site, the 05/24/2002 image contained 10% cloud cover. These affected areas were masked out from all images for the final analysis of each study site.

Within each study site, one image was chosen as the reference and the others were georeferenced to that image using Erdas Imagine Autosync (Leica Geosystems 2005). A second order polynomial model was applied, and images were resampled using nearest neighbor interpolation. Images were projected in UTM NAD83 zones 13, 15, and 17 North for the New Mexico, Ontario, and Virginia study sites, respectively.

A suite of texture measures were calculated for each of the 10 images using ENVI (Research Systems Inc. 2005) (Figure 2-2 D-I for example). For each image band, first-order texture measures: mean, variance, entropy, and skewness were calculated using window sizes of 3x3, 7x7, and 11x11. The second-order texture measures: correlation, contrast, angular second moment, homogeneity, dissimilarity, entropy, and variance were also calculated for each band. When calculating second order measures, care must be taken to avoid sparsely populated GLCMs (Haralick et al. 1973, Vega-Garcia and Chuvieco 2006). With small window sizes, the number of pixel adjacencies is relatively small, and a GLCM of 8-bit data will have 65,536 cells (256 by 256). This results in a value of 0 in most cells of the GLCM, causing instability in the texture measurement. For this reason, we calculated second-order measures with larger window sizes of 11x11 and 15x15, and we reduced the radiometric resolution to 6 bits (64 values, yielding a GLCM with 4,096 cells) instead of the 8 bits of the original data. GLCMs were calculated for the horizontal direction with a distance parameter of 1 pixel.

Within each study site, the calculated texture measures were compared among image dates on a pixel-by-pixel basis. Because variation in texture measures was consistently higher in pixels with a high mean texture value, the per-pixel coefficient of variation was chosen as a more representative measure of interseasonal variability. For each study site, band, texture measure, and window size combination, the coefficient of variation of each pixel was calculated among the different image dates in order to assess the inter-date variability of the textures measures (Figure 2-3). With three study sites, six bands, four first-order measures with three window sizes, and seven second-order measures with two window sizes, this processing yielded 216 single-band coefficient of variation images for first-order texture measures and 252 images for second-order texture measures (Figure 2-4). To facilitate comparison between texture measures, cloud-contaminated areas were masked, and the image-wide mean was calculated for each of the single-band coefficient of variation images.

Results

All study sites showed substantial interseasonal variation in both first- and second-order texture measures. The overall mean coefficients of variation of the calculated texture measures were 0.52, 0.66, and 1.06 for the New Mexico, Ontario, and Virginia study sites, respectively. These levels are higher than we expected, and it can be seen that the level of variation was substantially higher in the Virginia study site. As a test sample, a small area of evergreen forest was selected from the Ontario study site, and 11x11 second-order texture measures of this area were plotted for each of the four image dates (Figure 2-5). The two images from very early in the growing season (04/29/00 and 05/21/2002) showed very similar texture measures. However, during the peak of the growing season (07/05/2001) most texture measures changed substantially in value. Entropy, contrast, variance, and dissimilarity show a marked increase in value, while correlation and homogeneity show a decrease. Late in the growing season (09/12/2000) texture measures returned to values similar to the two early images.

The ranking of seasonal variation in first-order texture measures was consistent between the Ontario and New Mexico sites with entropy and mean as the least variable measures, followed by variance, then skew (Figure 2-6). While the relative ordering of variability in texture measures of the Virginia site was similar, entropy, mean, and variance had noticeably higher seasonal variability. The variability of skew was similar in all three sites and substantially higher than the three other measures. Overall variation was high for variance and skew, with a mean coefficient of variation of approximately 0.7 and 1.75 respectively.

Seasonal variability of second-order texture measures was fairly complex (Figure 2-7). Variability of contrast, dissimilarity, entropy, homogeneity, and variance were very similar between the New Mexico and Ontario sites, with the New Mexico site being slightly less variable in each case. Differences between Ontario and New Mexico were much larger for angular second moment and correlation. Homogeneity and entropy were the most robust measures in these two sites, followed by dissimilarity, contrast, and variance. However, the variation of texture measures of the Virginia site was substantially higher, with most coefficients of variation near 1.0. It is difficult to ascertain the relative robustness of angular second moment and correlation given that the level of variation was inconsistent among the three study sites.

There were noticeable differences in robustness of texture measures among biomes. The Virginia site had the highest level of variation in 9 of the 11 texture measures, for an overall average coefficient of variation of 1.06. For most of the texture measures, the level of variation was similar between the New Mexico and Ontario sites, with New Mexico yielding a slightly lower overall mean coefficient of variation of 0.52 compared to 0.66 for the Ontario site.

With regard to window size, there appeared to be a slight trend of decreasing interseasonal variability with increasing window size when comparing coefficients of variation averaged across all bands and texture measures (Figure 2-8).

It was expected that texture measures of different Landsat spectral bands would behave differently with regard to robustness to seasonal change. Band 4 (near infra-red) was of particular interest as this band is especially sensitive to vegetative vigor, which varies substantially over the growing season. Measures calculated from band 4 did not show substantially higher interseasonal variation than those of other bands. The mean per-band level of variability averaged across all texture measures was relatively constant for first order measures (Figure 2-9), with the exception of band 3 in the New Mexico and Ontario site and band 4 in the Ontario site.

The mean per-band variability averaged across second-order texture measures showed a stronger pattern (Figure 2-10). Once again the Virginia site consistently had the highest variation. Ontario and New Mexico showed higher variability between bands and followed a similar pattern with the coefficient of variation increasing to a peak around band 3 then decreasing.

Although some texture measures appeared to vary similarly across an individual study site, with other textures, patterns did emerge. For example, in the Virginia study site, homogeneity showed noticeable differences in coefficient of variation between the agricultural areas in the valleys, and the mountainous forested areas (Figure 2-4 D-F). The coefficient of variation for band 4 was strikingly higher in the agricultural areas. Homogeneity heavily weights the main diagonal of the GLCM, so areas composed of many adjacent pixels with highly similar DNs yielded a high value. In agricultural areas, homogeneity was very high within-field, and low between fields, especially in this study site where some images contained vegetatively active fields (high NIR/red ratio) adjacent to fields with low activity (nearly even NIR/red ratio). In contrast, while the forested mountainous areas varied in band 4 values over the growing season, each forested area varied relatively consistently, resulting in a smaller coefficient of variation for homogeneity. This highlights the importance of considering land cover and texture characteristics of the setting of interest when considering the effects of vegetation phenology on texture measures.

Discussion

The most significant finding of our study was that all texture measures varied substantially with phenology. This variation can significantly impact analyses utilizing texture measures and should be of special concern in studies using multi-temporal imagery or a very large spatial extent requiring many images. Even in single-date, single-image analyses, care should be taken in the choice of image date, as the textural measures of specific features will vary based on the phenological stage of the image.

While overall variation was high, some patterns did emerge. Among the three study sites, first-order measures were consistently ranked in their robustness to phenological variation, with mean and entropy being the most robust, followed by variance then skew. In contrast, no clear pattern of robustness emerged in second-order measures, as the Virginia site did not follow the patterns observed at the other sites. Because of this, it is inconclusive if there is a consistent ordering of robustness of second-order texture measures, although homogeneity, entropy, and dissimilarity appeared to be the most robust.

One of our more striking results was that while the boreal forest of Ontario was a substantially different ecosystem than the desert scrub of southern New Mexico, both sites behaved quite similarly with respect to interseasonal variability in both first- and second-order texture measures. We expected the Virginia site to behave similar to the Ontario site, since both are heavily forested, but found substantial differences.

One possible explanation is the relatively large areas of agriculture in the Virginia site. The Ontario site had no agriculture and the New Mexico site had a limited amount. Agricultural fields can show substantial spectral variability across the growing season, potentially greatly increasing interseasonal variability.

To further investigate this, we manually selected several areas of agriculture and forest in the Virginia study site and compared their interseasonal variability. Contrary to our expectation, the overall mean level of variability was nearly identical between the two classes, with a mean coefficient of variation of 0.98 for agriculture, and 1.09 for forest. Therefore the higher level of agriculture in the Virginia study site did not explain the site's higher variability.

As we expected, interseasonal variability in texture measures was relatively unaffected by the window size chosen for the texture calculations. This allows the flexibility to choose a window size based on a spatial scale(s) that is appropriate for a specific research question (Coburn and Roberts 2004, Franklin et al. 1996) as long as the window is large enough to avoid sparsely populated GLCMs (Vega-Garcia and Chuvieco 2006).

In contrast to our predictions, robustness to interseasonal variability was relatively consistent across spectral bands, especially for first-order texture measures. Our findings imply that there are not specific spectral bands that are universally more sensitive to phenological variation than others.

We believe most of the observed variability in the texture measures can be attributed to changes in phenology, but other factors may have contributed to the variability. As with all studies using imagery from different points of the year, sun angle varies between images, yielding different illumination. In areas of more complex vertical structure, such as forests, this lighting effect will be more pronounced, due to sunlit portions of crowns being brighter, and due to shadows cast by taller trees. These changes in highlight and shadow will yield changes in texture measures. It is also possible that atmospheric conditions varied among (and within) the images, and we did not apply atmospheric correction in this study. Atmospheric contamination can reduce the contrast of an image, which would reduce the values of texture measures responding to heterogeneity (e.g. variance), and increase the value of texture measures that respond to homogeneity (e.g. angular second moment). As with all multi-temporal analyses, precise co-registration of imagery is very important. Misregistration between image dates would artificially inflate variability because the texture values would be calculated from a slightly different area in each image. Lastly, because the imagery used in our study was not all acquired during the same year, in addition to the large seasonal differences in the images, there were likely some interannual differences contributing to variability.

Remote sensing has been used to explicitly monitor vegetation phenology (Reed et al. 1994, Zhang et al. 2003, Stockli and Vidale 2004). Much of the effort has focused on using time series to monitor vegetation phenology over very large spatial extents, often continental scale, from coarse spatial resolution imagery. The goal of these analyses is often to track specific points in vegetation phenology such as greenup or senescence over many years to monitor temporal shifts in phenology. Thus far, there have been relatively few mentions of the effect of phenology on texture measures. Many studies using measures of texture have relied on single-date imagery (Coburn and Roberts 2004, Franklin et al. 2001a, Tuttle et al. 2006, Kayitakire et al. 2006, Wunderle et al. 2007, Tuominen and Pekkarinen 2005, Johansen et al. 2007, Franklin et al. 2001b, Wulder et al. 1998, Peddle and Franklin 1991, Smits and Annoni 1999), and little mention was made regarding the choice of date in relation to texture measures. It is important to consider how texture measures may vary over the growing season in relation to the feature of interest. Even within the growing season, there may be specific windows of time during which certain texture measures will be most powerful in discerning the feature of interest.

It is critical that future studies consider the effects of phenology on texture measures. Some existing multi-temporal studies using texture measures (Hudak and Wessman 1998, Vega-Garcia and Chuvieco 2006, Peroni et al. 2000) have utilized anniversary date imagery, with some making explicit references to concern over phenological changes. However, the specific effect of phenology on texture measures was not explored.

Thus far, few studies have carried out texture analysis over very large spatial extents. In a study modeling bird species occurrence (Hepinstall and Sader 1997), textures measures were calculated from a 2001 Landsat TM mosaic of the state of Maine. It was unclear if the mosaic used same date imagery. Such large spatial extent studies are likely to increase in number as technical capabilities allow. In these cases the effects of phenology must be carefully considered, as cloud cover and other natural variability makes it difficult to create large image mosaics with all images on the same date or even within the same month.

Several actions can be taken to minimize the effect of phenological variation on texture measures. Foremost, whenever possible, imagery should be selected for the same date or phenological stage. The texture measures chosen should be based on the specific application, but if possible, measures that are more robust to phenological variation should be selected, such as first-order mean or entropy, or second-order homogeneity, entropy, or dissimilarity. Special attention should be paid to land cover types, such as agriculture, that show high interseasonal or interannual variability. Just as it is advisable to explore different texture measures and parameter settings for a specific application, the effects of seasonality should be explored in small test areas when possible.

The upside to phenological variation in image texture is that these changes may contain important information. As Figure 2-5 shows, a land cover class (in this case evergreen forest) can show a strong change in texture measures with change in phenology. With higher temporal resolution, the behavior of each texture measure could be further teased out to determine a more precise pattern. When these patterns are known for other land cover types or features of interest, the variability in texture measure can be exploited by choosing imagery at a specific phenological stage or stages to yield the best results.

The phenological variation of texture measures can also be exploited in image classification. Multi-temporal classification of spectral data has been shown to improve classification accuracy over single-date classifications (Homer et al. 2004). For example, some broadleaf tree species are spectrally similar during the growing season, but green-up and senesce at different time points, thus a multi-temporal classification that includes imagery across these points can yield higher accuracy than a single date classification (Wolter et al. 1995). A similar approach utilizing texture measures instead of spectral values seems promising and warrants further exploration.

Before this can be done, more understanding is needed on the trends of specific texture measures in different biomes over the growing season, and which parts of the growing season yield the best measures to characterize a specific process.

References

Bailey R. G. 1995. Description of the Ecoregions of the United States. United States Department of Agriculture.

Baraldi A., F. Parmiggiani. 1995. An Investigation of the textural characteristics associated with gray-level cooccurrence matrix statistical parameters. IEEE Transactions on Geoscience and Remote Sensing 33:293-304.

Bellis L. M., A. M. Pidgeon, V. C. Radeloff, V. St-Louis, J. L. Navarro, and M. B. Martella. 2008. Modeling habitat suitability for greater rheas based on satellite image texture. Ecological Applications 18:1956-1966.

Coburn C. A., A. C. B. Roberts. 2004. A multiscale texture analysis procedure for improved forest stand classification. International Journal of Remote Sensing 25:4287-4308.

Cody M. L. 1981. Habitat selection in birds - the roles of vegetation structure, competitors, and productivity. Bioscience 31:107-113.

Estes L. D., G. S. Okin, A. G. Mwangi, and H. H. Shugart. 2008. Habitat selection by a rare forest antelope: A multi-scale approach combining field data and imagery from three sensors. Remote Sensing of Environment 112:2033-2050.

Franklin S. E., A. J. Maudie, and M. B. Lavigne. 2001a. Using spatial co-occurrence texture to increase forest structure and species composition classification accuracy. Photogrammetric Engineering and Remote Sensing 67:849-855.

Franklin S. E., M. A. Wulder, and G. R. Gerylo. 2001b. Texture analysis of IKONOS panchromatic data for Douglas-fir forest age class separability in British Columbia. International Journal of Remote Sensing 22:2627-2632.

Franklin S. E., M. A. Wulder, and M. B. Lavigne. 1996. Automated derivation of geographic window sizes for use in remote sensing digital image texture analysis. Computers & Geosciences 22:665-673.

Franklin S. E., R. J. Hall, L. M. Moskal, A. J. Maudie, and M. B. Lavigne. 2000. Incorporating texture into classification of forest species composition from airborne multispectral images. International Journal of Remote Sensing 21:61-79.

Haralick R. M. 1979. Statistical and structural approaches to texture. Proceedings of the IEEE 67:786-804.

Haralick R. M., K. Shanmuga, and I. Dinstein. 1973. Textural features for image classification. IEEE Transactions on Systems Man and Cybernetics 3:610-621.

Hepinstall J. A., S. A. Sader. 1997. Using Bayesian statistics, Thematic Mapper satellite imagery, and breeding bird survey data to model bird species probability of occurrence in Maine. Photogrammetric Engineering and Remote Sensing 63:1231-1237.

Homer C., C. Huang, L. Yang, B. Wylie, and M. Coan. 2004. Development of a 2001 National Land-Cover Database for the United States. Photogrammetric Engineering and Remote Sensing 70:829-840.

Hudak A. T., C. A. Wessman. 1998. Textural analysis of historical aerial photography to characterize woody plant encroachment in South African savanna. Remote Sensing of Environment 66:317-330.

Johansen K., N. C. Coops, S. E. Gergel, and Y. Stange. 2007. Application of high spatial resolution satellite imagery for riparian and forest ecosystem classification. Remote Sensing of Environment 110:29-44.

Kayitakire F., C. Hamel, and P. Defourny. 2006. Retrieving forest structure variables based on image texture analysis and IKONOS-2 imagery. Remote Sensing of Environment, 102:390-401.

Leica Geosystems. 2005. ERDAS Imagine. 9.0.

MacArthur R. H., J. W. MacArthur. 1961. On bird species diversity. Ecology 42:594-598.

Musick H. B., H. D. Grover. 1991. Image textural measures as indices of landscape pattern. pp. 77-103 *In* M. G. Turner and K. J. Gaston, editors. Quantitative Methods in Landscape Ecology, Springer-Verlag, New York.

Peddle D. R., S. E. Franklin. 1991. Image texture processing and data integration for surface pattern-discrimination. Photogrammetric Engineering and Remote Sensing 57:413-420.

Peroni P., F. Ferri, and G. C. Avena. 2000. Temporal and spatial changes in a mountainous area of central Italy. Journal of Vegetation Science 11:505-514.

Reed B. C., J. F. Brown, D. VanderZee, T. R. Loveland, J. W. Merchant, and D. O. Ohlen. 1994. Measuring phenological variability from satellite imagery. Journal of Vegetation Science 5:703-714.

Research Systems Inc. 2005. ENVI. 4.2.

Smits P. C., A. Annoni. 1999. Updating land-cover maps by using texture information from very high-resolution space-borne imagery. IEEE Transactions on Geoscience and Remote Sensing 37:1244-1254.

St-Louis V., A. M. Pidgeon, V. C. Radeloff, T. J. Hawbaker, and M. K. Clayton. 2006. High-resolution image texture as a predictor of bird species richness. Remote Sensing of Environment 105:299-312.

St-Louis V., A. M. Pidgeon, M. K. Clayton, B. A. Locke, D. Bash, and V. C. Radeloff. 2009. Satellite image texture and a vegetation index predict avian biodiversity in the Chihuahuan Desert of New Mexico. Ecography 32:468-480.

Stockli R., P. L. Vidale. 2004. European plant phenology and climate as seen in a 20-year AVHRR land-surface parameter dataset. International Journal of Remote Sensing 25:3303-3330.

Tso B., P. Mather. 2001. Classification Methods for Remotely Sensed Data. Taylor & Francis, London.

Tucker C. J. 1979. Red and photographic infrared linear combinations for monitoring vegetation. Remote Sensing of Environment 8:127-150.

Tuominen S., A. Pekkarinen. 2005. Performance of different spectral and textural aerial photograph features in multi-source forest inventory. Remote Sensing of Environment 94:256-268.

Tuttle E. M., R. R. Jensen, V. A. Formica, and R. A. Gonser. 2006. Using remote sensing image texture to study habitat use patterns: a case study using the polymorphic white-throated sparrow (Zonotrichia albicollis). Global Ecology and Biogeography 15:349-357.

Vega-Garcia C., E. Chuvieco. 2006. Applying local measures of spatial heterogeneity to Landsat-TM images for predicting wildfire occurrence in mediterranean landscapes. Landscape Ecology 21:595-605.

Wiken E. B. 1986. Terrestrial ecozones of Canada. Ecological Land Classification Series No. 19. Environment Canada, Hull, Quebec.

Wolter P. T., D. J. Mladenoff, G. E. Host, and T. R. Crow. 1995. Improved forest classification in the Northern Lake-States using multitemporal Landsat imagery. Photogrammetric Engineering and Remote Sensing 61:1129-1143.

Wulder M. A., E. F. LeDrew, S. E. Franklin, and M. B. Lavigne. 1998. Aerial image texture information in the estimation of northern deciduous and mixed wood forest leaf area index (LAI). Remote Sensing of Environment 64:64-76.

Wunderle A. L., S. E. Franklin, and X. G. Guo. 2007. Regenerating boreal forest structure estimation using SPOT-5 pan-sharpened imagery. International Journal of Remote Sensing 28:4351-4364.

Zhang X. Y., M. A. Friedl, C. B. Schaaf, A. H. Strahler, J. C. F. Hodges, F. Gao, B. C. Reed, and A. Huete. 2003. Monitoring vegetation phenology using MODIS. Remote Sensing of Environment 84:471-475.

Tables

Table 2-1. Study imagery.

Site	Image Date (Sensor)
New Mexico	04/23/2000 (ETM+) 06/13/2001 (ETM+) 09/12/1999 (ETM+)
Ontario	04/29/2000 (ETM+) 05/21/2002 (ETM+) 07/05/2001 (ETM+) 09/12/2000 (TM)
Virginia	03/31/2000 (ETM+) 10/15/1999 (TM) 05/24/2002 (ETM+)

Table 2-2. Image texture measure formulae.

Type of Measure	**Texture Measure**	**Formula [11,22]**
1st Order	**Mean**	$\dfrac{\sum_{k=1}^{N} x_k}{N}$ Where N = the number of pixels in the window, and, x_k = the gray tone value of pixel k.
	Variance	$\dfrac{1}{N-1}\sum_{k=1}^{N}\left(x_k - \bar{x}\right)^2$
	Entropy	$-\sum_{g=1}^{G} P(g)\log\left[P(g)\right]$ Where G = the number of gray tone levels, and P(g) is the probability of occurrence of gray level g in the window.
	Skewness	$\dfrac{\frac{1}{N}\sum_{k=1}^{N}\left(x_k - \bar{x}\right)^3}{\left(\frac{1}{N}\sum_{k=1}^{N}\left(x_k - \bar{x}\right)^2\right)^{3/2}}$
2nd Order	**Angular Second Moment**	$\sum_i \sum_j \left\{p(i,j)\right\}^2$ Where p(i,j) is the (i,j)th entry in the normalized GLCM
	Correlation	$\dfrac{\sum_i \sum_j (ij)p(i,j) - \mu_x \mu_y}{\sigma_x \sigma_y}$ Where μ_x, μ_y, σ_x, and σ_y are the means and standard deviations of p_x and p_y, where p_x and p_y are the marginal probabilities of x and y in the normalized GLCM
	Contrast	$\sum_{n=0}^{N-1} n^2 \left\{\sum_{i=1}^{N}\sum_{j=1}^{N} p(i,j)\right\}$ **where n =** $\lvert i - j\rvert$
	Homogeneity (IDM)	$\sum_i \sum_j \dfrac{1}{1+(i-j)^2}\, p(i,j)$
	Dissimilarity	$\sum_{n=0}^{N-1} n \left\{\sum_{i=1}^{N}\sum_{j=1}^{N} p(i,j)\right\}$
	Entropy	$-\sum_i \sum_j p(i,j)\log\left(p(i,j)\right)$
	Variance	$\sum_i \sum_j (i-\mu)^2\, p(i,j)$

Figures

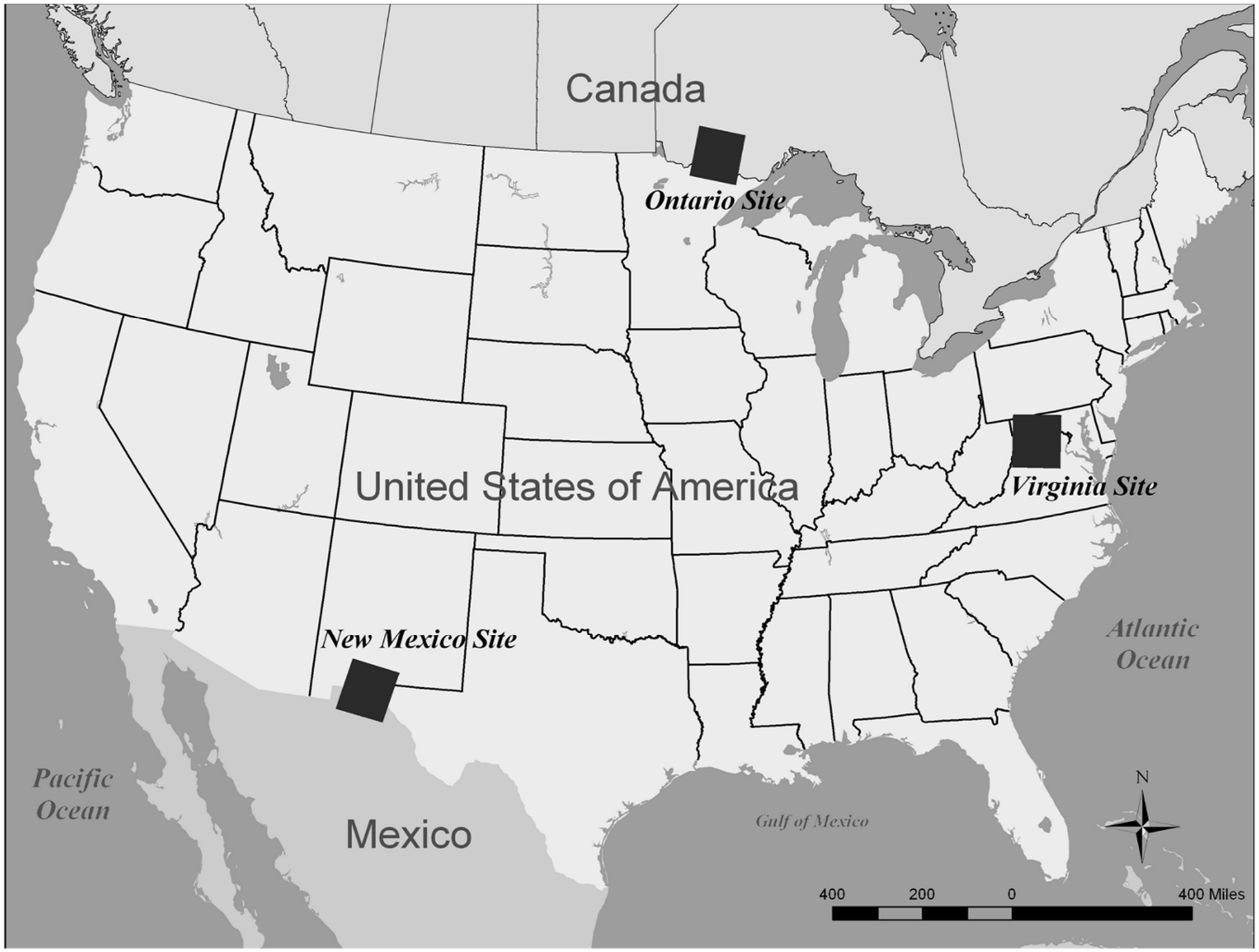

Figure 2-1. The three study sites: Landsat path 16 row 33, along the border of New Mexico, USA and Chihuahua, Mexico; path 33 row 38 along the border of Ontario, Canada and Minnesota, USA; and path 27 row 26, including parts of Virginia, West Virgina, and Maryland, USA.

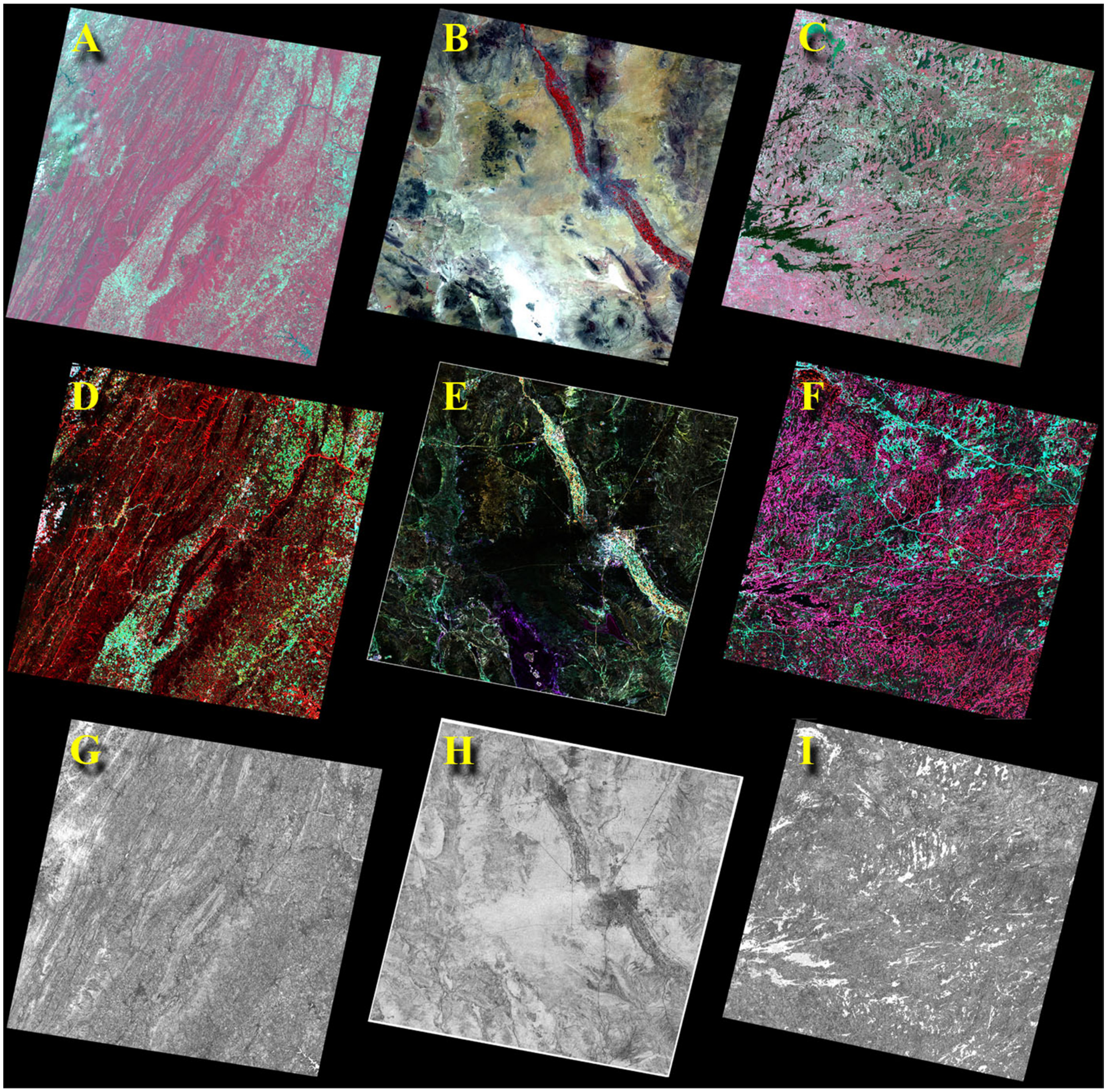

Figure 2-2. (A-C) Virginia, New Mexico, and Ontario Study sites, respectively, bands 4/3/2 false-color composite. (D-F) Second-order 11x11 variance of Virgina, New Mexico, and Ontario study sites, respectively, bands 4/3/2 false color composite. (G-I), Second-order 11x11 homogeneity of band 4 (near-infrared) of Virginia, New Mexico, and Virginia study sites, respectively.

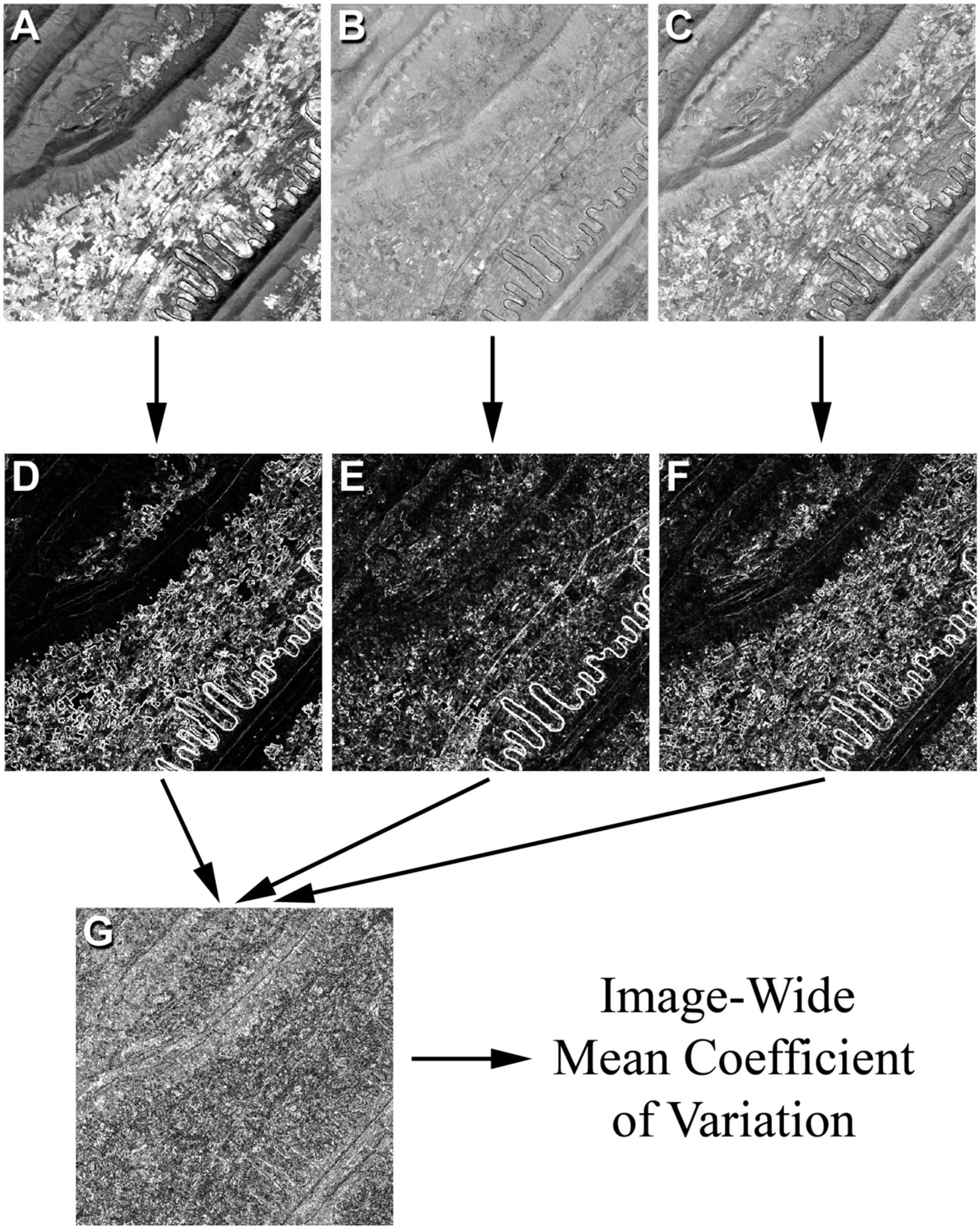

Figure 2-3. Processing flow example for a subset of Virginia study site. Original images, TM Band 4, 03/31/2000 (A), 05/24/2002 (B), 10/15/1999 (C). First-order variance TM band 4 3x3 window size 03/31/2000 (D), 05/24/2002 (E), 10/15/1999 (F). Pixel-wise coefficient of variation across dates (G).

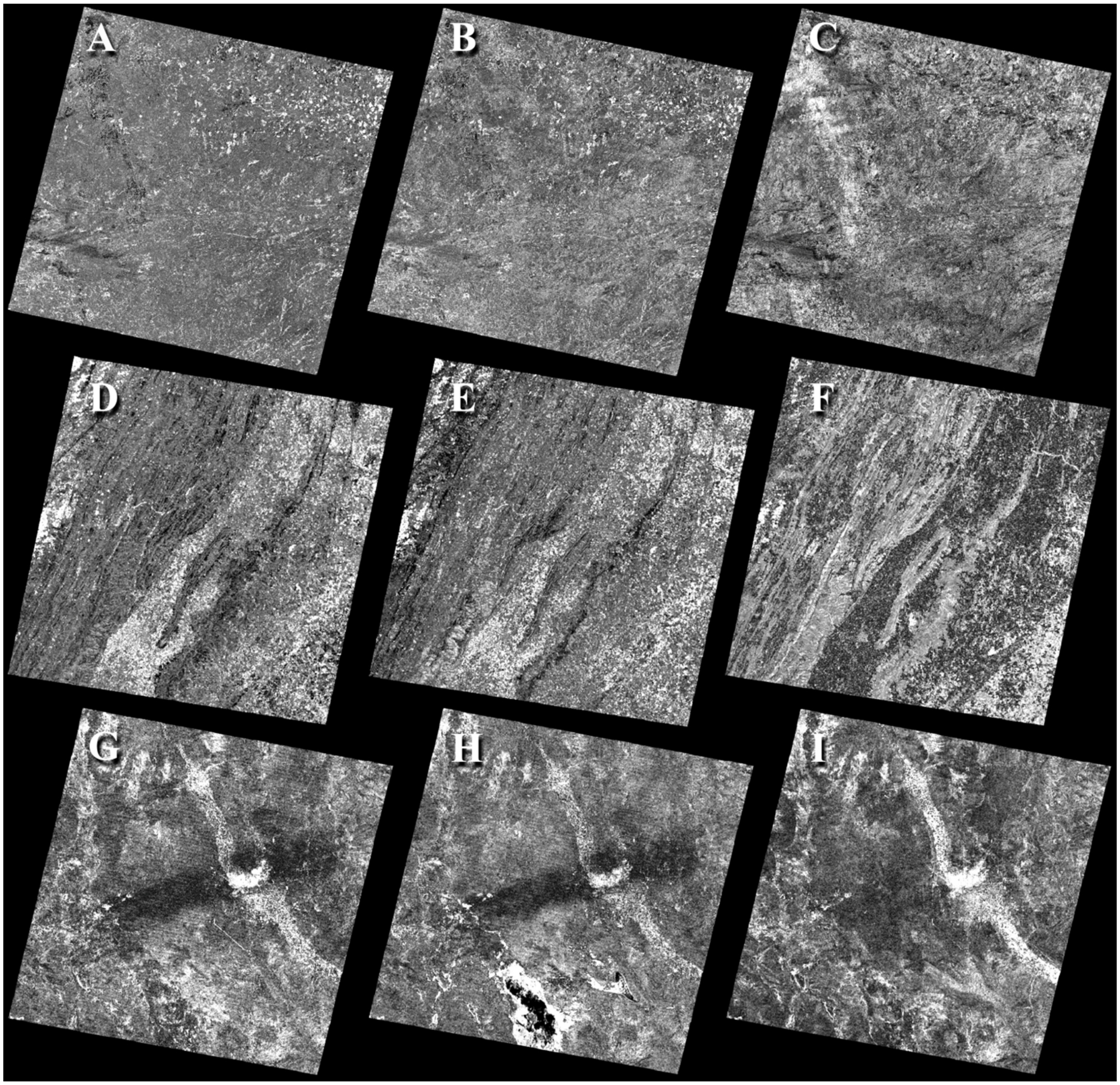

Figure 2-4. A sample of the 468 single-band interseasonal coefficient of variation images. (A-C) Ontario study site, first-order variance, 7x7 window size, bands 2, 3, and 4, respectively. (D-F) Virginia study site, second-order contrast, 15x15 window size, bands 2, 3, and 4, respectively. (G-I) New Mexico study site, second-order homogeneity, 15x15 window size, bands 2, 3, and 4, respectively.

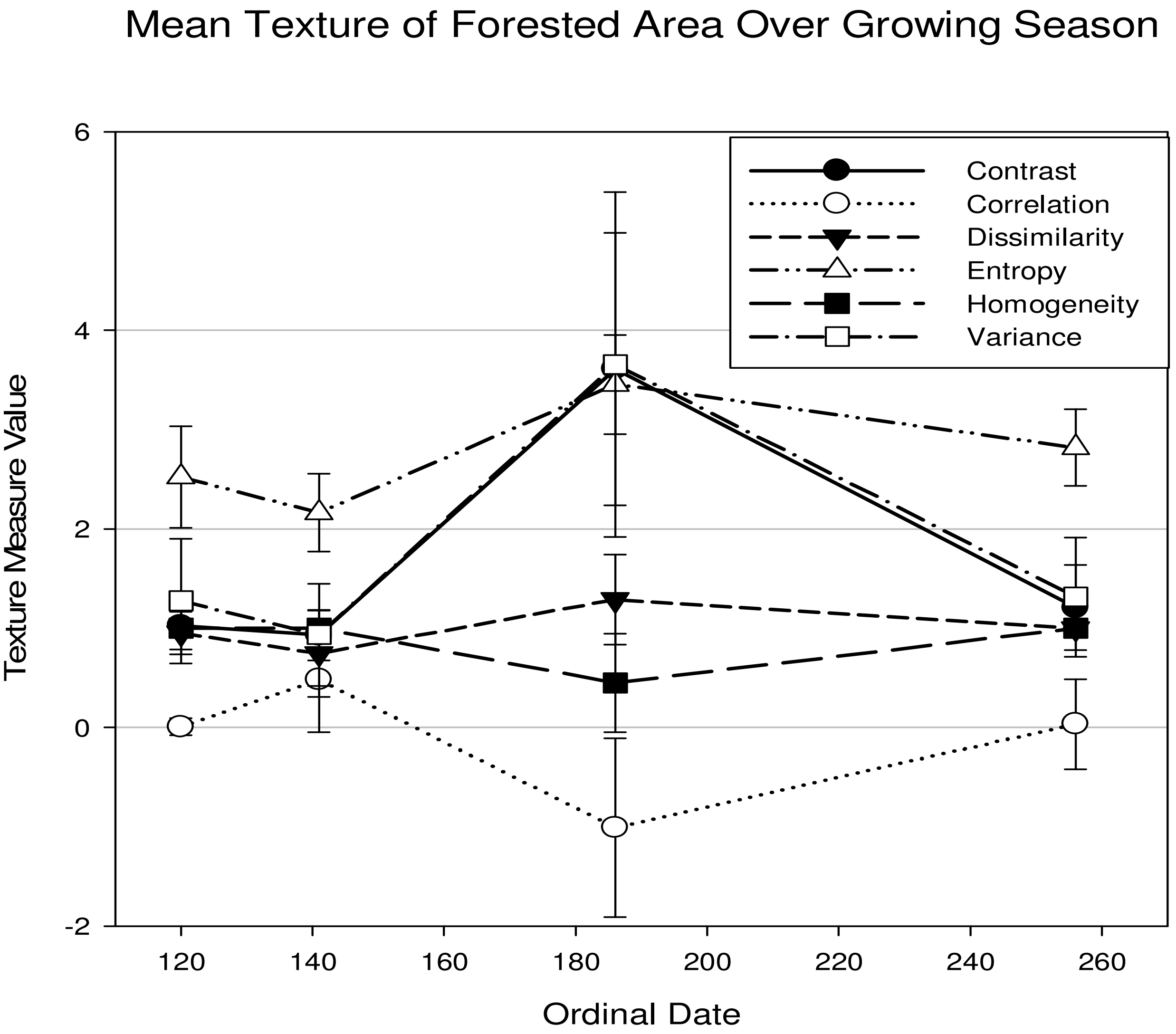

Figure 2-5. Mean values of 11x11 second-order texture measures of TM band 4 across the growing season for a small area of primarily coniferous forest in the Ontario site. Little variation occurred between the first two dates, which both occurred very early in the growing season. The peak of the growing season showed a substantial difference in texture measures. In the final date, which is in the late growing season, texture measures reverted close to early growing season levels. Error bars indicate plus and minus one standard deviation.

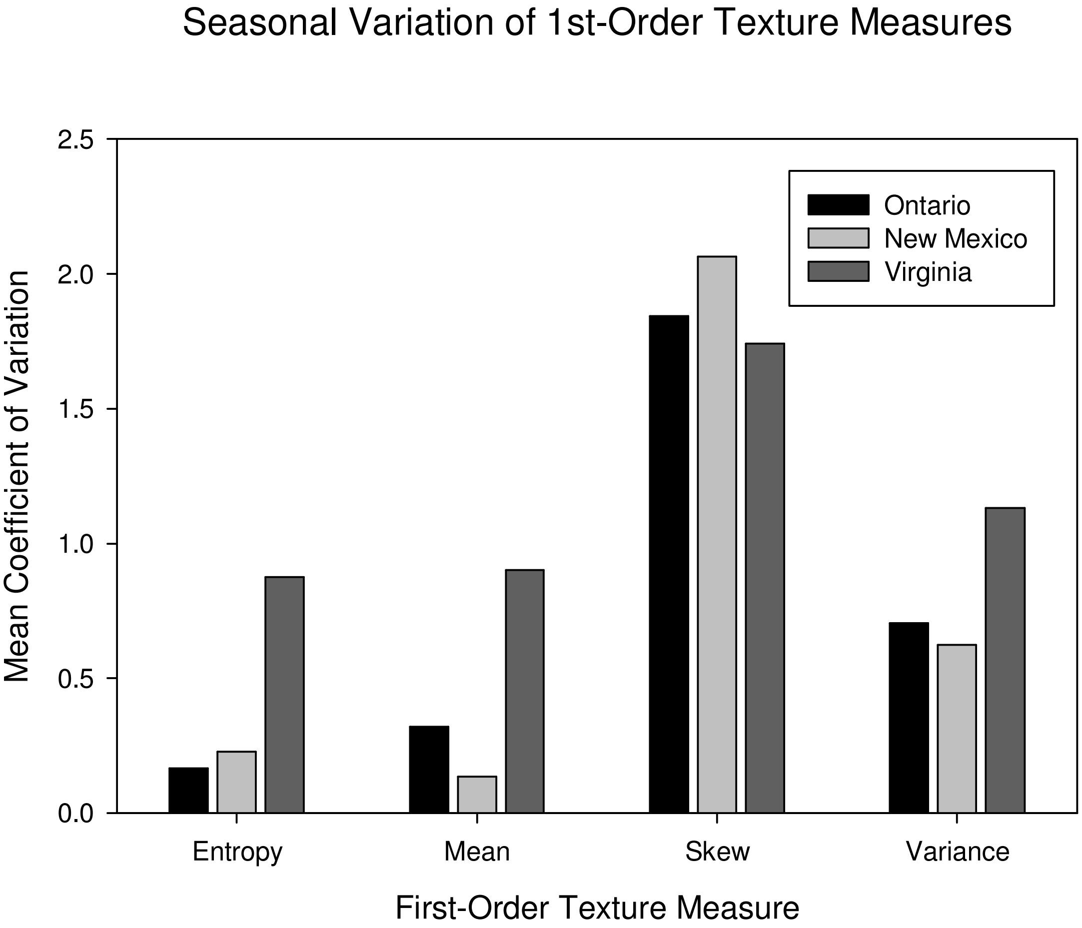

Figure 2-6. Mean image-wide coefficient of variation of first-order texture measures averaged across bands and three window sizes, for the three study sites. Entropy and mean had the lowest coefficient of variation. The Ontario and New Mexico study sites behaved similarly. Variation was generally higher in the Virginia site with a less distinct ranking of texture measure robustness.

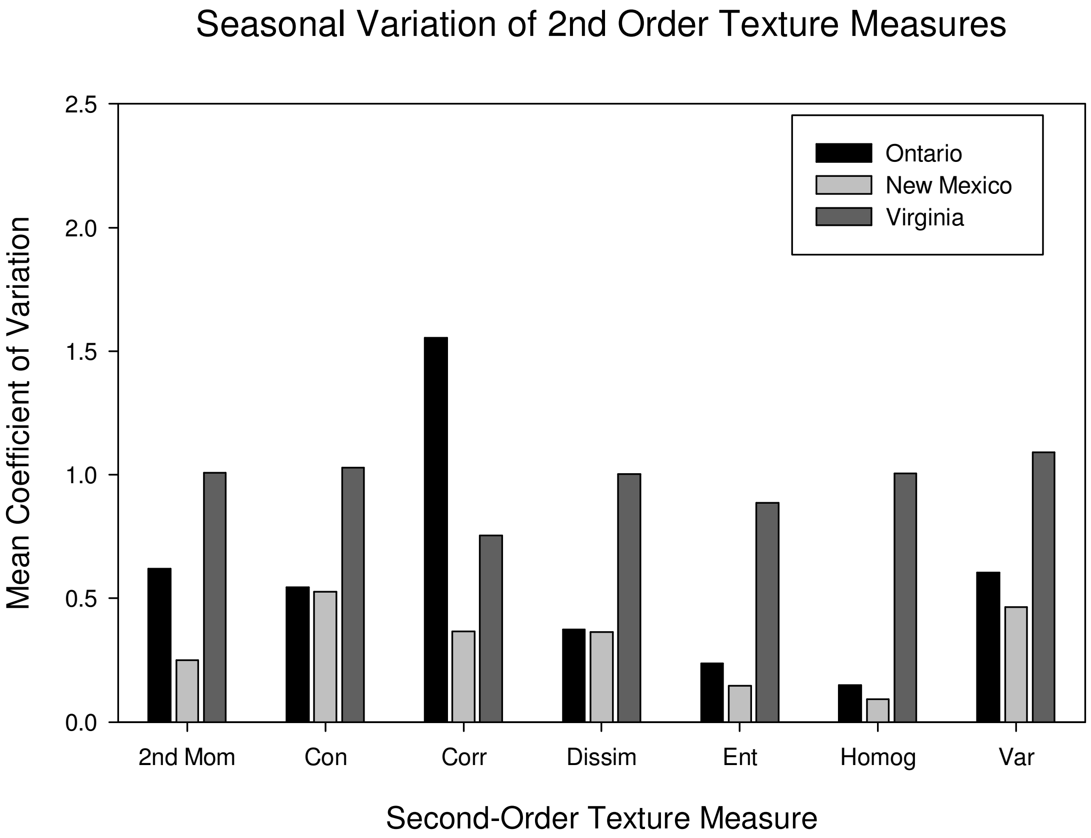

Figure 2-7. Mean image-wide coefficient of variation averaged across bands and three window sizes for each study site. Homogeneity and entropy were the most robust second-order measures. The Ontario and New Mexico sites behaved similarly. The Virginia site had higher variation and less distinction in robustness between different texture measures.

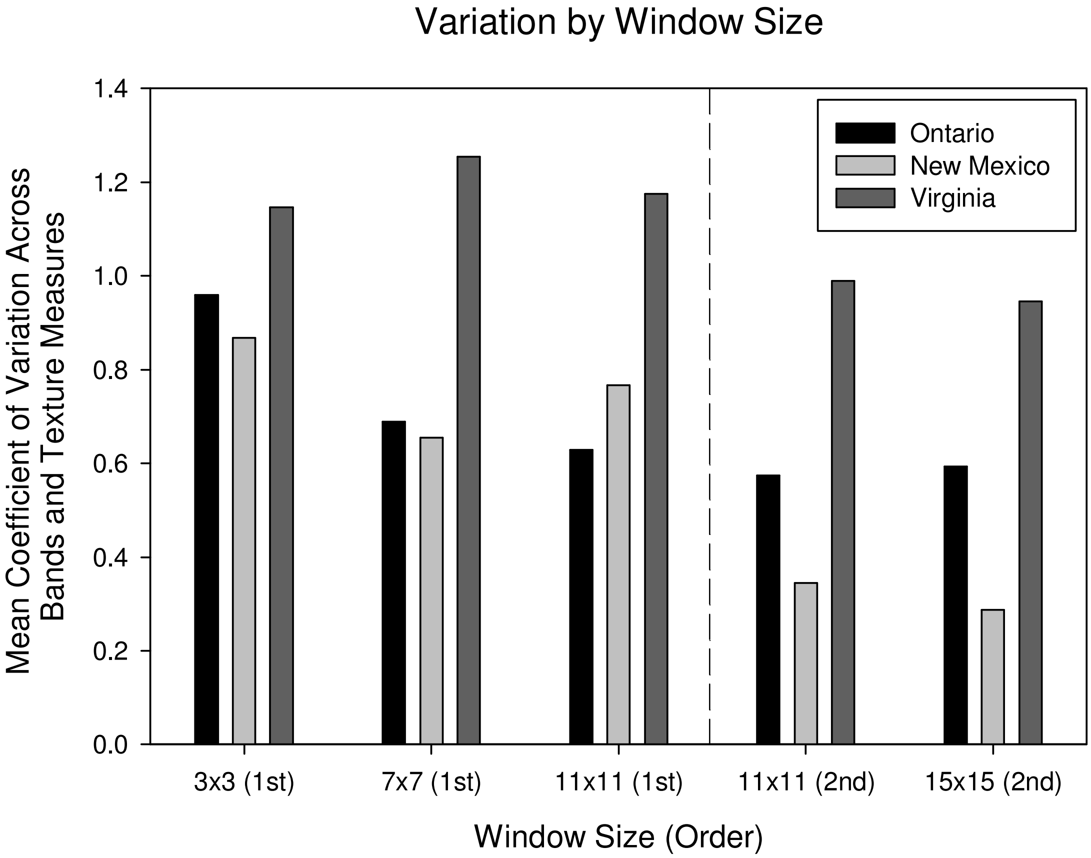

Figure 2-8. Mean coefficient of variation in texture measures summarized for first- and second-order measures for each window size. The mean coefficient of variation shows a slight decreasing trend as window size increases.

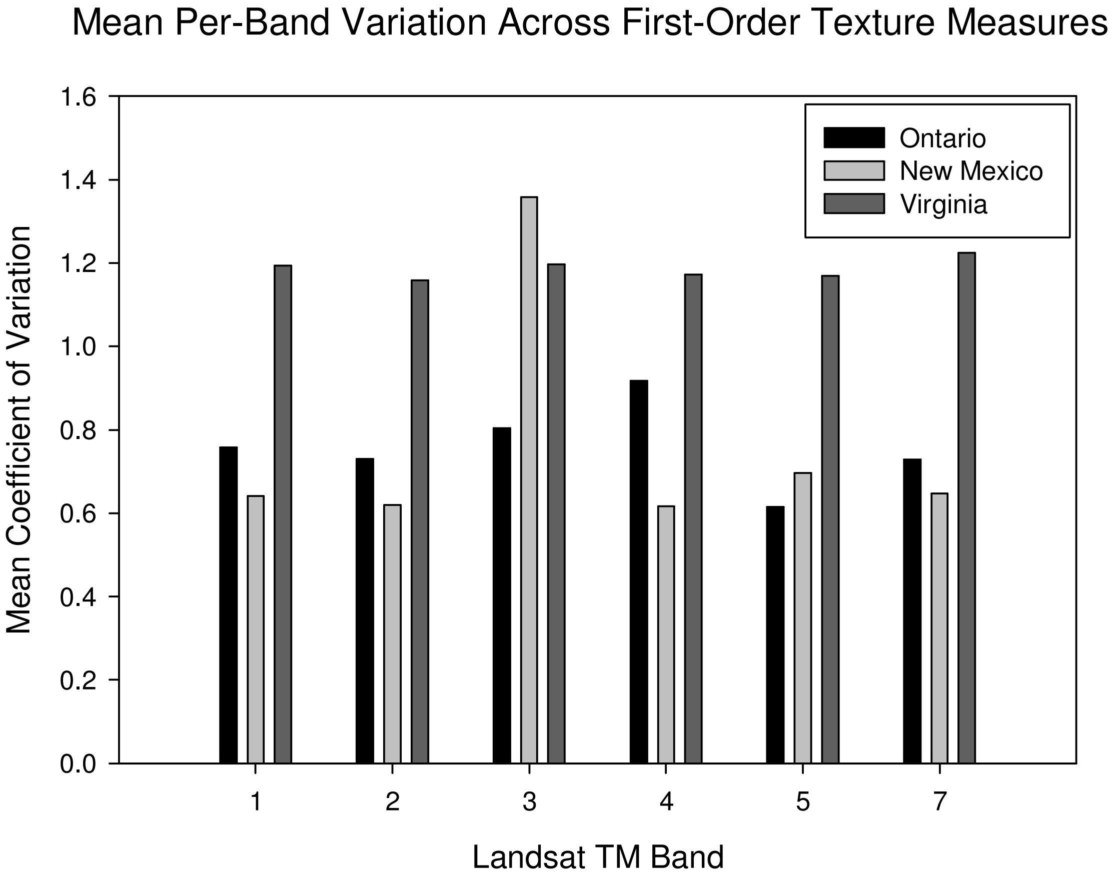

Figure 2-9. Mean variation in first order measures by band. Most bands behaved similarly with a slightly higher level of variation in bands 3 and 4.

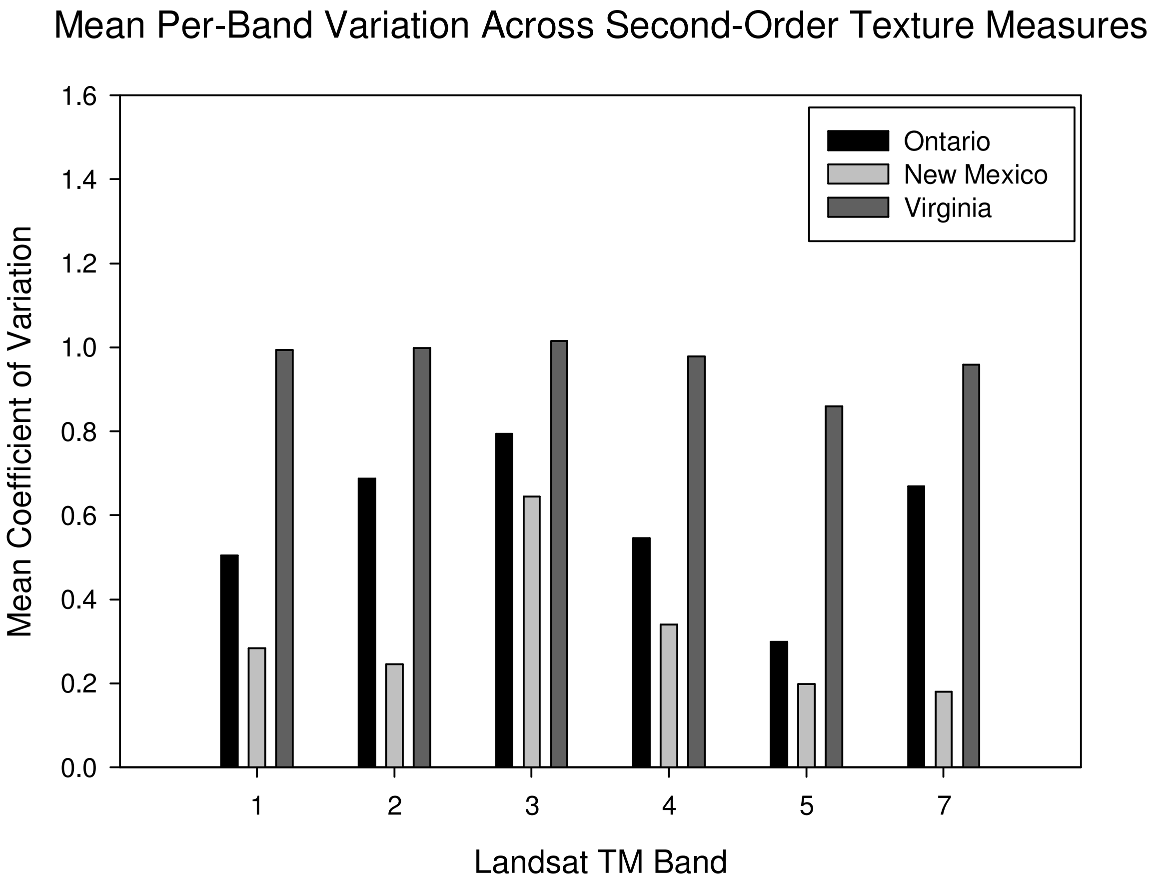

Figure 2-10. Mean variation in second-order measures by band. Variation was less consistent overall with an apparent peak at band 3.

Chapter 2

Modeling broad-scale patterns of avian species richness across the Midwestern United States with measures of satellite image texture

Abstract

Avian biodiversity is threatened, and in order to prioritize limited conservation resources and conduct effective conservation planning a better understanding of avian species richness patterns is needed. The use of image texture measures, as a proxy for the spatial structure of land cover and vegetation, has proven useful in explaining patterns of avian abundance and species richness. However, prior studies that modeled habitat with texture measures were conducted over small geographical extents and typically focused on a single habitat type. Our goal was to evaluate the performance of texture measures over broad spatial extents and across multiple habitat types with varying levels of vertical habitat structure. We calculated a suite of texture measures from 114 Landsat images over a study area of 1,498,000 km^2 in the Midwestern United States, which included habitats ranging from grassland to forest. Avian species richness was modeled for several functional guilds as a function of image texture. We subsequently compared the explanatory power of texture-only models with models fitted using landscape composition metrics derived from the National Land Cover Dataset, as well as models fitted using both texture and composition metrics. Measures of image texture were effective in modeling spatial patterns of avian species richness in multiple habitat types, explaining up to 51% of the variability in species richness of permanent resident birds. In comparison, landscape composition metrics explained up to 56% of the variability in permanent resident species richness. In the most heavily forested ecoregion, texture-measures outperformed landscape metrics, and the two types of measurements were complementary in multivariate models. However, in two out of three ecoregions examined, landscape composition metrics consistently performed slightly better than texture measures, and the variance explained by the two types of measures overlapped considerably. These results show that image texture measures derived from satellite imagery can be an important tool for modeling patterns of avian species richness at broad spatial extents, and thus assist in conservation planning. However, texture measures were slightly inferior to landscape composition metrics in about three-fourths of our models. Therefore texture measures are best considered in conjunction with landscape metrics (if available) and are best used when they show explanatory ability that is complementarity to landscape metrics.

Introduction

Avian biodiversity is under severe threat from human-caused habitat loss and fragmentation (Gaston et al., 2003). The identification of high-value habitat is critical for maintaining avian biodiversity, given that the resources available for habitat conservation are limited (Turner et al., 2003). While some broad-scale mapping of biodiversity has been conducted (Myers et al., 2000, Buckton & Ormerod, 2002), the spatial resolution of these maps is often too coarse to be directly relevant to resource managers and land use planners. Therefore, alternative approaches that can provide maps of avian species richness at a finer spatial resolution are needed for land management and biogeography alike. However, surveying avian species richness exhaustively is not feasible, and it is not clear which approaches can best explain and predict broad-scale avian species richness patterns while retaining a high level of detail.

Modeling and mapping of broad-scale patterns of biodiversity greatly benefits from the use of remotely sensed data (Kerr & Ostrovsky, 2003). A major advantage of remotely sensed data over field data is the availability of highspatial and temporal resolution data over very broad extents (Roy, 2003, Innes & Koch, 1998). Remote sensing-based approaches have played a major role in many recent studies attempting to understand and map patterns of biodiversity (Turner et al., 2003, Nagendra, 2001). Remote sensing approaches fall into three main categories: (1) direct mapping of individuals or assemblages of individuals, (2) indirect mapping based on inference derived from models based on habitat maps (such as landcover classifications) and observed species distribution patterns, or (3) indirect mapping based on relationships between spectral radiance information obtained from unclassified imagery and species distribution (Nagendra, 2001).

In order to infer biodiversity patterns from remotely sensed data, it is important to understand which environmental factors drive biodiversity. Three of the hypothesized primary drivers of biodiversity are climatic stability, productivity, and habitat structure (MacArthur, 1972). Of these three, remotely-sensed measures of climate and productivity are standardized and freely available over broad spatial extents such as PRISM (Daly et al., 2008) temperature and precipitation data, MODIS land surface temperature data (Wan et al., 2002), AVHRR NDVI and MODIS leaf area index data (Myneni et al., 1997, Myneni et al., 2002), vegetation indices (Huete et al., 2002), and net primary productivity (Turner et al., 2006). In contrast, there are no standardized measures of habitat structure for broad extents. For the purpose of our study, we define habitat structure as both the vertical structure of vegetation (such as the vertical configuration of vegetation layers in a forest) as well as horizontal vegetation structure (such as the existence of canopy gaps in a forest).

Habitat structure influences biodiversity, particularly in birds (MacArthur & MacArthur, 1961, MacArthur et al., 1966, Willson, 1974, Wiens, 1974, Tews et al., 2004, Luoto et al., 2004, Clawges et al., 2008), as greater variety in habitat leads to greater variety in species (Rosenzweig, 1995, Tews et al., 2004). Birds can finely partition foraging areas (MacArthur, 1958). Thus, more structure may support a higher number of foraging niches or support a larger food supply (such as insects) allowing for more species (Cody, 1981).

Direct field measurements of habitat structure, while effective in explaining avian distribution patterns, are time consuming and impractical to conduct at a state-wide or regional scale (Bergen et al., 2009), which are the very scales at which conservation planning and land management is conducted. LiDAR (light detection and ranging) technology has proven very effective at remotely measuring vegetation structure, especially in relation to patterns of avian abundance and biodiversity (Goetz et al., 2007, Clawges et al., 2008, Bergen et al., 2009, Seavy et al., 2009, Lesak et al., In Press). Unfortunately, operational LiDAR sensors have only recently become widespread, and most areas of the United States have not been imaged by LiDAR, or areas have been imaged by different types of sensors, complicating analyses. Therefore, broad-scale studies involving measurement of habitat structure by LiDAR remain impractical.

Landscape metrics derived from land cover classifications can also serve as habitat structure measures when explaining biodiversity patterns (Farina 1997, Atauri and De Lucio

2001, Donovan and Flather 2002, Kondo and Nakagoshi 2002). However, metrics are based on land cover classifications, which remove within-class heterogeneity. One promising alternative for characterizing habitat structure using remotely sensed data are image texture measures derived from remotely sensed imagery. Texture measures can capture both between-habitat and within-habitat structure, providing a potential advantage over landscape metrics.

Remotely sensed images are composed of both tone (spectral variation) and texture (spatial variation) (Haralick, 1979, Baraldi & Parmiggiani, 1995). Texture measures quantify spatial heterogeneity which is valuable for both land cover classification (Franklin et al., 2000, Franklin et al., 2001, Coburn & Roberts, 2004) and habitat modeling (Hepinstall & Sader, 1997, Tuttle et al., 2006, Estes et al., 2008). One of the most promising applications of texture measures is the characterization of habitat structure, such as forest structure (Kayitakire et al., 2006, Wunderle et al., 2007), woody plant encroachment of savanna (Hudak & Wessman, 1998), and leaf area index (Wulder et al., 1998).

The most commonly used measures of texture are divided into two groups: first-order (occurrence) and second-order (co-occurrence) (Haralick et al., 1973). First-order measures are summary statistics, such as mean and standard deviation, calculated from the spectral values of pixels in a defined neighborhood, typically implemented as a moving window. Second-order texture measures take into account the spatial distribution and dependencies of spectral values (Coburn & Roberts, 2004). Second-order measures are derived from a gray-level co-occurrence matrix (GLCM) (Haralick et al., 1973). The GLCM is a symmetric n-by-n matrix, where n is the number of possible gray-tone values. Entries P_{ij} in the matrix, represent the relative frequency of pixels with tone levels i and j co-occurring adjacent to one another (Haralick et al., 1973). The

GLCM is also calculated for a neighborhood, typically a moving window. Haralick (1973) originally proposed 14 texture measures derived from the GLCM. Many of these original second-order measures have been found to be highly correlated, and a subset of six measures is considered most useful for remote sensing analysis: angular second moment (ASM), contrast, correlation, homogeneity, variance, and entropy, with the first three being the least correlated (Baraldi & Parmiggiani, 1995, Kayitakire et al., 2006).

Broadly speaking, most second-order texture measures either measure homogeneity or heterogeneity in the digital numbers (DNs) of pixels within a specified neighborhood (Haralick et al., 1973, Baraldi & Parmiggiani, 1995). Measures of homogeneity include homogeneity and angular second moment. Homogeneity is high when adjacent pixels have similar reflectance DNs. Angular second moment measures “uniformity” meaning that certain pairs of DN values occur adjacent to one another in the image very frequently. An image where all pixels have the same DN would have high uniformity, but so would a regular checkerboard image as the white-black adjacency would occur very frequently. Measures of heterogeneity include entropy, contrast, and variance. Entropy measures disorder. The highest entropy values occur when the GLCM is uniform, indicating a perfectly random arrangement of DNs in the original image. Contrast has high values when adjacent pixels have a very large difference in DNs. Variance measures the amount of variability in the GLCM, and is very highly correlated with first-order variance. Correlation measures the correlation in DN of pixel pairs. For this reason, either a very homogenous image or a very heterogenous image could exhibit strong correlation.

The properties of different texture measures explain how they relate to what is visible in a satellite image. A given landcover class, e.g., a deciduous forest, will exhibit homogeneity if adjacent pixels have similar reflectance values. A more heterogeneous forest may include tree species with different spectral properties, or canopy gaps resulting in shadows which will tend to have different reflectance values and texture measures capturing heterogeneity will be higher. Textural features of course also depend on heterogeneity and homogeneity among landcover classes. For example, a patchwork of agricultural fields planted to different crops or at different stages (e.g., bare soil versus mature crop) would have high within-field homogeneity, but high between-field heterogeneity. Similarly, sharp transitions among different land cover classes, such as between forest and pasture, will increase measures of heterogeneity, such as sum of squares variance or contrast.

Given that image texture measures can characterize habitat structure (Franklin et al., 2001, Kayitakire et al., 2006), texture measures have been used successfully to map habitat of species as varied as the mountain bongo (an endangered antelope species) (Estes et al., 2008, Estes et al., 2010), the redtail monkey (Stickler & Southworth, 2008), and avian communities. In Maine, for example, texture measures derived from remotely sensed imagery proved useful in bird presence/absence models (Hepinstall & Sader, 1997). In Argentina, texture measures captured meaningful variation within grasslands, improving habitat suitability models for the Greater Rhea (Bellis et al., 2008). In a desert scrub ecosystem of the Chihuahuan Desert of New Mexico, texture measures derived from Landsat imagery and 1-m resolution digital aerial photographs explained patterns of avian species richness well (St-Louis et al., 2006, St-Louis et al., 2009). Similarly, texture measures derived 0.5-m resolution photographs were successful in explaining avian species richness in prairies and savannas in western Wisconsin (Wood et al., 2007).

These studies show the promise of texture measures for mapping patterns of biodiversity but also present questions for further research. The ecosystems where most of these studies took place (i.e., Grassland, desert scrub, and prairie savanna) have little vertical structure. The ability to characterize the lower strata of structurally complex, closed-canopy habitats, such as forests, is a potential limitation of texture measures derived from passive remote sensing imagery (Estes et al., 2008, Gottschalk et al., 2005). Furthermore, most of the studies investigating the use of image texture for biodiversity modeling were conducted at relatively small spatial extents (4782 km^2, Bellis et al. 2008; 250 km^2, Wood et al. 2007; 2800 km^2, St-Louis et al. 2006, St-Louis et al. 2009). A study modeling avian species occurrence over a much larger study area, i.e., the state of Maine (91,600 km^2) (Hepinstall & Sader, 1997), showed that texture was effective, but considered only first-order texture measures. Thus, it remains unclear whether image texture is equally useful in explaining avian species richness at broader spatial extents and in areas with more vertically complex habitat structure, such as forests.

Our overall goal was to evaluate the ability of satellite image texture measures to explain avian species richness. We were specifically interested in understanding: 1) whether measures of image texture can explain patterns of avian species richness across broad regions that include vertically complex habitats such as forests, and 2) if measures of image texture compare favorably with landscape composition metrics derived from land cover classifications, such as the proportion of specific land cover classes, for modeling patterns of avian species richness. Our predictions were that:

1. The ability of image texture to explain patterns of species richness over small extents will scale-up to broad extents.

2. Measures of image texture will better explain patterns of avian species richness in habitats with simple vertical structure, such as grasslands, than in habitats with complex vertical structure, such as forests.
3. Measures of image texture will better explain avian species richness patterns than landscape composition metrics, because landscape metrics ignore within-habitat variability while texture measures capture both between-habitat and within-habitat variability. However, these two groups of measures will be complementary in multivariate models.
4. Because texture measures are associated with landcover and vegetation, which relate to habitat type, they will hold higher explanatory power for habitat-based avian guilds than migratory guilds.

Methods

Study Area

Our study area encompassed three ecoregions at the province level (hereafter ecoregions) totaling 1,498,000 km^2 of the Midwestern United States: ecoregion 251 (Prairie Parkland, Temperate) and most of ecoregions 212 (Laurentian Mixed Forest) and 222 (Eastern Broadleaf Forest, Continental) (Bailey, 1995) (Figure 2-1). The Prairie Parkland ecoregion was historically composed of prairie alternating with deciduous trees. Today, it is dominated by agriculture, with remnant patches of prairie and small groves and strips of deciduous forest. The Eastern Broadleaf Forest ecoregion is composed primarily of deciduous broadleaf forests, mixed with agriculture. We included the portion of this ecoregion from approximately the state of Michigan and westward. (It should be noted that the Eastern Broadleaf Forest included roughly half of our data points, thereby weighting our full-study-area analysis to this ecoregion.) The Laurentian Mixed Forest is in the transition area between broadleaf deciduous forest zones and the boreal forest. The ecoregion is composed of pure stands of deciduous trees, pure stands of conifers, and mixed stands. We included the areas of this ecoregion in Minnesota, Wisconsin, and Michigan, while excluding areas east of Michigan in order to maintain a contiguous study area.

In order to quantify differences in landcover composition (and inferred vertical habitat structure) between ecoregions, we calculated the proportion of forest, agriculture, grassland, and shrubland surrounding the Breeding Bird Survey routes included in our analysis (Table 2-1). The Laurentian Mixed forest was dominated by forest, indicating the highest level of vertical habitat structure. The Eastern Broadleaf Forest was heavily in agriculture, but with a significant component in forest. The Prairie Parkland was clearly agriculture-dominated, reflecting the lowest level of vertical habitat structure.

Bird Data

We calculated species richness (our measure of biodiversity) from the North American Breeding Bird Survey (BBS), an annual survey of approximately 3,000 routes across the U.S. (Figure 2-1). A typical BBS survey consists of recording all birds observed or heard at 50 regularly spaced 3-min point counts along a 39.4-km route (USGS Patuxent Wildlife Research Center 2008). We centered our analysis on the year 2000, calculating the mean species richness of each BBS route from 1998 to 2002. We included only BBS routes that fall entirely within one of the three ecoregions of study. The BBS data were preprocessed to remove route-years collected by first year observers, or those carried out in suboptimal weather (e.g., high wind or rain). A total of 586 BBS routes fulfilled our criteria, including 161 in Prairie Parkland, 113 in Laurentian Mixed Forest, and 312 in Eastern Broadleaf Forest. Because we did not expect all bird species to respond uniformly to measures of textures, we calculated overall species richness as well as richness within three migratory guilds: permanent residents, short-distance migrants (i.e., species that spend the non-breeding season primarily in the southern portion of the U.S.), and Neotropical migrants (Rappole, 1995, Peterjohn & Sauer, 1999, Pidgeon et al., 2007). We also calculated species richness of avian guilds organized by the structural form of habitat they are commonly associated with: forest, shrubland, and grassland (Peterjohn & Sauer, 1999, Pidgeon et al., 2007).

To adjust for detection probability bias (i.e., the problem that not all bird species are uniformly detectable at a given site), it is recommended that a correction be applied to raw count data to adjust the species richness estimate (Kéry & Schmid, 2004). We used the software program COMDYN (Hines et al., 1999) to adjust our species richness estimates. COMDYN considers the raw BBS route richness data from a capture-recapture model perspective and uses a jackknife estimator to calculate estimated species richness (Nichols et al., 1998).

Image Texture Data

We acquired 114 Landsat TM/ETM+ scenes (Figure 2-2 A) from the LEDAPS database (Masek et al., 2006), a collection of atmospherically corrected Landsat images based on the GeoCover dataset (Tucker et al., 2004). We selected scenes from approximately the year 2000, to temporally coincide with our species richness data. All images were acquired during the growing season, however due to the extent of study, it was not possible to obtain all images for the same phenological stage. Therefore, some extraneous phenological variability in the texture measures was likely present (Culbert et al., 2009). For each image, a suite of first- and second-order texture measures were calculated using Matlab® R2010a (The MathWorks, 1984-2010), with scripts adapted from St-Louis et al. (2006) (Table 2-2). First-order mean and standard deviation were calculated for TM bands 1, 2, 3, 4, 5, and 7, with 5x5 and 21x21 moving windows. We also calculated second-order angular second moment (ASM), contrast, correlation, entropy, homogeneity (Figure 2-2 B), and sum of squares variance (SSVar). Among all second-order texture measures, these six are considered the most useful for remote sensing analyses, and angular second moment, contrast, and correlation are the three least correlated measures (Baraldi & Parmiggiani, 1995, Kayitakire et al., 2006). We expected this set of texture measures would adequately characterize vegetation structure and therefore be an appropriate set with which to relate avian species richness. We quantized the imagery to 64 values to limit the size of the GLCM and avoid matrices that are too sparsely populated to provide robust results. To determine minimum and maximum values for the quantization, we calculated the 2.5th and 97.5th percentiles for each band of each image. We then calculated the 2.5th and 97.5th percentile of these values for each band across all images, and we used these values as our minimum and maximum digital numbers (DNs) for the quantization. Second-order textures were calculated using an omni-directional GLCM (calculated as the mean of the four possible directional GLCMs). Preliminary analysis found strong correlation between texture measures derived from 5x5 and 21x21 window sizes, so due to the substantial computational requirements, second-order texture measures were calculated only with a 5x5 window and only for TM bands 2, 3, 4, and 5. Bands 1 and 7 were excluded because we expected band 1 results to be highly correlated with band 2, and band 7 was less useful than other bands in prior exploratory analysis. This resulted in a total of 48 texture measures (24 first-order and 24 second-order).

In order to relate our texture measures to individual BBS routes, we derived 19.7 km-radius (one-half the length of a BBS route) circular buffers around the centroid of each BBS route (Flather & Sauer, 1996, Rittenhouse et al., 2010, Albright et al., 2010, 2011). We chose this radius because it encompasses the entire BBS route, regardless of varying route path, thus resulting in a uniform area and shape for each route. Furthermore, this distance is comparable to the median maximum natal dispersal distance (31 km) of 76 avian species (Sutherland et al., 2000) estimated from body size relationships, and is consistent with the recommendation that landscape effects on songbirds should be examined over tens of kilometers to capture dispersal effects (Tittler et al., 2009). For each BBS route, we calculated the within-buffer mean and standard deviation of each of the 48 texture measures, yielding 96 explanatory variables total. We calculated buffer summary statistics from a single Landsat scene whenever possible. Of the 586 BBS route buffers, 164 did not fall entirely within a single Landsat footprint. In those cases, the buffer summary statistics were calculated from mosaics of adjacent Landsat scenes.

Land Cover Data

We derived landscape composition metrics for each BBS route for comparison with our texture results. Landscape metrics were calculated from the 2001 National Land-Cover Database (NLCD) (Homer et al., 2004). Within each BBS route buffer, the relative abundance was calculated for 13 land-cover classes: developed (NLCD 2001 classes 21, 22, 23, and 24), barren (31), deciduous forest (41), evergreen forest (42), mixed forest (43), shrub-scrub (52), grassland (71), pasture (81), cultivated crops (82), woody wetland (90), and herbaceous wetland (95). Additionally, the total number of landcover classes present and the Shannon diversity index (Shannon, 1948) of class distribution were calculated for each buffer.

Statistical Analysis

The Landsat image texture processing generated 96 potential explanatory variables. Given our sample sizes (161, 113, 312, and 586), this was an unreasonably large pool of explanatory variables. Furthermore, many texture measures are correlated (Baraldi & Parmiggiani, 1995) and we also expected there would be correlation between some of the bands, window sizes, and summary statistics (mean or standard deviation). We therefore analyzed the correlation in this variable pool in order to exclude collinear variables ($|r| > 0.8$) and reduce the number of variables. Additionally, we created a univariate linear model for each combination of texture measure variable (96) and avian guild (7) for a total of 672 models. We ranked the individual texture variables based on their R^2 value for the "all birds" guild (results not shown). Rankings of texture measure variables based on performance for other guilds were similar. Correlation analysis first focused on within-texture measure correlation. For each texture measure (mean, standard deviation, angular second moment, contrast, correlation, entropy, homogeneity, and sum of squares variance), correlations between bands, window sizes, or summary statistics were analyzed. For variable pairs with $|r| > 0.8$, the variable with the lower univariate R^2 ranking was dropped. After within-texture correlations were accounted for, the remaining between-texture correlations were then eliminated by dropping the variable with the poorer univariate R^2 rank.

The relationships between texture measures and avian species richness were explored using multiple linear regression models. Model selection was implemented with the *step* function in R (R Development Core Team, 2009). For each guild, a candidate model was selected using forward selection, backward selection, and bi-directional selection starting from both the full and null models. Of the four candidate models produced by stepwise selection, we selected the model with the lowest Akaike's information criterion (AIC) value as our best model. This analysis was carried out for the entire study area, as well as for each ecoregion separately.

In addition to the texture-based models, we modeled avian species richness as a function of landscape composition metrics only, in order to have a benchmark with which to compare the performance of texture measures. Lastly, we were interested in whether texture measures were complimentary to landscape metrics, so we modeled avian species richness as a function of both texture and landcover metrics.

Results

Correlation analysis of the 96 texture measure variables showed that 441 (9.7%) of the 4,560 unique combinations of variable pairs exceeded our collinearity threshold ($|r| > 0.8$). Once all correlations greater than our threshold were addressed, 22 texture variables remained (Table 2-3).

Over the full study area, all but the models for short-distance migrant explained at least 26% of the variability of species richness with an average adjusted R^2 value of 0.30 (Table 2-4).

The forest bird and permanent resident models were the best (as determined by R^2), with adjusted R^2 values of 0.42 and 0.40, respectively. Three of the texture measures, standard deviation of 21x21 band 4 mean, standard deviation of 5x5 band 2 correlation, and mean of 5x5 band 5 homogeneity were included in six of the seven models.

Model performance in the Laurentian Mixed Forest showed strong differences compared to the full study area models (Table 2-4). The average model adjusted R^2 was similar, at 0.24. However, the grassland bird model was the strongest model with an adjusted R^2 value of 0.41, while adjusted R^2 values for the other six models ranged from 0.16 (permanent residents) to 0.25 (forest birds). The permanent residents model performed the worst in this ecoregion, though it was one of the strongest models for the study area as a whole. The forest bird model also performed more poorly in this ecoregion (adjusted $R^2 = 0.25$) than in the full study area (adjusted $R^2 = 0.42$), even though the Laurentian Mixed Forest ecoregion is the most heavily forested of the three ecoregions in our study area. The three texture measures that were most frequently included in the models were mean of 5x5 band 4 homogeneity (all seven models), standard deviation of 21x21 band 7 mean (six models), and standard deviation of 5x5 band 2 homogeneity (six models).

The Eastern Broadleaf Forest had the models with the highest explanatory power, with an average adjusted R^2 value of 0.32 and top model R^2 values up to 0.46 (permanent residents) and 0.45 (forest birds) (Table 2-4). Three texture variables were frequently included in models: standard deviation of 5x5 band 5 correlation (all seven models), standard deviation of 5x5 band 2 correlation (six models), and standard deviation of 21x21 band 4 mean (five models).

The Prairie Parkland (Temperate) ecoregion had the strongest-performing single model, with texture measures explaining up to 51% of the variation in permanent resident species richness (Table 2-4). The average adjusted R^2 value of the seven models was 0.27. The standard deviation of 5x5 band 2 correlation (six of seven models), standard deviation of 5x5 band 7 mean (five models), and mean of 5x5 band 5 correlation (five models) were frequently included in the best models.

For each ecoregion, and for the study area as a whole, the model selection process was repeated with landscape composition metrics derived from the NLCD as the explanatory variables. Over the entire study area, models using only landscape metrics almost always explained more variance than models based on texture measures (Table 2-5). Only in the case of permanent residents did the texture-only model have a higher adjusted R^2 value than the landscape metric-only model. Models including both texture measures and landscape metrics showed consistent but modest increases in adjusted R^2 over models including landscape metrics or texture alone, with absolute gains of around 0.04 to 0.08.

In the Laurentian Mixed Forest, species richness models including only texture variables were superior to landscape metric-only models for every guild (Table 2-6), with texture-only models outperforming landscape metric-only models by, on average, an absolute adjusted R^2 difference of 0.09 for a relative improvement of 34%. This was in sharp contrast to the other ecoregions. When both texture and landscape variables were included in the explanatory variable pool, the resulting models showed strong absolute and relative gains in adjusted R^2 values.

In the Eastern Broadleaf Forest (Continental), landscape composition metrics were superior to texture variables for explaining species richness (Table 2-7), but the differences in adjusted R^2 values were small (average adjusted R^2 values of 0.36 for landscape metrics-only models compared to 0.32 for texture-only models for a 0.03 absolute or 10% relative increase). Models including both landscape composition metric and texture variables showed modest gains, with an average absolute increase in adjusted R^2 of 0.07 and an average relative gain of 18%.

In the Prairie Parkland (Temperate), landscape metric-only models outperformed texture-only models for five out of seven guilds (Table 2-8). On average, texture-only models had an adjusted R^2 of 0.27 versus 0.31 for landscape metric-only models, a difference of 0.04. Models including both texture and landscape composition metric variables showed only marginal gains over models that included landscape composition metrics alone, with an average absolute adjusted R^2 improvement of 0.04 or a relative improvement of 11%.

Lastly, due to the spatial nature of our study, we expected spatial autocorrelation may have been present in the data. We therefore generated semivariograms of the residuals of all 48 of the final species richness models. Inspection of the semivariograms found no evidence of spatial autocorrelation, and thus no corrective action was necessary.

Discussion

We found strong evidence supporting our first prediction that image texture measures can explain the variability in avian species richness over broad areas. Our results support earlier studies modeling avian species richness in savanna (Wood et al., 2007) and desert-scrub ecosystems (St-Louis et al., 2006, St-Louis et al., 2009), as well as studies modeling habitat suitability for individual grassland (Bellis et al., 2008) and forest (Hepinstall & Sader, 1997) bird species. However, our study expanded texture analysis to a much broader spatial extent (1,498,000 km^2) than previously attempted, and we showed that image texture derived from Landsat satellite imagery can explain variability in avian species richness even in habitats with high levels of vertical habitat structure, such as forests.

The broad-extent texture-only multivariate models that we developed had similar explanatory power to models developed for smaller spatial extents (St-Louis et al., 2006, Wood et al., 2007). Our final multivariate models showed that measures of texture can explain up to 51% of the variability in avian species richness, with most of our final models explaining 20-40% of the variability. In comparison, texture measures derived from orthophotos within a single habitat type (savanna) yielded univariate R^2 values of up to 0.54 (Wood et al., 2007). This was a much stronger relationship than in our univariate models (results not shown), but our multivariate models approached this level of explanatory power. In a 2820 km^2 Chihuahuan Desert landscape, multivariate models explained up to 62% of the variability in avian species richness (St-Louis et al., 2006). This somewhat higher predictive power supports the theory that habitat structure (and therefore texture measures) is more effective at explaining bird species richness patterns over small to medium extents than at broader extents (Hutto, 1985).

Another potential source of the slightly higher explanatory power of these smaller-extent studies is the finer spatial resolution of imagery used. These studies used 1-m (St-Louis et al., 2006) and 0.5-m resolution imagery (Wood et al., 2007). At this resolution, individual trees or large shrubs that have an extent of several pixels can be captured by the imagery and canopy gaps or variability in the spatial distribution of shrubs would thus be well sampled. In contrast, our 30-m resolution imagery is too coarse for a single-tree canopy gap to be captured in a single pixel. While small features may still be included in the spectral information, their contribution to image texture is likely weaker than with fine-resolution imagery.

Modeling suitable avian habitat and biodiversity with image texture measures has been effective in habitats with little vertical structure such as grassland (Bellis et al., 2008), desert scrub (St-Louis et al., 2006, St-Louis et al., 2009), and savanna (Wood et al., 2007). Of the three ecoregions that we analyzed, the Prairie Parkland had the least vertical habitat structure while the Laurentian Mixed Forest had the most. Adjusted R^2 values (Table 2-4) from species richness models were higher in the Laurentian Mixed Forest for all birds, grassland birds, and Neotropical migrants. The Prairie Parkland models had superior adjusted R^2 values for forest birds, shrubland birds, permanent residents, and short-distance migrants.

These results refute our second prediction that image texture would perform better in ecosystems with simple vertical structure. Models calculated for an ecoregion dominated by agriculture and grassland performed similarly to models for a forest-dominated ecoregion. While satellite imagery cannot characterize the structure of lower vegetation in forests (Gottschalk et al., 2005), if understory structural characteristics are correlated with canopy features, then useful information may be derived (Estes et al., 2008). It is possible that in our study area understory vegetation features are either less important in explaining patterns of avian species richness than canopy features, or that understory features are sufficiently correlated with the canopy. This is an important finding, as it indicates that, in the context of avian species richness modeling, the usefulness of image texture measures is *not* limited to habitats with low vertical habitat structure.

A significant shortcoming of landscape metrics is that the landcover classifications on which landscape metrics are based do not retain any information on within-class heterogeneity (Turner et al., 2001). We therefore expected that texture measures would outperform landscape metrics in modeling avian species richness. In addition, we expected some complementarity; that both approaches would characterize some unique information useful in explaining species richness patterns.

Contrary to our third prediction, we found that across our study area (Table 2-5), and also in the Eastern Broadleaf Forest (Table 2-7) and the Prairie Parkland (Table 2-8), models of avian species richness using landscape composition metrics were generally slightly superior to models based on texture measures. This supports the theory that habitat structure is more effective at explaining bird species richness patterns over small to medium extents, and habitat type is more important at broader extents (Hutto, 1985). The notable exception was the Laurentian Mixed Forest (Table 2-6), where texture models yielded higher adjusted R^2 values than landscape metric models for all seven guilds. We speculate that this is due to the predominance of forest in the ecoregion (Table 2-1), which may render within-forest structure as particularly important in explaining patterns of avian species richness.

Because landscape metrics ignore within-habitat heterogeneity, while texture measures do not, our third prediction also stated that texture measures and landscape metrics would prove complementarity in their ability to explain patterns of avian species richness. For the overall study area and for all three ecoregions, models generated using both NLCD-derived landscape composition metrics and texture measures yielded higher adjusted R^2 values than models derived from only landscape composition metrics or only texture measures. The final joint models included a relatively even mix of texture and landscape variables (results not shown). This indicates some level of complementarity, but we caution that this could potentially result from model over-fitting. For the overall study area (Table 2-5), the Eastern Broadleaf Forest (Table 2-7), and the Prairie Parkland (Table 2-8), the improvement in adjusted R^2 was small, and the joint models were not very parsimonious (full study region: average of 20.0 variables per model; Eastern Broadleaf Forest: 17.4 variables per model; Prairie Parkland: 12.4 variables per model).

However, in the Laurentian Mixed Forest, four of the seven landscape and texture models showed absolute improvement in adjusted R^2 greater than 0.10, and six of the seven models had relative adjusted R^2 improvement greater than 30% (Table 2-6). Gains of this magnitude cannot be explained by over-fitting alone, and we thus conclude that at least in the Laurentian Mixed Forest, measures of image texture and landscape metrics are complementary.

Because measures of image texture characterize spatial heterogeneity in landcover and vegetation, two key components of avian habitat, our fourth prediction was that our texture measure models would perform better for guilds based on habitat preference compared with guilds based on migratory habit (Figure 2-3). This prediction held overall with texture models explaining, on average, 32% of the variation in species richness of habitat guilds and 26% of variation of migratory guilds. We do note, however, that the strongest model overall was for species richness of permanent residents, though it was followed by the three habitat guilds.

We were also surprised to see which habitat guilds showed the strongest models in certain ecoregions (Figure 2-3). Texture measure-based models explained the most variation in grassland bird species richness in the Laurentian Mixed Forest (adjusted $R^2 = 0.41$) followed by the Eastern Broadleaf Forest (0.37), and the Prairie Parkland (0.20). Texture measures explained twice as much of the variation in grassland bird species richness in the most forested region than in the region with the most agriculture and grassland. Similarly, models of forest bird species richness were strongest in the Eastern Broadleaf Forest (adjusted $R^2 = 0.45$), then the Prairie Parkland (0.29), then the Laurentian Mixed Forest (0.25). Again, models of forest bird species richness were strongest in a moderately forested ecoregion and weakest in the most heavily forested ecoregion. This suggests that it is easier to model species richness of certain groups of birds in areas where there is less suitable habitat for them. For example, in a grassland area with only a few small "islands" of forest, forest bird richness will be very low in the grassland areas and very high in the forest area. On the other hand, in a completely forested area, it will be harder to predict which areas of forest will have the highest forest bird richness since the entire area is potentially suitable habitat for forest birds.

An important caveat for this study, as mentioned earlier, is that while all our satellite images were acquired during the growing season, they were not all from the same phenological stage. In most remote sensing analyses, it is ideal for imagery to have the same acquisition date, as image phenological stage may affect analysis, including image texture analysis (Culbert et al., 2009). However, when analyzing very large areas, this is not always possible. This likely introduced extraneous variability into our texture measurements, and had all our images been acquired at the same phenological stage, the relationships between image texture measures and avian species richness would likely have been even stronger.

The use of image texture measures for habitat and biodiversity analyses has two potential drawbacks: significant computational requirements and difficulties in interpreting the ecological relevance of specific texture measures. First, calculations of second-order image texture are computationally much more demanding than other common remote sensing data analyses. While this challenge will become less significant as computing power continues to increase, it is currently non-trivial to calculate second-order texture measures over a broad extent. Second, interpreting the ecological meaning of specific texture measures is challenging. Many of the texture measures, especially second-order measures, are difficult to conceptualize in terms of what they represent "on the ground". This means that texture measures provide only limited additional insights into the ecology of birds. However, there are many applications, such as conservation planning, for which the variables selected may matter much less than the quality of the output map, and texture metrics can be valuable for such tasks.

In summary, our study showed that image-texture can be an important tool to explain avian species richness patterns over broad areas. Image texture measures were effective in modeling species richness for several avian guilds, and over varied habitats, ranging from grassland to forest. In particular, texture measures showed superior performance to landscape composition metrics in the most forested ecoregion, and the two types of measures showed strong complementarity. However, in about three-fourths of our models, texture measures had slightly less explanatory power than landscape composition metrics. For this reason the simultaneous use of texture measures and landscape metrics should be considered. The use of image texture measures is also highly useful when an accurate landcover map is unavailable for a given study area, or when the classes of existing maps do not capture the ecological attributes relevant to the study. The use of image texture is a valuable approach for characterizing structure from continuous data sources and should therefore be considered in the spatial modeling of species diversity and habitat suitability for conservation planning.

References

Albright, T.P., Pidgeon, A.M., Rittenhouse, C.D., Clayton, M.K., Flather, C.H., Culbert, P.D. (2011). Heat waves measured with MODIS land surface temperature data predict changes in avian community structure. Remote Sensing of Environment 115:245-254.

Albright, T.P., Pidgeon, A.M., Rittenhouse, C.D., Clayton, M.K., Flather, C.H., Culbert, P.D. (2010). Effects of drought on avian community structure. Global Change Biology 16: 2158-2170.

Bailey, R.G. (1995). Description of the Ecoregions of the United States. United States Department of Agriculture.

Baraldi, A., & Parmiggiani, F. (1995). An investigation of the textural characteristics associated with gray-level cooccurrence matrix statistical parameters. IEEE Transactions on Geoscience and Remote Sensing 33:293-304.

Bellis, L.M., Pidgeon, A.M., Radeloff, V.C., St-Louis, V., Navarro, J.L., & Martella, M.B. (2008). Modeling habitat suitability for Greater Rheas based on satellite image texture. Ecological Applications 18:1956-1966.

Bergen, K.M., Goetz, S.J., Dubayah, R.O., Henebry, G.M., Hunsaker, C.T., Imhoff, M.L., et al. (2009). Remote sensing of vegetation 3-D structure for biodiversity and habitat: Review and implications for lidar and radar spaceborne missions. Journal of Geophysical Research-Biogeosciences 114, G00E06.

Buckton, S.T., & Ormerod, S.J. (2002). Global patterns of diversity among the specialist birds of riverine landscapes. Freshwater Biology 47:695-709.

Clawges, R., Vierling, K., Vierling, L., & Rowell, E. (2008). The use of airborne lidar to assess avian species diversity, density, and occurrence in a pine. Remote Sensing of Environment 112:2064-2073.

Coburn, C.A., & Roberts, A.C.B. (2004). A multiscale texture analysis procedure for improved forest stand classification. International Journal of Remote Sensing 25:4287-4308.

Cody, M.L. (1981). Habitat selection in birds - the roles of vegetation structure, competitors, and productivity. Bioscience 31:107-113.

Culbert, P.D., Pidgeon, A.M., St-Louis, V., Bash, D., & Radeloff, V.C. (2009). The impact of phenological variation on texture measures of remotely sensed imagery. IEEE Journal of selected topics in applied earth observations and remote sensing 2:299-309.

Daly, C., Halbleib, M., Smith, J.I., Gibson, W.P., Doggett, M.K., Taylor, G.H., et al. (2008). Physiographically sensitive mapping of climatological temperature and precipitation across the conterminous United States. International Journal of Climatology 28:2031-2064.

Estes, L.D., Okin, G.S., Mwangi, A.G., & Shugart, H.H. (2008). Habitat selection by a rare forest antelope: A multi-scale approach combining field data and imagery from three sensors. Remote Sensing of Environment 112:2033-2050.

Estes, L.D., Reillo, P.R., Mwangi, A.G., Okin, G.S., & Shugart, H.H. (2010). Remote sensing of structural complexity indices for habitat and species distribution modeling. Remote Sensing of Environment 114:792-804.

Flather, C.H., & Sauer, J.R. (1996). Using landscape ecology to test hypotheses about large-scale abundance patterns in migratory birds. Ecology 77:28-35.

Franklin, S.E., Maudie, A.J., & Lavigne, M.B. (2001). Using spatial co-occurrence texture to increase forest structure and species composition classification accuracy. Photogrammetric Engineering and Remote Sensing 67:849-855.

Franklin, S.E., Hall, R.J., Moskal, L.M., Maudie, A.J., & Lavigne, M.B. (2000). Incorporating texture into classification of forest species composition from airborne multispectral images. International Journal of Remote Sensing 21:61-79.

Gaston, K.J., Blackburn, T.M., & Goldewijk, K.K. (2003). Habitat conversion and global avian biodiversity loss. Proceedings of the Royal Society B: Biological Sciences 270:1293-1300.

Goetz, S., Steinberg, D., Dubayah, R., & Blair, B. (2007). Laser remote sensing of canopy habitat heterogeneity as a predictor of bird species richness in an eastern temperate forest, USA. Remote Sensing of Environment 108:254-263.

Gottschalk, T.K., Huettmann, F., & Ehlers, M. (2005). Thirty years of analysing and modelling avian habitat relationships using satellite imagery data: a review. International Journal of Remote Sensing 26:2631-2656.

Haralick, R.M. (1979). Statistical and structural approaches to texture. Proceedings of the IEEE 67:786-804.

Haralick, R.M., Shanmuga, K., & Dinstein, I. (1973). Textural features for image classification. IEEE Transactions on Systems Man and Cybernetics SMG3:610-621.

Hepinstall, J.A., & Sader, S.A. (1997). Using Bayesian statistics, Thematic Mapper satellite imagery, and breeding bird survey data to model bird species probability of occurrence in Maine. Photogrammetric Engineering and Remote Sensing 63:1231-1237.

Hines, J.E., Boulinier, T., Nichols, J.D., Sauer, J.R., & Pollock, K.H. (1999). COMDYN: software to study the dynamics of animal communities using a capture-recapture approach. Bird Study 46:209-217.

Homer, C., Huang, C.Q., Yang, L.M., Wylie, B., & Coan, M. (2004). Development of a 2001 national land-cover database for the United States. Photogrammetric Engineering and Remote Sensing 70:829-840.

Hudak, A.T., & Wessman, C.A. (1998). Textural analysis of historical aerial photography to characterize woody plant encroachment in South African savanna. Remote Sensing of Environment 66:317-330.

Huete, A., Didan, K., Miura, T., Rodriguez, E.P., Gao, X., & Ferreira, L.G. (2002). Overview of the radiometric and biophysical performance of the MODIS vegetation indices. Remote Sensing of Environment 83:195-213.

Hutto, R.L. (1985). Habitat Selection by nonbreeding migratory birds. In M.L. Cody (Ed.), Habitat selection in birds (pp. 455-476). NY: Academic Press.

Innes, J.L., & Koch, B. (1998). Forest biodiversity and its assessment by remote sensing. Global Ecology and Biogeography 7:397-419.

Kayitakire, F., Hamel, C., & Defourny, P. (2006). Retrieving forest structure variables based on image texture analysis and IKONOS-2 imagery. Remote Sensing of Environment 102:390-401.

Kerr, J.T., & Ostrovsky, M. (2003). From space to species: ecological applications for remote sensing. Trends in Ecology & Evolution 18:299-305.

Kéry, M., & Schmid, H. (2004). Monitoring programs need to take into account imperfect species detectability. Basic and Applied Ecology 5:65-73.

Lesak, A.A., Radeloff, V.C., Hawbaker, T.J., Pidgeon, A.M., Gobakken, T., & Contrucci, K. (In Press). Modeling forest songbird species richness using LiDAR-derived measures of forest structure. Remote Sensing of Environment.

Luoto, M., Virkkala, R., Heikkinen, R.K., & Rainio, K. (2004). Predicting bird species richness using remote sensing in boreal agricultural-forest mosaics. Ecological Applications 14:1946-1962.

MacArthur, R., Recher, H., & Cody, M. (1966). On the relation between habitat selection and species diversity. The American Naturalist 100:319-332.

MacArthur, R.H. (1972). Geographical Ecology: Patterns in the Distribution of Species. Harper & Row.

MacArthur, R.H. (1958). Population ecology of some warblers of northeastern coniferous forests. Ecology 39:599-619.

MacArthur, R.H., & MacArthur, J.W. (1961). On bird species diversity. Ecology 42:594-598.

Masek, J.G., Vermote, E.F., Saleous, N.E., Wolfe, R., Hall, F.G., Huemmrich, K.F., et al. (2006). A Landsat surface reflectance dataset for North America, 1990-2000. IEEE Geoscience and Remote Sensing Letters 3:68-72.

Myers, N., Mittermeier, R.A., Mittermeier, C.G., da Fonseca, G.A.B., & Kent, J. (2000). Biodiversity hotspots for conservation priorities. Nature 403:858.

Myneni, R.B., Nemani, R.R., & Running, S.W. (1997). Estimation of global leaf area index and absorbed par using radiative transfer models. IEEE Transactions on Geoscience and Remote Sensing 35:1380-1393.

Myneni, R.B., Hoffman, S., Knyazikhin, Y., Privette, J.L., Glassy, J., Tian, Y., et al. (2002). Global products of vegetation leaf area and fraction absorbed PAR from year one of MODIS data. Remote Sensing of Environment 83:214-231.

Nagendra, H. (2001). Using remote sensing to assess biodiversity. International Journal of Remote Sensing 22:2377-2400.

Nichols, J.D., Boulinier, T., Hines, J.E., Pollock, K.H., & Sauer, J.R. (1998). Inference methods for spatial variation in species richness and community composition when not all species are detected. Conservation Biology 12:1390-1398.

Peterjohn, B.G., & Sauer, J.R. (1999). Population status of North American grassland birds from the North American breeding bird survey, 1966-1996. In P.D. Vickery, & J.R. Herkert (Eds.), Ecology and Conservation of Grassland Birds of the Western Hemisphere (pp. 27-44). Camarillo, CA: Cooper Ornithological Society.

Pidgeon, A.M., Radeloff, V.C., Flather, C.H., Lepczyk, C.A., Clayton, M.K., Hawbaker, T.J., et al. (2007). Associations of forest bird species richness with housing and landscape patterns across the USA. Ecological Applications 17:1989-2010

R Development Core Team. (2009). R: A language and environment for statistical computing.

Rappole, J.H. (1995). *The Ecology of Migrant Birds.* Washington, D.C.: Smithsonian Institute Press.

Rittenhouse, C.D., Pidgeon, A.M., Albright, T.P., Culbert, P.D., Clayton, M.K., Flather, C.H., et al. (2010). Avifauna response to hurricanes: regional changes in community similarity. Global Change Biology 16:905-917

Rosenzweig, M.L. (1995). Species Diversity in Space and Time. Cambridge University Press.

Rowhani, P., Lepczyk, C.A., Linderman, M.A., Pidgeon, A.M., Radeloff, V.C., Culbert, P.D., et al. (2008). Variability in energy influences avian distribution patterns across the USA. Ecosystems 11:854-867.

Roy, P.S. (2003). Biodiversity conservation - Perspective from space. National Academy Science Letters-India 26:169-184.

Seavy, N.E., Viers, J.H., & Wood, J.K. (2009). Riparian bird response to vegetation structure: a multiscale analysis using LiDAR measurements of canopy height. Ecological Applications 19:1848-1857.

Shannon, C.E. (1948). A mathematical theory of communication. Bell System Technical Journal 27:379-423 and 623-656.

Stickler, C.M., & Southworth, J. (2008). Application of multi-scale spatial and spectral analysis for predicting primate occurrence and habitat associations in Kibale National Park, Uganda. Remote Sensing of Environment 112:2170-2186.

St-Louis, V., Pidgeon, A.M., Radeloff, V.C., Hawbaker, T.J., & Clayton, M.K. (2006). High-resolution image texture as a predictor of bird species richness. Remote Sensing of Environment 105:299-312.

St-Louis, V., Pidgeon, A.M., Clayton, M.K., Locke, B.A., Bash, D., & Radeloff, V.C. (2009). Satellite image texture and a vegetation index predict avian biodiversity in the Chihuahuan Desert of New Mexico. Ecography 32:468-480.

Sutherland, G.D., Harestad, A.S., Price, K., & Lertzman, K.P. (2000). Scaling of natal dispersal distances in terrestrial birds and mammals. Conservation Ecology 4:16.

Tews, J., Brose, U., Grimm, V., Tielborger, K., Wichmann, M.C., Schwager, M., et al. (2004). Animal species diversity driven by habitat heterogeneity. Journal of Biogeography 31:79-92.

The MathWorks, I. (1984-2010). Matlab R2010a.

Tittler, R., Villard, M., & Fahrig, L. (2009). How far do songbirds disperse? Ecography 32:1051-1061.

Tucker, C.J., Grant, D.M., & Dykstra, J.D. (2004). NASA's global orthorectified landsat data set. Photogrammetric Engineering and Remote Sensing 70:313-322.

Turner, D.P., Ritts, W.D., Cohen, W.B., Gower, S.T., Running, S.W., Zhao, M., et al. (2006). Evaluation of MODIS NPP and GPP products across multiple biomes. Remote Sensing of Environment 102:282-292.

Turner, M.G., Gardner, R.H., & O'Neill, R.V. (2001). *Landscape ecology in theory and practice.* New York: Springer.

Turner, W., Spector, S., Gardiner, N., Fladeland, M., Sterling, E., & Steininger, M. (2003). Remote sensing for biodiversity science and conservation. Trends in Ecology & Evolution 18:306-314.

Tuttle, E.M., Jensen, R.R., Formica, V.A., & Gonser, R.A. (2006). Using remote sensing image texture to study habitat use patterns: a case study using the polymorphic white-throated sparrow (Zonotrichia albicollis). Global Ecology and Biogeography 15:349-357.

Wan, Z.M., Zhang, Y.L., Zhang, Q.C., & Li, Z.L. (2002). Validation of the land-surface temperature products retrieved from Terra Moderate Resolution Imaging Spectroradiometer data. Remote Sensing of Environment 83:163-180.

Wiens, J.A. (1974). Habitat Heterogeneity and Avian Community Structure in North-American Grasslands. American Midland Naturalist 91:195-213.

Willson, M.F. (1974). Avian Community Organization and Habitat Structure. Ecology 55:1017-1029.

Wood, E.M., Pidgeon, A.M., & Radeloff, V.C. (2007). Comparing image texture from infrared versus panchromatic aerial photographs for predicting avian species richness in a Midwest prairie savanna. 68th Midwest Fish and Wildlife Conference. December 9-12, 2007. Madison, WI.

Wulder, M.A., LeDrew, E.F., Franklin, S.E., & Lavigne, M.B. (1998). Aerial image texture information in the estimation of northern deciduous and mixed wood forest leaf area index (LAI). Remote Sensing of Environment 64:64-76.

Wunderle, A.L., Franklin, S.E., & Guo, X.G. (2007). Regenerating boreal forest structure estimation using SPOT-5 pan-sharpened imagery. International Journal of Remote Sensing 28:4351-4364.

Tables

Table 2-1. Landcover composition of BBS route buffers by ecoregion.

Ecoregion	Laurentian Mixed Forest	Eastern Broadleaf Forest (Continental)	Prairie Parkland (Temperate)	All 3 Ecoregions Combined
Proportion Forest	0.47	0.29	0.11	0.27
Proportion Agriculture	0.17	0.52	0.69	0.50
Proportion Grassland	0.03	0.02	0.08	0.04
Proportion Shrubland	0.01	0.01	0.00	0.01
Number of BBS Buffers	113	312	161	586

Table 2-2. Combinations of texture, window size, and Landsat TM band that were calculated for the study area.

Order	Texture	Window Size(s)	TM Bands
1st	Mean	5x5, 21x21	1,2,3,4,5,7
1st	Standard Deviation	5x5, 21x21	1,2,3,4,5,7
2nd	Angular Second Moment (ASM)	5x5	2,3,4,5
2nd	Contrast	5x5	2,3,4,5
2nd	Correlation	5x5	2,3,4,5
2nd	Entropy	5x5	2,3,4,5
2nd	Homogeneity	5x5	2,3,4,5
2nd	Sum of Squares Variance (SSVar)	5x5	2,3,4,5

Table 2-3. Texture variables calculated from Landsat imagery. Based on correlation analysis, 74 variables (marked "-") were excluded from subsequent analysis, and 22 variables (marked "X") were retained.

Texture	Landsat TM Band					
	1	2	3	4	5	7
Mean_5x5_Mean	-	-	-	-	-	-
Mean_21x21_Mean	-	X	-	X	-	-
Mean_5x5_SD	X	-	-	X	-	X
Mean_21x21_SD	X	-	-	X	-	X
SD_5x5_Mean	-	-	-	-	-	-
SD_21x21_Mean	-	-	-	-	-	-
SD_5x5_SD	X	-	-	X	X	-
SD_21x21_SD	-	-	-	-	-	-
ASM_5x5_Mean	■	-	-	-	-	■
ASM_5x5_SD	■	X	-	-	-	■
Contrast_5x5_Mean	■	-	-	-	-	■
Contrast_5x5_SD	■	-	-	-	-	■
Correlation_5x5_Mean	■	-	X	X	X	■
Correlation_5x5_SD	■	X	-	-	X	■
Entropy_5x5_Mean	■	-	-	-	-	■
Entropy_5x5_SD	■	-	-	-	-	■
Homogeneity_5x5_Mean	■	-	-	X	X	■
Homogeneity_5x5_SD	■	X	-	X	-	■
SSVariance_5x5_mean	■	-	X	-	-	■
SSVariance_5x5_SD	■	-	-	-	-	■

Table 2-4. Final guild species richness models as determined by stepwise selection using AIC.

Texture Measure	All Birds	Forest Birds	Grassland Birds	Shrubland Birds	Neotropical Migrants	Permanent Residents	Short-Distance Migrants
Mean_21x21_B2_Mean	A E	A E	L P	A	A E P	A E	
Mean_21x21_B4_Mean	L	A L	A	A E	L	A L E	E
Mean_5x5_B1_SD		E		A	E	A	L
Mean_5x5_B4_SD			A E	L P	E P	A E P	E P
Mean_5x5_B7_SD	L P	P	A E P	A L E	P	A E P	A L
Mean_21x21_B1_SD	A	A			A E	P	
Mean_21x21_B4_SD	A E	A E	A L E	P	A E P	A L E P	A
Mean_21x21_B7_SD	L	A L	A L E P	A L E P	L	A E	A L P
SD_5x5_B1_SD	A L E	A E	E P		A E P	L	
SD_5x5_B4_SD	L E	L	A E	E P	L E P	A E P	
SD_5x5_B5_SD	A		A L E	E	A	A E P	A
ASM_5x5_B2_SD				P	P		E P
Corr_5x5_B3_Mean	A	A	A P	E P	A	A P	
Corr_5x5_B4_Mean	L		L E	A L E P	L	A E P	L
Corr_5x5_B5_Mean	L E P	P	A P	L P	L	E P	L
Corr_5x5_B2_SD	A E P	A E P	L	A E P	A E P	A E P	A E P
Corr_5x5_B5_SD	A E	A E	E	A E	E	A E	A E
Homog_5x5_B4_Mean	L	L E	L P	L	L E	A L	A L P
Homog_5x5_B5_Mean	A P	A E P	A	A P	A	P	A
Homog_5x5_B2_SD	L	L		A L E P	L P	L E	L P
Homog_5x5_B4_SD	E		P				P
SSVar_5x5_B3_Mean			E	L E P	A E	A P	L E P
Model Adjusted R^2	0.29(A) 0.23(L) 0.29(E) 0.19(P)	0.42(A) 0.25(L) 0.45(E) 0.29(P)	0.26(A) 0.41(L) 0.37(E) 0.20(P)	0.28(A) 0.25(L) 0.33(E) 0.32(P)	0.35(A) 0.20(L) 0.24(E) 0.15(P)	0.40(A) 0.16(L) 0.46(E) 0.51(P)	0.07(A) 0.19(L) 0.12(E) 0.24(P)
Number of Variables / Degrees of Freedom	9/576(A) 9/103(L) 8/303(E) 4/156(P)	10/575(A) 5/107(L) 8/303(E) 4/156(P)	10/575(A) 7/105(L) 10/301(E) 8/152(P)	10/575(A) 8/104(L) 11/300(E) 12/148(P)	9/576(A) 7/105(L) 11/300(E) 9/151(P)	16/569(A) 5/107(L) 13/298(E) 12/148(P)	8/577(A) 8/104(L) 6/305(E) 8/152(P)

A = all three ecoregions together, L = Laurentian Mixed Forest, E = Eastern Broadleaf Forest (Continental), P = Prairie Parkland (Temperate)

Table 2-5. Adjusted R2 and Akaike's information criterion (AIC) values of best models of avian species richness by guild for the models that used texture variables only, NLCD-derived landscape composition metrics only, and a combination of both for the entire study area. Bolded R2 and AIC values indicate the superior (texture-only or landscape metric-only) model.

	Texture-*Only* Models			Landscape Metric-*Only* Models			Texture *and* Landscape Metric Models				
Guild	Adj. R^2	AIC	# of Vars	Adj. R^2	AIC	# of Vars	Adj. R^2	AIC	# of Vars	Abs. R^2 Gain	Rel. R^2 Gain
All Birds	0.29	2844.1	9	**0.41**	**2738.0**	6	0.45	2710.2	21	0.039	9%
Forest Birds	0.42	2683.3	10	**0.51**	**2579.7**	7	0.55	2536.5	18	0.042	8%
Grassland Birds	0.26	1018.1	10	**0.31**	**971.1**	8	0.39	910.4	20	0.078	25%
Shrubland Birds	0.28	1001.2	10	**0.31**	**974.0**	3	0.39	913.7	19	0.077	25%
Neotropical Migrants	0.35	2426.8	9	**0.46**	**2324.9**	7	0.48	2311.2	24	0.025	6%
Permanent Residents	**0.40**	**1113.3**	16	0.35	1158.9	8	0.46	1058.6	18	0.055	14%
Short-Distance Migrants	0.07	1302.9	8	**0.17**	**1241.6**	4	0.23	1203.3	20	0.070	42%
Average	0.30	1770.0	10.3	0.36	1712.6	6.1	0.42	1663.4	20	0.055	15%

Table 2-6. Adjusted R2 and Akaike's information criterion (AIC) values of best models of avian species richness by guild for the models that used texture variables only, NLCD-derived landscape metrics only, and a combination of both for the Laurentian Mixed Forest. Bolded R2 and AIC values indicate the superior (texture-only or landscape metric-only) model.

	Texture-*Only* Models			Landscape Metric-*Only* Models			Texture *and* Landscape Metric Models				
Guild	Adj. R^2	AIC	# of Vars	Adj. R^2	AIC	# of Vars	Adj. R^2	AIC	# of Vars	Abs. R^2 Gain	Rel. R^2 Gain
All Birds	**0.23**	**586.7**	9	0.15	592.1	3	0.31	576.4	11	0.078	35%
Forest Birds	**0.25**	**548.8**	5	0.21	555.1	5	0.36	536.3	11	0.110	43%
Grassland Birds	**0.41**	**223.9**	7	0.38	227.9	5	0.53	208.9	21	0.125	31%
Shrubland Birds	**0.24**	**234.3**	8	0.15	242.5	4	0.35	220.7	14	0.118	50%
Neotropical Migrants	**0.20**	490.8	7	0.18	**490.7**	4	0.31	480.6	14	0.107	53%
Permanent Residents	**0.16**	**244.2**	5	0.07	253.6	3	0.17	244.0	6	0.008	5%
Short-Distance Migrants	**0.19**	**328.3**	8	0.11	333.7	3	0.25	322.7	11	0.057	30%
Average	0.24	379.6	7	0.18	385.1	3.9	0.33	369.9	12.6	0.086	36%

Table 2-7. Adjusted R2 and Akaike's information criterion (AIC) values of best models of avian species richness by guild for the models that used texture variables only, NLCD-derived landscape metrics only, and a combination of both for the Eastern Broadleaf Forest (Continental). Bolded R2 and AIC values indicate the superior (texture-only or landscape metric-only) model.

	Texture-*Only* Models			Landscape Metric-*Only* Models			Texture *and* Landscape Metric Models				
Guild	Adj. R^2	AIC	# of Vars	Adj. R^2	AIC	# of Vars	Adj. R^2	AIC	# of Vars	Abs. R^2 Gain	Rel. R^2 Gain
All Birds	0.29	1383.4	8	**0.32**	**1368.3**	6	0.37	1351.7	13	0.049	15%
Forest Birds	0.45	1311.9	8	**0.47**	**1296.1**	7	0.53	1265.6	15	0.061	13%
Grassland Birds	0.37	482.0	10	**0.40**	**465.0**	9	0.49	421.1	14	0.086	21%
Shrubland Birds	0.33	450.4	11	**0.39**	**423.3**	10	0.48	383.2	21	0.092	24%
Neotropical Migrants	0.24	1206.4	11	**0.28**	**1185.2**	5	0.32	1174.6	12	0.039	14%
Permanent Residents	0.46	474.0	13	**0.46**	**468.0**	8	0.54	434.2	20	0.072	16%
Short-Distance Migrants	0.12	578.7	6	**0.19**	**557.0**	8	0.25	539.9	15	0.060	32%
Average	0.32	841.0	9.6	0.36	823.27	7.6	0.42	795.8	15.7	0.066	18%

Table 2-8. Adjusted R2 and Akaike's information criterion (AIC) values of best models of avian species richness by guild for the models that used texture variables only, NLCD-derived landscape metrics only, and a combination of both for the Prairie Parkland (Temperate). Bolded R2 and AIC values indicate the superior (texture-only or landscape metric-only) model.

	Texture-*Only* Models			Landscape Metric-*Only* Models			Texture *and* Landscape Metric Models				
Guild	Adj. R^2	AIC	# of Vars	Adj. R^2	AIC	# of Vars	Adj. R^2	AIC	# of Vars	Absolute R^2 Gain	Percent R^2 Gain
All Birds	0.19	728.8	4	**0.24**	**719.0**	6	0.27	715.4	9	0.030	12%
Forest Birds	0.29	688.9	4	**0.36**	**675.5**	7	0.40	673.4	17	0.044	12%
Grassland Birds	0.20	200.8	8	**0.28**	**184.1**	8	0.30	186.3	15	0.019	7%
Shrubland Birds	**0.32**	**255.9**	12	0.28	256.4	3	0.36	247.2	13	0.039	12%
Neotropical Migrants	0.15	603.9	9	**0.23**	**585.6**	7	0.27	584.3	14	0.036	16%
Permanent Residents	0.51	316.9	12	**0.56**	**296.3**	8	0.59	286.0	9	0.030	5%
Short-Distance Migrants	**0.24**	**254.7**	8	0.19	262.0	4	0.29	244.4	8	0.047	20%
Average	0.27	435.7	8.1	0.31	425.5	6.1	0.35	419.6	12.1	0.035	11%

Figures

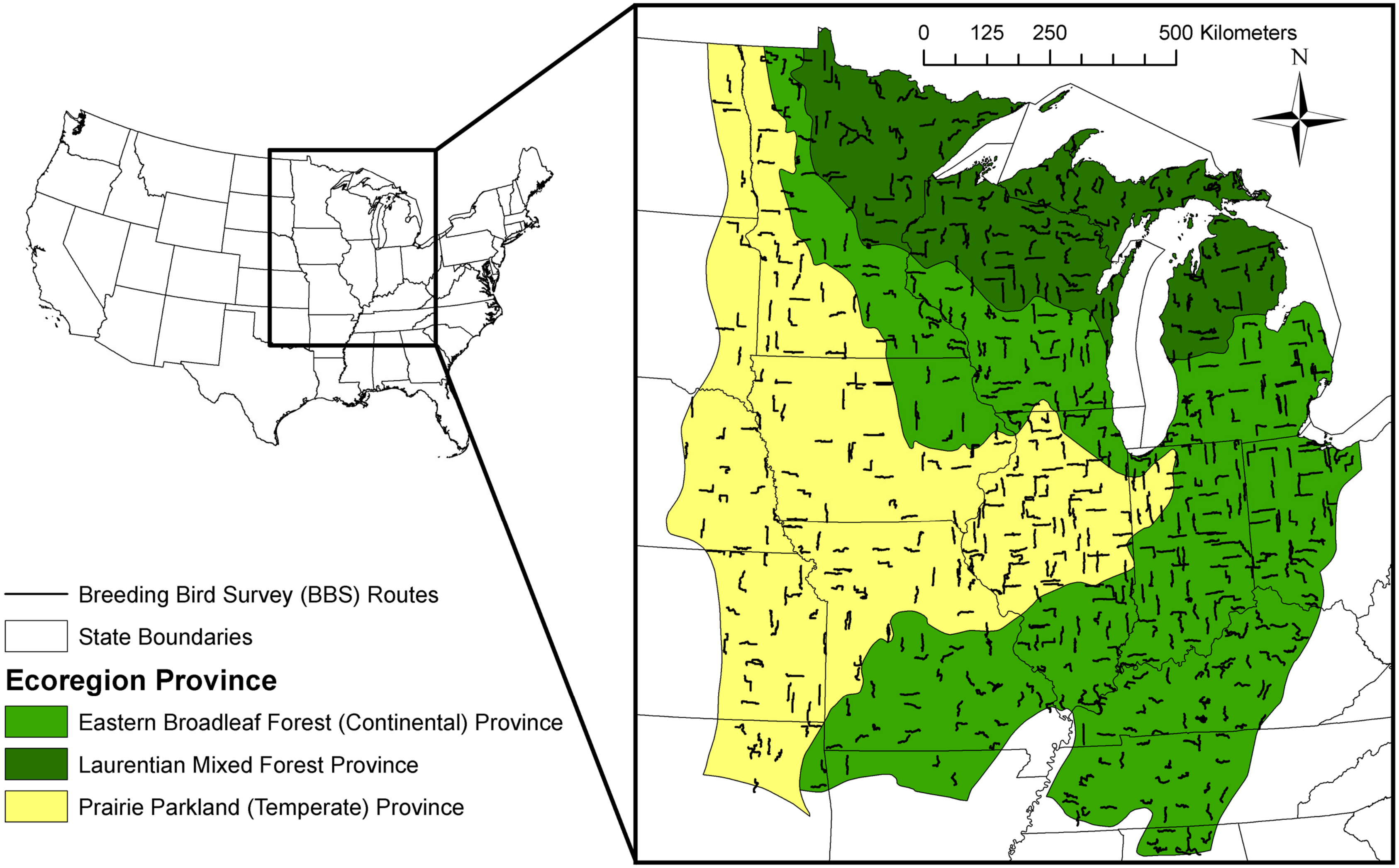
0
125
250
500 Kilometers
N
Breeding Bird Survey (BBS) Routes
State Boundaries
Ecoregion Province
Eastern Broadleaf Forest (Continental) Province
Laurentian Mixed Forest Province
Prairie Parkland (Temperate) Province

Figure 2-1. Study area, including ecoregion boundaries and Breeding Bird Survey (BBS) routes.

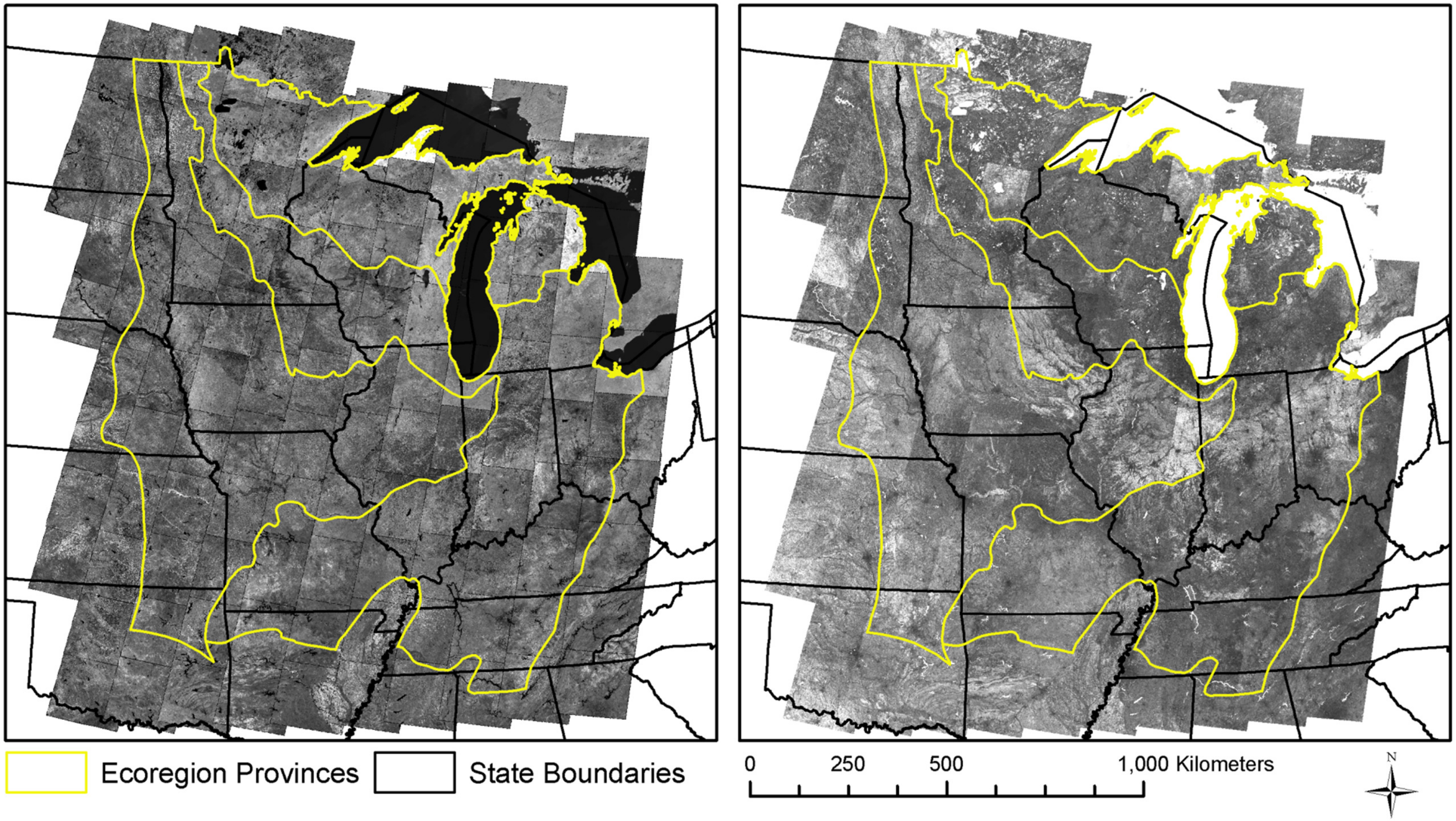

Figure 2-2. (A) Landsat (band 4) data for the study area. (B) Second-Order Homogeneity of band 4.

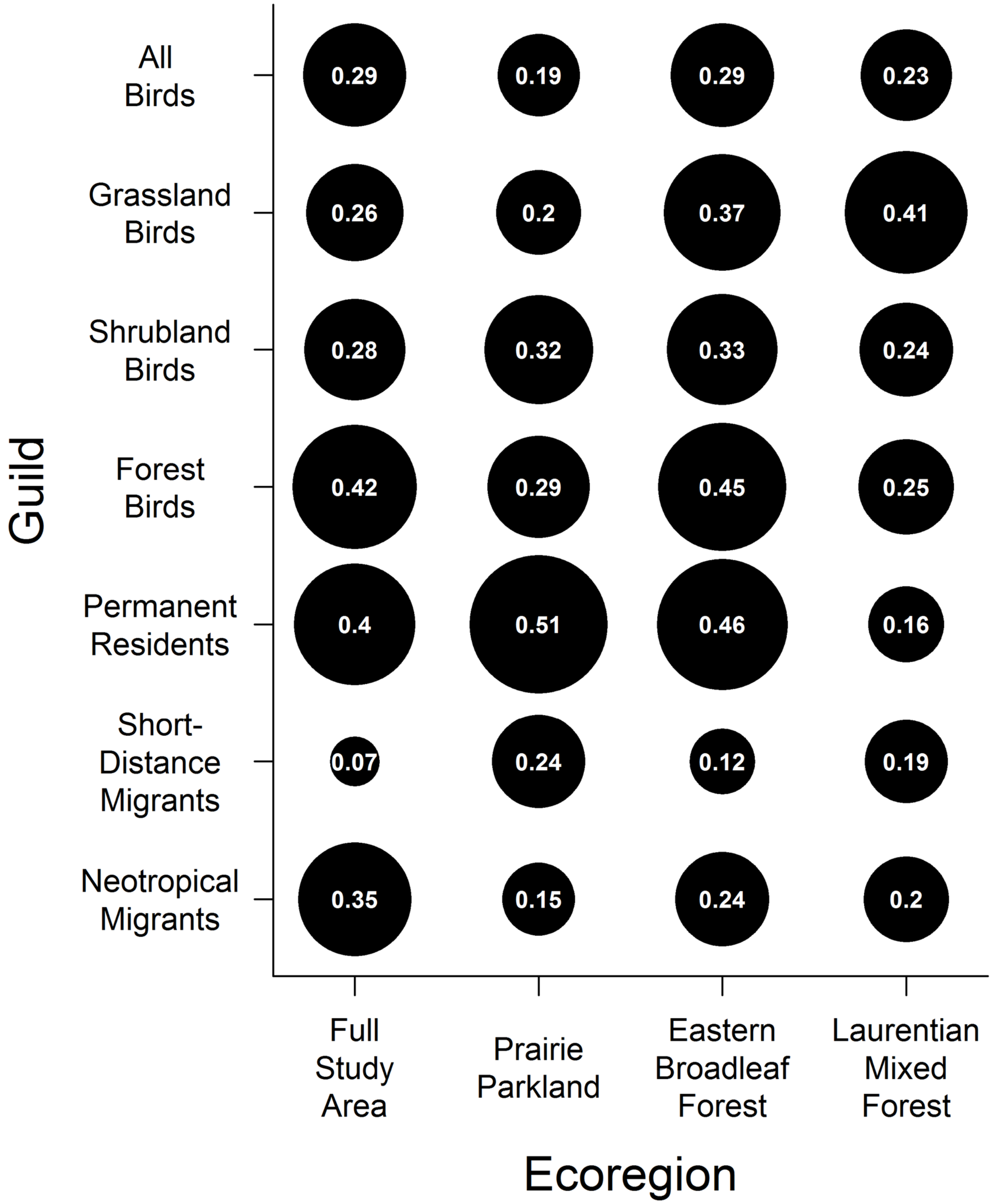

Figure 2-3. Adjusted R^2 values of best multivariate models of avian species richness based on measures of image texture for each avian guild and ecoregion. Circle diameter is proportional to adjusted R^2 value.

Chapter 3

The Influence of Vertical and Horizontal Habitat Structure on Nationwide Patterns of Avian Biodiversity

Abstract

Avian biodiversity is under threat, primarily from human influences. With limited resources for habitat conservation, the accurate identification of high-value bird habitat is crucial. One major factor known to influence avian biodiversity is habitat structure, though this is generally difficult to quantify over broad extents. Our goal was to identify which measures of vertical and horizontal habitat structure are most strongly related to patterns of avian biodiversity across the conterminous United States and to determine whether horizontal and vertical measures are complementary or redundant. We evaluated the performance of metrics derived from the National Biomass and Carbon Dataset (NBCD), as measures of vertical habitat structure, and metrics derived from the 2001 National Land Cover Database (NLCD), as measures of horizontal habitat structure. We calculated estimated vegetation height and biomass from the NBCD as well as landcover composition and configuration metrics for different NLCD classes for 2,546 North American Breeding Bird Survey routes across the conterminous US. Avian species richness was calculated for each route for all birds as well as for three migratory guilds and three habitat guilds. Analyses were carried out nationwide, as well as individually for three ecoregion provinces of varying dominant vegetation type. Measures derived from both the

NBCD and NLCD were significantly related to avian species richness. For forest bird and grassland bird species richness, NBCD mean canopy height yielded R^2 values of 0.55 and 0.22 respectively. The combination of both horizontal and vertical habitat structure measures was most powerful, and nationwide multivariate models of forest and grassland bird species richness yielded adjusted R^2 values of 0.70 and 0.48 respectively. Models developed at the scale of single ecoregion provinces had slightly weaker performance but still showed strong relationships between species richness and measures of both vertical and horizontal structure. This suggests that measures derived from canopy height estimates and land cover classifications are useful methods for characterizing habitat structure. New measures of vertical structure proved complementary to measures of horizontal structure. These data thus allow the efficient prediction of avian diversity with fine spatial resolution, advancing the identification of biodiversity hotspots, and thus contributing to better land management and bird conservation.

Introduction

Avian biodiversity is under severe threat from human-caused habitat loss and fragmentation (Gaston et al. 2003). With limited resources for habitat conservation, the accurate identification of high-value bird habitat is crucial (Turner et al. 2003). While some broad-extent mapping of biodiversity has been carried out (Myers et al. 2000, Buckton and Ormerod 2002), the spatial resolution of these maps is too coarse to be of direct relevance for resource managers. Therefore, spatially detailed maps of avian species richness are needed for land management and biogeography alike. However, surveying avian species richness exhaustively is not feasible, and it is not clear which variables can predict avian species richness best.

Habitat structure has long been recognized as a major factor influencing biodiversity (MacArthur and MacArthur 1961, MacArthur et al. 1966, Willson 1974, Wiens 1974, Tews et al. 2004, Clawges et al. 2008). However, studies relating biodiversity patterns to habitat structure have focused primarily on local scales. When considering the influence of habitat structure on avian biodiversity, it is useful to consider both vertical and horizontal structure. Vertical habitat (or vegetation) structure is defined as the bottom to top configuration of aboveground vegetation at a given site (Brokaw and Lent 1999). We define horizontal habitat structure as the composition and configuration of a landscape with regard to land cover class (Turner et al. 2001). Due to the logistical challenges of assessing vertical habitat structure (Gottschalk et al. 2005), broad-extent measurements have been non-existent thus far (Bergen et al. 2009).

Vertical habitat structure exhibits a strong relationship with avian species richness. Vertical structure directly affects birds through its effect on perching, nesting, and foraging sites (Brokaw and Lent 1999), and areas with higher vertical structure thus provide more niches. Avian species richness is positively correlated with foliage height diversity (MacArthur and MacArthur 1961, MacArthur et al. 1966, Erdelen 1984, Erdelen 1984) as well as canopy height (Goetz et al. 2007).

Horizontal habitat structure strongly affects biodiversity at broad scale. Landscape metrics derived from land-cover classifications that are particularly strong predictors capture, for example, habitat fragmentation (Donovan and Flather 2002), proportion of vegetation class (Farina 1997), landscape heterogeneity (Atauri and de Lucio 2001), and habitat isolation (Krauss et al. 2003). In general, there is a positive relationship between high horizontal habitat structure (generally defined as habitat heterogeneity) and biodiversity (Tews et al. 2004). However, the relationship varies among species groups, as different groups vary in the threshold at which the positive aspects of increased structure (or heterogeneity) are replaced by the negative aspects of fragmentation (Tews et al. 2004).

Vertical habitat structure measurements have traditionally been limited to local scales because fine-scale field measurements are prohibitively costly and time-consuming to acquire (Clawges et al. 2008). The use of LiDAR (light detection and ranging) has greatly improved the ability to measure vertical habitat structure at the landscape scale (Bergen et al. 2009, Hyde et al. 2006) including direct application to avian biodiversity (Clawges et al. 2008, Goetz et al. 2007, Seavy et al. 2009, Lesak et al. 2011). Unfortunately there are currently no LiDAR datasets with wall-to-wall national coverage, so the use of LiDAR is not feasible for national-scale projects. However, a recently released data set has the potential to capture high-resolution vertical vegetation structure at the national scale. The National Biomass and Carbon Dataset 2000 (NBCD 2000), derived from multiple datasets including the Shuttle Radar Topography Mission, provides high resolution (30-m) nationwide estimates of basal area-weighted canopy height and aboveground live dry biomass (Kellndorfer et al. 2004a, Kellndorfer et al. 2006, Walker et al. 2007, Kellndorfer et al. 2011). The NBCD appears very promising; however the ability of this dataset to characterize ecologically meaningful vertical habitat structure has not yet been tested.

Our overall goal was to evaluate the relationship of avian species richness with vertical and horizontal habitat structure for different habitat- and migratory habit-based guilds for the conterminous United States as a whole, as well as for three individual ecoregion provinces. A key focus was the effectiveness of the NBCD in characterizing vertical habitat structure in a manner sufficient to explain avian species richness patterns, and subsequently, to investigate whether measures of vertical and horizontal structure are complementary in this regard. We made several predictions regarding the relationship among our explanatory variables and avian species richness by guild (Table 3-1). We expected a positive relationship between overall bird diversity and (1) vegetation height, (2) vegetation height variability, (3) biomass, and (4) biomass variability, as an increase in these measures indicates an increase in the number of potential habitat niches. For the three habitat-based guilds, (5, 6, and 7) we anticipated that the abundance of that habitat should be the strongest explanatory variable. In terms of other measures of horizontal structure, we expected that (8) higher levels of landscape diversity would lead to higher species richness. Lastly we expected that (9) measures of vertical habitat structure from the NBCD would capture new information that was not already present in the measures of horizontal structure, and that multivariate models combining measures of both horizontal and vertical structure would exhibit the highest explanatory power.

Methods

Our study included the entire contiguous United States. Avian species richness was calculated from the North American Breeding Bird Survey (BBS), an annual survey of approximately 3,000 routes across the U.S. (Figure 3-1). Along each 39.4-km route, 50 3-minute point counts are conducted, and all birds heard or seen are recorded (USGS Patuxent Wildlife Research Center 2008). Analysis was centered on the year 2000, and we calculated the mean species richness of each BBS route over the period 1998-2002. The BBS data set was preprocessed to remove observations collected by first year observers (Kendall et al. 1996) and those conducted in suboptimal weather. We also excluded poorly sampled species, which we defined as species with fewer than 30 route-year observations during the entire history of the BBS. After the removal of these routes as well as routes for which we did not have a full set of explanatory variables, we retained 2,546 routes.

We expected that relationships between species richness and habitat structure would differ among different functional guilds. Therefore in addition to overall species richness, we calculated species richness within three guilds, organized by their migratory strategy: permanent residents, short-distance migrants (i.e., those that spend the non-breeding season in the southern U.S.), and Neotropical migrants. We also calculated species richness of avian guilds organized by the structural form of habitat they require or are associated with: forest, shrubland, and grassland.

Because bird species are not uniformly detectable, the number of species identified on a route is almost certainly less than the actual number of species present. For this reason it is recommended that a correction be applied to raw species richness counts (Kéry and Schmid 2004). In studies of avian species richness, the software program COMDYN (Hines et al. 1999) is frequently used to correct for this problem and derive estimated species richness (Boulinier et al. 1998, Hamer et al. 2006). COMDYN considers the raw BBS route species richness data from a capture-recapture model perspective and uses a jackknife estimator to calculate estimated species richness (Nichols et al. 1998, Nichols et al. 1998). We used estimated species richness as calculated by COMDYN for all species, and for the six guilds mentioned above, as our measures of biodiversity for each route.

In order to relate our explanatory variables to individual BBS routes, we created 19.7 km-radius (one-half the length of a BBS route) circular buffers around the centroid of each BBS route (Flather and Sauer 1996). This radius was chosen because it encompasses the entire BBS route, regardless of route path, and we chose a circular buffer because it provides a uniform area and shape around each BBS route. This distance is also comparable to the median maximum natal dispersal distance (31 km) of 76 avian species for which it has been observed (Sutherland et al. 2000), indicating that the buffer captures a biologically relevant area. This approach has been used successfully in several studies using BBS data (Flather and Sauer 1996, Rittenhouse et al. 2010, Rowhani et al. 2008, Pidgeon et al. 2007).

To characterize vertical habitat structure, we derived measures of vegetation canopy height (Figure 3-2) and aboveground live dry biomass from the 30-m resolution NBCD2000. These measures are based on an empirical modeling approach combining data from the USDA Forest Inventory and Analysis (FIA), the National Elevation Dataset, the 2000 Shuttle Radar Topography Mission, and the USGS National Land Cover Dataset 2001 (NLCD) (Kellndorfer et al. 2006, Walker et al. 2007, Kellndorfer et al. 2011, Kellndorfer et al. 2004b) . The NBCD 2000 estimates of canopy height and biomass provided a unique opportunity to estimate the relative importance of horizontal versus vertical vegetation structure on avian species richness patterns at a national scale. From this dataset we calculated mean, standard deviation, and coefficient of variation of both basal area-weighted canopy height and aboveground live dry biomass (using the NBCD's FIA-derived biomass model) for each BBS route buffer, yielding six variables in all.

Analysis of horizontal habitat structure included landscape metrics calculated from the 2001 National Land-Cover Database (NLCD) (Homer et al. 2004). We used measures of both land-cover composition and configuration. Within each BBS route buffer, we calculated the proportion of landscape for 12 land-cover classes: water (NLCD 2001 class 11), developed (21, 22, 23, and 24), barren (31), deciduous forest (41), evergreen forest (42), mixed forest (43), shrub-scrub (52), grassland (71), pasture (81), cultivated crops (82), woody wetland (90), and herbaceous wetland (95). Additionally, we calculated the total number of land cover classes present and the Shannon diversity index (Shannon 1948) of land cover class distribution for each buffer.

To quantify landscape configuration, we used morphological spatial pattern analysis (MSPA) (Vogt et al. 2009, Vogt et al. 2007, Vogt et al. 2007). MSPA can be used to classify habitat pixels, based on their context, into ecologically relevant classes. We used the software program GUIDOS and applied it to the 2001 NLCD. The software program GUIDOS (Graphical User Interface for the Description of image Objects and their Shapes) (Vogt 2010) uses MSPA to perform a pixel-wise classification on binary habitat/non-habitat raster images, assigning each pixel to a context-based class. The resulting classes are core, islet, loop, bridge, perforation, edge, and branch (Soille and Vogt 2009).

We calculated context-based classes for three habitat types: forest, shrubland, and grassland. The forest habitat images included all pixels classified as deciduous forest (NLCD 2001 class 41), evergreen forest (42), or mixed forest (43). Shrubland habitat images included only pixels classified as shrub/scrub (52). Grassland habitat images included pixels classified as grassland/herbaceous (71) or pasture/hay (81). We ran GUIDOS with an 8-neighbor window, and edge distances of 60, 60, and 120 m for grassland, shrubland, and forest, respectively. To limit the number of explanatory variables, we grouped the GUIDOS results into two classes: core habitat (consisting of the core habitat class) and edge habitat (consisting of islet, loop, bridge, perforation, edge, and branch). For each BBS route buffer, we calculated the total area of forest core, forest edge, grassland core, grassland edge, shrubland core, and shrubland edge.

In addition to our nationwide analysis, we modeled avian species richness using the same variables and procedures for three ecoregion provinces: Central Appalachian Broadleaf Forest—Coniferous Forest—Meadow (province M221), Eastern Broadleaf Forest (Continental) (province 222), and Great Plains-Palouse Dry Steppe (province 331) (Bailey 1995)). The Central Appalachian Broadleaf forest is composed of open, low mountains and valleys with mixed pine-oak forest, Appalachian oak forest, northeastern hardwood forest, and spruce-fir forest and meadows, following a gradient of low elevation to high elevation. The Eastern Broadleaf Forest Province is dominated by relatively flat, rolling hills covered with broadleaf deciduous forest. The Great Plains-Palouse Dry Steppe is defined by rolling plains in the rain-shadow of the Cascade and Rocky Mountains with predominantly steppe vegetation. These provinces are well sampled by the BBS, and our analysis included 130 routes in the Central Appalachian Broadleaf Forest, 326 routes in the Eastern Broadleaf Forest, and 156 in the Great Plains. We selected these provinces to provide a gradient in land cover type from mostly forested (Central Appalachian Broadleaf forest) to agriculture with forest (Eastern Broadleaf Forest) to grassland with agriculture (Great Plains). Within the BBS route buffers, the Central Appalachian Broadleaf forest has 66% forest and 22% agriculture, the Eastern Broadleaf Forest has only 29% forest, though 52% agriculture, and the Great Plains has 7% forest, 26% agriculture, 52% grassland, and 10% shrubland.

Statistical analysis

We carried out our statistical analysis four separate times, once for the entire data set, and once for each of the three ecoregion provinces. Our input data consisted of 14 land-cover composition variables, six vertical habitat structure variables, and six land-cover configuration variables, for a total of 26 explanatory variables. As an initial step, a univariate model was created for species richness of each avian guild as a function of each explanatory variable, to identify those variables with very low explanatory power. A scatter plot of each model was inspected for evidence of non-linear relationships. Only variables that yielded an R^2 value > 0.05 for at least one avian guild were retained for further analysis.

Because several of the variables measured properties that were potentially correlated, and most statistical analyses require independence between variables, we investigated potential collinearity. The correlation coefficient was calculated for each pair of explanatory variables. Correlations greater than 0.8 were investigated, and one variable of each correlated pair was dropped from further analysis. Drop decisions were made based on variable performance in the univariate models in an attempt to arrive at the most parsimonious pool of explanatory variables.

The explanatory power of the remaining variables was evaluated using best-subsets regression (Miller 1990) and hierarchical partitioning (Chevan and Sutherland 1991). Best-subsets regression uses an exhaustive approach to find the best models (in this case based on adjusted R^2 value) with a specified number of explanatory variables. We used the LEAPS package (Lumley and Miller 2009) in R (Lumley and Miller 2009, R Development Core Team 2009) to carry out best-subsets selection to calculate the top 10 and top 20 models for each guild with one, two, three, four, and five explanatory variables. We then calculated how many times each explanatory variable had appeared in one of the top 10 and top 20 models.

While best-subsets regression gives a good idea of the explanatory power of individual variables, especially when there is a large pool of explanatory variables, the analysis parameters that are used, such as the number of top models considered and the number of variables per model, can affect the outcome, and within a given model there is no ranking of variable explanatory contribution. For these reasons, we relied more heavily on hierarchical partitioning because it yields a more objective measure of the contribution of each variable.

Hierarchical partitioning measures the relative explanatory contribution of each variable in the context of others (Chevan and Sutherland 1991). Like best-subsets, hierarchical partitioning is an exhaustive approach. For each explanatory variable, two linear models are created for every combination of the remaining variables, one model including the variable of interest, and one excluding it. The difference in a fitness parameter (adjusted R^2 in our case) is calculated for the models with and without the variable of interest, and reported as that variable's independent contribution to the model. We performed hierarchical partitioning with the *hier.part* function (Walsh and Mac Nally 2008) in R (R Development Core Team 2009). Due to computational constraints, this function limits the maximum number of explanatory variables to 12. We were therefore unable to include all of our explanatory variables, so we dropped the variables that ranked beyond 12th place in the best-subsets regression. In addition, there is a known rounding error in the *hier.part* routine which can significantly influence the results when more than 9 explanatory variables are included (Olea et al. 2010). The error is affected by the ordering of the explanatory variables, so to account for this behavior when we used more than nine explanatory variables, we ran the routine 1000 times, randomly permuting the order of our explanatory variables each time.

Results

Nationwide Analysis

We fit univariate models for each combination of species richness of the 7 avian guilds and the 26 explanatory variables, yielding 182 models (Table 3-2). The variables mean biomass, and standard deviation of biomass showed some evidence of non-linearity in their relationship to avian species richness, so these variables were log-transformed. Variables with the strongest relationships to avian species richness were: mean canopy height, standard deviation of canopy height, mean biomass, and forest edge area (all with R^2 values > 0.50 for at least one guild); proportion deciduous forest, standard deviation of biomass, and forest core area (all with R^2 values > 0.25 for at least one guild); and proportion evergreen forest, proportion scrub-shrub, proportion grassland, proportion cultivated crops, number of land cover classes, Shannon diversity of land cover classes, shrubland core area, and grassland core area (all with R^2 values > 0.15 for at least one guild). Among these variables, the directions of the relationships were as expected (e.g. forest birds were positively associated with canopy height and variability, while grassland birds were negatively associated with both).

Of the 26 explanatory variables, four failed to meet our criterion of $R^2 > 0.05$ for at least one guild, and were thus dropped from subsequent analysis (Table 3-3). Collinearity among the predictor variables in our dataset was rare, with only seven of 231 variable pair combinations exceeding our predefined threshold of $|r| > 0.8$. To remove the collinearity, five variables were excluded from subsequent analysis (Table 3-3).

Best-subsets regression was carried out with the 17 remaining explanatory variables. The rankings of the most frequently included variables was similar in our analyses of the top 10 models and the top 20 models, with only a few variables switching position with an adjacent variable in the ordered ranking, and two variables changing rank by two places (results not shown). Therefore, for simplicity, we show here only the results from the top 10 models (Table 304).

Standard deviation and mean of canopy height were the most frequently included variables, each appearing in at least half of the top 10 models of species richness for three guilds. The third most common variable overall was proportion of deciduous forest, which was common in models of species richness for all guilds except grassland birds, permanent residents, and short-distance migrants. The remaining common variables were included less often across the board, but appeared frequently in models of specific guilds: e.g., grassland core area was frequently included in grassland bird species richness models.

In addition to determining the top-performing variables we were interested in evaluating whether the horizontal and vertical variables contained redundant or complementary information. Of the 17 explanatory variables, we considered three representative of vertical structure (mean canopy height, standard deviation of canopy height, and coefficient of variation of canopy height) and the remaining 14 representative of horizontal structure (**Table 3-4**). For the best-subsets models with two, three, four, and five variables, we examined how many times both a horizontal and vertical variable were included in the model. We observed that 61% (43/70) of the 2-variable models contained both horizontal and vertical variables, as well as 86% (60/70), 99% (69/70), and 97% (68/70) of the three-, four-, and five- variable models, respectively. Because there were 14 horizontal variables and only three vertical variables, if there was equal probability that each variable would be included in the models, one would expect (based on probability) that both horizontal and vertical variables would be present in 31%, 46%, 58%, and 68% of the two-, three-, four-, and five-variable models, respectively. Since the proportion of our models with both horizontal and vertical variables was substantially higher than expected, this lends support to our view that these two types of variables are in fact complementary.

For each model, we derived the relative independent contribution of each variable to that model's total adjusted R^2 (Table 3-5). Mean canopy height, standard deviation of canopy height, and forest edge area had independent contribution values that were substantially higher than the values for the remaining variables. Interestingly, these top-three variables include both of the vertical structure variables included in this analysis, suggesting that vertical habitat structure is at least as effective, if not more so, in explaining avian diversity distribution than common measures of horizontal structure.

Individual Ecoregion Province Analysis

Statistical analysis was conducted individually for the Eastern Broadleaf Forest (EBF), Central Appalachian Broadleaf Forest (CABF), and Great Plains – Palouse Dry Steppe (GP).

Based on univariate linear models of avian species richness (Table 3-3), variables with high maximum univariate R^2 values among guilds included proportion deciduous forest (0.40), forest edge area (0.39), and mean canopy height (0.39) in the EBF; mean canopy height (0.24), mean biomass (0.23), and standard deviation of biomass (0.22) in the CABF, and standard deviation of canopy height (0.53), standard deviation of biomass (0.48), and forest edge area (0.48) in the GP. Some variables failed to meet our criterion of $R^2 > 0.05$ for at least one guild, and thus 10 variables were dropped from EBF, 9 from the CABF, and 2 variables from the GP. To reduce explanatory variable correlation, seven, eight, and eight additional variables were dropped from the EBF, CABF, and GP, respectively, leaving nine, nine, and 16 variables for subsequent analysis.

Best-subsets regression was carried out for each ecoregion province separately with the set of explanatory variables retained for that ecoregion. Results for top-10 and top-20 model best subset analyses were again very similar, so we present only the results from the top 10 models.

In the EBF (**Table 3-6**), mean canopy height, proportion developed, and standard deviation of canopy height were clearly the strongest performing variables, appearing in over half of the models. In the CABF (Table 3-7), proportion developed was the strongest performing variable, appearing in more than half of the models for most guilds. Grassland core area, mean canopy height, and standard deviation of biomass were the next most frequently included variables. In the GP (Table 3-8), results were less uniform among guilds compared to the other two ecoregions. Shannon diversity of land cover class was the strongest overall performer, appearing in 180 models; however, this variable was rarely included in models of forest bird or permanent resident species richness. Standard deviation of canopy height was the next most included variable, appearing in 161 models, however this variable was rarely included in models of shrubland bird or permanent resident species richness.

For the EBF and CABF, only nine variables remained in our explanatory variable pool, so we did not need to drop any remaining variables before performing hierarchical partitioning. For the GP, 16 variables remained. We selected the top 12 variables as ranked from the best subsets regression to reduce the number of variables to within computational limits.

In the EBF (Table 3-9), mean canopy height had the highest total (summed across guilds) independent contribution (191.9) followed by proportion developed and standard deviation of canopy height (155.6 and 141.7, respectively). The remaining variables had substantially lower total independent contribution values (21.5 – 57.9). Adjusted R^2 values for guild species richness as a function of the nine explanatory variables were calculated for all birds ($R^2 = 0.27$), forest birds ($R^2 = 0.47$), grassland birds ($R^2 = 0.42$), shrubland birds ($R^2 = 0.37$), Neotropical migrants ($R^2 = 0.23$), permanent residents ($R^2 = 0.44$), and short-distance migrants ($R^2 = 0.11$) (Figure 3-3).

For the CABF (Table 3-10), proportion developed had the highest total independent contribution across guilds (193.3). Standard deviation of canopy height, grassland core area, and mean canopy height followed at 90.8, 79.4, and 79.2. The remaining variables had a total independent contribution value ranging from 28.7 – 71.8. Adjusted R^2 values for guild species richness as a function of the nine explanatory variables were calculated for all birds ($R^2 = 0.14$), forest birds ($R^2 = 0.16$), grassland birds ($R^2 = 0.29$), shrubland birds ($R^2 = 0.08$), Neotropical migrants ($R^2 = 0.18$), permanent residents ($R^2 = 0.06$), and short-distance migrants ($R^2 = 0.27$) (Figure 3-3).

In the GP (Table 3-11), standard deviation of canopy height had the highest total independent contribution across guilds (118.8). Shannon diversity of land cover classes and mean biomass followed with 81.0 and 75.9, respectively. The remaining variables had total independent contribution values ranging from 36.3 – 61.4. Adjusted R^2 values for guild species richness as a function of the nine explanatory variables were calculated for all birds ($R^2 = 0.48$), forest birds ($R^2 = 0.57$), grassland birds ($R^2 = 0.63$), shrubland birds ($R^2 = 0.40$), Neotropical migrants ($R^2 = 0.44$), permanent residents ($R^2 = 0.46$), and short-distance migrants ($R^2 = 0.27$) (Figure 3-3).

To further illustrate the relative explanatory contribution of vertical versus horizontal measures of habitat structure, for each model we summed the independent contribution of horizontal variables and vertical variables. The difference between these sums was plotted on a number line (Figure 3-4). (When interpreting these plots, it should be noted that the number of vertical versus horizontal habitat structure variables was unbalanced in the models, with two vertical and six horizontal in the national models, three vertical and six horizontal in the EBF and CABF, and 3 vertical and 9 horizontal in the GP.)

Discussion

We showed that vertical habitat structure, represented as measures of canopy height and biomass from the National Biomass and Carbon Dataset, was important in explaining the nationwide and ecoregion province level patterns of overall bird species richness and of the species richness of several avian habitat and migratory guilds. As expected, methods of characterizing horizontal habitat structure, such as proportion of land cover class, also contributed to explanation of species richness patterns. While measures of both vertical and horizontal structure were individually useful in explaining avian species richness patterns, the combination of both types of variables resulted in the highest predictive power as shown by the high proportion of models from the best-subsets regression that included both a horizontal and vertical structure variable. This suggests that our measures of vertical and horizontal habitat structure were complementary rather than redundant, each characterizing different components of habitat structure that explain avian species richness patterns.

Nationwide analysis

We expected that the measures of vertical habitat structure would add information not already present in the measures of horizontal structure (Table 3-1, prediction 9). This was conclusively shown to be true and is perhaps the most significant finding of our study. The univariate models showed that variables related to vertical structure were at least as strongly associated with avian species richness as variables related to horizontal structure. For example, mean canopy height and mean biomass had the strongest relationship with forest bird richness (both had R2 = 0.55). Forest edge area was the only explanatory variable with R2 values similar to measures of canopy height and biomass. For all guilds, the vertical structure measures were as strong as or stronger than horizontal measures.

We expected positive relationships between overall avian species richness and vegetation height, vegetation height variability, biomass, and biomass variability, as increases in these measures usually correspond to an increase in potential habitat niches (Table 3-1, predictions 1-4). Our univariate models did indeed concur with expectations in all of these cases (Table 3-2). The finding of a positive relationship between mean canopy height and forest bird species richness supports previous local-scale LiDAR-based findings (Goetz et al. 2007), however our study expands this result to a national scale.

Although we excluded measures of biomass from the national analysis due to correlation with other variables, mean and standard deviation of biomass were strongly related with avian species richness in the univariate models. This concurs with previous findings that radar-based measures of forest biomass improved bird species habitat modeling over vegetation type alone (Bergen et al. 2007), and we extend this finding beyond habitat mapping to measures of biodiversity.

In addition to increasing the number of habitat niches, high canopy height and biomass may influence species richness through increased food availability. Lepidoptera species comprise much of the diet of many bird species, especially migrants. In the mid-Atlantic, deciduous trees such as *Quercus* spp., *Prunus* spp., *Salix* spp., *Betula* spp., and *Populus* spp. support the greatest species diversity of Lepidoptera (Tallamy and Shropshire 2009), and these tree species are common throughout the eastern United States. Food (arthropod) availability has been shown to influence bird distribution (Johnson and Sherry 2001). Since higher canopy height and biomass should equate to higher food availability for Lepidoptera, and availability of Lepidoptera drives higher avian reproductive success (Holmes et al. 1986), high canopy height and biomass should positively influence avian abundance and therefore species richness.

Within habitat-based guilds, we predicted that the proportion of area in the associated habitat type would be the strongest explanatory variable in species richness models (Table 3-1, predictions 5-7). Contrary to our prediction, the hierarchical partitioning analysis revealed that measures of habitat abundance were less effective in explaining variation in species richness than the other habitat structure variables. Surprisingly, in our final variable ranking based on hierarchical partitioning, proportion of deciduous forest was only the fourth strongest predictor of forest bird species richness (after mean canopy height, forest edge area, and standard deviation of canopy height). This indicates that measures of horizontal and vertical structure other than vegetation type are just as important, at least for forest birds. We expected that proportion of a given land cover class would be strongly related to canopy height (e.g. an area of forest should consistently have high canopy height compared to other landcover classes), but the nationwide hierarchical partitioning analysis showed that measures of canopy height and proportion deciduous forest all made independent contributions to explain richness of forest birds. This indicates that while vegetation type is important, canopy height yields additional information that helps explain forest bird species richness.

Though the proportion grassland variable was dropped from analysis prior to hierarchical partitioning, a similar measure, grassland core area, was the third highest ranked variable for explaining grassland bird richness, behind forest edge area and standard deviation of canopy height (both negatively related to grassland bird species richness in univariate models). Similarly, the proportion of shrub-scrub had to be excluded from the hierarchical partitioning, though both shrubland core area and shrubland edge area were included. Both variables contributed relatively little to explaining shrubland bird species richness with shrubland core area ranked seventh and shrubland edge tied for 10th. For shrubland birds, standard deviation of canopy height, mean canopy height, and forest edge area were the strongest predictors, with positive, positive, and negative relationships with shrubland bird richness, respectively. These results emphasize the importance of measures of habitat structure normally associated with forest, which are still strong predictors (positive or negative) even for species not associated with forests.

We predicted that higher levels of landscape diversity (as a measure of landscape heterogeneity) should lead to increased species richness (Atauri and de Lucio 2001) (Table 3-1 prediction 8). While the number of land-cover classes and the Shannon diversity of land-cover classes indeed exhibited positive univariate relationships with species richness of all guilds except grassland birds, these relationships were relatively weak for permanent residents, short-distance migrants, grassland birds, and shrubland birds. These measures were too general, and we found that measures specific to individual land-cover classes were more important than the synthetic variables. However, forest edge area was strongly related to avian species richness overall, reflecting both the fact that edge habitat tends to have higher species richness (Conner and Adkisson 1975, Kunin 1998), and the dominance of the forest guild and shrubland guild (of which some members use forest edge) in overall species richness.

Our all species and Neotropical migrant models compared favorably in explanatory power with other nationwide studies of bird species richness. The adjusted R^2 values of our multivariate models (including all variables considered in the hierarchical partitioning) were 0.46 for all species as a group, 0.70, 0.48, and 0.27 for forest, grassland, and shrubland birds, and 0.50, 0.20, and 0.24 for Neotropical migrants, permanent residents, and short-distance migrants, respectively (Figure 3-3). This is comparable to other studies with similar methodology. Nationwide avian species richness models based on energy availability and variability yielded adjusted R^2 values of 0.43, 0.36, and 0.27 for all species, Neotropical migrants, and permanent residents, respectively (Rowhani et al. 2008). Avian species richness has also been related to measures of housing and population density, land cover type, and traditional landscape indices such as number of patches, mean patch size, and edge density (Pidgeon et al. 2007). Nationwide models including only forested ecoregions resulted in adjusted R^2 values of 0.35, 0.48, 0.16, and 0.19 for forest birds, Neotropical migrants, short-distance migrants, and permanent residents, respectively. Our adjusted R^2 values were slightly higher for the last three guilds, and our adjusted R^2 value for forest birds was twice as big. This is likely because our study was nationwide while Pidgeon et al. (2007) studied only forested ecoregions. Models for forest bird species richness improve when including non-forested areas such as grasslands and deserts, because the dynamic range of species richness is greater than when working only in ecoregions dominated by forest.

Individual Ecoregion Analysis

Our most important prediction, that measures of vertical habitat structure would add new information not already present in horizontal measures (Table 3-1 prediction 9), was strongly supported by the single-province analyses. This was most clearly seen in the hierarchical partitioning analysis. Variables representing both vertical and horizontal habitat structure ranked in the top five for all 3 ecoregions (Table 3-9 through Table 3-11). This is an exciting finding, as it shows that measures of vertical and horizontal vegetation structure remain complementary at the ecoregion scale. It is also notable that our measures of vertical structure from the NBCD showed strong performance at the ecoregion level, even in the GP, which has comparatively low vertical vegetation structure.

Our other predictions received mixed support from the single-ecoregion analyses. Predictions 1-4 (Table 3-1), that relationships between overall species richness and mean canopy height, canopy height variability, biomass, and biomass variability (Table 3-1 predictions 1-4) would be positive and highly significant (Bergen et al. 2009, Goetz et al. 2007), held in the GP and EBF (except biomass, which was non-significant). None of these univariate relationships showed statistical significance in the CABF. For the habitat-based guilds, our predictions that proportion of the preferred habitat type would be the strongest predictor (Table 3-1 predictions 5-7) was refuted by the univariate relationships. Some positive, significant relationships existed (e.g., grassland birds in the GP and forest birds in all three ecoregions), however in none of these cases was the proportion of preferred habitat type the strongest univariate predictor.

Our prediction that higher landscape diversity would lead to increased avian species richness (Atauri and de Lucio 2001) (Table 3-1 prediction 8) was strongly supported by the univariate relationships. Of the 22 of 42 univariate models relating guild species richness to the number of landcover classes or Shannon diversity of landcover classes were statistically significant, with 20 of those showing a positive relationship.

The combination of best subsets selection and hierarchical partitioning worked well. When relating measures of multiple landscape attributes to species abundance, distribution, or species richness, it is highly likely that collinearity will be present among explanatory variables (Mac Nally 2000, Heikkinen et al. 2004). While traditional multivariate analyses, such as stepwise-selection, are useful in producing models, it is difficult (and unwise) to interpret the influence of individual variables within the model. The strength of hierarchical partitioning is the averaging of variable influence over all possible models, which alleviates multicollinearity issues (Mac Nally 2000). Though we removed variables in our analyses to limit correlation, we expected some level of correlation remained in our dataset. Hiearchical partitioning has been successfully used to gauge the influence of different environmental variables in models of invasive exotic plant species richness (Gavier-Pizarro et al. 2010), butterfly distribution (Heikkinen et al. 2005), vascular plant species richness (Marini et al. 2008), and bird abundance (Heikkinen et al. 2004). Since the release of the "hier.part" package for R (Walsh and Mac Nally 2008), the use of hierarchical partitioning in ecological studies has been increasing (Olea et al. 2010). We found hierarchical partitioning to be a useful and effective method for evaluating the relative contribution of different variables in explaining patterns of avian species richness.

Our study showed that measures of vertical structure, as characterized by estimates of biomass and canopy height from NBCD2000 capture information not present in measures of horizontal structure, and thus improve models of avian species richness on a national scale. These findings are especially timely given the cancellation of the NASA DesdynI mission (DESDynI Writing Committee 2007), a LiDAR and radar satellite that was expected to provide detailed measurement of vertical vegetation structure. Such a mission is still of critical importance, however, the NBCD2000 is a useful data source that fills the gap in knowledge by providing data on vegetation structure in the meantime (at least for the United States).

The horizontal and vertical measures of structure proved to be complementary, rather than redundant, in their explanation of species richness patterns. For this reason, we recommend that future studies of broad scale avian biodiversity include measures of both vertical and horizontal structure.

References

Atauri J. A., J. V. de Lucio. 2001. The role of landscape structure in species richness distribution of birds, amphibians, reptiles and lepidopterans in Mediterranean landscapes. Landscape Ecology 16:147-159.

Bailey R. G. 1995. Description of the Ecoregions of the United States. United States Department of Agriculture.

Bergen K. M., A. M. Gilboy, and D. G. Brown. 2007. Multi-dimensional vegetation structure in modeling avian habitat. Ecological Informatics 2:9-22.

Bergen K. M., S. J. Goetz, R. O. Dubayah, G. M. Henebry, C. T. Hunsaker, M. L. Imhoff, R. F. Nelson, G. G. Parker, and V. C. Radeloff. 2009. Remote sensing of vegetation 3-D structure for biodiversity and habitat: Review and implications for lidar and radar spaceborne missions. Journal of Geophysical Research-Biogeosciences 114:G00E06.

Boulinier T., J. D. Nichols, J. E. Hines, J. R. Sauer, C. H. Flather, and K. H. Pollock. 1998. Higher temporal variability of forest breeding bird communities in fragmented landscapes. Proceedings of the National Academy of Sciences of the United States of America 95:7497-7501.

Brokaw N. V., R. A. Lent. 1999. Vertical Structure. Pages 373-373-399 *In* M. L. Hunter, editor. Maintaining Biodiversity in Forest Ecosystems, Cambridge University Press, Cambridge, U.K., 1999.

Buckton S. T., S. J. Ormerod. 2002. Global patterns of diversity among the specialist birds of riverine landscapes. Freshwater Biology 47:695-709.

Chevan A., M. Sutherland. 1991. Hierarchical Partitioning. American Statistician 45:90-96.

Clawges R., K. Vierling, L. Vierling, and E. Rowell. 2008. The use of airborne lidar to assess avian species diversity, density, and occurrence in a pine. Remote Sensing of Environment 112:2064-2073.

Conner R. N., C. S. Adkisson. 1975. Effects of Clearcutting on Diversity of Breeding Birds. Journal of Forestry 73:781-785.

DESDynI Writing Committee. Report of the July 17-19, 2007 Orlando, Florida Workshop to Assess the National Research Council Decadal Survey Rocommendation for the DESDynI Radar/Lidar Space Mission. National Aeronautics and Space Administration, Earth Sciences Division; July 17-19, 2007.

Donovan T. M., C. H. Flather. 2002. Relationships among north American songbird trends, habitat fragmentation, and landscape occupancy. Ecological Applications 12:364-374.

Erdelen M. 1984. Bird communities and vegetation structure. 1. Correlations and comparisons of simple and diversity indexes. Oecologia 61:277-284.

Farina A. 1997. Landscape structure and breeding bird distribution in a sub-Mediterranean agro-ecosystem. Landscape Ecology 12:365-378.

Flather C. H., J. R. Sauer. 1996. Using landscape ecology to test hypotheses about large-scale abundance patterns in migratory birds. Ecology 77:28-35.

Gaston K. J., T. M. Blackburn, and K. K. Goldewijk. 2003. Habitat conversion and global avian biodiversity loss. Proceedings of the Royal Society B: Biological Sciences 270:1293-1300.

Gavier-Pizarro G., V. C. Radeloff, S. I. Stewart, C. D. Huebner, and N. S. Keuler. 2010. Housing is positively associated with invasive exotic plant species richness in New England, USA. Ecological Applications 20:1913-1925.

Goetz S., D. Steinberg, R. Dubayah, and B. Blair. 2007. Laser remote sensing of canopy habitat heterogeneity as a predictor of bird species richness in an eastern temperate forest, USA. Remote Sensing of Environment 108:254-263.

Gottschalk T. K., F. Huettmann, and M. Ehlers. 2005. Thirty years of analysing and modelling avian habitat relationships using satellite imagery data: a review. International Journal of Remote Sensing 26:2631-2656.

Hamer T. L., C. H. Flather, and B. R. Noon. 2006. Factors associated with grassland bird species richness: The relative roles of grassland area, landscape structure, and prey. Landscape Ecology 21:569-583.

Heikkinen R. K., M. Luoto, M. Kuussaari, and J. Poyry. 2005. New insights into butterfly-environment relationships using partitioning methods. Proceedings of the Royal Society B-Biological Sciences 272:2203-2210.

Heikkinen R. K., M. Luoto, R. Virkkala, and K. Rainio. 2004. Effects of habitat cover, landscape structure and spatial variables on the abundance of birds in an agricultural-forest mosaic. Journal of Applied Ecology 41:824-835.

Hines J. E., T. Boulinier, J. D. Nichols, J. R. Sauer, and K. H. Pollock. 1999. COMDYN: software to study the dynamics of animal communities using a capture-recapture approach. Bird Study 46:209-217.

Holmes R. T., T. W. Sherry, and F. W. Sturges. 1986. Bird Community Dynamics in a Temperate Deciduous Forest - Long-Term Trends at Hubbard Brook. Ecological Monographs 56:201-220.

Homer C., C. Q. Huang, L. M. Yang, B. Wylie, and M. Coan. 2004. Development of a 2001 National Land-Cover Database for the United States. Photogrammetric Engineering and Remote Sensing 70:829-840.

Hyde P., R. Dubayah, W. Walker, J. B. Blair, M. Hofton, and C. Hunsaker. 2006. Mapping forest structure for wildlife habitat analysis using multi-sensor (LiDAR, SAR). Remote Sensing of Environment 102:63-73.

Johnson M., T. Sherry. 2001. Effects of food availability on the distribution of migratory warblers among habitats in Jamaica. Journal of Animal Ecology 70:546-560.

Kellndorfer, J.M., Walker, W.S., LaPointe, E., Hoppus, M., & Westfall, J. 2006. Modeling Height, Biomass, and Carbon in U.S. Forests from FIA, SRTM, and Ancillary National

Scale Data Sets. IEEE International Geoscience and Remote Sensing Symposium 2006. IGARSS'06 (pp. 3591-3594). Denver, Co.

Kellndorfer J., W. Walker, L. LaPoint, J. Bishop, T. Cormier, G. Fiske, and K. Kirsch. 2011. The National Biomass and Carbon Dataset - A hectare-scale dataset of vegetation height, aboveground biomass and carbon stock of the conterminous United States. Data Published by the Woods Hole Research Center. http://whrc.org/nbcd.

Kellndorfer J., W. Walker, L. Pierce, C. Dobson, J. A. Fites, C. Hunsaker, J. Vona, and M. Clutter. 2004a. Vegetation height estimation from shuttle radar topography mission and national elevation datasets. Remote Sensing of Environment 93:339-358.

Kellndorfer J., W. Walker, L. Pierce, C. Dobson, J. Fites, C. Hunsaker, J. Vona, and M. Clutter. 2004b. Vegetation height estimation from shuttle radar topography mission and national elevation datasets. Remote Sensing of Environment 93:339-358.

Kendall W. L., B. G. Peterjohn, and J. R. Sauer. 1996. First-Time Observer Effects in the North American Breeding Bird Survey. The Auk 113:823-829.

Kéry M., H. Schmid. 2004. Monitoring programs need to take into account imperfect species detectability. Basic and Applied Ecology 5:65-73.

Krauss J., I. Steffan-Dewenter, and T. Tscharntke. 2003. How does landscape context contribute to effects of habitat fragmentation on diversity and population density of butterflies? Journal of Biogeography 30:889-900.

Kunin W. E. 1998. Biodiversity at the edge: A test, of the importance of spatial "mass effects" in the Rothamsted Park Grass experiments. Proceedings of the National Academy of Sciences of the United States of America 95:207-212.

Lesak A. A., V. C. Radeloff, T. J. Hawbaker, A. M. Pidgeon, T. Gobakken, and K. Contrucci. 2011. Modeling forest songbird species richness using LiDAR-derived measures of forest structure. Remote Sensing of Environment 115:2823-2835.

Lumley T., L. Miller. 2009. Leaps: Regression Subset Selection. R package version 2.9.

Mac Nally R. 2000. Regression and model-building in conservation biology, biogeography and ecology: The distinction between and reconciliation of 'predictive' and 'explanatory' models. Biodiversity and Conservation 9:655-671.

MacArthur R., H. Recher, and M. Cody. 1966. On the relation between habitat selection and species diversity. The American Naturalist 100:319-332.

MacArthur R. H., J. W. MacArthur. 1961. On bird species diversity. Ecology 42:594-598.

Marini L., F. Prosser, S. Klimek, and R. H. Marrs. 2008. Water-energy, land-cover and heterogeneity drivers of the distribution of plant species richness in a mountain region of the European Alps. Journal of Biogeography 35:1826-1839.

Miller A. J. 1990. Subset Selection in Regression. Chapman and Hall, London.

Myers N., R. A. Mittermeier, C. G. Mittermeier, G. A. B. da Fonseca, and J. Kent. 2000. Biodiversity hotspots for conservation priorities. Nature 403:858.

Nichols J. D., T. Boulinier, J. E. Hines, K. H. Pollock, and J. R. Sauer. 1998. Inference methods for spatial variation in species richness and community composition when not all species are detected. Conservation Biology 12:1390-1398.

Olea P. P., P. Mateo-Tomas, and A. de Frutos. 2010. Estimating and modelling bias of the hierarchical partitioning public-domain software: implications in environmental management and conservation. Plos One 5:e11698.

Pidgeon A. M., V. C. Radeloff, C. H. Flather, C. A. Lepczyk, M. K. Clayton, T. J. Hawbaker, and R. B. Hammer. 2007. Associations of forest bird species richness with housing and landscape patterns across the USA. Ecological Applications 17:1989-2010.

R Development Core Team. 2009. R: A language and environment for statistical computing. :.

Rittenhouse C. D., A. M. Pidgeon, T. P. Albright, P. D. Culbert, M. K. Clayton, C. H. Flather, C. Huang, J. G. Masek, and V. C. Radelof. 2010. Avifauna response to hurricanes: regional changes in community similarity. Global Change Biology 16:905-917.

Rowhani P., C. A. Lepczyk, M. A. Linderman, A. M. Pidgeon, V. C. Radeloff, P. D. Culbert, and E. F. Lambin. 2008. Variability in energy influences avian distribution patterns across the USA. Ecosystems 11:854-867.

Seavy N. E., J. H. Viers, and J. K. Wood. 2009. Riparian bird response to vegetation structure: a multiscale analysis using LiDAR measurements of canopy height. Ecological Applications 19:1848-1857.

Shannon C. E. 1948. A mathematical theory of communication. Bell System Technical Journal 27:379-423 and 623-656.

Soille P., P. Vogt. 2009. Morphological segmentation of binary patterns. Pattern Recognition Letters 30:456-459.

Tallamy D. W., K. J. Shropshire. 2009. Ranking lepidopteran use of native versus introduced plants. Conservation Biology 23:941-947.

Tews J., U. Brose, V. Grimm, K. Tielborger, M. C. Wichmann, M. Schwager, and F. Jeltsch. 2004. Animal species diversity driven by habitat heterogeneity. Journal of Biogeography 31:79-92.

Turner M. G., R. H. Gardner, and R. V. O'Neill. 2001. Landscape ecology in theory and practice. Springer, New York.

Turner W., S. Spector, N. Gardiner, M. Fladeland, E. Sterling, and M. Steininger. 2003. Remote sensing for biodiversity science and conservation. Trends in Ecology & Evolution 18:306-314.

Vogt P. 2010. GUIDOS. 1.3.

Vogt P., K. H. Riitters, C. Estreguil, J. Kozak, and T. G. Wade. 2007. Mapping spatial patterns with morphological image processing. Landscape Ecology 22:171-177.

Vogt P., J. R. Ferrari, T. R. Lookingbill, R. H. Gardner, K. H. Riitters, and K. Ostapowicz. 2009. Mapping functional connectivity. Ecological Indicators 9:64-71.

Vogt P., K. H. Riitters, M. Iwanowski, C. Estreguil, J. Kozak, and P. Soille. 2007. Mapping landscape corridors. Ecological Indicators 7:481-488.

Walker W. S., J. M. Kellndorfer, E. LaPoint, M. Hoppus, and J. Westfall. 2007. An empirical InSAR-optical fusion approach to mapping vegetation canopy height. Remote Sensing of Environment 109:482-499.

Walsh C., R. Mac Nally. 2008. hier.part: Hierarchical Partitioning. R package version 1.0-3.

Wiens J. A. 1974. Habitat heterogeneity and avian community structure in North-American grasslands. American Midland Naturalist 91:195-213.

Willson M. F. 1974. Avian community organization and habitat structure. Ecology 55:1017-1029.

Tables

Table 3-1. Predicted relationships between avian species richness and explanatory variables.

	Guild	**Variable**	**Hypothesized Relationship**
1.	All Birds	Vegetation height	Positive
2.	All Birds	Vegetation height variability	Positive
3.	All Birds	Biomass	Positive
4.	All Birds	Biomass variability	Positive
5.	Grassland birds	Grassland	Positive, strongest univariate relationship
6.	Shrubland birds	Shrubland	Positive, strongest univariate relationship
7.	Forest birds	Forest	Positive, strongest univariate relationship
8.	All Guilds	Landscape diversity	Positive
9.	All Guilds	Vertical and Horizontal measures of habitat structure	Complementary in ability to explain avian species richness

Table 3-2. Univariate R^2 values for nationwide models of avian species richness.

		Habitat Association			Migratory Habit		
	All Species	Forest Birds	Grassland Birds	Shrubland Birds	Neotropical Migrants	Permanent Residents	Short-Distance Migrants
Proportion Water	0.00(+)*	0.01(+)***	0.01(-)***	0.00(-)	0.00(+)**	0.00(-)	0.00(+)
Proportion Developed	0.00(-)*	0.02(-)***	0.02(-)***	0.00(-)***	0.00(-)*	0.01(-)***	0.00(-)*
Proportion Barren	0.05(+)***	0.05(+)***	0.00(-)**	0.01(+)***	0.04(+)***	0.02(+)***	0.03(+)***
Proportion Deciduous Forest	**0.25(+)*****	**0.34(+)*****	0.06(-)***	0.10(+)***	**0.34(+)*****	0.02(+)***	0.05(+)***
Proportion Evergreen Forest	0.03(+)***	0.06(+)***	**0.15(-)*****	0.00(+)	0.01(+)***	0.03(+)***	0.02(+)***
Proportion Mixed Forest	0.08(+)***	0.13(+)***	0.08(-)***	0.00(+)***	0.12(+)***	0.00(+)**	0.01(+)***
Proportion Scrub-Shrub	0.12(-)***	**0.25(-)*****	0.00(+)***	0.00(+)***	**0.16(-)*****	0.00(-)***	0.07(-)***
Proportion Grassland	0.09(-)***	**0.16(-)*****	**0.20(+)**	0.09(-)	0.09(-)***	0.05(-)	0.03(-)***
Proportion Pasture	0.03(+)***	0.05(+)***	0.00(-)***	0.02(+)***	0.03(+)***	0.03(+)***	0.02(+)***
Proportion Cultivated Crops	0.02(-)***	0.03(-)***	**0.18(+)**	0.03(-)***	0.02(-)***	0.06(-)***	0.00(+)***
Proportion Woody Wetland	0.00(+)***	0.03(+)***	0.05(-)***	0.00(-)***	0.00(+)***	0.02(+)***	0.00(-)*
Proportion Herbaceous Wetland	0.01(-)**	0.01(-)***	0.00(+)***	0.02(-)**	0.01(-)***	0.00(-)***	0.01(-)**
Number of Land Cover Classes	0.12(+)***	**0.15(+)*****	0.01(-)	0.01(+)***	0.13(+)***	0.01(+)*	0.05(+)***
Shannon Diversity of Land Cover Classes	0.13(+)***	**0.23(+)*****	0.06(-)***	0.02(+)***	0.13(+)***	0.05(+)***	0.05(+)***
Mean Canopy Height	**0.35(+)*****	**0.55(+)*****	**0.22(-)*****	0.11(+)***	**0.32(+)*****	0.10(+)***	**0.16**(+)***
Standard Deviation Of Canopy Height	**0.32(+)*****	**0.53(+)*****	**0.25(-)*****	0.12(+)***	**0.25(+)*****	0.13(+)***	**0.17**(+)***
Coefficient of Variation of Canopy Height	0.07(-)***	0.09(-)***	0.03(+)***	0.03(-)***	0.06(-)***	0.02(-)***	0.04(-)***
Log of Mean Biomass	**0.36(+)*****	**0.55(+)*****	**0.23(-)*****	0.12(+)***	**0.32(+)*****	0.10(+)***	**0.16**(+)***
Log of Standard Deviation of Biomass	**0.23(+)*****	**0.35(+)*****	0.14(-)***	0.07(+)***	**0.19(+)*****	0.06(+)***	0.13(+)***
Coefficient of Variation of Biomass	0.07(-)***	0.10(-)***	0.03(+)***	0.03(-)***	0.06(-)***	0.02(-)***	0.04(-)***
Forest Core Area	**0.17(+)*****	**0.26(+)*****	**0.18(-)*****	0.03(+)***	**0.20(+)*****	0.02(+)***	0.04(+)***

Forest Edge Area	**0.35(+)*****	**0.54(+)*****	**0.28(-)*****	0.12(+)***	**0.34(+)*****	0.10(+)***	0.10(+)***
Shrubland Core Area	0.12(-)***	**0.22(-)*****	0.00(+)***	0.00(+)***	0.13(-)***	0.00(-)***	0.07(-)***
Shrubland Edge Area	0.05(-)***	0.12(-)***	0.00(+)	0.00(+)'	0.10(-)***	0.00(+)***	0.02(-)***
Grassland Core Area	0.07(-)***	0.11(-)***	**0.20(+)**	0.08(-)	0.06(-)***	0.05(-)**	0.02(-)***
Grassland Edge Area	0.01(-)***	0.00(-)***	0.04(+)***	0.00(+)***	0.00(-)***	0.00(+)***	0.00(+)***

Sign indicates direction of relationship. *** p-value < 0.001, ** p-value < 0.01, * p-value < 0.05. Values > 0.15 bolded for emphasis.

Table 3-3. Maximum univariate R^2 value among 7 avian guilds, by ecoregion. Struck-through entries denote variables excluded from further analysis (for that ecoregion) due to low R^2 value (R) or high correlation with other explanatory variables (C).

	Contiguous United States	Eastern Broadleaf Forest (Continental)	Central Appalachian Broadleaf Forest	Great Plains - Palouse Dry Steppe
Proportion Water	~~0.01~~ (R)	~~0.04~~ (R)	~~0.02~~ (R)	0.12
Proportion Developed	~~0.02~~ (R)	0.13	0.13	0.11
Proportion Barren	0.05	~~0.02~~ (R)	~~0.03~~ (R)	~~0.02~~ (R)
Proportion Deciduous Forest	0.34	~~0.40~~ (C)	~~0.18~~ (C)	0.16
Proportion Evergreen Forest	0.15	0.15	~~0.02~~ (R)	~~0.42~~ (C)
Proportion Mixed Forest	0.13	0.06	~~0.03~~ (R)	0.13
Proportion Scrub-Shrub	~~0.25~~ (C)	~~0.03~~ (R)	0.09	0.13
Proportion Grassland	~~0.20~~ (C)	~~0.02~~ (R)	~~0.04~~ (R)	~~0.10~~ (C)
Proportion Pasture	0.05	0.08	~~0.13~~ (C)	0.16
Proportion Cultivated Crops	0.18	~~0.26~~ (C)	0.19	0.11
Proportion Woody Wetland	0.05	~~0.02~~ (R)	~~0.01~~ (R)	0.13
Proportion Herbaceous Wetland	~~0.02~~ (R)	0.12	~~0.04~~ (R)	0.11
Number of Land Cover Classes	0.15	~~0.05~~ (R)	0.08	0.19
Shannon Diversity of Land Cover Classes	0.23	~~0.03~~ (R)	0.20	0.26
Mean Canopy Height	0.55	0.39	0.24	~~0.38~~ (C)
Standard Deviation Of Canopy Height	0.53	0.28	0.11	0.53
Coefficient of Variation of Canopy Height	0.09	~~0.32~~ (C)	~~0.16~~ (C)	~~0.14~~ (C)
Log of Mean Biomass	~~0.55~~ (C)	~~0.04~~ (R)	~~0.23~~ (C)	0.36
Log of Standard Deviation of Biomass	~~0.35~~ (C)	~~0.02~~ (R)	0.22	~~0.48~~ (C)
Coefficient of Variation of Biomass	~~0.10~~ (C)	0.17	~~0.18~~ (C)	0.14

Forest Core	0.26	~~0.25~~ (C)	~~0.18~~ (C)	~~0.35~~ (C)
Forest Edge	0.54	~~0.39~~ (C)	~~0.04~~ (R)	~~0.48~~ (C)
Shrubland Core	0.22	~~0.01~~ (R)	~~0.03~~ (R)	~~0.03~~ (R)
Shrubland Edge	0.12	~~0.03~~ (R)	~~0.09~~ (C)	~~0.14~~ (C)
Grassland Core	0.20	~~0.06~~ (C)	0.06	0.11
Grassland Edge	~~0.04~~ (R)	~~0.06~~ (C)	~~0.15~~ (C)	0.09

Table 3-4. Number of times explanatory variables appeared in top 10 models of nationwide species richness for models with 1, 2, 3, 4, and 5 explanatory variables. Variables are marked as measures of vertical (V) or horizontal (H) habitat structure.

		Habitat Association			Migratory Habit			
TOP10	All Species	Forest Birds	Grassland Birds	Shrubland Birds	Neotropical Migrants	Permanent Residents	Short-Distance Migrants	Sum
Standard Deviation of Canopy Height (V)	11	29	24	21	6	41	37	169
Mean Canopy Height (V)	35	31	5	21	26	2	22	142
Proportion Deciduous Forest (H)	30	27	2	26	35	1	3	124
Forest Edge Area (H)	25	22	6	8	17	5	4	87
Proportion Cultivated Crops (H)	3	4	35	2	7	13	22	86
Proportion Barren (H)	19	4	1	2	4	19	10	59
Shrubland Core Area (H)	2	7	3	31	4	4	6	57
Shrubland Edge Area (H)	1	5	8	11	4	26	1	56
Grassland Core Area (H)	1	0	35	5	0	8	1	50
Proportion Woody Wetland (H)	1	0	8	5	0	5	29	48
Proportion Mixed Forest (H)	7	9	5	0	19	0	0	40
Number of Land Cover Classes (H)	4	1	3	0	14	6	6	34
Forest Core Area (H)	3	5	5	7	5	1	3	29
Proportion Evergreen Forest (H)	5	4	7	5	6	1	0	28
Proportion Pasture (H)	0	0	0	2	0	15	1	18
Shannon Diversity of Land Cover Classes (H)	3	2	3	1	3	2	2	16
Coefficient of Variation of Canopy Height (V)	0	0	0	3	0	1	3	7

Table 3-5. Independent contribution values for nationwide avian species richness models as determined by hierarchical partitioning. Variables are marked as measures of vertical (V) or horizontal (H) habitat structure.

		Habitat Association			Migratory Habit			
	All Species	Forest Birds	Grassland Birds	Shrubland Birds	Neotropical Migrants	Permanent Residents	Short-Distance Migrants	Sum
Standard Deviation of Canopy Height (V)	15.1***	16.3***	14.6***	14.7***	11.1	19.7***	20.2***	111.6
Mean Canopy Height (V)	17.1***	16.7***	13.1**	14.4***	14.3***	15.1*	18.4***	109.2
Forest Edge Area (H)	16.7***	16.5***	15.8	14.2*	15.7***	14.7	12.0*	105.7
Proportion Deciduous Forest (H)	12.7***	11.0***	5.4***	13.4***	17.0***	5.1	6.8	71.3
Grassland Core Area (H)	5.2**	5.3	13.2***	11.4*	4.6**	8.5*	4.6***	52.8
Shrubland Core Area (H)	6.7**	7.7*	3.8	5.4***	7.0*	4.0	9.3	43.9
Proportion Cultivated Crops (H)	3.6***	3.5**	12.3***	5.8***	3.4***	10.2***	4.0***	42.8
Number of Land Cover Classes (H)	6.6**	5.7	3.5***	4.0	7.2***	3.7***	7.4*	38.2
Proportion Mixed Forest (H)	5.1***	5.3***	6.3***	3.6	6.9***	3.4**	3.2	33.8
Shrubland Edge Area (H)	4.1***	5.3	3.2***	4.0***	6.1	4.9***	4.5***	32.2
Proportion Barren (H)	4.5***	3.7***	3.3**	4.8***	4.2***	5.8***	5.4***	31.7
Proportion Woody Wetland (H)	2.6	3.0**	5.3**	4.4	2.7	4.8**	4.1***	26.8
Sum	100.0	100.0	100.0	100.0	100.0	100.0	100.0	
Adjusted R^2 (full model)	0.46	0.70	0.48	0.27	0.50	0.20	0.24	

Table 3-6. Number of times explanatory variables appeared in top 10 models of species richness in the Eastern Broadleaf Forest (Continental) ecoregion, for models with 1, 2, 3, 4, and 5 explanatory variables. Variables are marked as measures of vertical (V) or horizontal (H) habitat structure, and bold typeface indicates the most frequently included variable for each guild.

		Habitat Association			Migratory Habit			
	All Species	Forest Birds	Grassland Birds	Shrubland Birds	Neotropical Migrants	Permanent Residents	Short-Distance Migrants	Sum
Mean Canopy Height (V)	30	**38**	**39**	21	**39**	**35**	22	224
Proportion Developed (H)	**34**	31	29	31	29	30	**39**	223
Standard Deviation of Canopy Height (V)	29	24	12	**35**	16	25	27	168
Coefficient of Variation of Biomass (V)	8	14	16	21	6	17	7	89
Proportion Herbaceous Wetland (H)	14	7	21	7	24	7	8	88
Number of Land Cover Classes (H)	6	10	12	12	10	13	9	72
Proportion Mixed Forest (H)	12	8	5	6	8	6	20	65
Proportion Pasture (H)	7	8	10	6	10	8	11	60
Proportion Evergreen Forest (H)	9	9	5	10	7	8	6	54

Table 3-7. Number of times explanatory variables appeared in top 10 models of species richness in Ecoregion province Central Appalachian Broadleaf Forest, for models with 1, 2, 3, 4, and 5 explanatory variables. Variables are marked as measures of vertical (V) or horizontal (H) habitat structure, and bold typeface indicates the most frequently included variable for each guild.

		Habitat Association			Migratory Habit			
	All Species	Forest Birds	Grassland Birds	Shrubland Birds	Neotropical Migrants	Permanent Residents	Short-Distance Migrants	Sum
Proportion Developed (H)	**39**	**39**	17	28	**39**	**29**	27	218
Grassland Core Area (H)	16	15	19	21	23	27	16	137
Mean Canopy Height (V)	10	12	30	14	11	20	**33**	130
Log of Standard Deviation of Biomass (V)	27	23	**32**	7	22	9	7	127
Proportion Cultivated Crops (H)	14	9	13	17	11	28	10	102
Standard Deviation of Canopy Height (V)	8	13	6	**39**	10	15	5	96
Proportion Scrub-Shrub (H)	13	11	17	9	15	7	14	86
Number of Land Cover Classes (H)	14	22	11	6	14	6	10	83
Shannon Diversity of Land Cover Classes (H)	8	5	4	8	4	8	27	64

Table 3-8. Number of times explanatory variables appeared in top 10 models of species richness in the Great Plains – Palouse Dry Steppe Ecoregion, for models with 1, 2, 3, 4, and 5 explanatory variables. Variables are marked as measures of vertical (V) or horizontal (H) habitat structure, and bold typeface indicates the most frequently included variable for each guild.

		Habitat Association			Migratory Habit			
	All Species	Forest Birds	Grassland Birds	Shrubland Birds	Neotropical Migrants	Permanent Residents	Short-Distance Migrants	Sum
Shannon Diversity of Land Cover Classes (H)	32	9	**24**	**41**	**36**	4	**34**	180
Standard Deviation of Canopy Height (V)	**39**	**41**	18	4	22	5	32	161
Proportion Cultivated Crops (H)	14	12	11	27	10	**23**	30	127
Proportion Deciduous Forest (H)	13	32	9	15	10	19	3	101
Number of Land Cover Classes (H)	13	16	1	6	32	5	5	78
Grassland Core Area (H)	12	7	22	0	9	22	3	75
Proportion Open Water (H)	5	7	8	8	14	4	3	49
Log of Mean Biomass (V)	3	1	18	1	2	19	5	49
Coefficient of Variation of Biomass (V)	5	5	0	23	1	1	13	48
Grassland Edge Area (H)	2	1	7	3	2	22	3	40
Proportion Scrub-Shrub (H)	3	3	12	2	2	6	4	32
Proportion Developed (H)	1	5	2	10	4	3	2	27
Proportion Mixed Forest (H)	5	2	2	4	4	5	3	25
Proportion Herbaceous Wetland (H)	1	4	7	1	1	7	1	22
Proportion Pasture (H)	1	3	9	0	0	1	0	14
Proportion Woody Wetland (H)	1	2	0	5	1	2	2	13

Table 3-9. Independent contribution values for avian species richness models for the Eastern Broadleaf Forest (Continental), as determined by hierarchical partitioning. Variables are marked as measures of vertical (V) or horizontal (H) habitat structure.

		Habitat Association			Migratory Habit			
	All Species	Forest Birds	Grassland Birds	Shrubland Birds	Neotropical Migrants	Permanent Residents	Short-Distance Migrants	Sum
Mean Canopy Height (V)	26.6**	35.3***	34.9***	23.2*	35.5***	27.5***	8.9**	191.9
Proportion Developed (H)	30.3***	15.0***	8.6***	12.0***	17.4***	13.0***	59.4***	155.6
Standard Deviation of Canopy Height (V)	21.3**	22.4***	16.9	27.4***	17.9	22.0***	13.9***	141.7
Coefficient of Variation of Biomass(V)	3.5	9.3*	12.1**	16.0**	2.4	13.8**	0.7	57.9
Proportion Evergreen Forest (H)	6.8	8.8	6.1	8.6	7.1	8.8	1.2	47.3
Proportion Herbaceous Wetland (H)	2.9*	1.1	10.4*	2.9	7.8**	4.1	2.5	31.7
Proportion Pasture (H)	3.9	3.7	4.2**	4.9	4.1	5.5*	3.1	29.3
Proportion Mixed Forest (H)	1.9	2.6	4.4	2.0	2.7	2.2	7.4	23.1
Number of Land Cover Classes (H)	2.8	1.9*	2.5**	3.1**	5.3	3.1***	3.0	21.5
Model Adjusted R^2	0.27	0.47	0.42	0.37	0.23	0.44	0.11	

Table 3-10. Independent contribution values for avian species richness models for the Central Appalachian Broadleaf Forest, as determined by hierarchical partitioning. Variables are marked as measures of vertical (V) or horizontal (H) habitat structure.

		Habitat Association			Migratory Habit			
	All Species	Forest Birds	Grassland Birds	Shrubland Birds	Neotropical Migrants	Permanent Residents	Short-Distance Migrants	Sum
Proportion Developed (H)	48.4***	53.2***	5.1*	11.6	49.6***	18.9	6.5*	193.3
Standard Deviation of Canopy Height (V)	4.0*	5.0	3.2	50.5	4.8*	14.0	9.3	90.8
Grassland Core Area (H)	8.7	6.5	5.8	16.5	9.9	26.7	5.2	79.4
Mean Canopy Height (H)	5.7	9.6	18.2	7.4	7.8	8.9	21.5	79.2
Proportion Cultivated Crops (H)	9.5	5.5	15.0	5.2	5.7	16.5	14.4	71.8
Log of Mean Biomass (V)	3.0	3.8	23.6	4.1	3.6	9.6	15.8	63.5
Proportion Scrub-Shrub (H)	13.6	6.9	12.7	1.4***	11.6	1.8	3.5	51.7
Shannon Diversity of Land Cover Classes (H)	2.6	2.7	7.9	2.7	3.4	2.2	20.2	41.7
Number of Land Cover Classes (H)	4.5	6.7	8.5	0.6	3.5	1.4	3.5	28.7
Model Adjusted R^2	0.14	0.16	0.29	0.08	0.18	0.06	0.27	

Table 3-11. Independent contribution values for avian species richness models for the Great Plains - Palouse Dry Steppe, as determined by hierarchical partitioning. Variables are marked as measures of vertical (V) or horizontal (H) habitat structure.

		Habitat Association			Migratory Habit			
	All Species	Forest Birds	Grassland Birds	Shrubland Birds	Neotropical Migrants	Permanent Residents	Short-Distance Migrants	Sum
Standard Deviation of Canopy Height (V)	18.6**	26.2***	14.6*	10.8	13.7*	18.0	17.0	118.8
Shannon Diversity of Land Cover Classes (H)	13.7**	7.3	7.4***	19.2**	16.5**	4.6	12.3	81.0
Log of Mean Biomass (V)	7.1	14.0	19.1	4.1	4.9	20.4	6.5	75.9
Proportion Deciduous Forest (H)	10.2	9.4*	4.9**	10.1	10.9	9.2**	6.6	61.4
Proportion Cultivated Crops (H)	8.5	7.4	5.6**	7.3	5.9	7.7***	12.0*	54.4
Number of Land Cover Classes (H)	10.2	8.2	3.7	6.6	13.9**	4.0**	7.5	54.1
Coefficient of Variation of Biomass (V)	8.6	6.5	3.7	10.7*	8.1	4.7	10.6	52.8
Proportion Scrub-Shrub (H)	4.5	4.3	9.6	6.6	3.7	7.6	6.0	42.3
Grassland Edge Area (H)	5.2	3.4	5.7***	7.7	6.2	6.4***	7.0	41.6
Grassland Core Area (H)	4.5	5.7	9.5***	4.9	4.2	8.1*	4.5	41.4
Proportion Open Water (H)	4.5	3.0	8.6**	7.3*	8.1**	4.8**	3.8	40.1
Proportion Developed (H)	4.5	4.7	7.7	4.7	3.9	4.6*	6.2	36.3
Model Adjusted R^2	0.48	0.57	0.63	0.40	0.44	0.46	0.27	

Figures

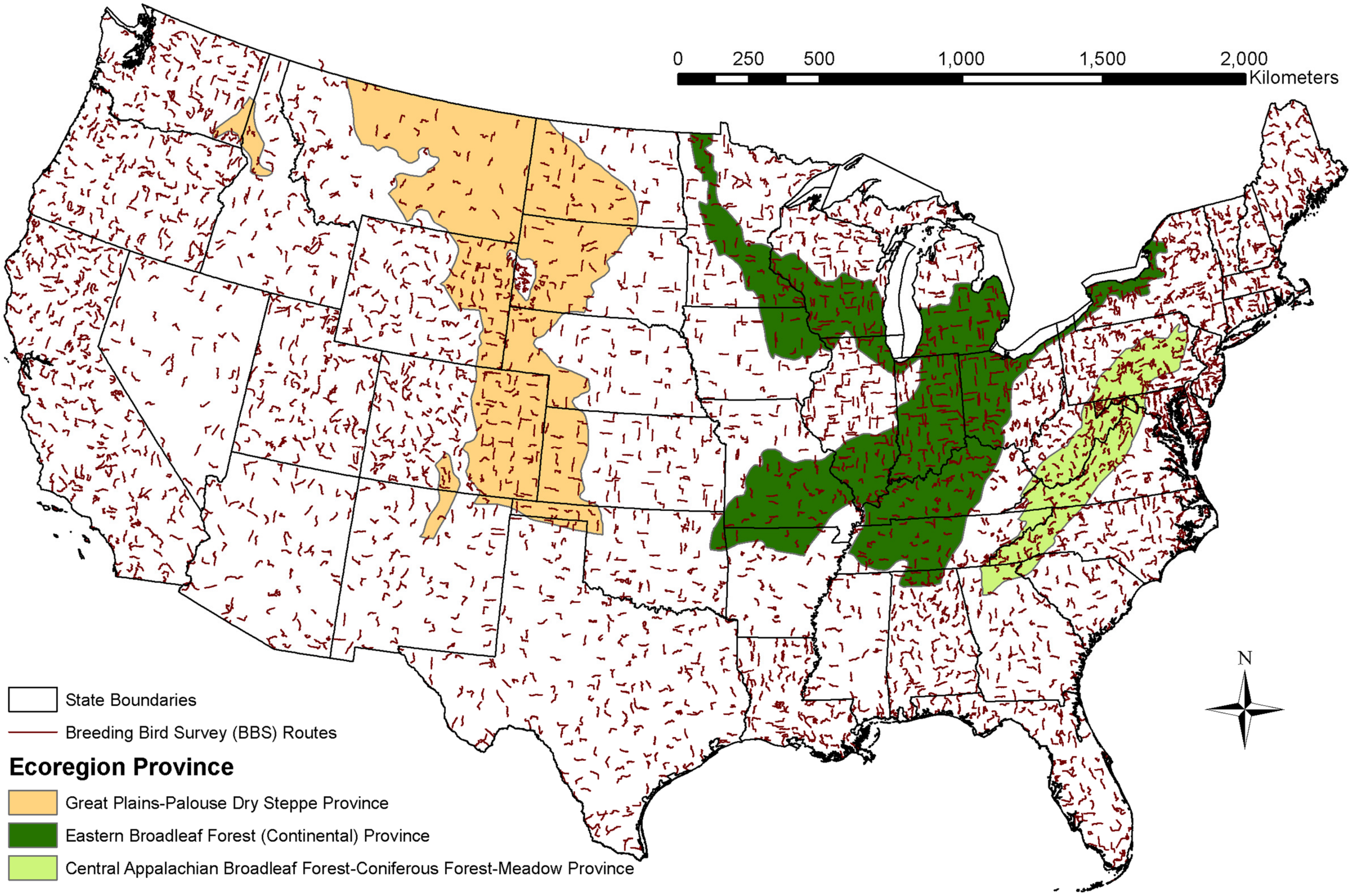

Figure 3-1. Study area, including Breeding Bird Survey (BBS) routes and ecoregion provinces used in analysis.

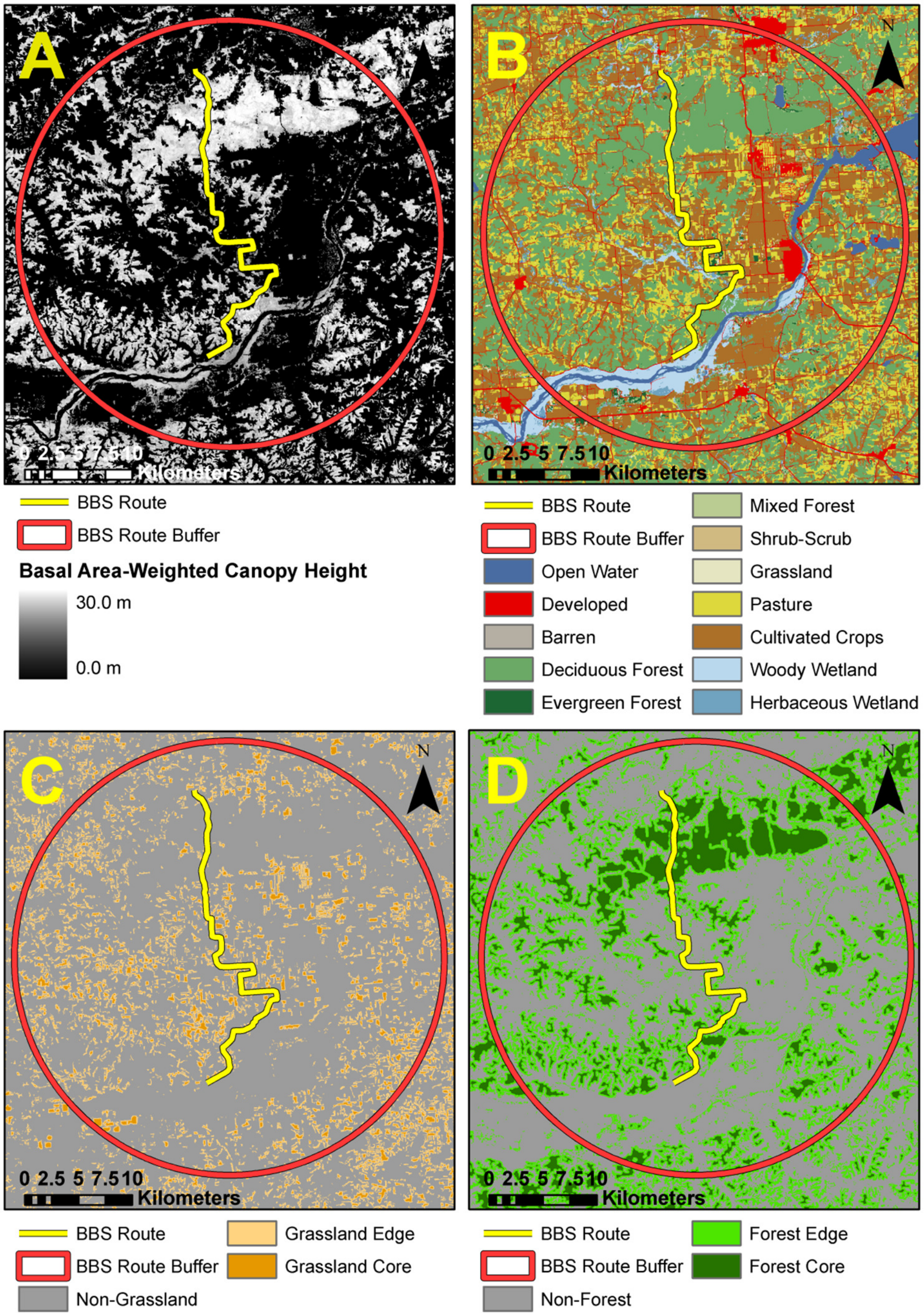

Figure 3-2. Data layers corresponding to a single BBS route in the study area. (A) Basal area-weighted canopy height from the National Biomass and Carbon Dataset (NBCD). (B) Land cover from 2001 National Land Cover Dataset (NLCD). (C) Grassland edge and grassland core, as calculated from 2001 NLCD. (D) Forest edge and forest core, as calculated from 2001 NLCD.

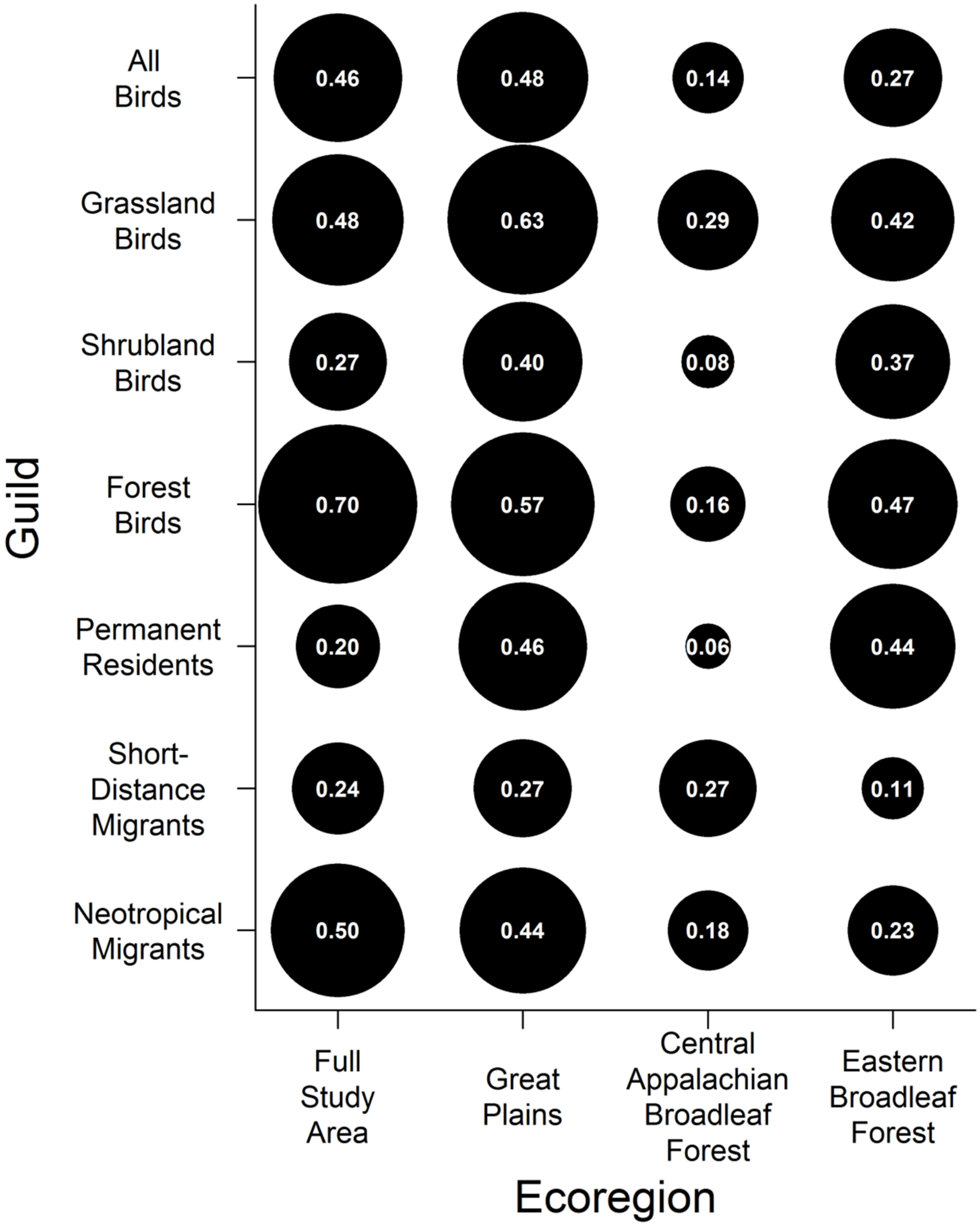

Figure 3-3. Adjusted R^2 values of final models of avian species richness as a function of vertical and horizontal measures of habitat structure, by avian guild and ecoregion. Circle diameter is proportional to adjusted R^2 value.

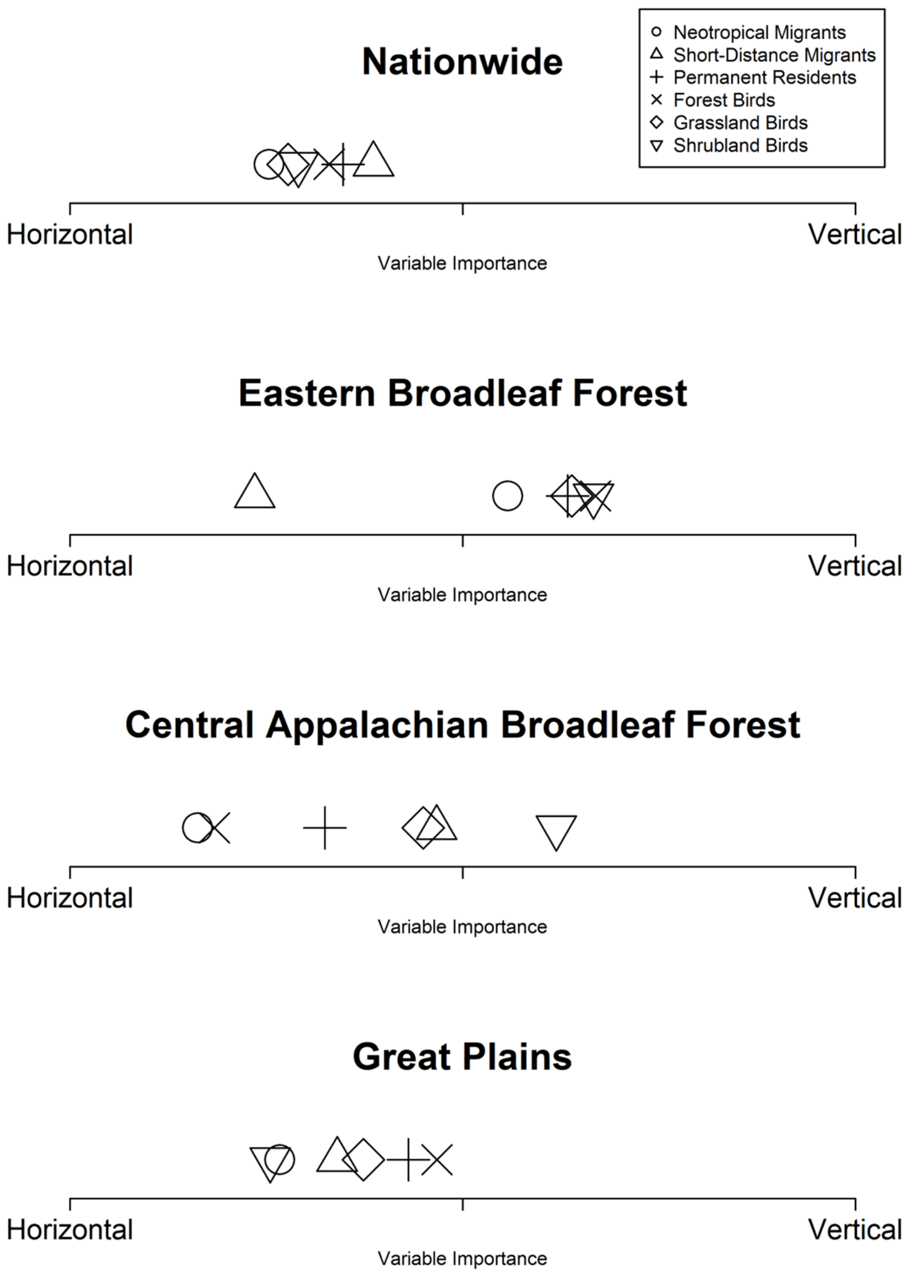

Figure 3-4. For each model of avian species richness, the difference was calculated between the sum of independent contributions (as determined by hierarchical partitioning) of variables representing horizontal structure and variables representing vertical structure. The nationwide model included 2 vertical variables and 10 horizontal variables, the Eastern Broadleaf forest model, 3 vertical, 6 horizontal, the Central Appalachian Broadleaf Forest model, 3 vertical, 6 horizontal, and the Great Plains, 3 vertical, 9 horizontal.

Chapter 4

The Influence of Productivity, Climatic Stability, and Habitat Structure on Nationwide Patterns of Avian Species Richness

Abstract

Understanding the drivers of geographic patterns in species richness is an important aim in ecology. Biodiversity has been hypothesized to be a function of productivity, climatic stability, and habitat structure. These factors have been rarely studied in conjunction with one another. We used remotely sensed measures of productivity, climatic stability, and habitat structure to model nationwide patterns of species richness for seven avian guilds. Our aims were to determine which groups of measures had the most predictive power and to evaluate complementarity between these groups. Avian species richness was derived from the Breeding Bird Survey. Measures of productivity included annual sum and annual minimum fraction of photosynthetically active radiation (fPAR), a measure strongly related to vegetative productivity. Seasonal variation of fPAR, and ecoregion province were used as measures of climatic stability. Image texture measures, canopy height, biomass, and landcover composition metrics were used to represent habitat structure. We used best subset selection and hierarchical partitioning to evaluate the relative explanatory contribution of individual variables as well as the broader groups they represented. All three categories made some contribution to explaining avian species richness patterns, with habitat structure measures the strongest overall. For five of seven

guilds (all birds, forest birds, shrubland birds, Neotropical migrants, and short-distance migrants), measures of habitat structure contributed the bulk of explanatory power followed by a moderate contribution from productivity measures and a small contribution from measures of climatic stability. For grassland birds, habitat structure was still the strongest predictor, though to a lesser extent, and productivity and climatic stability had a larger influence then in the previously mentioned guilds. For permanent residents, the contribution of different variable groups was roughly split three ways, with productivity explaining the most, followed by climatic stability, then habitat structure. Though habitat structure measures were dominant on the whole, the top-performing individual variables included measures from all three categories. In fact, the strongest performing variable overall was mean annual sum of fPAR (productivity).

Introduction

Understanding the causes of spatial heterogeneity in biodiversity is still one of the most pressing challenges for ecologists (Gaston 2000). One shortcoming of the current pool of biodiversity studies is that most explore only one or two factors in isolation. A broader perspective of the drivers of biodiversity is needed. MacArthur (1972) hypothesized that biodiversity is a function of productivity, climatic stability, and habitat structure (Figure 4-1). Because this hypothesis encompasses many of the recognized patterns of biodiversity, and these three factors are amenable to measurement by remote sensing, this is an ideal framework for studying patterns of biodiversity over a broad extent. Even though MacArthur's framework has existed for 40 years, few studies have considered these three factors jointly. This is a critical step to determine the relative importance of the factors, as well as whether complementarity truly exists among them as expected.

Geographic patterns in biodiversity exhibit strong variability. Numerous patterns have been identified, including a positive relationship between biodiversity and area (Williams 1943, Preston 1962, MacArthur and Wilson 1967), decreasing biodiversity with increasing latitude (Wallace 1878, Pianka 1966, Fischer 1960, Klopfer 1959), a positive relationship between biodiversity and habitat structure (MacArthur and MacArthur 1961, MacArthur 1972), highest biodiversity at intermediate scales of disturbance (Connell 1978, Sousa 1979, Sousa 1984), decreasing biodiversity with increasing trophic level (Lindeman 1942, Schoener 1989), monotonically or unimodally increasing biodiversity with increasing available energy or productivity (Wright 1983, Currie 1991), higher biodiversity in areas of high environmental or climatic stability (Fischer 1960, Fjeldsa and Lovett 1997), and decreasing biodiversity with increasing elevation (Stevens 1992). Many of these trends fall under MacArthur's framework as relationships between biodiversity and productivity, climatic stability, and habitat structure.

Productivity is a measure of environmental energy available to organisms. Productivity is generally recognized to have an important influence on biodiversity (Gaston 2000) though there is no consensus on the underlying mechanisms of this relationship. One of the most common hypotheses states that an increase in productivity allows an increase in overall abundance, resulting in higher biodiversity (Wright 1983, Evans et al. 2005, Rosenzweig 1995, Currie et al. 2004). A study in Kenya showed a strong positive monotonic relationship between normalized difference vegetation index (NDVI) and species richness, with the relationship especially strong in arid to semi-arid zones (Oindo et al. 2000). In an analysis of avian diversity patterns across North America (Hurlbert and Haskell 2003), a positive monotonic relationship was found between species richness and NDVI. In contrast, avian biodiversity showed a unimodal response to primary productivity across the United States (Currie 1991). When partitioned by ecoregion at the province level, avian richness responded negatively to productivity in some provinces, and positively in others (Rowhani et al. 2008).

Climatic stability influences levels of biodiversity (Fischer 1960, Klopfer 1959, MacArthur 1972, Sanders 1968). The primary hypothesis is that stable environments allow more niches and therefore higher faunal diversity (Klopfer 1959), since resources with high seasonality cannot be subdivided into as many niches as constant resources, thus limiting the number of coexisting species (MacArthur 1969). In Kenya, large herbivore richness is negatively correlated with the standard deviation of maximum average NDVI (Oindo 2002a). Biodiversity hot spots show higher ecoclimatic stability than similar areas with lower biodiversity (Fjeldsa et al. 1997). Studies of avian biodiversity also reflect this pattern. Avian species richness is negatively correlated with standard deviation of maximum average NDVI in Kenya (Oindo et al. 2000). Across the United States, increasing variability in energy, measured as EVI, is associated with decreasing species richness, explaining 30% of the variability (Rowhani et al. 2008). In some ecoregions, interannual variability in energy explains more than half of variation in avian richness (Rowhani et al. 2008). Seasonal variation in vegetative productivity also strongly affects avian species richness at the regional level in the United States (Coops et al. 2009).

It is hypothesized that a more complex structural arrangement within a habitat or a heterogeneous arrangement of habitats contains a larger number of potential niches, which can therefore be exploited by more species, thus supporting higher biodiversity. While the terms habitat structure and habitat heterogeneity have been used somewhat interchangeably, we take a broad approach, and use the term habitat structure to refer to the composition and configuration of vegetation and habitat types. Habitat structure has been studied across a range of spatial scales. Measurements such as foliage height diversity and vegetation cover exhibit a positive relationship to species richness (MacArthur and MacArthur 1961, MacArthur et al. 1966, Willson 1974, Erdelen 1984, Rotenberry and Wiens 1980). Studies considering context and landscape structure in addition to, or in place of fine scale vegetation measurements (Atauri and de Lucio 2001, Donovan and Flather 2002, Farina 1997, Kondo and Nakagoshi 2002, Krauss et al. 2003, Mcgarigal and Mccomb 1995) also show positive relationships between level of habitat structure and biodiversity (Tews et al. 2004).

Our overall goal was to determine the relative importance and complementarity of measures of productivity, climatic stability, and habitat structure, in explaining nationwide patterns of avian species richness. Prior to analysis, we made several predictions.

1. When combined, variables representing productivity, climatic stability, and habitat structure will all retain some level of importance, showing complementarity between these categories.
2. Because we are predicting species richness at a relatively fine scale (at the level of Breeding Bird Survey routes), measures of habitat structure will be the most important variables, as measures of productivity and climatic stability have stronger influence at a regional level (Mackey and Lindenmayer 2001, Pearson and Dawson 2003).

3. Among variables quantifying habitat structure, proportion of habitat type will be an important factor influencing habitat guild species richness (e.g. proportion grassland and grassland birds). Proportion deciduous forest and canopy height measures will have strong positive relationships with species richness for all birds, forest birds, and Neotropical migrants (as found in Chapter 3).
4. Among migratory guilds, permanent resident species richness will have a strong negative relationship with seasonal variability and a strong positive relationship with annual minimum productivity, as these species remain in the same location year-round. In contrast, Neotropical migrant and short-distance migrant species richness will be relatively unaffected by these measures, since these species are only present in their breeding areas during the most productive seasons.
5. Total productivity will be strongly and positively associated with species richness of all guilds, except shrubland birds, as shrubland habitat generally has low productivity (Coops et al. 2009).

Methods

Our study included the entire contiguous United States. Avian species richness was calculated from the North American Breeding Bird Survey (BBS) (USGS Patuxent Wildlife Research Center 2008). Analysis was centered on the year 2000, and we calculated the mean species richness of each BBS route over the period 1998-2002. The BBS data set was preprocessed to remove observations collected by first year observers or in suboptimal weather, and poorly sampled species were excluded. After the removal of these routes as well as routes for which we did not have a full set of explanatory variables, we retained 2,555 routes. We expected that relationships between species richness and productivity, climatic stability and habitat structure would differ among different functional guilds. Therefore in addition to overall species richness, we calculated species richness within three migratory guilds: permanent residents, short-distance migrants, and Neotropical migrants, and three habitat guilds: forest, shrubland, and grassland. Because bird species detectability likely leads to undercounting of species, we used the software program COMDYN (Hines et al. 1999) to calculate estimated species richness, which was used as our measure of biodiversity for each BBS route.

In order to relate our explanatory variables to individual BBS routes, we created 19.7 km-radius (one-half the length of a BBS route) circular buffers around the centroid of each BBS route (Flather and Sauer 1996). This radius encompasses the entire BBS route, regardless of route path, and a circular buffer provides a uniform area and shape. This distance is comparable to the median maximum natal dispersal distance (31 km) of 76 avian species (Sutherland et al. 2000) and is consistent with the recommended scale for considering landscape effects on songbirds (Tittler et al. 2009). This approach has been used successfully in several studies using BBS data (Flather and Sauer 1996, Rittenhouse et al. 2010, Albright et al. 2010, Albright et al. 2011, Pidgeon et al. 2007).

Explanatory Variables

Remotely sensed data have been increasingly utilized in a variety of ecological applications (Kerr and Ostrovsky 2003). A major advantage of remotely sensed data over field acquired data is the ease of quickly acquiring high-spatial and -temporal resolution data over very broad extents (Innes and Koch 1998, Roy 2003). Methods of measuring biodiversity from remotely sensed data can be roughly divided into three categories (Nagendra 2001): 1 – direct mapping of individuals or assemblages that are visible from remotely sensed imagery (Innes and Koch 1998, Guinet et al. 1995), 2 – generating habitat maps for individual species (Pearlstine et al. 2002), and 3 - directly relating species distribution patterns to spectral reflectance or indices (Oindo et al. 2000, Oindo 2002b, Laurent et al. 2005).

Because we were studying patterns of biodiversity for many species over a broad extent, we opted for the third approach by directly relating avian species richness to remotely sensed measures of productivity, climatic stability, and habitat structure. Of these three factors, climate and productivity can be measured by relatively mature remote sensing techniques. Multiple indices of weather, vegetation, and productivity are widely available (e.g. DAYMET temperature and precipitation, MODIS land surface temperature, MODIS fraction of photosynthetically active radiation, MODIS net primary productivity, etc.) In contrast, there are no standardized measures of habitat structure for broad areas. Over small extents, lidar (light detection and ranging) has been effective (Clawges et al. 2008), but it is not currently feasible to acquire lidar data over broad extents. Approaches that have shown success applicable to broad extent analyses include landscape composition and configuration metrics (Atauri and de Lucio 2001, Donovan and Flather 2002, Farina 1997, Kondo and Nakagoshi 2002), measures of image texture (St-Louis et al. 2006, St-Louis et al. 2009, Culbert et al. 2012, Wood et al. 2012), and measures of canopy height (see Chapter 3).

To quantify productivity, our primary measures were of fraction of photosynthetically active radiation (fPAR). This measure, captured by the MODIS sensor, quantifies the proportion of the available solar radiation (in the photosynthetically active wavelengths) that is absorbed by vegetation. This is therefore a good measure of vegetative productivity (Sellers et al. 1997). We used two measures of fPAR from a nationwide 1-km resolution dataset including data from 2000-2006 (Coops et al. 2009) to quantify productivity, average annual sum of fPAR and the average annual minimum fPAR. Annual minimum fPAR is a measure of productivity during most severe annual conditions (winter in most regions of the country). This measure is therefore a potential limiting factor for permanent residents (Coops et al. 2009). We also included elevation, as measured by the Shuttle Radar Topography Mission (SRTM) (Rabus et al. 2003) as a proxy for productivity, as productivity and elevation are related over a broad elevational scale. For each of these mentioned measures, we calculated the mean and standard deviation within each BBS route buffer, for a total of six variables.

To quantify climatic stability, we again used a measure of fPAR. Variability in fPAR is also a good measure of climatic stability, as vegetative productivity is strongly influenced by climate. We included average intra-annual seasonality of fPAR over the period 2000-2006 (Coops et al. 2009). We calculated the mean and standard deviation of this measure within each BBS route buffer, for a total of two variables. Lastly, ecoregion at the province level (Bailey 1995) was added to capture other regional scale patterns in stability not already accounted for, adding one additional explanatory variable.

Because we expected habitat structure to be the strongest factor influencing species richness patterns at fine scales, we included several different measures of vertical and horizontal habitat structure. First, we used measures of land-cover composition and configuration calculated from the 2001 National Land-Cover Database (Homer et al. 2004). To quantify composition, we calculated proportion of 12 different landcover classes, total number of landcover classes, and Shannon diversity index (Shannon 1948) of landcover classes within each BBS route buffer. To quantify landscape configuration, we used the software program GUIDOS (Vogt 2010) to calculate the area of core and edge forest, grassland, and shrubland for each BBS route buffer. Together this yielded 20 explanatory variables.

To characterize vertical habitat structure, we derived measures of vegetation canopy height and aboveground live dry biomass from the 30-m resolution National Biomass and Carbon Dataset 2000 (NBCD2000) (Kellndorfer et al. 2011). From this dataset we calculated mean, standard deviation, and coefficient of variation of both basal area-weighted canopy height and aboveground live dry biomass (using the NBCD's FIA-derived biomass model) for each BBS route buffer, yielding six variables in all.

We calculated image texture measures from satellite imagery to further characterize within-landcover class heterogeneity. Texture measures were calculated from 114 Landsat TM/ETM+ scenes acquired from the LEDAPS database (Masek et al. 2006), a collection of atmospherically corrected Landsat images based on the GeoCover dataset (Tucker et al. 2004). We selected scenes from approximately the year 2000, to temporally coincide with our species richness data. All images were acquired during the growing season, however, due to the extent of study, it was not possible to obtain all images for the same phenological stage. Therefore, some extraneous phenological variability (and therefore noise) in the texture measures was likely present (Culbert et al. 2009). For each image, a suite of first- and second-order texture measures were calculated using Matlab® R2010a (The MathWorks 1984-2010), with scripts adapted from (St-Louis et al. 2006). First-order mean and standard deviation were calculated for TM bands 2, 3, 4, and 5, with 5x5 and 21x21 moving windows. We also calculated second-order angular second moment (ASM), contrast, correlation, entropy, homogeneity, and sum of squares variance (SSVar). Among all second-order texture measures, these six are considered the most useful for remote sensing analyses (Baraldi and Parmiggiani 1995, Kayitakire et al. 2006). We expected this set of texture measures would adequately characterize vegetation structure and therefore be an appropriate set with which to relate avian species richness. We quantized the imagery to 64 values to limit the size of the GLCM and avoid matrices that are too sparsely populated to provide robust results (Vega-Garcia and Chuvieco 2006). Second-order textures were calculated using an omni-directional GLCM (calculated as the mean of the four possible directional GLCMs). Preliminary analysis found strong correlation between texture measures derived from 5x5 and 21x21 window sizes, so, due to the substantial computational requirements, second-order texture measures were calculated only with a 5x5 window and only for TM bands 2, 3, 4, and 5. Bands 1 and 7 were excluded because we expected band 1 results to be highly correlated with band 2, and band 7 was less useful than other bands in prior exploratory analysis. This resulted in a total of 40 texture measures (16 first-order and 24 second-order). For each BBS route, we calculated the within-buffer mean and standard deviation of each of the 40 texture measures, yielding 80 variables total.

Statistical analysis

Our explanatory variable pool included 115 candidate variables. Though we had a large sample size, this was still a large number of variables, and we expected there would be a high level of correlation, particularly among the texture variables (Baraldi and Parmiggiani 1995).

We used a multi-step process to reduce the variable pool. First, we created univariate models for species richness of each guild as a function of each explanatory variable in order to identify those variables with very low explanatory power, and we inspected a scatter plot of each model for evidence of non-linear relationships. Only variables that yielded an R^2 value > 0.05 for at least one avian guild were retained for further analysis. We then analyzed the correlation of the remaining variables in order to exclude correlated variables and further reduce the number of explanatory variables. We ranked the individual explanatory variables based on their R^2 value for the all birds guild univariate models (results not shown). Rankings of variables based on performance for other guilds were similar. For each explanatory variable pair with correlation coefficient $|r| > 0.6$, the variable with the lower univariate rank was dropped from subsequent analysis. This was carried out in stages, first examining correlation within a texture measure (e.g. correlation among different window sizes and bands of the same texture), then examining correlation between remaining texture measures, and finally considering correlation among the remaining texture measures and the rest of the candidate explanatory variables.

Once correlated variables were removed from the pool, variable contribution was evaluated in two stages. First, best subset regression (Miller 1990) was used to determine the models with the highest adjusted-R^2. For each avian guild, the 10 best models with 1 though 10 variables were determined (100 models total), and the number of times each variable was included in a model was counted. For each guild, the top 12 variables were selected. As in Chapter 3, we first used best subset regression. The advantages of best subset regression are that it is an exhaustive procedure and can handle a large pool of candidate explanatory variables, as was the case in this study. The disadvantage is that the choices of the number of top models and the number of variables per model are relatively arbitrary and can affect the results.

For this reason we relied on hierarchical partitioning (Chevan and Sutherland 1991) as the method for determining our final variable contribution (as in Chapter 3). Like best subset regression, hierarchical partitioning is also an exhaustive approach. The advantages of hierarchical partitioning are that this method calculates the contribution of each variable in the context of other explanatory variables, and there are no arbitrary parameters to set. The disadvantage is that, due to computational limitations, the maximum number of variables that can be considered is twelve. We used the variable ranking from best subset regression to determine the top 12 variables (for each guild species richness model) to be considered in the hierarchical partitioning. The calculation was carried out in R (R Development Core Team 2012) using the *hier.part* library (Walsh and Mac Nally 2008). Because we included more than 9 variables, the hierarchical partitioning was carried out 1000 times, randomly permuting the variable order each time, in order to compensate for a known rounding error in the computation (Olea et al. 2010).

Results

Correlation

As expected, there was substantial correlation among the variables in the candidate explanatory variable pool. After ranking the texture measures by univariate R^2 (results not shown) and removing lower ranking variables from all variable pairs with correlation coefficient

$|r| > 0.6$, 8 of 80 texture measures were retained for further analysis (Table 4-1). The retained variables included two first-order and six second-order measures.

We then fitted univariate models for species richness of each guild as a function of each of the retained texture variables and the other candidate explanatory variables (Table 4-2). These models revealed many strong relationships. Mean of fPAR annual sum, mean canopy height, standard deviation of canopy height, and mean of 5x5 band 3 mean each had an R^2 value > 0.50 for one of the seven guilds. Mean of fPAR annual minimum, mean of fPAR annual seasonality, mean biomass, standard deviation of biomass, and proportion deciduous forest had an R^2 value > 0.30 for at least one guild. A correlation matrix was calculated for these 37 variables (not shown), and for variable pairs with a correlation coefficient $|r| > 0.6$ the variable with the lowest univariate R^2 values was dropped from further analysis. This yielded 23 remaining variables (Table 4-3), including 3 productivity variables, 3 climatic stability variables, and 17 habitat structure variables. The retained variables included 9 of 14 landcover composition metrics, 0 of 6 landcover configuration metrics, ecoregion province, 4 of 6 fPAR measures, 1 of 32 first-order texture measures, 6 of 48 second-order texture measures, 1 of 6 canopy height/biomass variables, and 1 of 2 elevation variables.

Best Subset Analysis

The results of the best subset regression analysis (Figure 4-3) showed that some variables were included in the best models with much higher frequency than others. Of the productivity variables, mean fPAR sum and standard deviation of fPAR minimum were frequently included in models for nearly all guilds. Mean elevation was a top 12 variable for 4 of the seven guilds, but it was much less frequently included than other variables. Of climatic stability measures, mean of fPAR seasonality ranked in the top 12 variables for all guilds and was very frequently included in those models. Standard deviation of fPAR seasonality and ecoregion province ranked in the top 12 variables in only 4 and 2 guilds, respectively, and were much less frequently included. Of the measures of habitat structure, landcover composition metrics performed well, with proportion deciduous forest, proportion evergreen forest, and proportion grassland frequently included in models of most guilds. Among the texture measures, standard deviation of band 2 ASM and mean of band 5 homogeneity ranked in the top 12 for 7 and 5 guilds, respectively, although the number of times these variables were included was less than the top variables in other categories. Of the five other texture measures, four ranked in the top 12 variables of at least one guild, but overall these variables were infrequently included in models.

When considering the results by guild, a few patterns were noticeable. The models for all birds, forest birds, and Neotropical migrants are quite similar, with the most-frequently included variables nearly identical for the three guilds. Proportion deciduous forest was the most frequently included variable for all birds and Neotropical migrants, and the second-most included guild for forest birds. This was expected, as these guilds are dominated by forest-associated birds. Grassland bird models frequently included proportion grassland, proportion pasture, and proportion cultivated crops. Short-distance migrants showed a slightly different pattern than the other guilds, with measures of productivity and climatic stability the three most frequently included variables. Seasonality was key for permanent residents, with mean fPAR seasonality included in 91 of 100 models.

Overall the models showed some balance between measures of productivity, climatic stability, and habitat structure. All guilds except for shrubland birds had at least one variable from each of the three groups included in 50 (out of 100) or more models. Shrubland birds had a comparatively weaker response to measures of productivity and climatic stability. Among highly-included variables, productivity variables were included in at least 70 of 100 models for a given guild 3 times, climatic stability 4 times, and habitat structure 5 times.

Hierarchical Partitioning Analysis

Hierarchical partitioning analysis (Figure 4-4) showed similar results to best-subsets selection overall, but there were some noticeable differences. Measures of productivity were again shown be important in models of species richness across all guilds, this was especially apparent for mean fPAR sum and standard deviation of fPAR Minimum. The contribution of measures of climatic stability was much lower than expected based on the best subset results. In the best subsets regression, mean fPAR seasonality was the strongest measure of climatic stability, and was included in models with frequency similar to productivity measures. In hierarchical partitioning, mean fPAR seasonality still had some contribution across all guilds, but the magnitude was much lower than measures of productivity. The notable exception was the independent contribution for the permanent residents model, which remained very high. Among habitat structure measures, proportion deciduous forest remained a key variable, outranking all other habitat structure variables in independent contribution for all birds, forest birds, shrubland birds, and Neotropical migrants. Proportion grassland remained important as the habitat structure variable with the highest and second-highest independent contribution for grassland bird and shrubland bird models, respectively. Assorted texture variables had moderate independent contribution values for different guild models, but none performed exceptionally.

To gain insight into overall variable explanatory contribution, the independent contribution of each variable was summed across the seven models (Table 4-4). Mean fPAR sum was clearly the most dominant variable with a total independent contribution of 98.1. Proportion deciduous forest, standard deviation of fPAR minimum, and mean fPAR seasonality were the next strongest variables with total independent contributions in the range 66.7-69.8. When these independent contribution values are summed by variable category (Table 4-5), habit structure measures have the highest total independent contribution with 417.5, followed by productivity with 190.6, and climatic stability with 91.9, though it is important to note that there were substantially more habitat structure variables (17) than productivity (3) or climatic stability (3).

Total independent contribution by variable category and guild (Figure 4-5), also showed habitat structure to be dominant over productivity and climatic stability. In all birds, forest birds, Neotropical migrants, and short-distance migrants, habitat structure accounted for 60-70% of the total independent contribution, productivity 20-35%, and climatic stability less than 10%. In shrubland birds, habitat structure was even more dominant, with 80% of the independent contribution, compared to roughly 10% each for productivity and climatic stability. The contribution of different variable categories was more balanced for grassland birds, with habitat structure still the highest at 51%, but productivity and climatic stability contributing 28% and 22% respectively. Permanent residents had the most balanced contribution across variable categories, as the only guild where habitat structure was not the highest-contributing category.

For this guild, productivity variables contributed 36%, climatic stability 32% and habitat structure 32%.

The adjusted R^2 values of the final models for each guild (including the 12 top-performing explanatory variables) varied widely by guild. The model for forest birds was the strongest with an adjusted R^2 of 0.67. The grassland birds and Neotropical migrant models had the next highest adjusted R^2 values of 0.59 and 0.53, respectively. The models for all species and permanent residents each had an adjusted R^2 value of 0.45. The shrubland birds and short-distance migrant models were the weakest, with adjusted R^2 values of 0.29 and 0.21, respectively.

Discussion

We found that measures of productivity, climatic stability, and habitat structure, when considered jointly, all played a role in explaining nationwide avian species richness patterns for all birds, three habitat guilds, and three migratory habit guilds. Of the five variables with the highest independent contribution to models of avian species richness, two were measures of productivity, one was a measure of climatic stability, and two were measures of habitat structure. Though all three of these measures contributed explanatory power, our analysis found measures of habitat structure to be most important overall, followed by productivity, then climatic stability. This ranking held in models of all guilds except permanent residents, where productivity variables had the largest independent contribution, followed by climatic stability and then habitat structure.

There was mixed support for our first hypothesis: that even when combined, variables representing productivity, climatic stability and habitat structure would all make a contribution to the explanation of avian species richness. Considering all variables, habitat structure was clearly a dominant factor in our results (Figure 4-5), but measures of productivity, and, to a lesser extent, climatic stability also made contributions. Climatic stability measures were particularly important in species richness models of grassland birds and permanent residents. When considering individual variables, the fact that variables from all three categories ranked in the top five (Table 4-4) supports our prediction of complementarity, especially considering that there were substantially more variables representing habitat structure than productivity or climatic stability.

On the other hand, comparison of coefficients of determination between these models and those in Chapter 3 tells a somewhat different story. In Chapter 3, we followed a similar statistical approach, but included only measures of habitat structure. The final habitat structure-based models of species richness from Chapter 3 for all birds, forest birds, shrubland birds, Neotropical migrants, and short-distance migrants yielded adjusted R^2 values within 0.03 of the corresponding models from this analysis. The grassland bird species richness model showed improvement over the habitat structure-only model, increasing in adjusted R^2 from 0.48 to 0.59. The standout model was that for permanent resident species richness, where adjusted R^2 more than doubled from the habitat structure- only model (0.45 versus 0.20). The strong improvement in models of grassland bird and permanent resident richness with the addition of measures of productivity and climatic stability indicate complementarity in these cases. In contrast, the lack of improvement for the other guilds indicates that measures of productivity and climatic stability failed to introduce additional explanatory power. One possible explanation for this is the relationship between mean canopy height and mean fPAR sum. In Chapter 3, standard deviation of canopy height and mean canopy height were the explanatory variables with the highest and second-highest independent contribution of habitat structure variables. In this Chapter (Chapter 4), mean canopy height and standard deviation of canopy height were excluded from analysis because they were highly correlated with mean fPAR sum ($r = 0.78$ and $r = 0.75$, respectively), our primary measure of productivity. This indicates that the reduction in explanatory power from removing the canopy height variables was offset by the explanatory power of mean fPAR sum with little net change, thus these variables appear to be redundant. It is clear these variables are confounded, as areas with high canopy height have high productivity (and conversely, areas with high productivity are capable of supporting high canopy height). It is difficult to determine if the birds are responding more to the increased structural complexity with the higher canopy height, the high level of productivity, or both.

We predicted that because we were modeling avian species richness at a fine scale (that of a BBS route), habitat structure variables would be the most important (prediction 2), since measures of habitat structure have been shown to be more influential at a local scale, while productivity and climatic stability are stronger drivers at a regional scale (Mackey and Lindenmayer 2001, Pearson and Dawson 2003). We found this to be the case, with habitat structure variables making the strongest contribution to models for six of seven guilds (Figure 4-5). It is important to note though, that the magnitude of this difference may be inflated since we had many more variables representing habitat structure than productivity or climatic stability. Though productivity and climatic stability appeared less influential at this scale, it was important to include them because models of species richness and species distribution that include environmental predictors for various scales have higher accuracy, even if the scale of different predictors is not explicitly considered (Meyer and Thuiller 2006).

Our third prediction was that habitat-based guild models would be strongly influenced by the proportion of the relevant habitat type, and that proportion deciduous forest and measures of canopy height would have strong positive relationships to species richness for all birds, forest birds, and Neotropical migrants. Proportion forest and proportion grassland did have a strongly positive relationship to forest bird and grassland bird species richness, respectively, but shrubland bird species richness was not significantly related to proportion scrub shrub (Table 4-2). Proportion deciduous forest, mean canopy height, and standard deviation of canopy height had very strong, positive univariate relationships with species richness of all birds, Neotropical migrants, and forest birds, however, as previously mentioned, the two canopy height measures were highly correlated with mean sum of fPAR, and were thus excluded from multivariate analysis. These findings concur with our findings from Chapter 3.

Prediction four stated that permanent residents would have a strong negative relationship with seasonality and a positive relationship with annual minimum productivity, while Neotropical and short-distance migrants would have a weak relationship with these variables. Univariate models (Table 4-2) showed this to be conclusively true, with permanent residents species richness showing a significant positive relationship to mean of fPAR annual minimum ($R^2 = 0.34$) and a significant negative relationship with mean of fPAR annual seasonality ($R^2 = 0.30$), while relationships with the other two migratory guilds were negligible (R^2 values from 0.00 to 0.05). In the multivariate models (Figure 4-4), mean of fPAR seasonality had a much higher independent contribution to permanent resident richness (23.5) than Neotropical (5.8) or short-distance migrant richness (8.2). Mean of fPAR annual minimum was excluded from multivariate analysis due to correlation with mean of fPAR sum, but the independent contribution of standard deviation of fPAR annual minimum was higher for permanent residents (14.0) than Neotropical (5.4) or short-distance migrants (8.4). Our findings concur with both the expectations and findings of Coops (2009), which was expected since we used the same measures of fPAR in our study. The distinction is that we modeled species richness at the BBS route level as compared to regional species richness.

Our final prediction was that total productivity would be strongly and positively associated with species richness of all guilds except shrubland birds, as shrublands are areas of relatively low vegetative productivity. Our results were mostly in support of this prediction. Species richness in all seven guilds was significantly related to mean of fPAR annual sum with strong, positive relationships for all birds, Neotropical migrants, permanent residents, and forest birds (R^2 from 0.21 to 0.54), weak positive relationships for short-distance migrants and shrubland birds (R^2 of 0.07 and 0.09 respectively, and surprisingly, a strong negative relationship with grassland birds ($R^2 = 0.28$). The relationship with shrubland birds was as expected, but the response of grassland birds was a surprise. It is likely that the negative relationship is due to grasslands having lower productivity than forested areas, with grassland birds obviously being more associated with the former. In our multivariate models (Figure 4-4), mean of fPAR sum was the variable with the highest overall contribution, and as expected, it was strongly related to all guilds except shrubland birds, where it had been previously excluded for not ranking in the top 12 variables in the best subsets analysis. This finding stands in contrast to Coops (2009) who found that, at the regional level, seasonal variability was as stronger driver of species richness than annual fPAR sum. We did find that seasonality was more important than productivity for permanent residents, and the two measures had similar contributions for grassland birds, but for the other guilds, productivity (mean fPAR sum) had a substantially higher independent contribution than mean fPAR seasonality. It is not clear what would cause this difference between a regional and local scale analysis.

Among the seven guilds, contribution of variables for models of grassland bird and permanent resident species richness stood out as dissimilar from the other guilds. As already discussed in relation to our fourth prediction, in the permanent resident species richness model, measures of productivity and climatic stability had higher independent contributions than measures of habitat structure, in contrast to all other guilds. This is logical as permanent residents are more influenced by extreme conditions since they are present in their breeding area year-round, in contrast to Neotropical and short-distance migrants. Grassland bird richness models also had high independent contribution from measures of climatic stability, primarily mean fPAR seasonality (which showed a strong, positive univariate relationship with grassland bird species richness). This is somewhat puzzling, as one might expect grassland bird species richness to be negatively associated with seasonality, as grasslands provide little buffer against weather conditions (e.g., as opposed to forests).

We modeled patterns of avian species richness for multiple guilds at a fine-scale across the contiguous United States as a function of productivity, climatic stability, and productivity. We showed that measures of all three factors were important, though at our scale of analysis (BBS route level), habitat structure was clearly dominant for all guilds (except permanent residents), followed by productivity, then climatic stability. For models of permanent resident species richness, measures of productivity had the highest independent contribution, followed by climatic stability, then habitat structure. Future studies of spatial patterns of biodiversity will benefit from the inclusion of environmental variables representing productivity, climatic stability, and habitat structure.

References

Albright T. P., A. M. Pidgeon, C. D. Rittenhouse, M. K. Clayton, C. H. Flather, P. D. Culbert, and V. C. Radeloff. 2011. Heat waves measured with MODIS land surface temperature data predict changes in avian community structure. Remote Sensing of Environment 115:245-254.

Albright T. P., A. M. Pidgeon, C. D. Rittenhouse, M. K. Clayton, C. H. Flather, P. D. Culbert, B. D. Wardlow, and V. C. Radeloff. 2010. Effects of drought on avian community structure. Global Change Biology 16:2158-2170.

Atauri J. A., J. V. de Lucio. 2001. The role of landscape structure in species richness distribution of birds, amphibians, reptiles and lepidopterans in Mediterranean landscapes. Landscape Ecology 16:147-159.

Bailey R. G. 1995. Description of the Ecoregions of the United States. United States Department of Agriculture.

Baraldi A., F. Parmiggiani. 1995. An investigation of the textural characteristics associated with gray-level cooccurrence matrix statistical parameters. IEEE Transactions on Geoscience and Remote Sensing 33:293-304.

Chevan A., M. Sutherland. 1991. Hierarchical partitioning. American Statistician 45:90-96.

Clawges R., K. Vierling, L. Vierling, and E. Rowell. 2008. The use of airborne lidar to assess avian species diversity, density, and occurrence in a pine. Remote Sensing of Environment 112:2064-2073.

Connell J. H. 1978. Diversity in tropical rain forests and coral reefs - high diversity of trees and corals is maintained only in a non-equilibrium state. Science 199:1302-1310.

Coops N. C., R. H. Waring, M. A. Wulder, A. M. Pidgeon, and V. C. Radeloff. 2009. Bird diversity: a predictable function of satellite-derived estimates of seasonal variation in canopy light absorbance across the United States. Journal of Biogeography 36:905-918.

Culbert P. D., A. M. Pidgeon, V. St-Louis, D. Bash, and V. C. Radeloff. 2009. The impact of phenological variation on texture measures of remotely sensed imagery. IEEE Journal of Selected Topics in Applied Earth Observations and Remote Sensing 2:299-309.

Culbert P. D., V. C. Radeloff, V. St-Louis, C. H. Flather, C. D. Rittenhouse, T. P. Albright, and A. M. Pidgeon. 2012. Modeling broad-scale patterns of avian species richness across the Midwestern United States with measures of satellite image texture. Remote Sensing of Environment 118:140-150.

Currie D. J. 1991. Energy and large-scale patterns of animal-species and plant-species richness. American Naturalist 137:27-49.

Currie D. J., G. G. Mittelbach, H. V. Cornell, R. Field, J. F. Guegan, B. A. Hawkins, D. M. Kaufman, J. T. Kerr, T. Oberdorff, E. O'Brien, and J. R. G. Turner. 2004. Predictions and tests of climate-based hypotheses of broad-scale variation in taxonomic richness. Ecology Letters 7:1121-1134.

Donovan T. M., C. H. Flather. 2002. Relationships among North American songbird trends, habitat fragmentation, and landscape occupancy. Ecological Applications 12:364-374.

Erdelen M. 1984. Bird Communities and Vegetation Structure .1. Correlations and comparisons of simple and diversity indexes. Oecologia 61:277-284.

Evans K. L., P. H. Warren, and K. J. Gaston. 2005. Species-energy relationships at the macroecological scale: a review of the mechanisms. Biological Reviews 80:1-25.

Farina A. 1997. Landscape structure and breeding bird distribution in a sub-Mediterranean agro-ecosystem. Landscape Ecology 12:365-378.

Fischer A. G. 1960. Latitudinal variations in organic diversity. Evolution 14:64-81.

Fjeldsa J., J. C. Lovett. 1997. Biodiversity and environmental stability. Biodiversity and Conservation 6:315-323.

Fjeldsa J., D. Ehrlich, E. Lambin, and E. Prins. 1997. Are biodiversity 'hotspots' correlated with current ecoclimatic stability? A pilot study using the NOAA-AVHRR remote sensing data. Biodiversity and Conservation 6:401-422.

Flather C. H., J. R. Sauer. 1996. Using landscape ecology to test hypotheses about large-scale abundance patterns in migratory birds. Ecology 77:28-35.

Gaston K. J. 2000. Global patterns in biodiversity. Nature 405:220-227.

Guinet C., P. Jouventin, and J. Malacamp. 1995. Satellite remote-sensing in monitoring change of seabirds - use of spot image in king penguin population increase at Ile-Aux-Cochons, Crozet Archipelago. Polar Biology 15:511-515.

Hines J. E., T. Boulinier, J. D. Nichols, J. R. Sauer, and K. H. Pollock. 1999. COMDYN: software to study the dynamics of animal communities using a capture-recapture approach. Bird Study 46:209-217.

Homer C., C. Q. Huang, L. M. Yang, B. Wylie, and M. Coan. 2004. Development of a 2001 Nnational land-cover database for the United States. Photogrammetric Engineering and Remote Sensing 70:829-840.

Hurlbert A. H., J. P. Haskell. 2003. The effect of energy and seasonality on avian species richness and community composition. American Naturalist 161:83-97.

Innes J. L., B. Koch. 1998. Forest biodiversity and its assessment by remote sensing. Global Ecology and Biogeography 7:397-419.

Kayitakire F., C. Hamel, and P. Defourny. 2006. Retrieving forest structure variables based on image texture analysis and IKONOS-2 imagery. Remote Sensing of Environment, 102:390-401.

Kellndorfer J., W. Walker, L. LaPoint, J. Bishop, T. Cormier, G. Fiske, and K. Kirsch. 2011. The National Biomass and Carbon Dataset - A hectare-scale dataset of vegetation height, aboveground biomass and carbon stock of the conterminous United States. Data Published by the Woods Hole Research Center http://whrc.org/nbcd.

Kerr J. T., M. Ostrovsky. 2003. From space to species: ecological applications for remote sensing. Trends in Ecology & Evolution 18:299-305.

Klopfer P. H. 1959. Environmental determinants of faunal diversity. The American Naturalist 93:337-342.

Kondo T., N. Nakagoshi. 2002. Effect of forest structure and connectivity on bird distribution in a riparian landscape. Phytocoenologia 32:665-676.

Krauss J., I. Steffan-Dewenter, and T. Tscharntke. 2003. How does landscape context contribute to effects of habitat fragmentation on diversity and population density of butterflies? Journal of Biogeography 30:889-900.

Laurent E. J., H. Shi, D. Gatziolis, J. P. LeBouton, M. B. Walters, and J. Liu. 2005. Using the spatial and spectral precision of satellite imagery to predict wildlife occurrence patterns. Remote Sensing of Environment 97:249-262.

Lindeman R. L. 1942. The trophic-dynamic aspect of ecology. Ecology 23:399-418.

MacArthur R., H. Recher, and M. Cody. 1966. On the relation between habitat selection and species diversity. The American Naturalist 100:319-332.

MacArthur R. H. 1972. Geographical Ecology: Patterns in the Distribution of Species. Harper & Row.

MacArthur R. H. 1969. Species packing, and what interspecies competition minimizes. Proceedings of the National Academy of Sciences of the United States of America 64:1369.

MacArthur R. H., E. O. Wilson. 1967. The Theory of Island Biogeography. Princeton University Press, Princeton, NJ.

MacArthur R. H., J. W. MacArthur. 1961. On bird species diversity. Ecology 42:594-598.

Mackey B., D. Lindenmayer. 2001. Towards a hierarchical framework for modelling the spatial distribution of animals. Journal of Biogeography 28:1147-1166.

Masek J. G., E. F. Vermote, N. E. Saleous, R. Wolfe, F. G. Hall, K. F. Huemmrich, F. Gao, J. Kutler, and T. K. Lim. 2006. A Landsat surface reflectance dataset for North America, 1990-2000. IEEE Geoscience and Remote Sensing Letters 3:68-72.

Mcgarigal K., W. C. Mccomb. 1995. Relationships between landscape structure and breeding birds in the Oregon coast range. Ecological Monographs 65:235-260.

Meyer C., W. Thuiller. 2006. Accuracy of resource selection functions across spatial scales. Diversity and Distributions 12:288-297.

Miller A. J. 1990. Subset Selection in Regression. Chapman and Hall, London.

Nagendra H. 2001. Using remote sensing to assess biodiversity. International Journal of Remote Sensing 22:2377-2400.

Oindo B. O. 2002a. Patterns of herbivore species richness in Kenya and current ecoclimatic stability. Biodiversity and Conservation 11:1205-1221.

Oindo B. O. 2002b. Predicting mammal species richness and abundance using multi-temporal NDVI. Photogrammetric Engineering and Remote Sensing 68:623-629.

Oindo B. O., R. A. de By, and A. K. Skidmore. 2000. Interannual variability of NDVI and bird species diversity in Kenya. International Journal of Applied Earth Observation and Geoinformation, 2:172-180.

Olea P. P., P. Mateo-Tomas, and A. de Frutos. 2010. Estimating and modelling bias of the hierarchical partitioning public-domain software: implications in environmental management and conservation. Plos One 5:e11698.

Pearlstine L. G., S. E. Smith, L. A. Brandt, C. R. Allen, W. M. Kitchens, and J. Stenberg. 2002. Assessing state-wide biodiversity in the Florida Gap analysis project. Journal of environmental management 66:127-144.

Pearson R., T. Dawson. 2003. Predicting the impacts of climate change on the distribution of species: are bioclimate envelope models useful? Global Ecology and Biogeography 12:361-371.

Pianka E. R. 1966. Latitudinal gradients in species diversity - a review of concepts. American Naturalist 100:33-46.

Pidgeon A. M., V. C. Radeloff, C. H. Flather, C. A. Lepczyk, M. K. Clayton, T. J. Hawbaker, and R. B. Hammer. 2007. Associations of forest bird species richness with housing and landscape patterns across the USA. Ecological Applications 17:1989-2010.

Preston F. W. 1962. The canonical distribution of commonness and rarity: part I. Ecology 43:185-215.

R Development Core Team. 2012. R: A language and environment for statistical computing. V. 2.15.

Rabus B., M. Eineder, A. Roth, and R. Bamler. 2003. The shuttle radar topography mission - a new class of digital elevation models acquired by spaceborne radar. ISPRS Journal of Photogrammetry and Remote Sensing 57:241-262.

Rittenhouse C. D., A. M. Pidgeon, T. P. Albright, P. D. Culbert, M. K. Clayton, C. H. Flather, C. Huang, J. G. Masek, and V. C. Radelof. 2010. Avifauna response to hurricanes: regional changes in community similarity. Global Change Biology 16:905-917.

Rosenzweig M. L. 1995. Species Diversity in Space and Time. Cambridge University Press.

Rotenberry J. T., J. A. Wiens. 1980. Habitat structure, patchiness, and avian communities in North-American steppe Vvegetation - a multivariate-analysis. Ecology 61:1228-1250.

Rowhani P., C. A. Lepczyk, M. A. Linderman, A. M. Pidgeon, V. C. Radeloff, P. D. Culbert, and E. F. Lambin. 2008. Variability in energy influences avian distribution patterns across the USA. Ecosystems 11:854-867.

Roy P. S. 2003. Biodiversity conservation - perspective from space. National Academy Science Letters-India 26:169-184.

Sanders H. L. 1968. Marine benthic diversity - a comparative study. American Naturalist 102:243-282.

Schoener T. W. 1989. Food webs from the small to the large. Ecology 70:1559-1589.

Sellers P. J., R. E. Dickinson, D. A. Randall, A. K. Betts, F. G. Hall, J. A. Berry, G. J. Collatz, A. S. Denning, H. A. Mooney, C. A. Nobre, N. Sato, C. B. Field, and A. Henderson-Sellers. 1997. Modeling the exchanges of energy, water, and carbon between continents and the atmosphere. Science 275:pp. 502-509.

Shannon C. E. 1948. A mathematical theory of communication. Bell System Technical Journal 27:379-423 and 623-656.

Sousa W. P. 1984. The role of disturbance in natural communities. Annual Review of Ecology and Systematics 15:353-391.

Sousa W. P. 1979. Disturbance in marine inter-tidal boulder fields - the non-equilibrium maintenance of species-diversity. Ecology 60:1225-1239.

Stevens G. C. 1992. The Elevational Gradient in Altitudinal Range: An Extension of Rapoport's Latitudinal Rule to Altitude. The American Naturalist 140:893.

St-Louis V., A. M. Pidgeon, V. C. Radeloff, T. J. Hawbaker, and M. K. Clayton. 2006. High-resolution image texture as a predictor of bird species richness. Remote Sensing of Environment 105:299-312.

St-Louis V., A. M. Pidgeon, M. K. Clayton, B. A. Locke, D. Bash, and V. C. Radeloff. 2009. Satellite image texture and a vegetation index predict avian biodiversity in the Chihuahuan Desert of New Mexico. Ecography 32:468-480.

Sutherland G. D., A. S. Harestad, K. Price, and K. P. Lertzman. 2000. Scaling of natal dispersal distances in terrestrial birds and mammals. Conservation Ecology 4:16.

Tews J., U. Brose, V. Grimm, K. Tielborger, M. C. Wichmann, M. Schwager, and F. Jeltsch. 2004. Animal species diversity driven by habitat heterogeneity. Journal of Biogeography 31:79-92.

The MathWorks I. 1984-2010. Matlab. R2010a:.

Tittler R., M. Villard, and L. Fahrig. 2009. How far do songbirds disperse? Ecography 32:1051-1061.

Tucker C. J., D. M. Grant, and J. D. Dykstra. 2004. NASA's global orthorectified landsat data set. Photogrammetric Engineering and Remote Sensing 70:313-322.

USGS Patuxent Wildlife Research Center. 2008. North American Breeding Bird Survey ftp data set, version 2008.0.

Vega-Garcia C., E. Chuvieco. 2006. Applying local measures of spatial heterogeneity to Landsat-TM images for predicting wildfire occurrence in mediterranean landscapes. Landscape Ecology 21:595-605.

Vogt P. 2010. GUIDOS. 1.3.

Wallace A. R. 1878. Tropical Nature and Other Essays. MacMillan, London.

Walsh C., R. Mac Nally. 2008. hier.part: Hierarchical Partitioning. R package version 1.0-3:.

Williams C. B. 1943. Area and the number of species. Nature 152:264-267.

Willson M. F. 1974. Avian community organization and habitat structure. Ecology 55:1017-1029.

Wood E. M., A. M. Pidgeon, V. C. Radeloff, and N. S. Keuler. 2012. Image texture as a remotely sensed measure of vegetation structure. Remote Sensing of Environment 121:516-526.

Wright D. H. 1983. Species-energy theory - an extension of species-area theory. Oikos 41:496-506.

Tables

Table 4-1. Texture variables calculated from Landsat imagery. Based on correlation analysis, 72 variables (marked "-") were excluded from subsequent analysis, and 8 variables (marked "X") were retained.

Texture	Landsat Band			
	2	3	4	5
Mean of 5x5 Mean	-	X	-	-
Mean of 21x21 Mean	-	-	-	-
Standard Deviation of 5x5 Mean	-	X	-	-
Standard Deviation of 21x21 Mean	-	-	-	-
Mean of 5x5 Standard Deviation	-	-	-	-
Mean of 21x21 Standard Deviation	-	-	-	-
Standard Deviation of 5x5 Standard Deviation	-	-	-	-
Standard Deviation of 21x21 Standard Deviation	-	-	-	-
Mean of 5x5 Angular Second Moment	-	-	X	-
Standard Deviation of 5x5 Angular Second Moment	X	-	-	-
Mean of 5x5 Contrast	-	-	-	-
Standard Deviation of 5x5 Contrast	-	-	-	-
Mean of 5x5 Correlation	-	X	X	-
Standard Deviation of 5x5 Correlation	-	X	-	-
Mean of 5x5 Entropy	-	-	-	-
Standard Deviation of 5x5 Entropy	-	-	-	-
Mean of 5x5 Homogeneity	-	-	-	X
Standard Deviation of 5x5 Homogeneity	-	-	-	-
Mean of 5x5 Sum of Squares Variance	-	-	-	-
Standard Deviation of 5x5 Sum of Squares Variance	-	-	-	-

Table 4-2. R^2 values for univariate models of species richness. Sign indicates direction of relationship. *** p-value < 0.001, ** p-value < 0.01, * p-value < 0.05. Values > 0.15 bolded for emphasis. Struck-through variable names indicate variables dropped from subsequent analysis due to low R^2 values or correlation with other variables.

	All Species	Neotropical Migrants	Permanent Residents	Short-Distance Migrants	Forest Birds	Grassland Birds	Shrubland Birds
~~Proportion Water~~	0.00(+)*	0.00(+)**	0.00(+)	0.00(+)	0.01(+)***	0.01(-)***	0.00(-)
~~Proportion Ice~~	0.00(+)	0.00(+)	0.00(-)	0.00(+)	0.00(+)	0.00(-)**	0.00(-)
~~Proportion Developed~~	0.00(+)*	0.00(+)*	0.01(+)***	0.00(+)*	0.02(+)***	0.02(-)***	0.00(+)***
Proportion Barren	0.05(-)***	0.04(-)***	0.02(-)***	0.03(-)***	0.05(-)***	0.00(-)**	0.01(-)***
Proportion Deciduous Forest	**0.25(+)*** **	**0.34(+)*** **	0.02(+)***	0.05(+)***	**0.34(+)*** **	0.06(-)***	0.10(+)***
Proportion Evergreen Forest	0.03(+)***	0.01(+)***	0.03(+)***	0.02(+)***	0.06(+)***	**0.15(-)*** **	0.00(+)
Proportion Mixed Forest	0.08(+)***	0.12(+)***	0.00(+)**	0.01(+)***	0.13(+)***	0.08(-)***	0.00(+)***
~~Proportion Scrub Shrub~~	0.12(-)***	**0.16(-)*** **	0.00(-)	0.07(-)***	**0.25(-)*** **	0.00(+)	0.00(+)'
Proportion Grassland	0.09(-)***	0.09(-)***	0.05(-)***	0.03(-)***	**0.16(-)*** **	**0.20(+)*** **	0.09(-)***
Proportion Pasture	0.03(+)***	0.03(+)***	0.03(+)***	0.02(+)***	0.05(+)***	0.00(-)	0.02(+)***
Proportion Cultivated Crops	0.02(-)***	0.02(-)***	0.06(-)***	0.00(+)*	0.03(-)***	**0.18(+)*** **	0.03(-)***
Proportion Woody Wetland	0.00(+)**	0.00(+)***	0.02(+)***	0.00(-)**	0.03(+)***	0.05(-)***	0.00(-)**
~~Proportion Herbaceous Wetland~~	0.01(-)***	0.01(-)***	0.00(-)*	0.01(-)***	0.01(-)***	0.00(+)	0.02(-)***
Number of Classes	0.12(+)***	0.13(+)***	0.01(+)***	0.05(+)***	**0.15(+)*** **	0.01(-)***	0.01(+)***
~~Shannon Diversity of Landcover Classes~~	0.13(+)***	0.13(+)***	0.05(+)***	0.05(+)***	**0.22(+)*** **	0.06(-)***	0.02(+)***
~~Mean Canopy Height~~	**0.29(+)*** **	**0.31(+)*** **	0.07(+)***	0.07(+)***	**0.51(+)*** **	**0.34(-)*** **	0.06(+)***
~~Standard Deviation of Canopy Height~~	**0.32(+)*** **	**0.25(+)*** **	0.13(+)***	**0.17(+)*** **	**0.53(+)*** **	**0.25(-)*** **	0.12(+)***

Coefficient of Variation of Canopy Height	0.07(-)***	0.06(-)***	0.02(-)***	0.04(-)***	0.09(-)***	0.03(+)***	0.03(-)***
~~Mean Biomass~~	**0.23(+)*****	**0.25(+)*****	0.04(+)***	0.07(+)***	**0.40(+)*****	**0.22(-)*****	0.07(+)***
~~Standard Deviation of Biomass~~	**0.18(+)*****	0.12(+)***	0.08(+)***	0.10(+)***	**0.32(+)*****	**0.23(-)*****	0.06(+)***
~~Coefficient of Variation of Biomass~~	0.07(-)***	0.06(-)***	0.02(-)***	0.04(-)***	0.10(-)***	0.03(+)***	0.03(-)***
~~Mean of 5x5 Band 3 Mean~~	**0.33(-)*****	**0.34(-)*****	0.05(-)***	0.15(-)***	**0.52(-)*****	**0.09(+)*****	0.05(-)***
Standard Deviation of 5x5 Band 3 Mean	**0.14(-)*****	**0.19(-)*****	0.01(-)***	0.05(-)***	**0.21(-)*****	**0.01(+)*****	0.02(-)***
Mean of 5x5 Band 4 Angular Second Moment	0.12(-)***	0.13(-)***	0.02(-)***	0.04(-)***	**0.16(-)*****	0.03(+)***	0.07(-)***
Standard Deviation of 5x5 Band 2 Angular Second Moment	**0.10(-)*****	**0.08(-)*****	0.03(-)***	0.07(-)***	**0.11(-)*****	0.00(-)**	0.02(-)***
Mean of 5x5 Band 3 Correlation	0.06(-)***	**0.12(-)*****	0.00(-)	0.00(-)*	**0.14(-)*****	0.11(+)***	0.00(-)*
Mean of 5x5 Band 4 Correlation	0.00(-)	0.00(+)	0.03(-)***	0.00(+)'	0.02(-)***	0.08(+)***	0.00(+)
Standard Deviation of 5x5 Band 3 Correlation	0.02(+)***	0.03(+)***	0.00(+)*	0.02(+)***	0.06(+)***	0.00(-)*	0.00(+)
Mean of 5x5 Band 5 Homogeneity	0.05(-)***	0.02(-)***	0.10(-)***	0.02(-)***	0.06(-)***	0.05(+)***	0.07(-)***
Mean of fPAR Annual Sum	**0.28(+)*****	**0.24(+)*****	**0.21(+)*****	0.07(+)***	**0.54(+)*****	**0.28(-)*****	0.09(+)***
~~Standard Deviation of fPAR Annual Sum~~	0.02(+)***	0.00(+)	0.05(+)***	0.02(+)***	0.03(+)***	0.09(-)***	0.01(+)***
~~Mean of fPAR Annual Minimum~~	0.05(+)***	0.01(+)***	**0.34(+)*****	0.00(+)*	**0.17(+)*****	**0.27(-)*****	0.07(+)***
Standard Deviation of fPAR Annual Minimum	0.11(+)***	0.05(+)***	**0.18(+)*****	0.03(+)***	**0.21(+)*****	**0.28(-)*****	0.06(+)***
Mean of fPAR Annual Seasonality	0.00(-)	0.02(+)***	**0.30(-)*****	0.02(+)***	0.01(-)***	**0.22(+)*****	0.05(-)***
Standard Deviation of fPAR Annual Seasonality	0.00(+)***	0.01(+)***	0.03(-)***	0.01(+)***	0.00(+)*	0.01(-)***	0.00(-)***
Mean of SRTM Elevation	**0.04(-)*****	**0.04(-)*****	**0.07(-)*****	0.00(-)***	**0.11(-)*****	**0.11(-)*****	0.02(-)***
~~Standard Deviation of SRTM Elevation~~	0.00(+)	0.00(-)	0.00(-)	0.00(+)*	0.00(-)'	0.00(-)'	0.01(+)***

Table 4-3. Explanatory variables retained after correlation analysis.

Factor	Variable Type	Variable
Productivity	fPAR	Mean fPAR Sum
		Standard Deviation of fPAR Minimum
	Elevation	Mean Elevation
Climatic Stability	fPAR	Mean fPAR Seasonality
		Standard Deviation of fPAR Seasonality
	Ecoregion	Ecoregion Province
Habitat Structure	Landcover Composition	Proportion Barren
		Proportion Deciduous Forest
		Proportion Evergreen Forest
		Proportion Mixed Forest
		Proportion Grassland
		Proportion Pasture
		Proportion Cultivated Crops
		Proportion Woody Wetland
		Number of Landcover Classes
	1st-Order Texture	Standard Deviation of Band 3 Mean
	2nd-Order Texture	Standard Deviation of Band 2 ASM
		Mean Band 4 ASM
		Mean Band 3 Correlation
		Standard Deviation of Band 3 Correlation
		Mean Band 4 Correlation
		Mean of Band 5 Homogeneity
	Canopy Height / Biomass	CV Canopy Height

Table 4-4. The sum of the independent contribution of each variable from hierarchical partition. Independent contribution is summed across the models for all birds, forest birds, grassland birds, shrubland birds, Neotropical migrants, short-distance migrants, and permanent residents.

Rank	Variable	Category	Sum of Independent Contribution
1	Mean fPAR Sum	Productivity	98.1
2	Prop. Deciduous Forest	Habitat Structure	69.8
3	SD fPAR Minimum	Productivity	69.0
4	Mean fPAR Seasonality	Climatic Stability	66.7
5	Prop. Grassland	Habitat Structure	54.2
6	SD Band 2 ASM	Habitat Structure	50.6
7	Mean Band 4 ASM	Habitat Structure	37.7
8	Mean Band 5 Homogeneity	Habitat Structure	36.6
9	Num. Landcover Classes	Habitat Structure	36.1
10	Prop. Evergreen Forest	Habitat Structure	26.5
11	Mean Elevation	Productivity	23.5
12	Prop. Mixed Forest	Habitat Structure	20.0
13	SD fPAR Seasonality	Climatic Stability	16.7
14	Prop. Woody Wetland	Habitat Structure	16.7
15	Prop. Cultivated Crops	Habitat Structure	16.5
16	CV Canopy Height	Habitat Structure	14.0
17	Mean Band 3 Correlation	Habitat Structure	11.7
18	SD Band 3 Correlation	Habitat Structure	9.5
19	SD Band 3 Mean	Habitat Structure	9.1
20	Prop. Pasture	Habitat Structure	8.5
21	Ecoregion Province	Climatic Stability	8.5
22	Prop. Barren	Habitat Structure	0.0
23	Mean Band 4 Correlation	Habitat Structure	0.0

Table 4-5. Sum of independent contribution of explanatory variables by variable category.

Variable Category	Number of Variables	Sum of Independent Contribution
Habitat Structure	17	417.5
Productivity	3	190.6
Climatic Stability	3	91.9

Table 4-6. Adjusted R^2 values of models of avian species richness, by guild, for models including the 12 explanatory variables considered in the hierarchical partitioning analysis.

Guild	Adjusted R^2 Value
All Species	0.45
Forest Birds	0.67
Grassland Birds	0.59
Shrubland Birds	0.29
Neotropical Migrants	0.53
Permanent Residents	0.45
Short-Distance Migrants	0.21

Figures

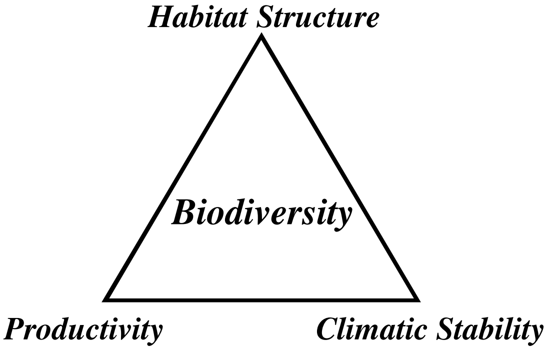

Figure 4-1. Three primary factors influencing biodiversity. Adapted from MacArthur 1972.

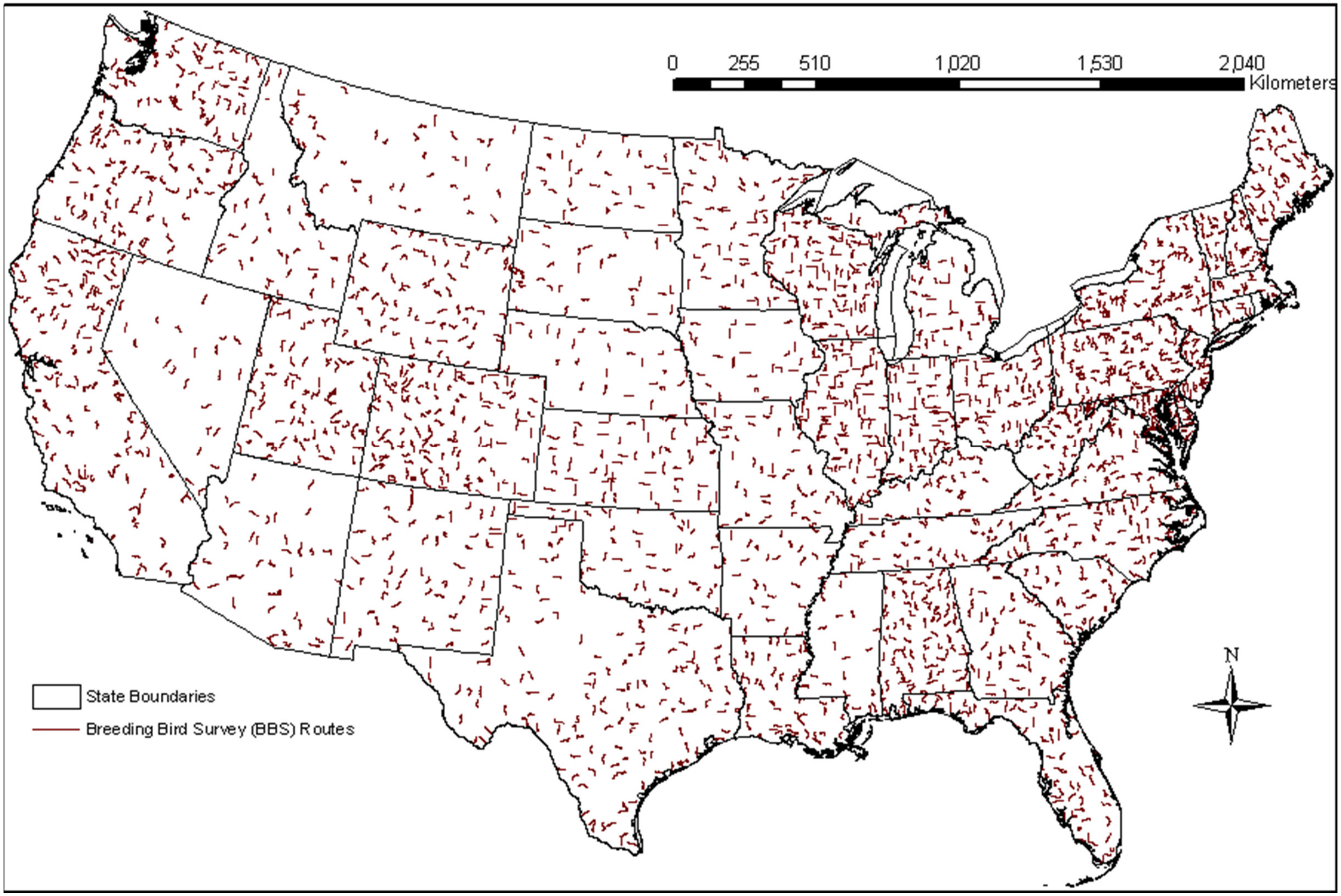

Figure 4-2. Breeding Bird Survey (BBS) routes (2,555) in the contiguous United States used to develop explanatory species richness models.

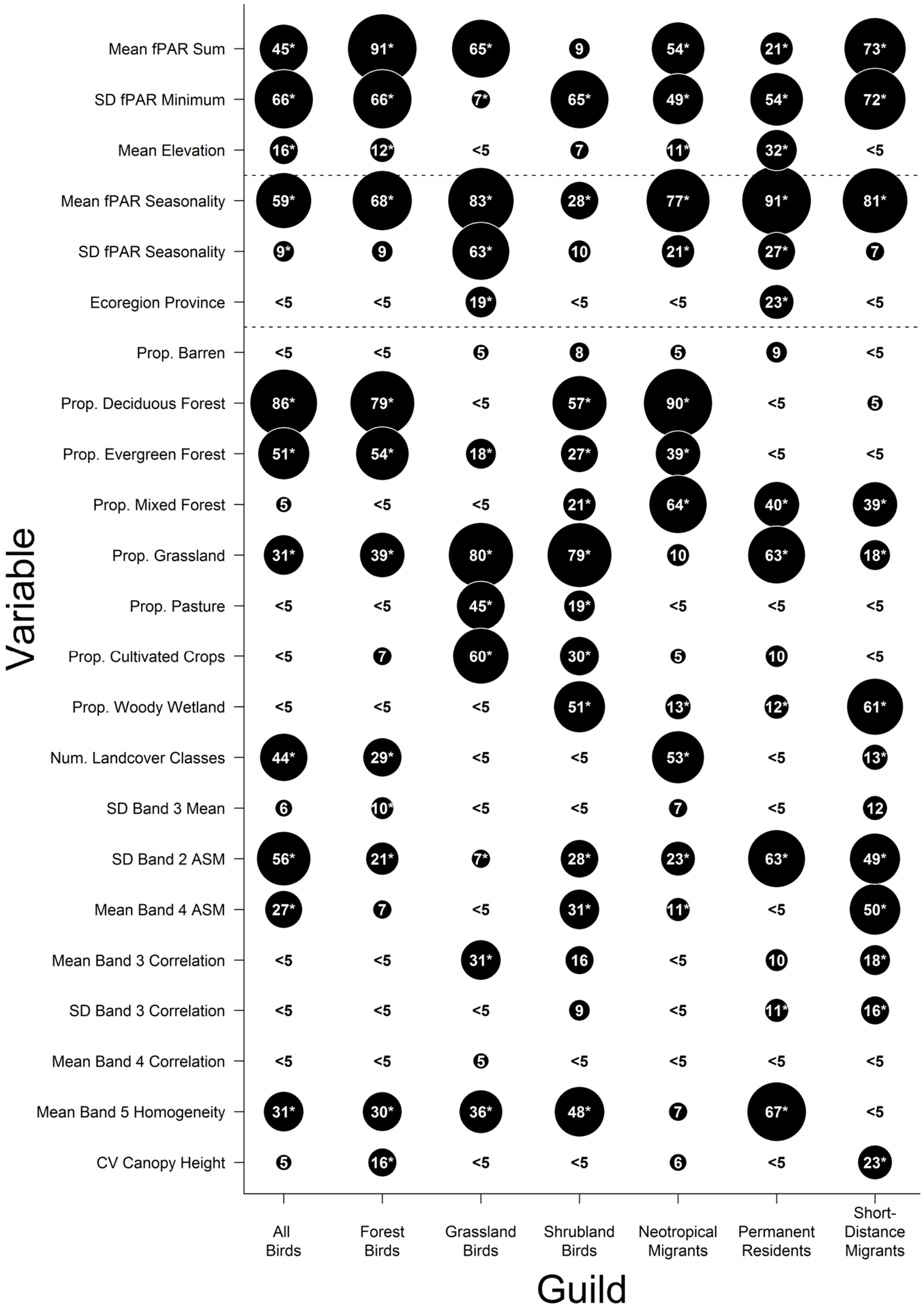

Figure 4-3. Best subsets regression was used to determine the 10 best models for each guild with 1, 2, 3, ..., 10 variables (100 models total). The number of times a variable was included in that guilds models is displayed, with a maximum value of 100. The circle diameter is proportional to the value. Asterisks ("*") indicate the variable ranked in the top 12 for that guild and was retained for further analysis.

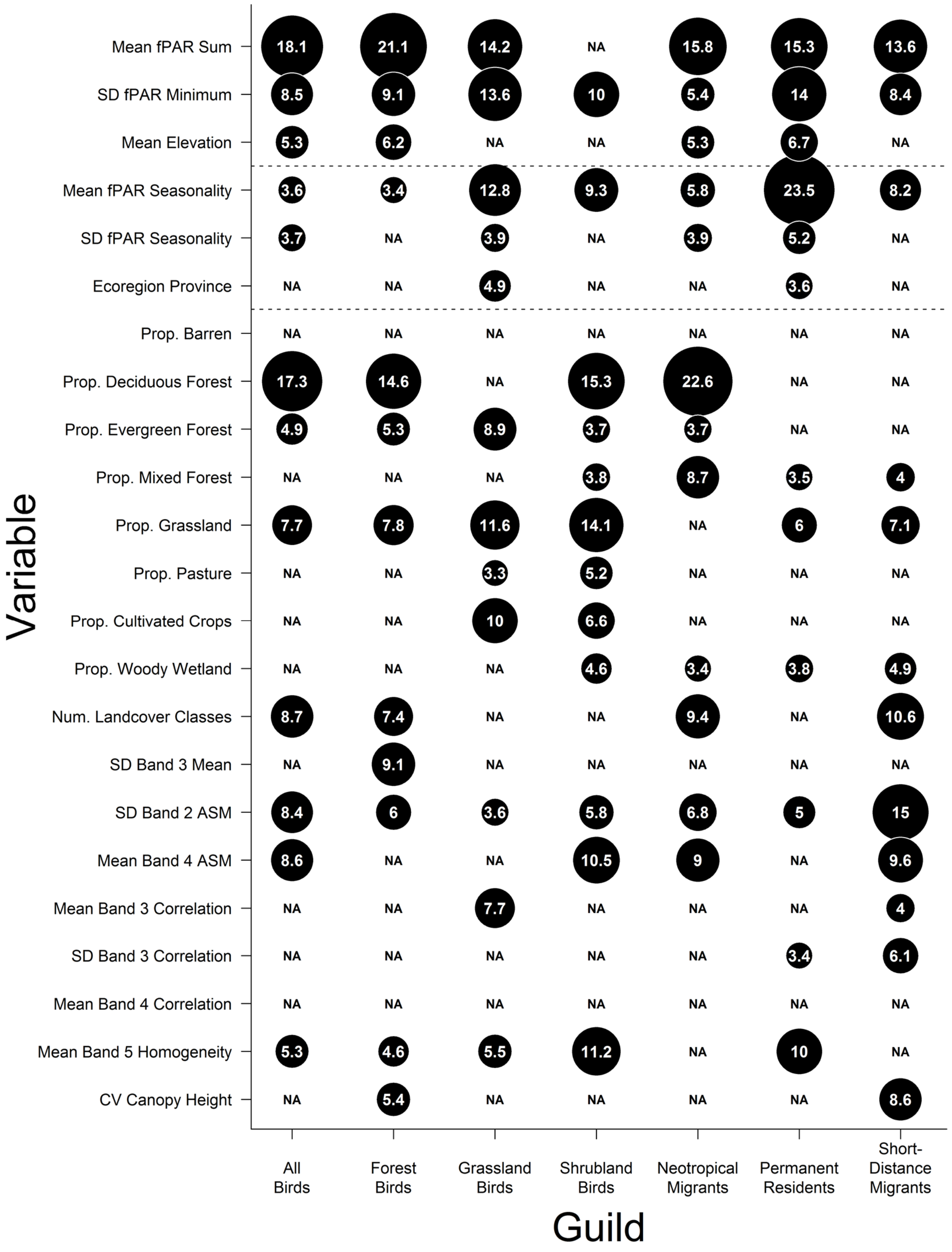

Figure 4-4. Independent contribution of each variable for the given avian guild model, as determined by hierarchical partitioning. Values within each guild sum to 100. Variables not considered in the hierarchical partitioning analysis for a given guild are marked "NA".

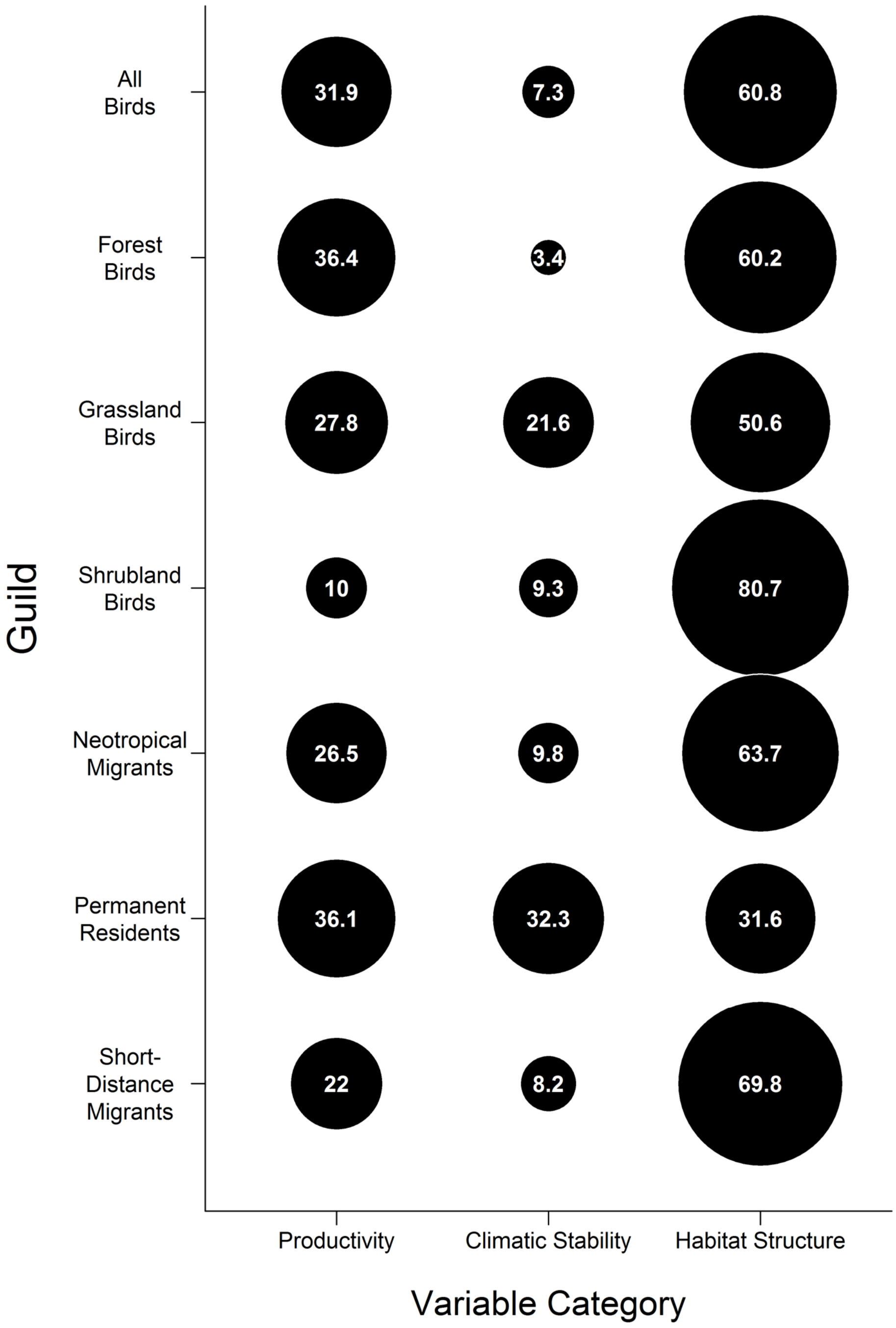

Figure 4-5. Sum of independent contribution of variables in each category (productivity, climatic stability, and habitat structure) by guild.

Chapter 5

Predicted Nationwide Avian Species Richness Maps for the United States

Abstract

Avian biodiversity is threatened, and in order for resource managers to informed conservation decisions, accurate, detailed maps of species richness must be available. We produced fine-scale resolution maps of predicted richness over the contiguous United States for seven avian guilds: all birds, forest birds, grassland birds, shrubland birds, Neotropical migrants, short-distance migrants, and permanent residents. We derived measures of species richness from the Breeding Bird Survey, and modeled richness as a function of remotely sensed measures of productivity, climatic stability, and productivity. We used two machine learning techniques, random forests and support vector regression to derive our predictive models. The random forest models were superior, and were used to create 1-km resolution nationwide maps of species richness, with each 1-km pixel representing the predicted species richness of a hypothetical Breeding Bird Survey centered at that location. Pseudo R^2 values for the predictive models were 0.36 for short-distance migrants, 0.50 for shrubland birds, 0.55 for all birds, 0.60 for Neotropical migrants, 0.66 for permanent residents, 0.68 for grassland birds, and 0.73 for forest birds.

Introduction

Avian biodiversity is under great threat from human-caused habitat conversion (Gaston et al. 2003). With limited resources for habitat conservation, the accurate identification of high-value bird habitat is crucial (Turner et al. 2003). While some mapping of biodiversity has been carried out (Myers et al. 2000, Buckton and Ormerod 2002), the spatial resolution of these maps is too coarse to be of great direct use to resource managers, and available fine-scale maps are based solely on one data source, such as land cover class (Scott et al. 1993, Pearlstine et al. 2002). Additionally, few nationwide maps of biodiversity exist, and those that do employ very coarse resolution (e.g., Dobson et al. 1997). Therefore, a spatially-detailed, nationwide map of avian species richness is needed.

It is also important that research results are shared in a form that is useful in making management decisions. One useful way of conveying information on biodiversity patterns is through maps of expected biodiversity. Issues of scale are of importance in producing maps that are useful for land use and management decisions. On one hand, it is helpful if the same methodology is used over a broad extent so that comparisons may be made at a state or national level. On the other hand, land use planners, resource managers, and land trusts typically work at a local or county scale, so the grain of predicted maps must also be fine enough to inform decisions at these scales. Ideal maps will therefore have broad extent and fine grain.

While different drivers of biodiversity have been heavily studied, these theoretical studies often fail to provide actionable information to land use planners and resource managers. One approach to this issue has been the identification of biodiversity "hot spots", or areas with a high level of endemism as well as habitat loss (Myers et al. 2000, Dobson et al. 1997). While the identification of these hotspots is important, many of these analyses are carried out at a coarse spatial scale. It is also important to recognize all areas of high biodiversity, not only areas where biodiversity is currently threatened. Another approach is the GAP analysis project in which statewide land cover classifications and known species-habitat relationships are used to map species distributions (Scott et al. 1993, Pearlstine et al. 2002). GAP analysis is an important and useful approach to this problem. However, since it is based primarily on land cover classifications, which ignore the continuous nature of habitat characteristics, the ability to predict species occurrence is limited (Laurent et al. 2005).

Another important consideration in biodiversity modeling is the issue of explanation versus prediction. In explanation, the primary aim is to gain insight into the relationships between an observed pattern and its putative causal factors, while in prediction, understanding the relationship between predictors and the response is of low priority compared to making accurate predictions of the response given a set of predictors (Elith and Leathwick 2009). When explanation is the aim, statistical techniques, such as those employing linear regression, may be used to develop models which are highly amenable to interpretation. These approaches also yield measures of significance for specific models or variables, as well as confidence intervals for estimated model coefficients. These advantages are offset by potential reduction in predictive performance, and a requirement of stronger assumptions (e.g. linear relationships between explanatory and response variables, normality, and independence of data). On the other hand, if prediction is the sole aim, machine learning techniques, such as neural networks, maximum entropy, random forests, or support vector regression may be used. These techniques produce highly accurate predictions and allow relaxed data requirements (e.g. no requirement of normality). The downside of these approaches is the limited interpretability of the models.

In modeling (and mapping) spatial distributions of individual species, there has been recent movement toward machine learning techniques. In a study comparing the species distribution modeling performance of 16 techniques (including 11 distinct methods and 5 additional variations on those methods), machine learning techniques (boosted regression trees and two variations of maximum entropy) ranked as three of the top four techniques (Elith et al. 2006). Other machine learning approaches have recently been employed in ecological contexts with promising results, including random forests (Prasad et al. 2006) and support vector machines (Drake et al. 2006).

When used to model species richness, these new approaches are frequently used to model distributions of individual species, and the resulting range maps are composited to calculate the species richness at any given point (Ferrier and Guisan 2006) (see for example Graham and Hijmans 2006). In community modeling, an alternative approach, environmental data are directly used to model richness of a group of similar species at once (Ferrier and Guisan 2006). The advantage of combining multiple species distribution models is that information about individual species is retained. Community level modeling gives up species-level detail in exchange for several advantages (Ferrier and Guisan 2006). If many species are involved, the complexity of analysis may be dramatically reduced versus computing distribution models for each species. In instances with groups of rare or sparsely-sampled species, patterns of similar response to environmental conditions may be detected. Lastly, and perhaps most importantly for our study, community level modeling has the power to synthesize complex data (e.g., distribution patterns of hundreds of species of birds) into a format that is much simpler and more readily understandable to scientists, decision-makers, and resource managers (e.g., maps of species richness for specific avian guilds). Though some of the information about individual species is lost, this may not be a disadvantage if the unit of management interest is a group of species, such as cavity-nesting birds or Neotropical migrants. In a comparison of these two approaches modeling plant species richness in relation to environmental variables (Dubuis et al. 2011), the community modeling approach produced an unbiased estimator of species richness and captured the observed hump-shaped pattern of species richness over an elevation gradient. The approach of directly mapping individual species had the advantage of retaining relatively accurate predictions of distribution of individual species, but the aggregation of these maps failed to capture the richness-elevation pattern.

Because our study aim was prediction and we were directly modeling species richness, we explored two machine learning approaches: random forests and support vector regression. A random forest is an ensemble classifier composed of many decision trees (Breiman 2001). Ensemble tree models solve a noted deficiency of single-tree models, poor predictive accuracy (Elith et al. 2008). A bootstrapped subsample of the data is drawn for the generation of each tree (i.e. bootstrap aggregating, or bagging), and only a random subset of variables are considered at each node. This process is repeated until the specified number of trees has been generated. Because the trees are each trained with slightly different data sets and are allowed to select from only some of the explanatory variables at each node, it is unlikely the trees will converge at identical solutions, and thus the risk of overfitting may be reduced. Once the model is trained, predictions are generated by feeding the explanatory variables to each of the trees, and averaging the output. While a random forest does not lend itself well to model interpretation and hypothesis testing, a measure of “relative importance” of each variable may be obtained. A comparison of random forests and several other statistical classifiers using three different ecological datasets found random forests to have very high classification accuracy compared to the other methods (Cutler et al. 2007).

Support vector machines (SVM) are a machine learning classification technique where a kernel function non-linearly maps input data into a higher-dimensional feature space where the classes may be separated by a hyperplane (Cortes and Vapnik 1995). SVMs have been widely used in many fields including medicine (Guyon et al. 2002), finance (Kim 2003), and satellite image classification (Foody and Mathur 2004). Support vector machines have only recently appeared in an ecological context, but have shown promising results in species distribution modeling (Drake et al. 2006, Guo et al. 2005) and modeling fish species richness (Knudby et al. 2010). While primarily used in classification, support vector machines may also be used in a regression context, known as Support Vector Regression (SVR) (Drucker et al. 1996, Smola and Scholkopf 2004).

Our goal was to produce fine-scale resolution maps of avian species richness, for multiple guilds, for the contiguous United States. In Chapter 4, our goal was to explain nationwide patterns of avian biodiversity and evaluate the relative contribution of factors driving those patterns. In this chapter, our aim was to produce highly accurate predictive maps, rather than draw inference about different drivers of biodiversity. We therefore took a machine learning statistical approach with the sole objective of high predictive accuracy.

Methods

Study Area and Avian Data

Our study included the entire contiguous United States. Avian species richness was calculated from the North American Breeding Bird Survey (BBS), an annual survey of approximately 3,000 routes across the contiguous U.S. Along each 39.4-km route, 50 3-minute point counts are conducted, and all birds heard or seen are recorded (USGS Patuxent Wildlife Research Center 2008). Analysis was centered on the year 2000, and we calculated the mean species richness of each BBS route over the period 1998-2002. The BBS data were preprocessed to remove observations collected by first year observers (Kendall et al. 1996) and those conducted in suboptimal weather. We also excluded poorly sampled species, which we defined as species with fewer than 30 route-year observations during the entire history of the BBS. After the removal of these routes as well as routes for which we did not have a full set of explanatory variables, we retained 2,555 routes (Figure 5-1).

As in Chapter 4, we calculated species richness by avian guild (all birds, forest birds, grassland birds, shrubland birds, Neotropical migrants, short-distance migrants, and permanent residents). However, our reasoning for doing this was not exactly the same here. First, since we are taking a community modeling approach to our predictive mapping, it is important to group species into meaningful assemblages that are expected to respond similarly to environmental data. From a more practical angle, much of habitat management is based on managing for specific groups of species, such as grassland birds or Neotropical migrants. We therefore expect that maps of species richness by avian guild will be most useful to resource managers.

Because bird species are not uniformly detectable, the number of species identified on a route is almost certainly less than the actual number of species present, and a correction should be applied to raw species richness counts (Kéry and Schmid 2004). In studies of avian species richness, the software program COMDYN (Hines et al. 1999) is frequently used to correct for this problem and derive estimated species richness (Boulinier et al. 1998, Hamer et al. 2006). COMDYN considers the raw BBS route species richness data from a capture-recapture model perspective and uses a jackknife estimator to calculate estimated species richness (Nichols et al. 1998, Nichols et al. 1998). As our measure of biodiversity for each BBS route, we used estimated species richness as calculated by COMDYN for all species as well as the six guilds mentioned above.

In order to relate our explanatory variables to individual BBS routes, we created 19.7 km-radius (one-half the length of a BBS route) circular buffers around the centroid of each BBS route (Flather and Sauer 1996) (Figure 5-2). This buffer size and shape was chosen because it encompasses the entire BBS route and provides a uniform area and shape around each BBS route, regardless of route shape. Furthermore, this distance is comparable to the median maximum natal dispersal distance (31 km) of 76 avian species (Sutherland et al. 2000) estimated from body size relationships, and is consistent with the recommendation that landscape effects on songbirds should be examined over tens of kilometers to capture dispersal effects (Tittler et al. 2009). This approach has been used in several studies using BBS data (Flather and Sauer 1996, Rittenhouse et al. 2010, Albright et al. 2010, Albright et al. 2011, Pidgeon et al. 2007).

Environmental Data

As discussed in Chapter 4, remotely sensed measures exist for each of MacArthur's three primary drivers of biodiversity. Of the three, productivity and climatic stability are expected to affect species richness patterns at regional scales, while habitat structure factors such as landcover type and vegetation structure have stronger influence at a local scale (Hutto 1985, Mackey and Lindenmayer 2001, Pearson and Dawson 2003). Including environmental measures with influence at different hierarchical scales improves predictive accuracy in species distribution modeling, even if scale is not considered explicitly (Meyer and Thuiller 2006). We used the same explanatory data sets as in Chapter 4 but we dropped the measures of landscape configuration derived from morphological spatial pattern analysis, since they were found to be highly correlated with other habitat structure measures and added little additional explanatory power. Our explanatory variables included measures of fPAR (Coops et al. 2009), ecoregion province (Bailey 1995), elevation (Rabus et al. 2003), landcover (Homer et al. 2004), canopy height and biomass (Kellndorfer et al. 2011), and image texture (Culbert et al. 2012). (See Chapter 4 for a detailed description of these data).

Model Development

We had an initial candidate pool of 107 explanatory variables. As in Chapter 4, we carried out a multi-step process to remove correlated variables and those with very little explanatory power. We followed the same process here, with one exception. Instead of using a threshold of $|r| > 0.6$ to determine correlated variables, we relaxed our definition of correlation to $|r| > 0.8$. Random forests and support vector machines have limited sensitivity to variable collinearity, and a study using support vector machines to model ecological niches found that removing poorly performing or correlated variables prior to analysis did not improve results (Drake et al. 2006). However, we chose to go ahead with variable removal for logistical reasons related to the challenges calculating and summarizing these variables for the contiguous United States.

The relationships between texture measures and avian species richness were explored using both random forests and support vector regression with the software program R (R Development Core Team 2012). Random forest models were generated with the "randomForest" library (Liaw and Wiener 2002), with 500 trees generated per model and one-third of the explanatory variables considered as candidates at each node. Support vector regression models were generated with the "e1071" library (Dimitriadou et al. 2011) using epsilon-regression and default parameters. For both approaches, species richness models were generated for all birds, the three habitat guilds, and the three migratory habit guilds.

To compare the performance of the random forest and support vector regression approaches, we generated 500 random forest and 500 support vector regression models for each guild, each from a randomly-selected training set consisting of 80% of the BBS routes. The remaining 20% of the data points were used as a test set to calculate error. To evaluate the relative performance of the two model types, we calculated mean squared error (MSE) for the training set and test set for the random forest and support vector regression models.

Prior to generating the predictive maps with the models, the explanatory variables needed to be summarized nationwide to allow for the calculation of predicted avian species richness at a 1 km resolution. The 19.7 km radius BBS route buffers have an area of 1,219 km^2, roughly corresponding in size to a 35 km by 35 km square (1,225 km^2). We therefore summarized the explanatory variables using a 35km moving window. This resulted in a nationwide, 1-km resolution raster, where, for each pixel, the explanatory variables were summarized for the surrounding 35 km by 35 km area. For each pixel in the nationwide 1-km resolution map, the random forest and support vector regression models were used to predict species richness for all birds, the three migratory guilds, and the three habitat guilds.

Results

As a result of correlation analysis of the texture measure variables, 68 of the 80 texture measure variables were excluded from subsequent analyses, with 12 variables retained (Table 5-1). The remaining texture measures and the other explanatory variables were then used to generate univariate models explaining species richness for each guild (Table 5-2). The variables mean biomass and standard deviation of biomass showed some evidence of non-linearity in their relationship to avian species richness, so these variables were log-transformed. The variables with the strongest univariate relationships to avian species richness were: mean of fPAR annual sum, standard deviation of canopy height, mean of 5x5 band 3 mean, and mean canopy height (all with R^2 values > 0.5 for at least one guild). A final correlation analysis led to the removal of 9 more explanatory variables (Table 5-2). After the addition of ecoregion province, the explanatory variable pool contained 33 variables.

Predictive models of avian species richness were developed for all birds and each of the six guilds, as a function of the 33 explanatory environmental variables using 2,555 BBS routes. We first compared the performance of the 500 random forest and 500 support vector regression models generated for each guild, each with a randomly selected training and testing set consisting of 80% and 20% of the data respectively. For each model, mean squared error (MSE) was calculated for the training set and the test set (Figure 5-3). For the training data, random forest models had substantially lower MSE than support vector regression models for every guild. For the test data, random forest models again had lower MSE than support vector regression models, but the difference was quite small (though statistically significant at $p < 0.05$).

Single random forest and support vector regression models were then produced for each guild, using all of the BBS data. We produced nationwide predicted avian species richness maps using both the random forest and support vector regression models created for each guild. A visual inspection of these maps showed strong discontinuities in the southwestern United States for the support vector regression-generated maps (Figure 5-4). For this reason, and because the random forest models had consistently lower MSE, we elected to use only the maps generated by the random forest models. The random forest model used for prediction had pseudo-R^2 values of 0.55 for all birds, 0.73, 0.68, and 0.50 for forest birds, grassland birds, and shrubland birds, and 0.60, 0.66, and 0.36 for Neotropical migrants, short-distance migrants, and permanent residents, respectively (Table 5-3).

When considering our maps of predicted species richness, it is import to remember the scale of our analysis and how it affects interpretation of the maps. Our predictive models were derived from the species richness of a BBS route considering the surrounding landscape. Therefore, *while we produced predicted species richness maps at 1-km resolution, the value of a given pixel does not indicate the number of species expected within that pixel; rather it is the number of species that could be expected to be present along a hypothetical 39.4 km BBS route centered at that point.*

Our predictive map for species richness of all birds (Figure 5-5) showed the highest predicted richness in the forested areas of the country. This primarily includes the eastern half of the country, with predicted richness highest in the Northeast, Minnesota, Wisconsin, and Michigan. The Great Plains and low elevation areas of the western United States had lower overall predicted richness.

The map of forest bird predicted species richness (Figure 5-6) showed a similar pattern to the map for all birds, as many of the bird species in the all birds guild are forest birds. As expected, predicted richness was highest in heavily forested areas. In the Eastern United States, this includes most areas except for heavily agricultural regions in southeastern Wisconsin, northern Illinois, northern Indiana, northwestern Ohio, and along the Mississippi River south of Illinois. In the western United States, predicted forest bird species richness was highest along the Pacific coast and in higher elevation areas such as the Rocky, Sierra Nevada, and Cascade Mountains.

Predicted grassland bird species richness (Figure 5-7) was highest in the Great Plains, stretching from Montana and North Dakota to Northern Texas. Areas of high richness also extend through Iowa, southern Minnesota, southern Wisconsin, northern Illinois, northern Indiana, and northwestern Ohio. West of the Rocky Mountains, species richness was highest in the Palouse of eastern Washington as well as southeastern Oregon, northern Nevada, and southern Idaho.

Shrubland bird species richness (Figure 5-8) was predicted to be highest in western Texas, the Transition zone (between the Colorado Plateau and Basin and Range region) of Arizona, and the chaparral regions of California. In the eastern United States, species richness for shrubland birds was predicted to be relatively uniform.

Neotropical migrants are strongly associated with forests, and thus predicted species richness for this guild (Figure 5-9) was highest in forested areas. However, in contrast to the forest birds predictive map, predicted richness appeared to be more strongly concentrated in northern Wisconsin, Northern Minnesota, the Upper Peninsula and northern Lower Peninsula of Michigan, and the northern Appalachian Mountains. In the western United States, predictions of high species richness were concentrated along the pacific coast and in higher-elevation forested areas.

Predicted species richness of short-distance migrants (Figure 5-10) in the eastern United States was concentrated in the Midwest, east of the Great Plains, with high species richness extending into Kentucky, Tennessee, Pennsylvania, and New York. In the western United States, species richness was higher in forested, mountainous areas, including strong concentrations in the Sierra Nevada, San Gabriel, San Bernardino, and San Jacinto Mountains in California, the Transition zone and Madrean Sky Islands in Arizona, and the Sacramento, Sangre de Cristo, and Jemez mountains in New Mexico.

Predicted species richness of permanent residents (Figure 5-11) was relatively uniform in the eastern United States, with a gradient of increasing richness going north to south. Species richness was lowest in the northern Great Plains and low elevation desert areas. Southern Texas, the Transition in Arizona, and coastal and high elevation areas in California had the highest predicted species richness.

A few patterns stood out from the nationwide maps. Grassland birds appeared to have relatively little “middle-ground” in their species richness distribution, with very high species richness concentrated in the Great Plains, and very low richness elsewhere. This is in contrast to shrubland birds, which, while concentrated in the southwest, had a moderate level of richness through most of the country. Distributions of predicted species richness between the eastern and western United States were notably, though not surprisingly, different. In the eastern United States, areas capable of supporting high species richness in all birds, forest birds and Neotropical migrants were distributed relatively uniformly and continuously. In contrast, areas supporting high species richness for these guilds in the western United States included primarily coastal and high elevation forests. This leads to a substantially patchier pattern with species richness concentrated in relatively small and often geographically isolated areas. Predicted species richness for short-distance migrants followed a similar spatial pattern, with relatively low variability and high uniformity in the eastern United States, and a very patchy distribution in the western United States, with much of the high predicted species richness located in small, relatively isolated patches in California, Arizona, and New Mexico.

In order to evaluate the predicted species richness maps at a finer scale, we examined the state of Wisconsin. Predicted species richness of all birds (Figure 5-12) was highest in forested areas in the northern third of the state, with the lowest richness in southeastern Wisconsin, including a noticeable low-species richness pocket in an agriculture-dominated area in Dodge, Fond du Lac, and Winnebago Counties. As was the case at the national level, forest bird species richness (Figure 5-13) was, unsurprisingly, highest in forested areas. This primarily includes the northern third of the state, as well as an area centered at Black River State forest and extending into Chippewa, Eau Claire, Clark, Jackson, Wood, Monroe, Juneau, and Adams counties. The area of lowest predicted forest species richness was a swath of agricultural land starting in Winnebago county and running south-southwest through Fond du Lac, Dodge, Jefferson, and Dane Counties. Predicted grassland bird species richness (Figure 5-14) was essentially the inverse of the forest bird map, with low species richness in forested areas, and higher species richness in agricultural areas. Another noticeable pocket of low predicted species richness was in the Milwaukee metropolitan area in Milwaukee and Waukesha counties. Predicted shrubland bird species richness (Figure 5-15) was generally higher in areas with high predicted forest bird species richness, although richness was lower in Iron, Vilas, and Oneida Counties in northern Wisconsin, and in contrast to forest birds, shrubland species richness was uniformly high in forested areas across the state, rather than just in northern forests. Predicted Neotropical migrant species richness (Figure 5-16), was uniformly high in forested areas of the northern third of the state, with moderate species richness in forests in the rest of the state. Predicted species richness of short-distance migrants (Figure 5-17) was very uniform across the state with a few small, isolated pockets of higher predicted species richness. Permanent resident predicted species richness (Figure 5-18) showed the most unique pattern. Species richness was low in northern forests except for a small hotspot in southern Sawyer County. Predicted species richness was higher overall in forested areas in the southern two-thirds of the state with a very strong hotspot in Jackson, Juneau, and Adams Counties, and a slightly less pronounced concentration in Vernon and Richland Counties.

A few are points of interest appeared in the Wisconsin maps. First, an oval area running roughly from Lake Winnebago south-southwest through Winnebago, Fond du Lac, and Dodge counties has noticeably low predicted species richness for all guilds except grassland birds. This was an area of intense agricultural production, interspersed with infrequent, small forest patches. Another point of interest was the boundary between the Laurentian Mixed Forest and Eastern Broadleaf Forest ecoregion provinces (to the north and south, respectively). This crisp boundary was clearly apparent in the map for all birds, and slightly less noticeable in the Neotropical migrant map, while it was not discernible in the maps for other guilds. This would seem to indicate that in the all bird and Neotropical migrant models, ecoregion province was an important variable representing information not present in other variables, while in the other guilds, it was unimportant and likely contained information redundant to the other explanatory variables. Lastly, an artifact of our methodology was noticeable along the shore of Lake Superior in Douglas, Bayfield, Ashland, and Iron Counties, and, to a lesser extent, along the shore of Lake Michigan (from Oconto County south). This artifact was manifested as a faint but discernible line along the Lake Michigan coast, and a drop in species richness (most noticeable in all birds, forest birds, and shrubland birds) along the Lake Superior coast. This was a result of our 35 km by 35 km moving window analysis, and therefore, was noticeable with roughly 10-15 km of the coast. Within this distance, much of the moving window was over open water, affecting measures of many of the explanatory variables, and apparently causing the species richness models to break down.

Discussion

We produced nationwide, fine-scale resolution maps of predicted avian biodiversity for all birds, three habitat guilds, and three migratory guilds. These maps provide an important aid to resource managers. Previous nationwide biodiversity maps are of coarse resolution (Buckton and Ormerod 2002), or only considered landcover data (Pearlstine et al. 2002, Scott and Jennings 1998), while our maps were produced with models including data on climatic stability, productivity, and numerous measures of habitat structure.

The predictive models used to create our maps explain a high level of the variability in the observed species richness from BBS routes, with pseudo-R^2 values ranging from 0.50 to 0.73 for six of the seven models (Table 5-3). These results compare favorably to previous studies (although those studies were more limited in scope). In a study modeling species richness of BBS routes as a function of energy availability and variability, models of all species, Neotropical migrant, and permanent resident richness yielded adjusted-R^2 values of 0.43, 0.36, and 0.27, respectively (Rowhani et al. 2008). This compares to our pseudo-R^2 measures of 0.55, 0.60, and

0.66. A similar study of avian species richness patterns in the forested ecoregions of the United States as a function of land cover, landscape configuration indices, and housing density yielded adjusted-R^2 values of 0.35, 0.48, 0.16, and 0.19 for forest birds, Neotropical Migrants, short-distance migrants, and permanent residents, respectively (Pidgeon et al. 2007). Our comparable pseudo-R^2 values were 0.73, 0.60, 0.36, and 0.66. Our results were much stronger, but it should be noted that we included non-forested landscapes in our analysis, and it would be expected that the forest bird model, for example, would have stronger explanatory power over a range of non-forest to forest, rather than in an entirely forested ecosystem. In comparison to the explanatory power of the species richness from Chapter 4, our predictive models here have pseudo-R^2 values ranging from 0.06 to 0.21 higher than the adjusted R^2 values of our explanatory models, with an average increase of 0.13. An important caveat to all of these comparisons however, is that pseudo-R^2 values may not be directly comparable to adjusted R^2 values, so although these values can give some indication of comparative performance, it would be unwise to draw strong conclusions from such comparisons.

Comparing the pseudo-R^2 values of the models among guilds can give further indication of relative model strength. The forest bird, grassland bird, and permanent resident models were strongest, followed by Neotropical migrants, all birds, and shrubland birds. The short-distance migrant model was clearly the weakest, with a pseudo-R^2 value of 0.36 compared to 0.50 to 0.73 for the other guilds. Though it is difficult to comprehensively test the accuracy of the predicted species richness maps, to the naked eye, the results appear very logical. For example, the numerical range of predicted species richness values is within the range of the (Comdyn-adjusted) species richness of the BBS Routes. The patterns of species richness are also as expected. For example, forest and Neotropical migrant species richness are heavily associated with forested areas, while grassland birds are concentrated in the Great Plains. These logical patterns are present at the small scale too. Examination of our maps for Wisconsin showed strong, logical relationships to known landcover and bird distribution patterns as well.

In the generation of our predictive models we explored two machine learning approaches, random forests and support vector regression. Both approaches have been widely used in other fields, but are only recently appearing in an ecological context (especially support vector regression). From the average model MSE from 500 model generation runs (Figure 5-3), it was clear that random forest models were superior to support vector regression models in fitting the training data. In a study of coral reef fish species richness, random forest models also consistently outperformed support vector machine models (Knudby et al. 2010). However, this substantial advantage in MSE in the training data all but disappeared when considering the test data. Though the test set MSE of the random forest models was still marginally superior to support vector regression models, this seems to indicate that support vector regression models were better able to generalize from the training data to the test data and/or the random forest models were overfitting to the training data. However, while the average MSEs of the test sets were quite similar between random forest and support vector regression models, there were some areas with sharp discontinuities in the maps predicted by support vector regression, while the random forest predictions were smoother. This concurs with a study comparing the predictive performance of several classification and regression tree techniques on an ecological data set, where bagging trees and random forests had the highest predictive accuracy, but random forests were judged superior for producing a smoother output (Prasad et al. 2006).

In addition to evaluating two relatively new and novel modeling techniques, we showed the value of community modeling to determine species richness patterns. While predicting species richness by modeling spatial distributions of individual species and compositing those distribution maps is a valid approach, it would have been challenging in our case. With 400 species in our all bird guild, developing a nationwide species distribution model for each of those species would have been a difficult undertaking, and models for rarely-sampled species may have been poor. Another important consideration is that our maps based on guild will be easier for resource managers to digest, and the guilds represent communities often managed as a whole. Our study was a good example of the strengths of community modeling, where species can be grouped into meaningful assemblages (in our case, habitat and migratory guilds) that can be modeled as a unit, making nationwide richness prediction with an immense dataset feasible, and our results readily interpretable (Ferrier and Guisan 2006).

When considering the maps of predicted species richness, it is import to be aware of some of the limitations. The most important point is the interpretation of the map. As already mentioned, based on our method of analysis, the value of a given pixel represents the predicted species richness of a hypothetical BBS route centered at that point, and not the predicted richness for that pixel alone. Secondly, caution should be taken when considering the coastal areas of the maps. As a roadside survey, the Breeding Bird Survey is not designed for sampling of shorebirds or waterfowl, and thus they are likely to be underrepresented. Because we modeled with a moving window approach, for coastal areas, the moving window extends into the ocean (or the Great Lakes). Since relatively few of the BBR route buffers used in training the models extended into the ocean, the models may not be making good predictions in those cases, as was evident along the shore of Lake Superior in some of the Wisconsin maps (e.g. Figure 5-12).

Keeping these limitations in mind, our maps have important value for informing conservation efforts. We suggest these maps be considered by land managers in identifying potential locations of high biodiversity for further field-based investigation. The maps also form a basis for comparison of relative levels of species richness within a region. We hope that producing these maps will help push forward nationwide modeling of species richness. Many modeling approaches may yield some insight into species richness relationships, but fail to produce a concrete product for comparison and improvement. We hope that others will expand on our approach and produce further nationwide, fine-resolution maps of species richness, hopefully yielding improved results over our maps. As the first nationwide, 1-km resolution maps of predicted avian species richness derived from numerous measures of climatic stability, productivity, and habitat structure, our study makes a significant contribution to the knowledge base for use in biodiversity modeling, conservation, and land-use planning.

References

Albright T. P., A. M. Pidgeon, C. D. Rittenhouse, M. K. Clayton, C. H. Flather, P. D. Culbert, and V. C. Radeloff. 2011. Heat waves measured with MODIS land surface temperature data predict changes in avian community structure. Remote Sensing of Environment 115:245-254.

Albright T. P., A. M. Pidgeon, C. D. Rittenhouse, M. K. Clayton, C. H. Flather, P. D. Culbert, B. D. Wardlow, and V. C. Radeloff. 2010. Effects of drought on avian community structure. Global Change Biology 16:2158-2170.

Bailey R. G. 1995. Description of the Ecoregions of the United States. United States Department of Agriculture.

Boulinier T., J. D. Nichols, J. E. Hines, J. R. Sauer, C. H. Flather, and K. H. Pollock. 1998. Higher temporal variability of forest breeding bird communities in fragmented landscapes. Proceedings of the National Academy of Sciences of the United States of America 95:7497-7501.

Breiman L. 2001. Random forests. Machine Learning 45:5-32.

Buckton S. T., S. J. Ormerod. 2002. Global patterns of diversity among the specialist birds of riverine landscapes. Freshwater Biology 47:695-709.

Coops N. C., R. H. Waring, M. A. Wulder, A. M. Pidgeon, and V. C. Radeloff. 2009. Bird diversity: a predictable function of satellite-derived estimates of seasonal variation in canopy light absorbance across the United States. Journal of Biogeography 36:905-918.

Cortes C., V. Vapnik. 1995. Support-vector networks. Machine Learning 20:273-297.

Culbert P. D., V. C. Radeloff, V. St-Louis, C. H. Flather, C. D. Rittenhouse, T. P. Albright, and A. M. Pidgeon. 2012. Modeling broad-scale patterns of avian species richness across the Midwestern United States with measures of satellite image texture. Remote Sensing of Environment 118:140-150.

Cutler D. R., T. C. Edwards Jr., K. H. Beard, A. Cutler, and K. T. Hess. 2007. Random forests for classification in ecology RID B-7177-2011. Ecology 88:2783-2792.

Dimitriadou E., K. Hornik, F. Leisch, D. Meyer, and A. Weingessel. 2011. e1071: Misc Functions of the Department of Statistics (e1071), TU Wien. 1.6.

Dobson A. P., J. P. Rodriguez, W. M. Roberts, and D. S. Wilcove. 1997. Geographic Distribution of Endangered Species in the United States. Science 275:550-553.

Drake J. M., C. Randin, and A. Guisan. 2006. Modelling ecological niches with support vector machines. Journal of Applied Ecology 43:424-432.

Support Vector Regression Machines. Advances in Neural Information Processing Systems 9; 1996; MIT Press; 1996. 155-161 p.

Dubuis A., J. Pottier, V. Rion, L. Pellissier, J. Theurillat, and A. Guisan. 2011. Predicting spatial patterns of plant species richness: a comparison of direct macroecological and species stacking modelling approaches. Diversity and Distributions 17:1122-1131.

Elith J., J. R. Leathwick, and T. Hastie. 2008. A working guide to boosted regression trees. Journal of Animal Ecology 77:802-813.

Elith J., C. H. Graham, R. P. Anderson, M. Dudik, S. Ferrier, A. Guisan, R. J. Hijmans, F. Huettmann, J. R. Leathwick, A. Lehmann, J. Li, L. G. Lohmann, B. A. Loiselle, G. Manion, C. Moritz, M. Nakamura, Y. Nakazawa, J. M. Overton, A. T. Peterson, S. J. Phillips, K. Richardson, R. Scachetti-Pereira, R. E. Schapire, J. Soberon, S. Williams, M. S. Wisz, and N. E. Zimmermann. 2006. Novel methods improve prediction of species' distributions from occurrence data. Ecography 29:129-151.

Elith J., J. R. Leathwick. 2009. Species distribution models: ecological explanation and prediction across space and time. Annual Review of Ecology Evolution and Systematics 40:677-697.

Ferrier S., A. Guisan. 2006. Spatial modelling of biodiversity at the community level. Journal of Applied Ecology 43:393-404.

Flather C. H., J. R. Sauer. 1996. Using landscape ecology to test hypotheses about large-scale abundance patterns in migratory birds. Ecology 77:28-35.

Foody G., A. Mathur. 2004. A relative evaluation of multiclass image classification by support vector machines. IEEE Transactions on Geoscience and Remote Sensing 42:1335-1343.

Gaston K. J., T. M. Blackburn, and K. K. Goldewijk. 2003. Habitat conversion and global avian biodiversity loss. Proceedings of the Royal Society B: Biological Sciences 270:1293-1300.

Graham C. H., R. J. Hijmans. 2006. A comparison of methods for mapping species ranges and species richness. Global Ecology and Biogeography 15:578-587.

Guo Q., M. Kelly, and C. H. Graham. 2005. Support vector machines for predicting distribution of Sudden Oak Death in California. Ecological Modelling 182:75-90.

Guyon I., J. Weston, S. Barnhill, and V. Vapnik. 2002. Gene selection for cancer classification using support vector machines. Machine Learning 46:389-422.

Hamer T. L., C. H. Flather, and B. R. Noon. 2006. Factors associated with grassland bird species richness: The relative roles of grassland area, landscape structure, and prey. Landscape Ecology 21:569-583.

Hines J. E., T. Boulinier, J. D. Nichols, J. R. Sauer, and K. H. Pollock. 1999. COMDYN: software to study the dynamics of animal communities using a capture-recapture approach. Bird Study 46:209-217.

Homer C., C. Q. Huang, L. M. Yang, B. Wylie, and M. Coan. 2004. Development of a 2001 national land-cover database for the United States. Photogrammetric Engineering and Remote Sensing 70:829-840.

Hutto R. L. 1985. Habitat selection by nonbreeding migratory birds. Pages 455-476 *In* M. L. Cody, editor. Habitat selection in birds, Academic Press, NY.

Kellndorfer J., W. Walker, L. LaPoint, J. Bishop, T. Cormier, G. Fiske, and K. Kirsch. 2011. The National Biomass and Carbon Dataset - A hectare-scale dataset of vegetation height, aboveground biomass and carbon stock of the conterminous United States. Data Published by the Woods Hole Research Center http://whrc.org/nbcd.

Kendall W. L., B. G. Peterjohn, and J. R. Sauer. 1996. First-time observer effects in the North American Breeding Bird Survey. The Auk 113:823-829.

Kéry M., H. Schmid. 2004. Monitoring programs need to take into account imperfect species detectability. Basic and Applied Ecology 5:65-73.

Kim K. 2003. Financial time series forecasting using support vector machines. Neurocomputing 55:307-319.

Knudby A., A. Brenning, and E. LeDrew. 2010. New approaches to modelling fish-habitat relationships RID E-6022-2011. Ecological Modelling 221:503-511.

Laurent E. J., H. Shi, D. Gatziolis, J. P. LeBouton, M. B. Walters, and J. Liu. 2005. Using the spatial and spectral precision of satellite imagery to predict wildlife occurrence patterns. Remote Sensing of Environment 97:249-262.

Liaw A., M. Wiener. 2002. Classification and Regression by randomForest. R News 2:18-22.

Mackey B., D. Lindenmayer. 2001. Towards a hierarchical framework for modelling the spatial distribution of animals. Journal of Biogeography 28:1147-1166.

Meyer C., W. Thuiller. 2006. Accuracy of resource selection functions across spatial scales. Diversity and Distributions 12:288-297.

Myers N., R. A. Mittermeier, C. G. Mittermeier, G. A. B. da Fonseca, and J. Kent. 2000. Biodiversity hotspots for conservation priorities. Nature 403:858.

Nichols J. D., T. Boulinier, J. E. Hines, K. H. Pollock, and J. R. Sauer. 1998. Inference methods for spatial variation in species richness and community composition when not all species are detected. Conservation Biology 12:1390-1398.

Pearlstine L. G., S. E. Smith, L. A. Brandt, C. R. Allen, W. M. Kitchens, and J. Stenberg. 2002. Assessing state-wide biodiversity in the Florida Gap analysis project. Journal of environmental management 66:127-144.

Pearson R., T. Dawson. 2003. Predicting the impacts of climate change on the distribution of species: are bioclimate envelope models useful? Global Ecology and Biogeography 12:361-371.

Pidgeon A. M., V. C. Radeloff, C. H. Flather, C. A. Lepczyk, M. K. Clayton, T. J. Hawbaker, and R. B. Hammer. 2007. Associations of forest bird species richness with housing and landscape patterns across the USA. Ecological Applications 17:1989-2010.

Prasad A., L. Iverson, and A. Liaw. 2006. Newer classification and regression tree techniques: Bagging and random forests for ecological prediction. Ecosystems 9:181-199.

R Development Core Team. 2012. R: A language and environment for statistical computing. 2.15.

Rabus B., M. Eineder, A. Roth, and R. Bamler. 2003. The shuttle radar topography mission - a new class of digital elevation models acquired by spaceborne radar. Isprs Journal of Photogrammetry and Remote Sensing 57:241-262.

Rittenhouse C. D., A. M. Pidgeon, T. P. Albright, P. D. Culbert, M. K. Clayton, C. H. Flather, C. Huang, J. G. Masek, and V. C. Radelof. 2010. Avifauna response to hurricanes: regional changes in community similarity. Global Change Biology 16:905-917.

Rowhani P., C. A. Lepczyk, M. A. Linderman, A. M. Pidgeon, V. C. Radeloff, P. D. Culbert, and E. F. Lambin. 2008. Variability in energy influences avian distribution patterns across the USA. Ecosystems 11:854-867.

Scott J. M., M. D. Jennings. 1998. Large-area mapping of biodiversity. Annals of the Missouri Botanical Garden 85:34-47.

Scott J. M., F. Davis, B. Csuti, R. Noss, B. Butterfield, C. Groves, H. Anderson, S. Caicco, F. D'Erchia, T. C. Edwards Jr., J. Ulliman, and R. G. Wright. 1993. Gap analysis: a geographic approach to protection of biological diversity. Wildlife Monographs :3-41.

Smola A., B. Scholkopf. 2004. A tutorial on support vector regression. Statistics and Computing 14:199-222.

Sutherland G. D., A. S. Harestad, K. Price, and K. P. Lertzman. 2000. Scaling of natal dispersal distances in terrestrial birds and mammals. Conservation Ecology 4:16.

Tittler R., M. Villard, and L. Fahrig. 2009. How far do songbirds disperse? Ecography 32:1051-1061.

Turner W., S. Spector, N. Gardiner, M. Fladeland, E. Sterling, and M. Steininger. 2003. Remote sensing for biodiversity science and conservation. Trends in Ecology & Evolution 18:306-314.

Tables

Table 5-1. Texture variables calculated from Landsat imagery. Based on correlation analysis, 68 variables (marked "-") were excluded from subsequent analysis, and 12 variables (marked "X") were retained.

Texture	Landsat Band			
	2	3	4	5
Mean_5x5_Mean	-	X	-	-
Mean_21x21_Mean	-	-	-	-
Mean_5x5_SD	-	X	-	-
Mean_21x21_SD	-	-	-	X
SD_5x5_Mean	-	X	-	-
SD_21x21_Mean	-	-	-	-
SD_5x5_SD	X	-	-	-
SD_21x21_SD	-	-	-	-
ASM_5x5_Mean	-	-	X	-
ASM_5x5_SD	X	-	-	-
Contrast_5x5_Mean	-	-	-	-
Contrast_5x5_SD	-	-	-	-
Correlation_5x5_Mean	-	X	X	-
Correlation_5x5_SD	-	X	-	-
Entropy_5x5_Mean	-	-	-	-
Entropy_5x5_SD	-	-	-	-
Homogeneity_5x5_Mean	-	-	-	X
Homogeneity_5x5_SD	-	-	X	-
SSVariance_5x5_mean	-	-	-	-
SSVariance_5x5_SD	-	-	-	-

Table 5-2. R^2 values for univariate models of species richness. Sign indicates direction of relationship. *** p-value < 0.001, ** p-value < 0.01, * p-value < 0.05. Values > 0.15 bolded for emphasis. Variable names in bold indicate variables retained after final correlation analysis, variables not in bold were dropped from subsequent analysis.

	All Species	Neotropical Migrants	Permanent Residents	Short-Distance Migrants	Forest Birds	Grassland Birds	Shrubland Birds
Proportion Water	0.00(+)*	0.00(+)**	0.00(+)	0.00(+)	0.01(+)***	0.01(-)***	0.00(-)
Proportion Ice	0.00(+)	0.00(+)	0.00(-)	0.00(+)	0.00(+)	0.00(-)**	0.00(-)
Proportion Developed	0.00(+)*	0.00(+)*	0.01(+)***	0.00(+)*	0.02(+)***	0.02(-)***	0.00(+)***
Proportion Barren	0.05(-)***	0.04(-)***	0.02(-)***	0.03(-)***	0.05(-)***	0.00(-)**	0.01(-)***
Proportion Deciduous Forest	**0.25(+)*****	**0.34(+)*****	0.02(+)***	0.05(+)***	**0.34(+)*****	0.06(-)***	0.10(+)***
Proportion Evergreen Forest	0.03(+)***	0.01(+)***	0.03(+)***	0.02(+)***	0.06(+)***	**0.15(-)*****	0.00(+)
Proportion Mixed Forest	0.08(+)***	0.12(+)***	0.00(+)**	0.01(+)***	0.13(+)***	0.08(-)***	0.00(+)***
Proportion Scrub Shrub	0.12(-)***	**0.16(-)*****	0.00(-)	0.07(-)***	**0.25(-)*****	0.00(+)	0.00(+)'
Proportion Grassland	0.09(-)***	0.09(-)***	0.05(-)***	0.03(-)***	**0.16(-)*****	**0.20(+)*****	0.09(-)***
Proportion Pasture	0.03(+)***	0.03(+)***	0.03(+)***	0.02(+)***	0.05(+)***	0.00(-)	0.02(+)***
Proportion Cultivated Crops	0.02(-)***	0.02(-)***	0.06(-)***	0.00(+)*	0.03(-)***	**0.18(+)*****	0.03(-)***
Proportion Woody Wetland	0.00(+)**	0.00(+)***	0.02(+)***	0.00(-)**	0.03(+)***	0.05(-)***	0.00(-)**
Proportion Herbaceous Wetland	0.01(-)***	0.01(-)***	0.00(-)*	0.01(-)***	0.01(-)***	0.00(+)	0.02(-)***
Number of Classes	0.12(+)***	0.13(+)***	0.01(+)***	0.05(+)***	**0.15(+)*****	0.01(-)***	0.01(+)***
Shannon Diversity of Landcover Classes	0.13(+)***	0.13(+)***	0.05(+)***	0.05(+)***	**0.22(+)*****	0.06(-)***	0.02(+)***
Mean Canopy Height	**0.29(+)*****	**0.31(+)*****	0.07(+)***	0.07(+)***	**0.51(+)*****	**0.34(-)*****	0.06(+)***
Standard Deviation of Canopy Height	**0.32(+)*****	**0.25(+)*****	0.13(+)***	**0.17(+)*****	**0.53(+)*****	**0.25(-)*****	0.12(+)***
Coefficient of Variation of Canopy Height	0.07(-)***	0.06(-)***	0.02(-)***	0.04(-)***	0.09(-)***	0.03(+)***	0.03(-)***
Mean Biomass	**0.23(+)*****	**0.25(+)*****	0.04(+)***	0.07(+)***	**0.40(+)*****	**0.22(-)*****	0.07(+)***
Standard Deviation of Biomass	**0.18(+)*****	0.12(+)***	0.08(+)***	0.10(+)***	**0.32(+)*****	**0.23(-)*****	0.06(+)***
Coefficient of Variation of Biomass	0.07(-)***	0.06(-)***	0.02(-)***	0.04(-)***	0.10(-)***	0.03(+)***	0.03(-)***
Mean of 5x5 Band 3 Mean	**0.33(-)*****	**0.34(-)*****	0.05(-)***	**0.15(-)*****	**0.52(-)*****	**0.09(+)*****	0.05(-)***
Standard Deviation of 5x5 Band 3 Mean	**0.14(-)*****	**0.19(-)*****	0.01(-)***	0.05(-)***	**0.21(-)*****	**0.01(+)*****	0.02(-)***
Standard Deviation of 21x21 Band 5 Mean	0.05(-)***	0.09(-)***	0.00(+)*	0.02(-)***	**0.06(-)*****	0.00(-)*	0.01(-)***
Mean of 5x5 Band 3 Standard Deviation	0.09(-)***	0.14(-)***	0.00(+)'	0.02(-)***	0.13(-)***	0.01(+)***	0.00(-)

Standard Deviation of 5x5 Band 2 Standard Deviation	0.04(-)***	0.05(-)***	0.00(+)	0.01(-)***	0.03(-)***	**0.00(-)***	0.00(-)*
Mean of 5x5 Band 4 Angular Second Moment	0.12(-)***	0.13(-)***	0.02(-)***	0.04(-)***	**0.16(-)*****	0.03(+)***	0.07(-)***
Standard Deviation of 5x5 Band 2 Angular Second Moment	**0.10(-)*****	**0.08(-)*****	0.03(-)***	0.07(-)***	**0.11(-)*****	0.00(-)**	0.02(-)***
Mean of 5x5 Band 3 Correlation	0.06(-)***	**0.12(-)*****	0.00(-)	0.00(-)*	**0.14(-)*****	0.11(+)***	0.00(-)*
Mean of 5x5 Band 4 Correlation	0.00(-)	0.00(+)	0.03(-)***	0.00(+)'	0.02(-)***	0.08(+)***	0.00(+)
Standard Deviation of 5x5 Band 3 Correlation	0.02(+)***	0.03(+)***	0.00(+)*	0.02(+)***	0.06(+)***	0.00(-)*	0.00(+)
Mean of 5x5 Band 5 Homogeneity	0.05(-)***	0.02(-)***	0.10(-)***	0.02(-)***	0.06(-)***	0.05(+)***	0.07(-)***
Standard Deviation of 5x5 Band 4 Homogeneity	0.06(-)***	0.06(-)***	0.03(-)***	0.01(-)***	**0.08(-)*****	0.03(+)***	0.05(-)***
Mean of fPAR Annual Sum	**0.28(+)*****	**0.24(+)*****	**0.21(+)*****	0.07(+)***	**0.54(+)*****	**0.28(-)*****	0.09(+)***
Standard Deviation of fPAR Annual Sum	0.02(+)***	0.00(+)	0.05(+)***	0.02(+)***	0.03(+)***	0.09(-)***	0.01(+)***
Mean of fPAR Annual Minimum	0.05(+)***	0.01(+)***	**0.34(+)*****	0.00(+)*	**0.17(+)*****	**0.27(-)*****	0.07(+)***
Standard Deviation of fPAR Annual Minimum	0.11(+)***	0.05(+)***	0.18(+)***	0.03(+)***	**0.21(+)*****	**0.28(-)*****	0.06(+)***
Mean of fPAR Annual Seasonality	0.00(-)	0.02(+)***	**0.30(-)*****	0.02(+)***	0.01(-)***	**0.22(+)*****	0.05(-)***
Standard Deviation of fPAR Annual Seasonality	0.00(+)***	0.01(+)***	0.03(-)***	0.01(+)***	0.00(+)*	0.01(-)***	0.00(-)***
Mean of SRTM Elevation	**0.04(-)*****	**0.04(-)*****	**0.07(-)*****	0.00(-)***	**0.11(-)*****	**0.11(-)*****	0.02(-)***
Standard Deviation of SRTM Elevation	0.00(+)	0.00(-)	0.00(-)	0.00(+)*	0.00(-)'	0.00(-)'	0.01(+)***

Table 5-3. Pseudo-R2 values for random forest models of nationwide avian species richness.

Guild	**Pseudo-R^2**
All Birds	0.55
Forest Birds	0.73
Grassland Birds	0.68
Shrubland Birds	0.50
Neotropical Migrants	0.60
Short-Distance Migrants	0.36
Permanent Residents	0.66

Figures

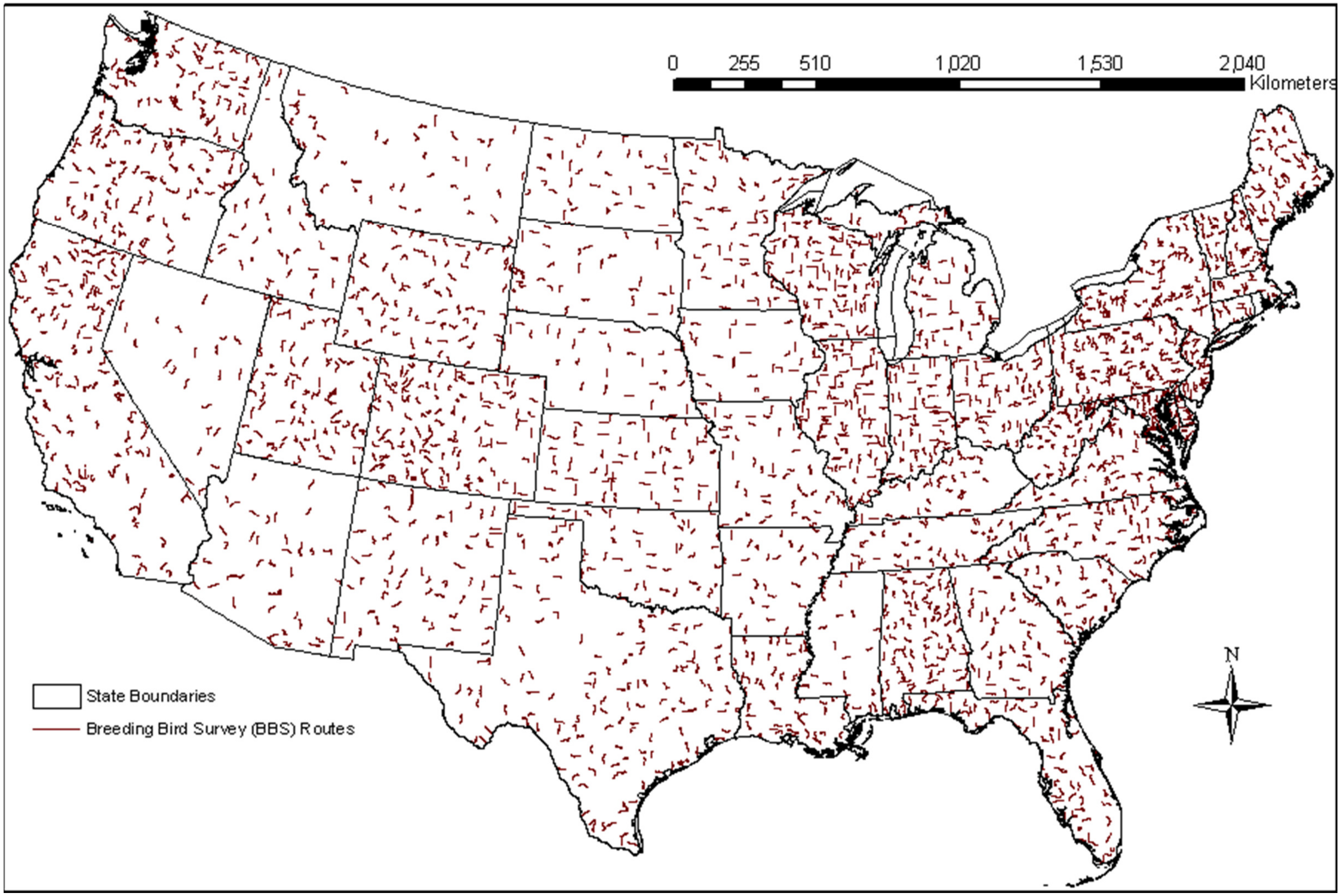

Figure 5-1. Breeding Bird Survey (BBS) routes (2,555) in the contiguous United States used to develop predictive richness models.

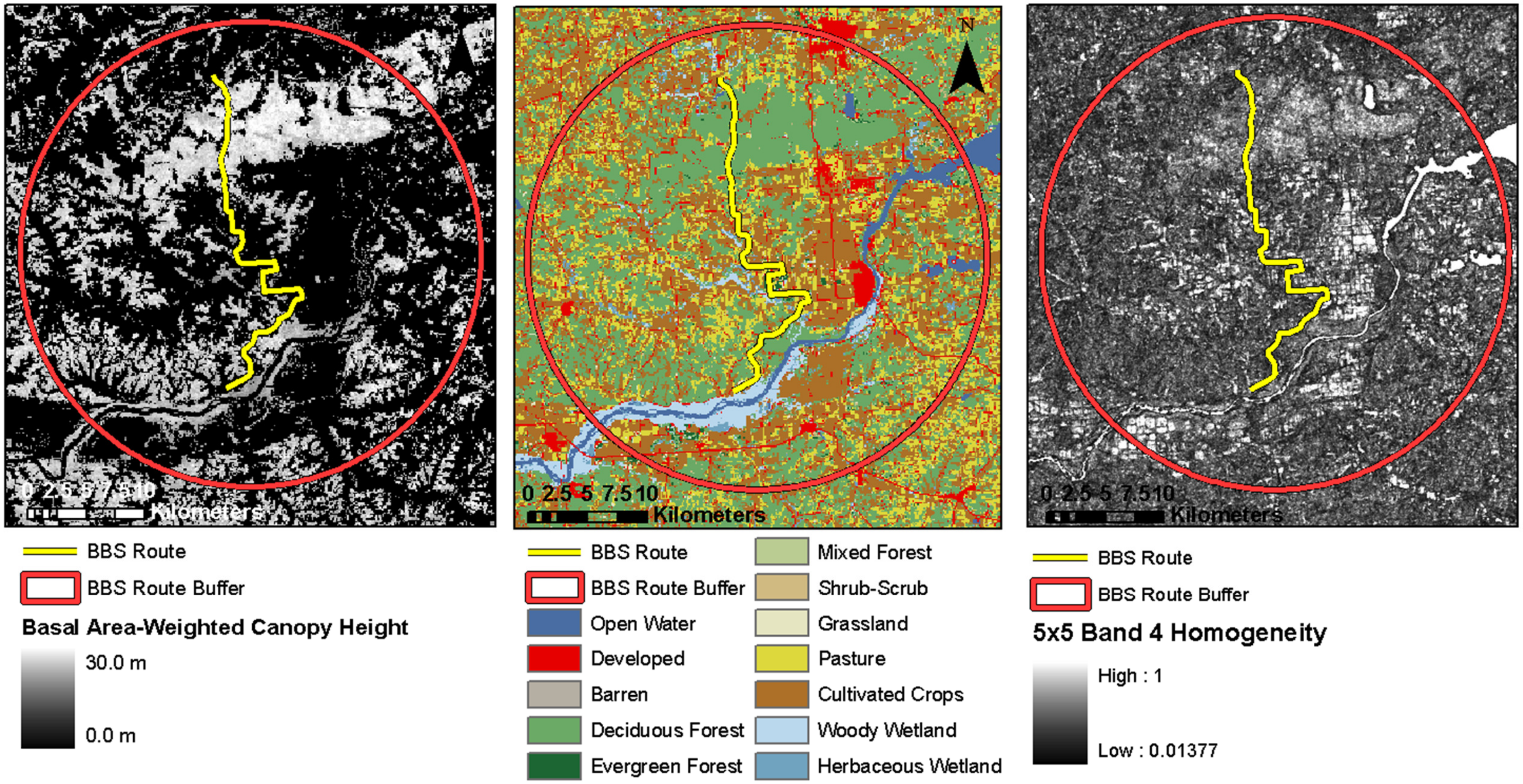

Figure 5-2. A single Breeding Bird Survey (BBS) route in southern Wisconsin. The 19.7 km radius circular buffer used in analysis is shown. Examples of environmental data include canopy height, land cover, and 5x5 TM band 4 homogeneity.

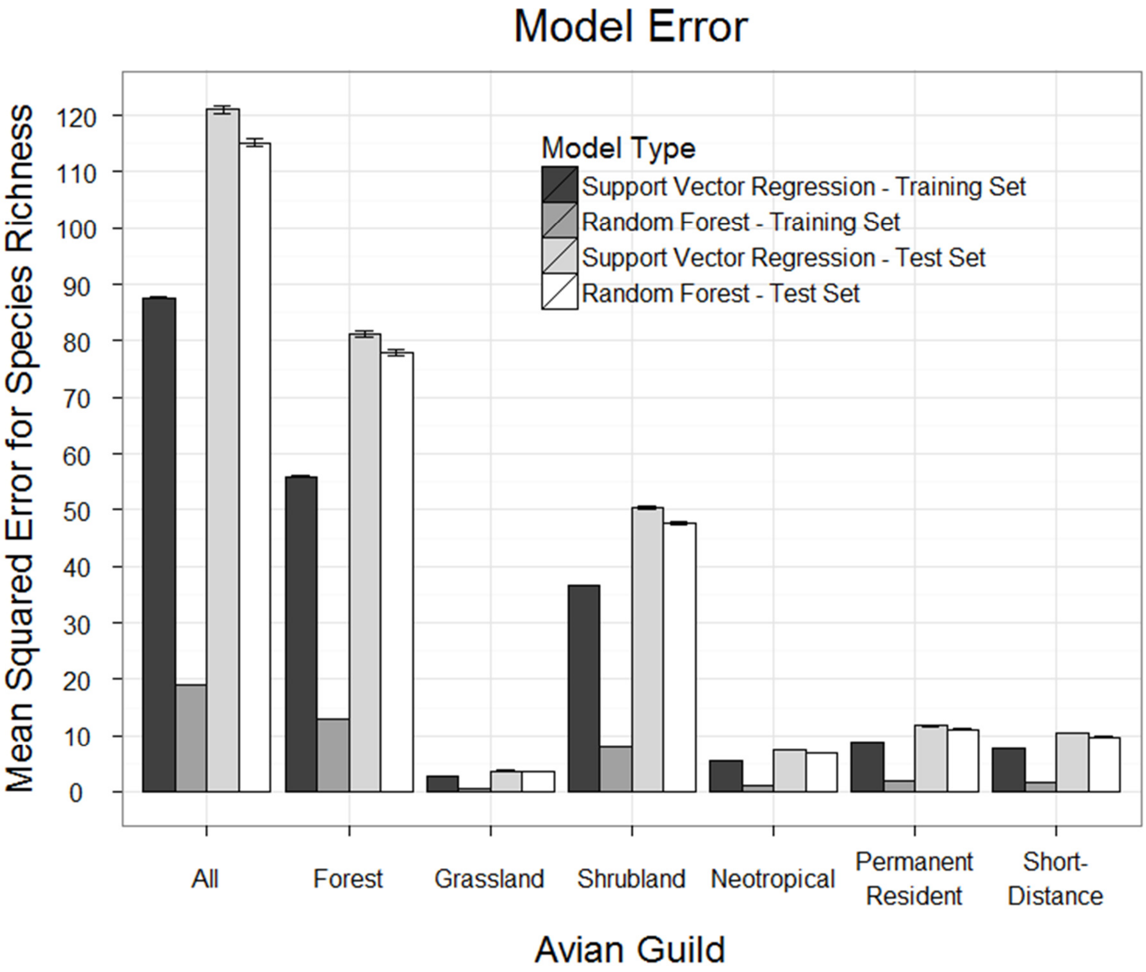

Figure 5-3. Average mean squared error (MSE) for training and test sets for models generated with support vector regression (SVR) and (RF) random forests. The dataset was randomly split 500 times, with 80% of the data comprising the training set, and 20% the test set. For each split, SVR and RF models were generated for each guild. Error bars indicate 95% confidence interval.

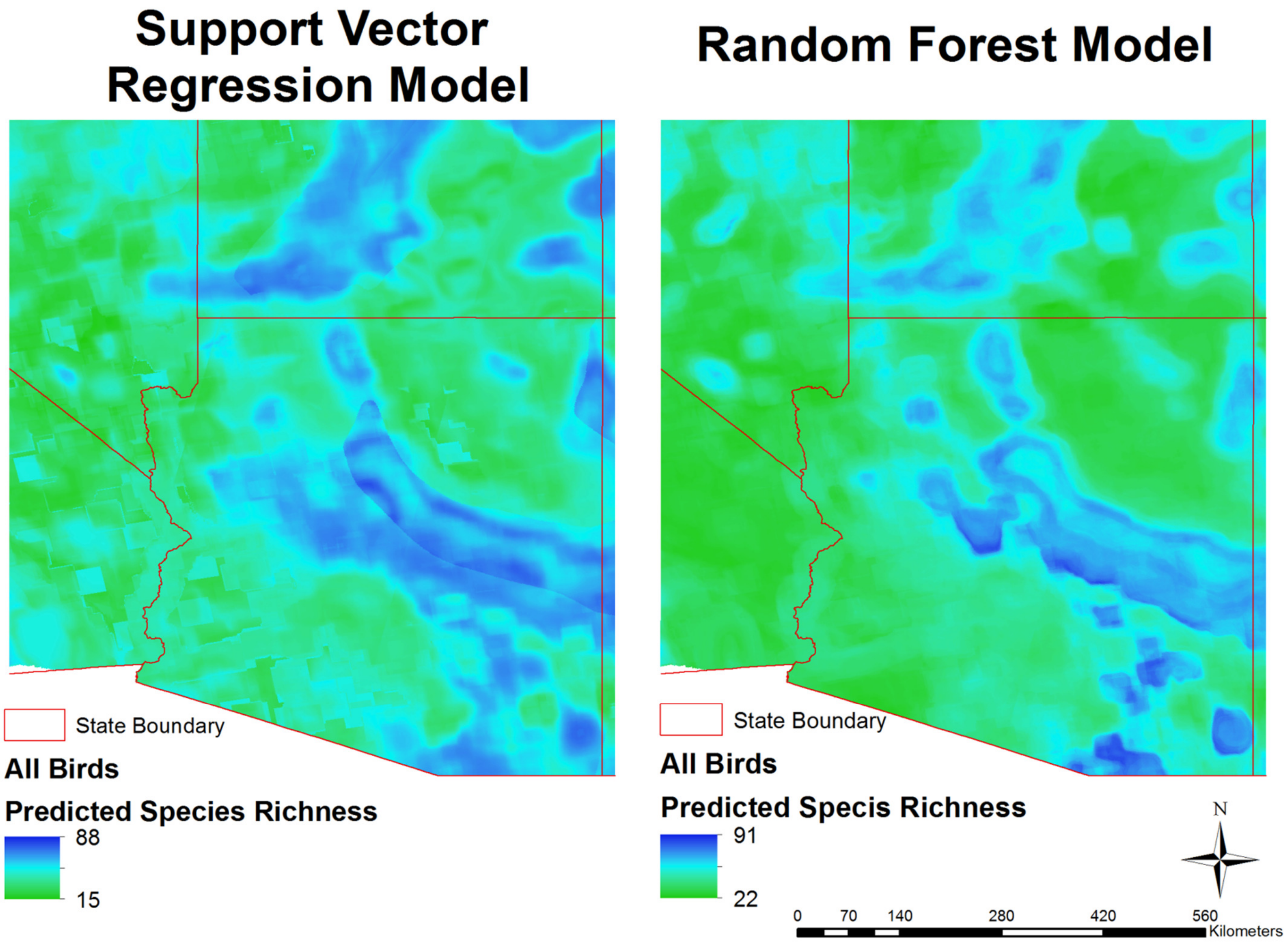

Figure 5-4. A selected portion of the predicted all bird species richness maps generated by the support vector regression model (left) and random forest model (right). The image shows Arizona and portions of Utah, Nevada, and California. While both models produced similar patterns overall, there are noticeable discontinuities in the support vector regression map, notably in the area of the Arizona – California border.

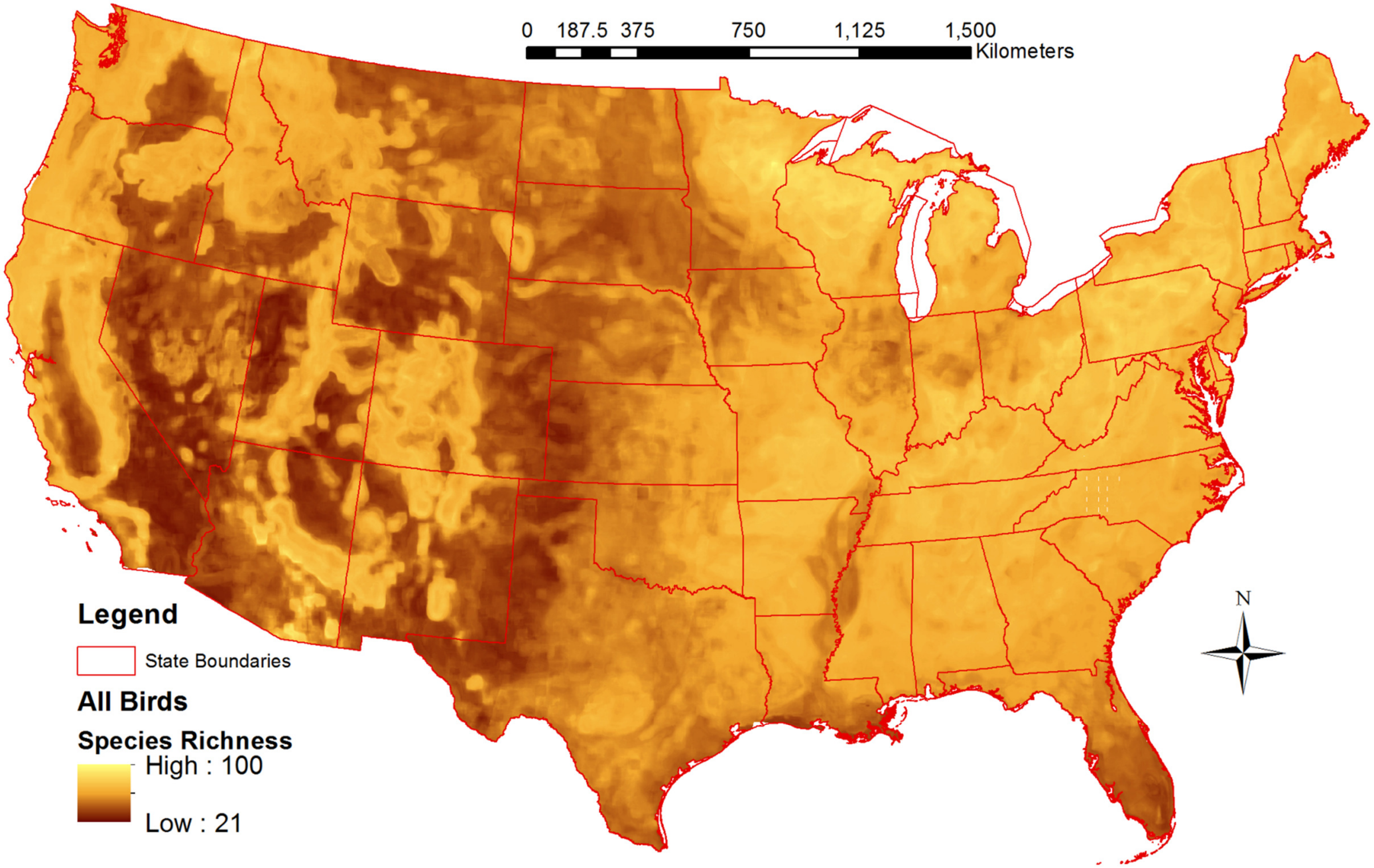

Figure 5-5. Predicted species richness for all birds. Map indicates the predicted species richness of a hypothetical Breeding Bird Survey centered at a given point. The pseudo-R^2 for this model is 0.55.

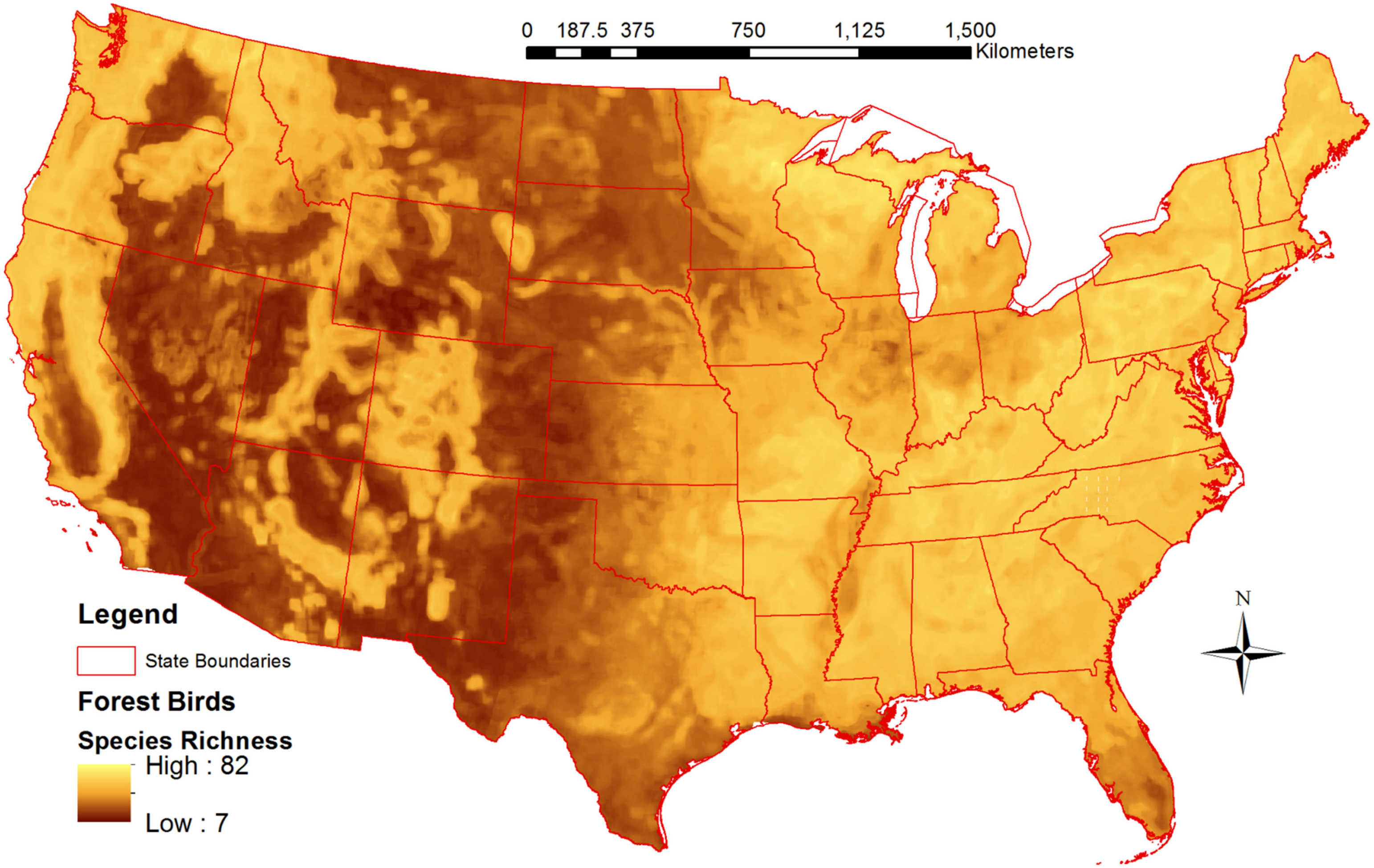

Figure 5-6. Predicted species richness for forest birds. Map indicates the predicted species richness of a hypothetical Breeding Bird Survey centered at a given point. The pseudo-R^2 for this model is 0.73.

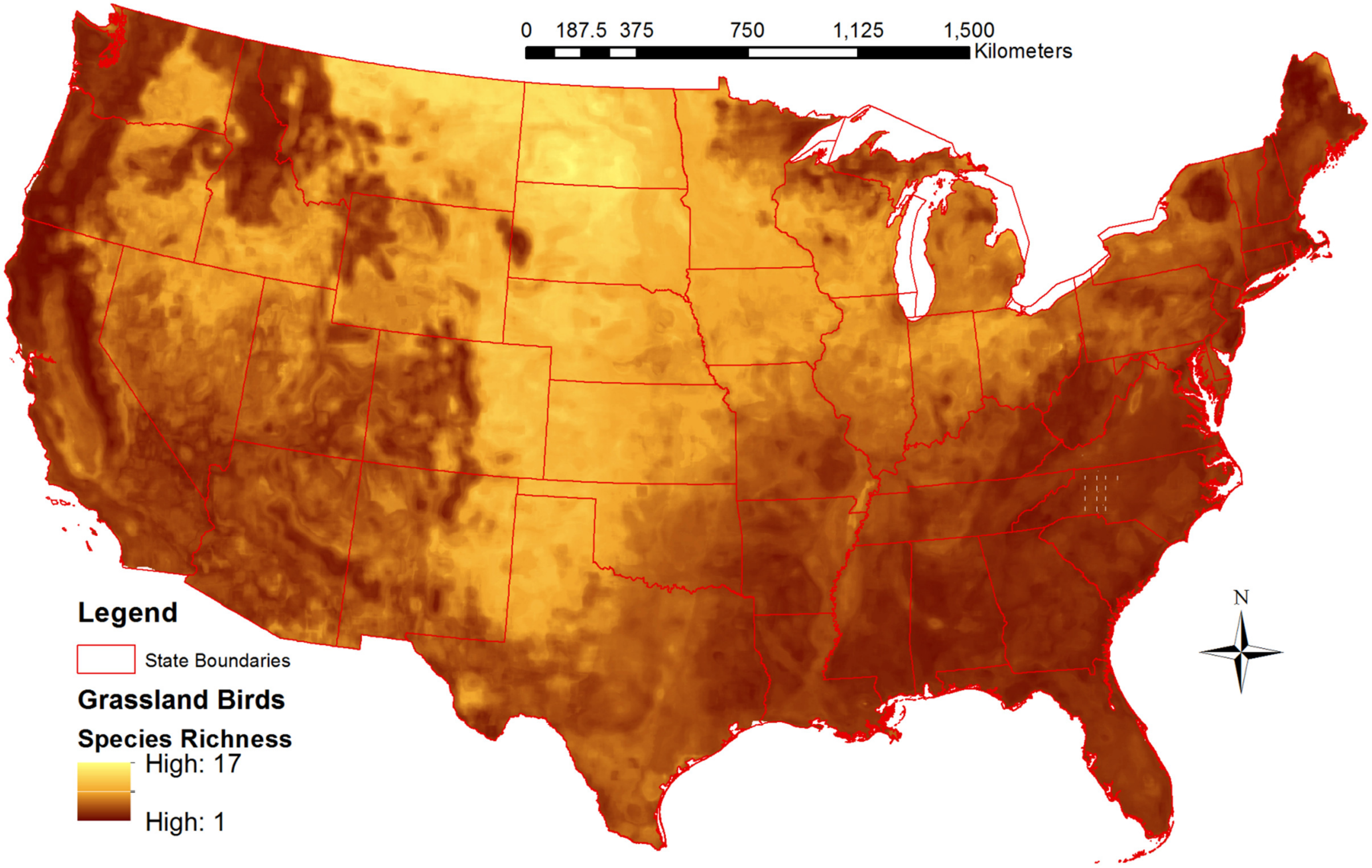

Figure 5-7. Predicted species richness for grassland birds. Map indicates the predicted species richness of a hypothetical Breeding Bird Survey centered at a given point. The pseudo-R^2 for this model is 0.68.

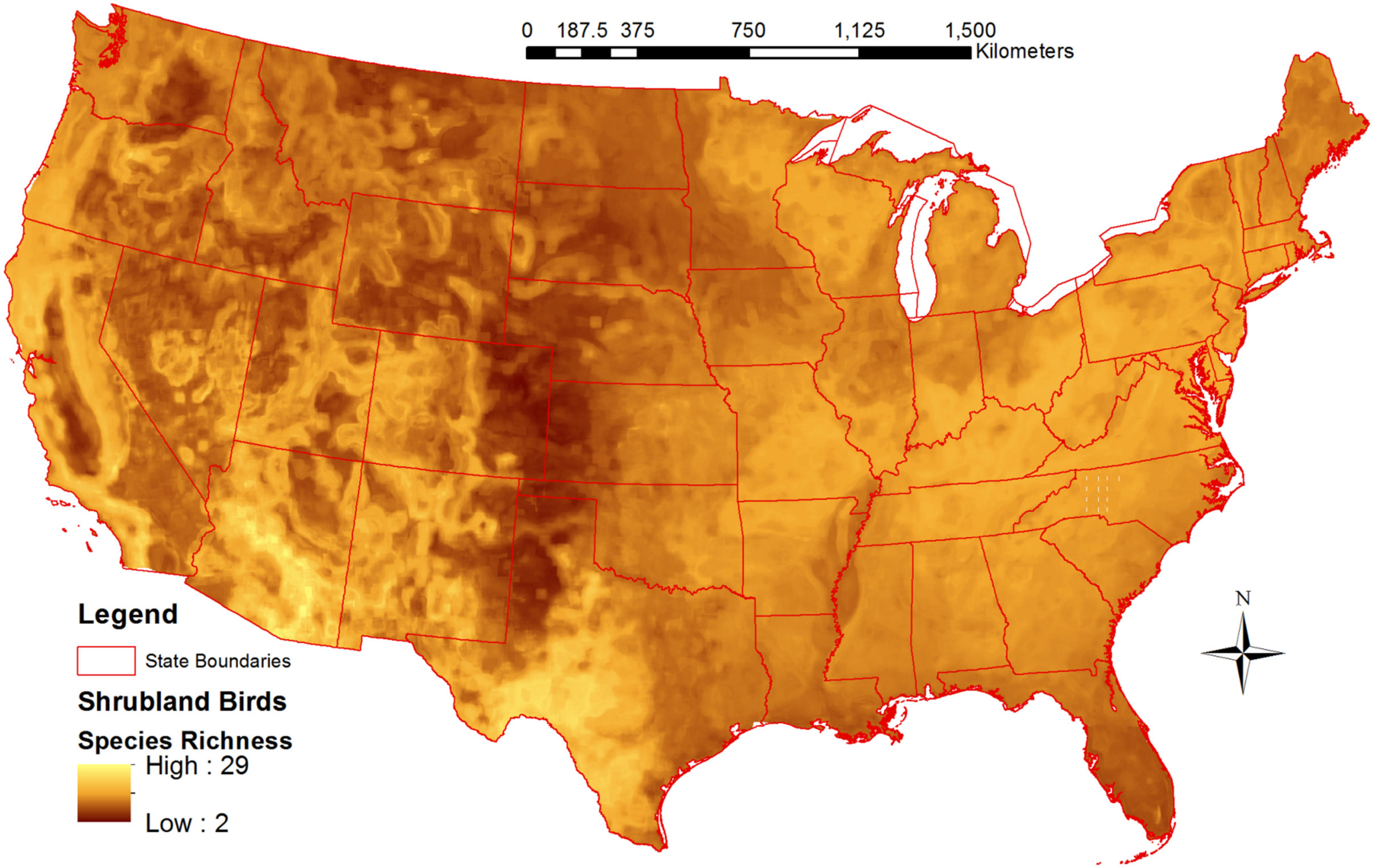

Figure 5-8. Predicted species richness for shrubland birds. Map indicates the predicted species richness of a hypothetical Breeding Bird Survey centered at a given point. The pseudo-R^2 for this model is 0.50.

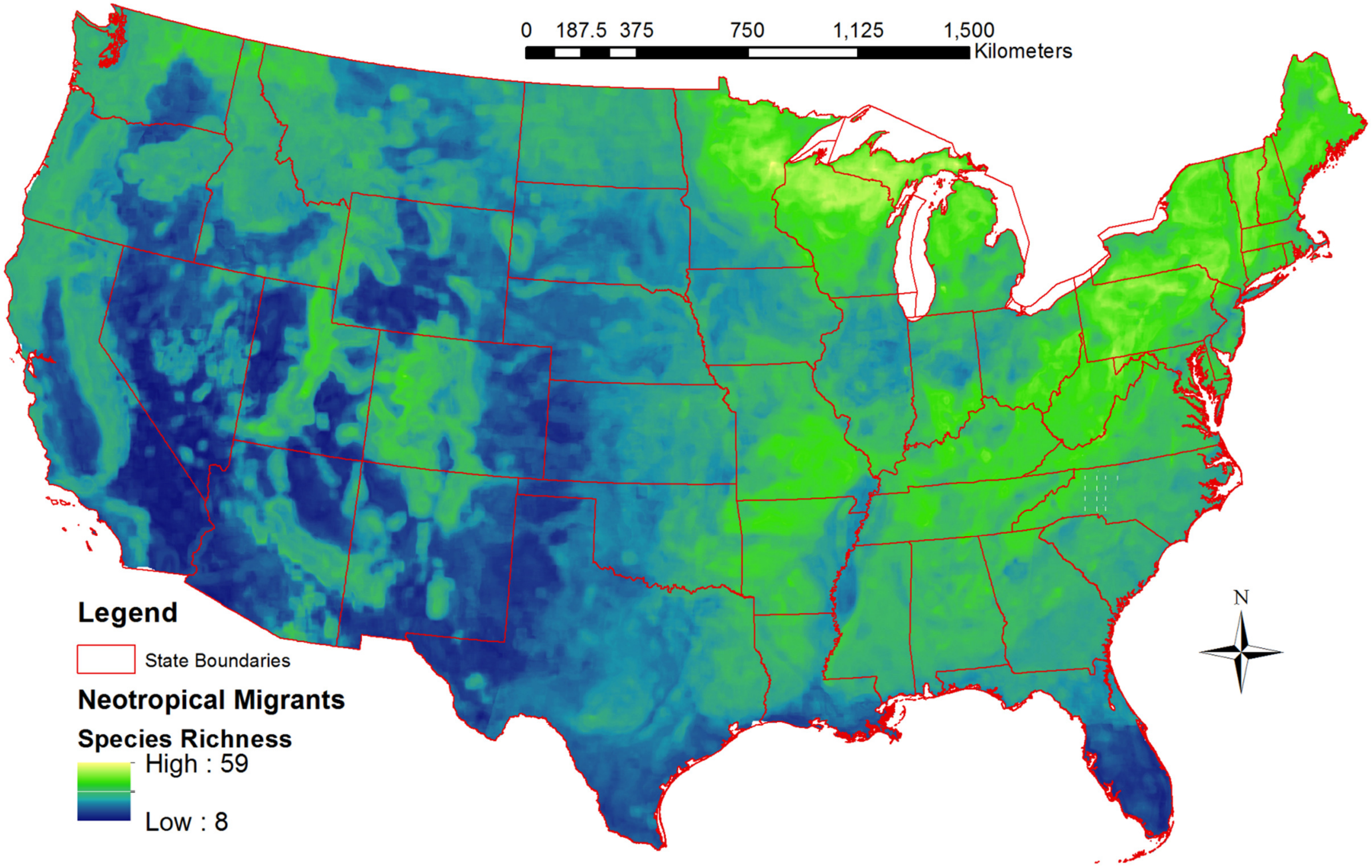

Figure 5-9. Predicted species richness for Neotropical migrant birds. Map indicates the predicted species richness of a hypothetical Breeding Bird Survey centered at a given point. The pseudo-R^2 for this model is 0.60.

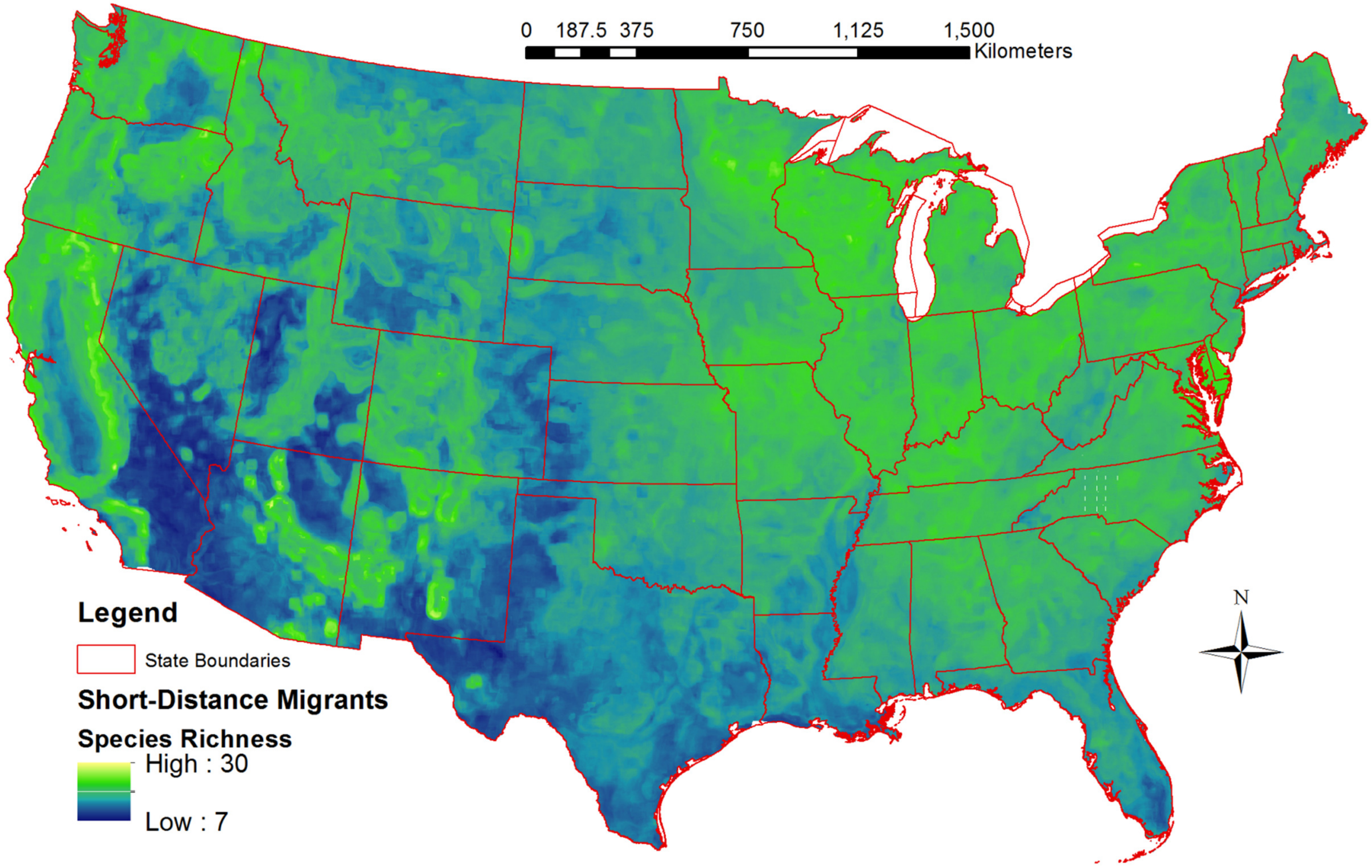

Figure 5-10. Predicted species richness for short-distance migrant birds. Map indicates the predicted species richness of a hypothetical Breeding Bird Survey centered at a given point. The pseudo-R^2 for this model is 0.36.

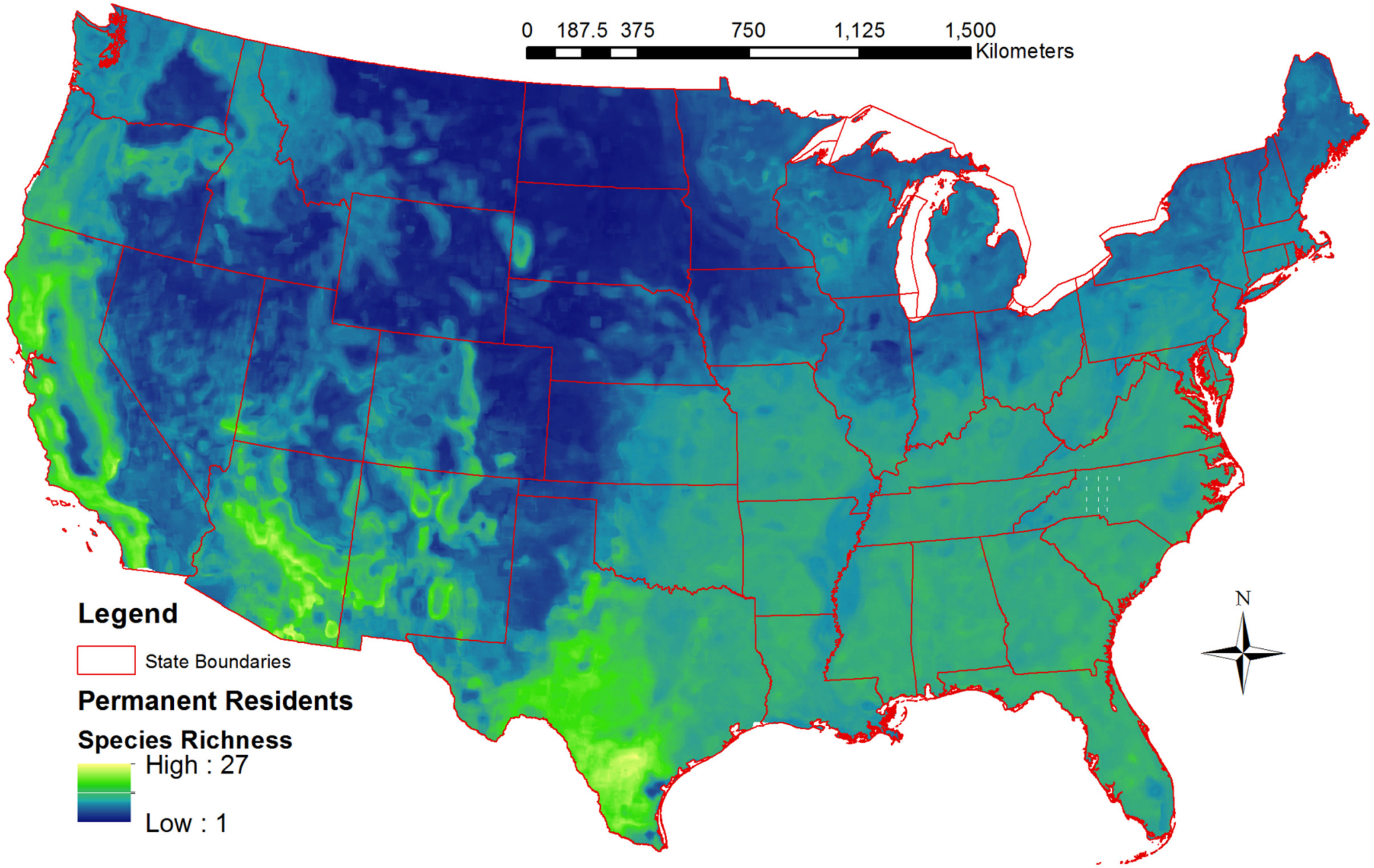

Figure 5-11. Predicted species richness for permanent resident birds. Map indicates the predicted species richness of a hypothetical Breeding Bird Survey centered at a given point. The pseudo-R^2 for this model is 0.66.

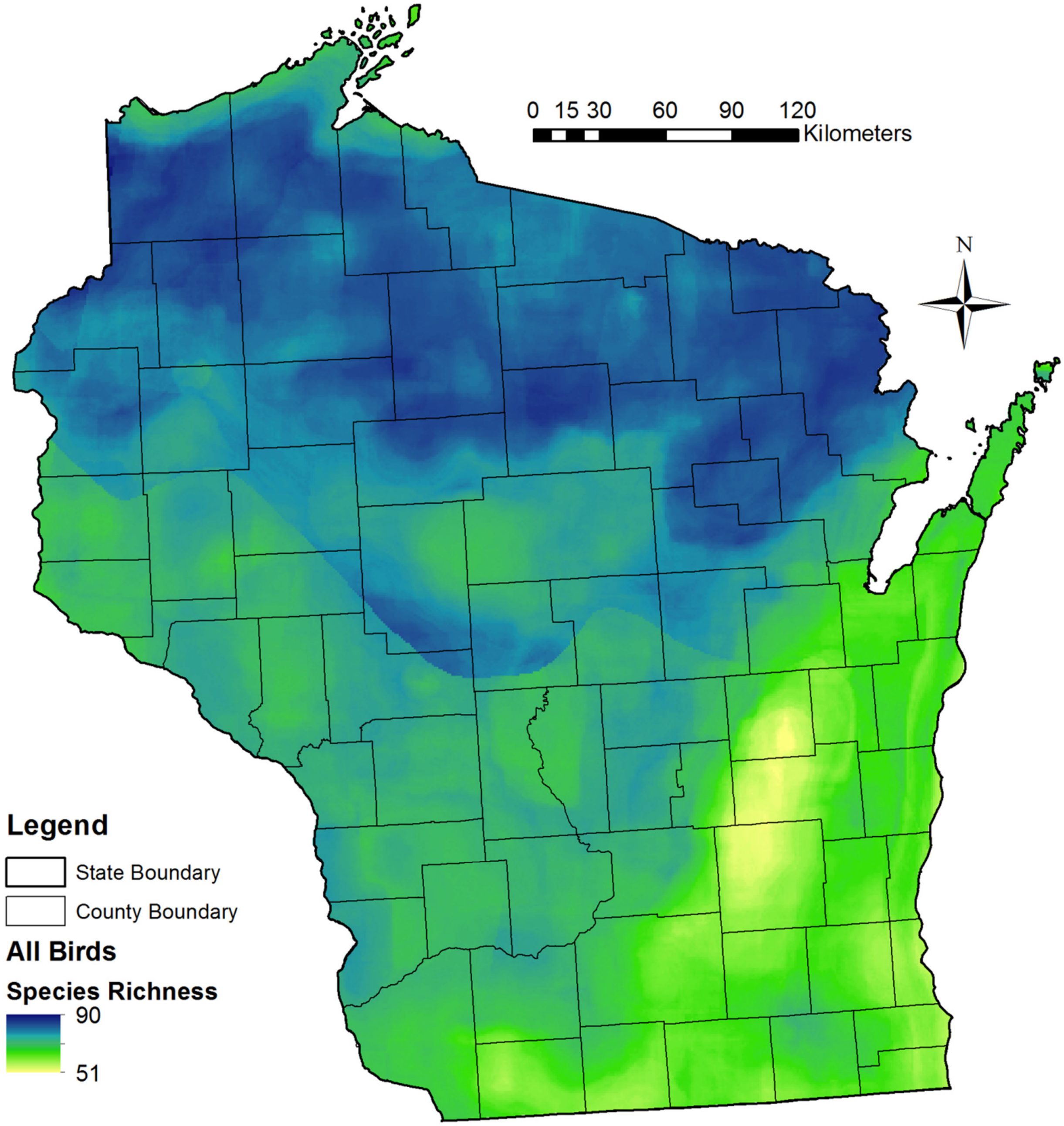

Figure 5-12. Predicted species richness for all birds in the state of Wisconsin. Map indicates the predicted species richness of a hypothetical Breeding Bird Survey centered at a given point. The pseudo-R^2 for this model at the national level is 0.55.

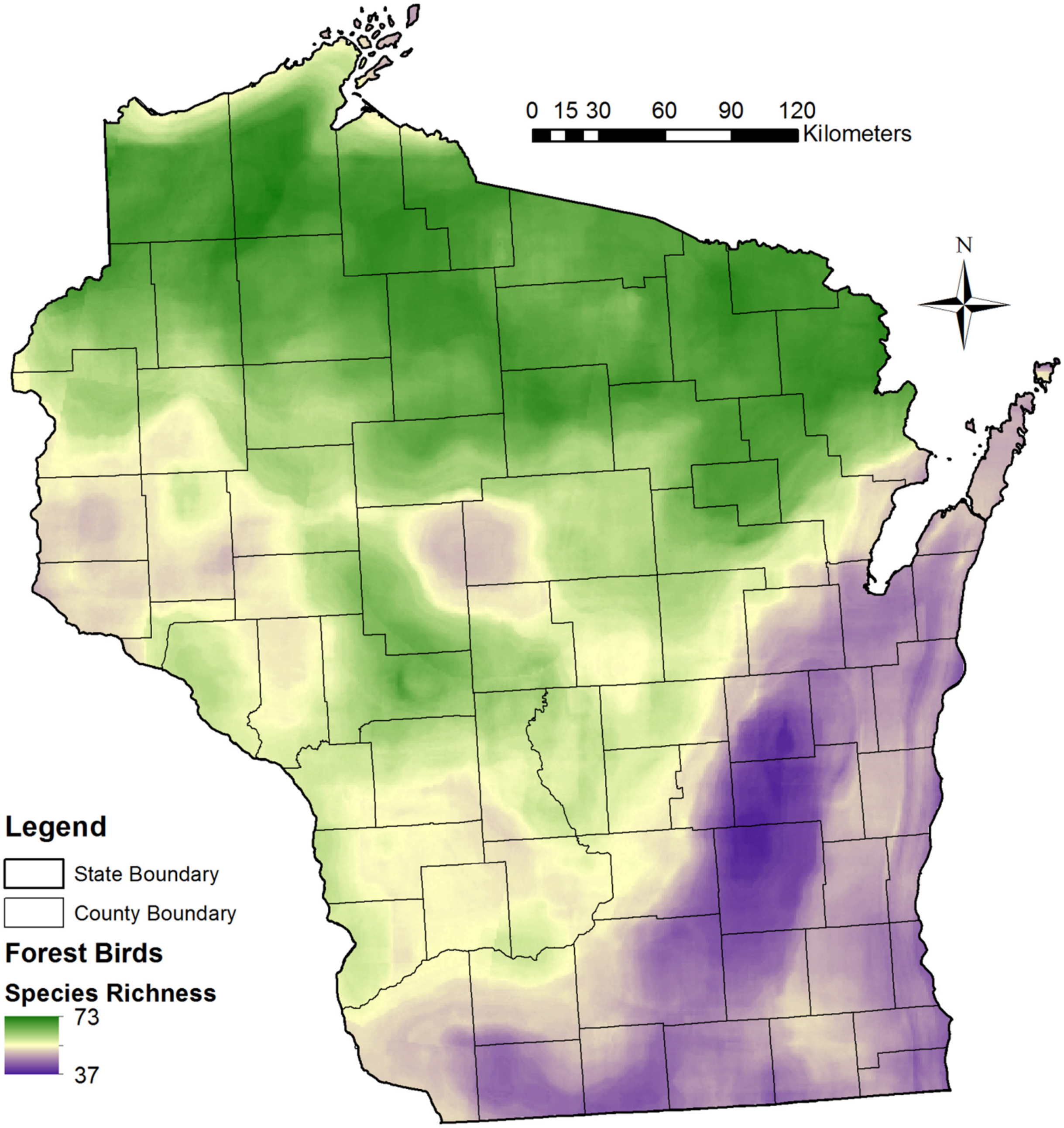

Figure 5-13. Predicted species richness for forest birds in the state of Wisconsin. Map indicates the predicted species richness of a hypothetical Breeding Bird Survey centered at a given point. The pseudo-R^2 for this model at the national level is 0.73.

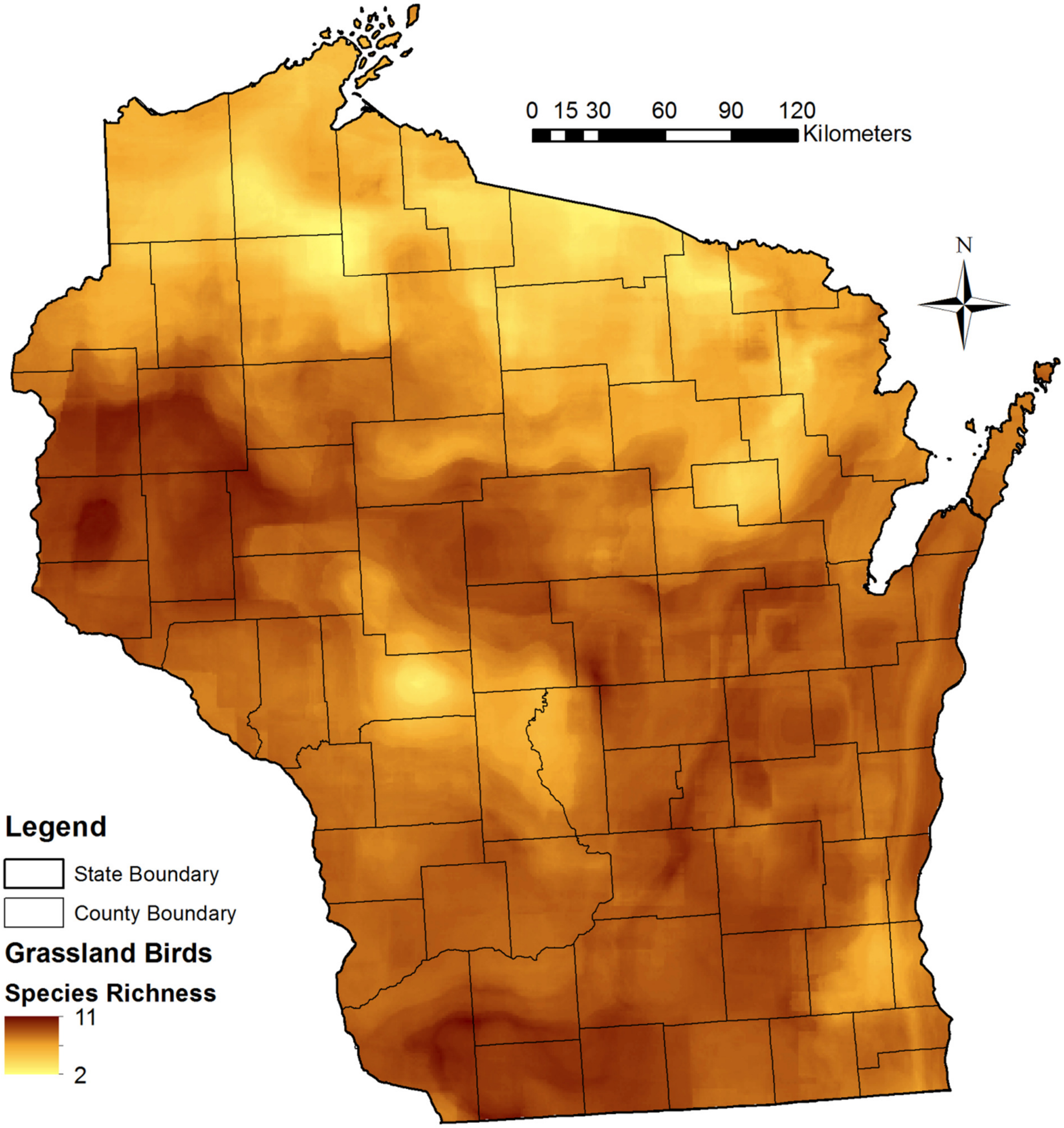

Figure 5-14. Predicted species richness for grassland birds in the state of Wisconsin. Map indicates the predicted species richness of a hypothetical Breeding Bird Survey centered at a given point. The pseudo-R^2 for this model at the national level is 0.68.

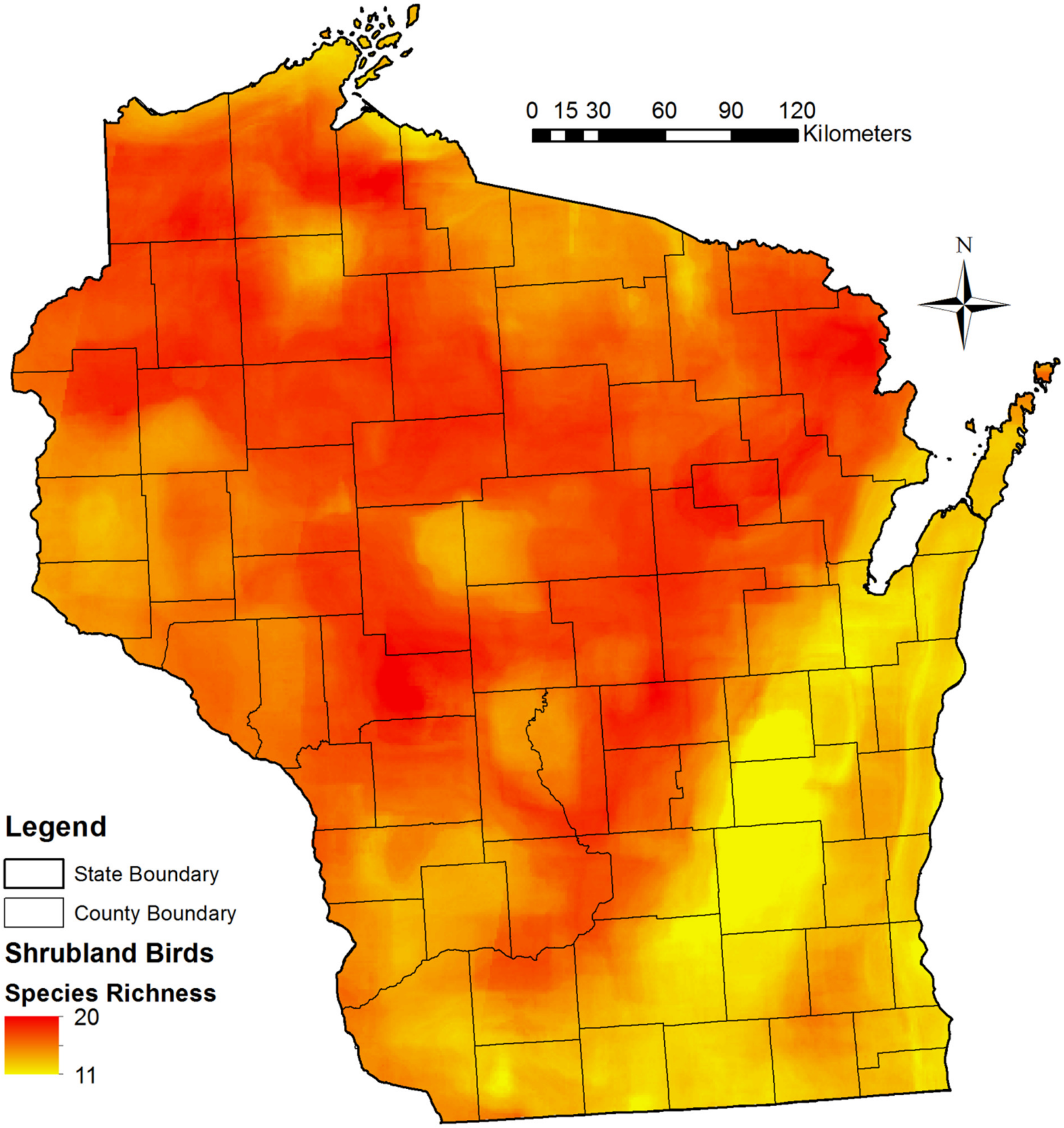

Figure 5-15. Predicted species richness for shrubland birds in the state of Wisconsin. Map indicates the predicted species richness of a hypothetical Breeding Bird Survey centered at a given point. The pseudo-R^2 for this model at the national level is 0.50.

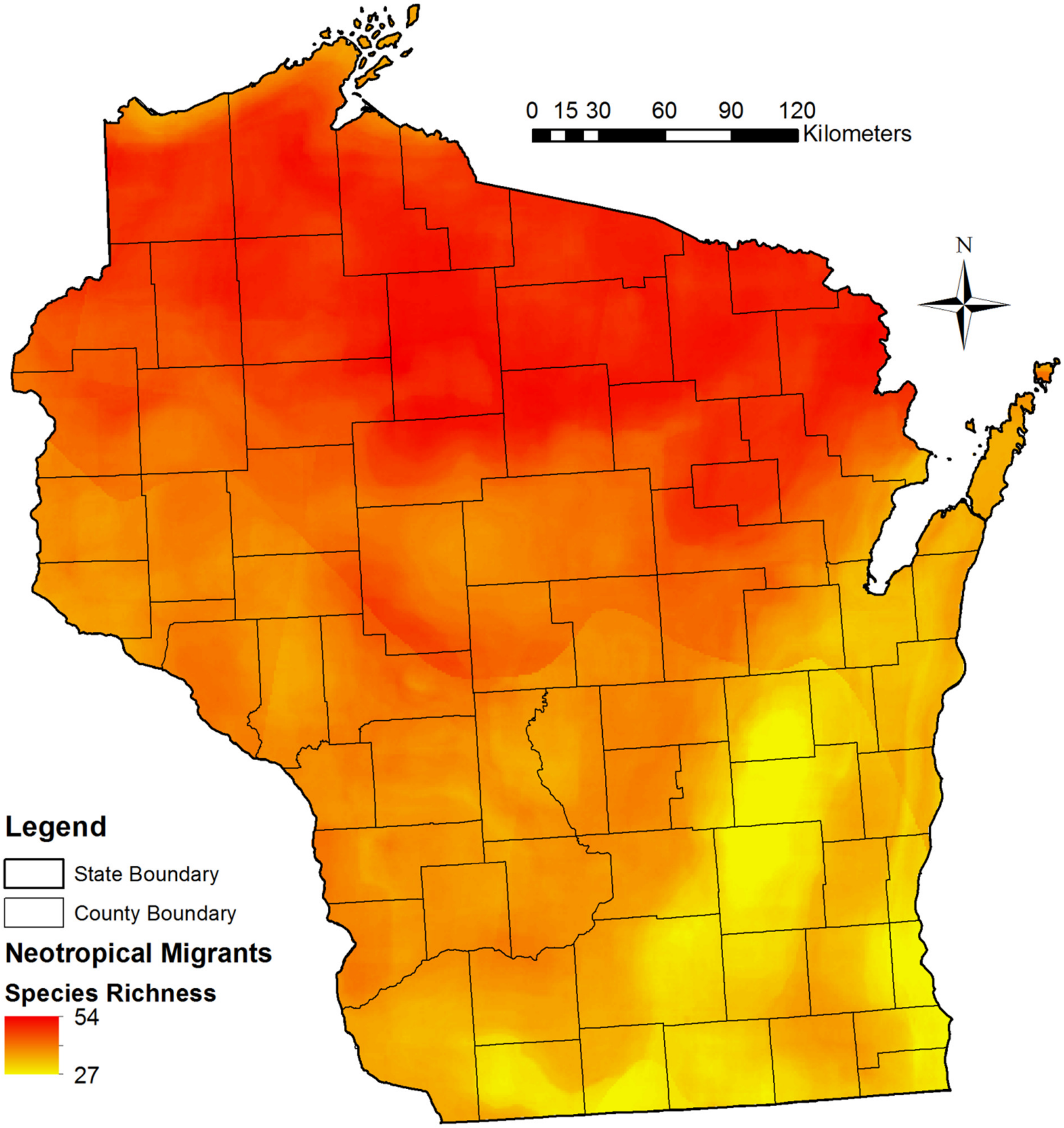

Figure 5-16. Predicted species richness for Neotropical migrant birds in the state of Wisconsin. Map indicates the predicted species richness of a hypothetical Breeding Bird Survey centered at a given point. The pseudo-R^2 for this model at the national level is 0.60.

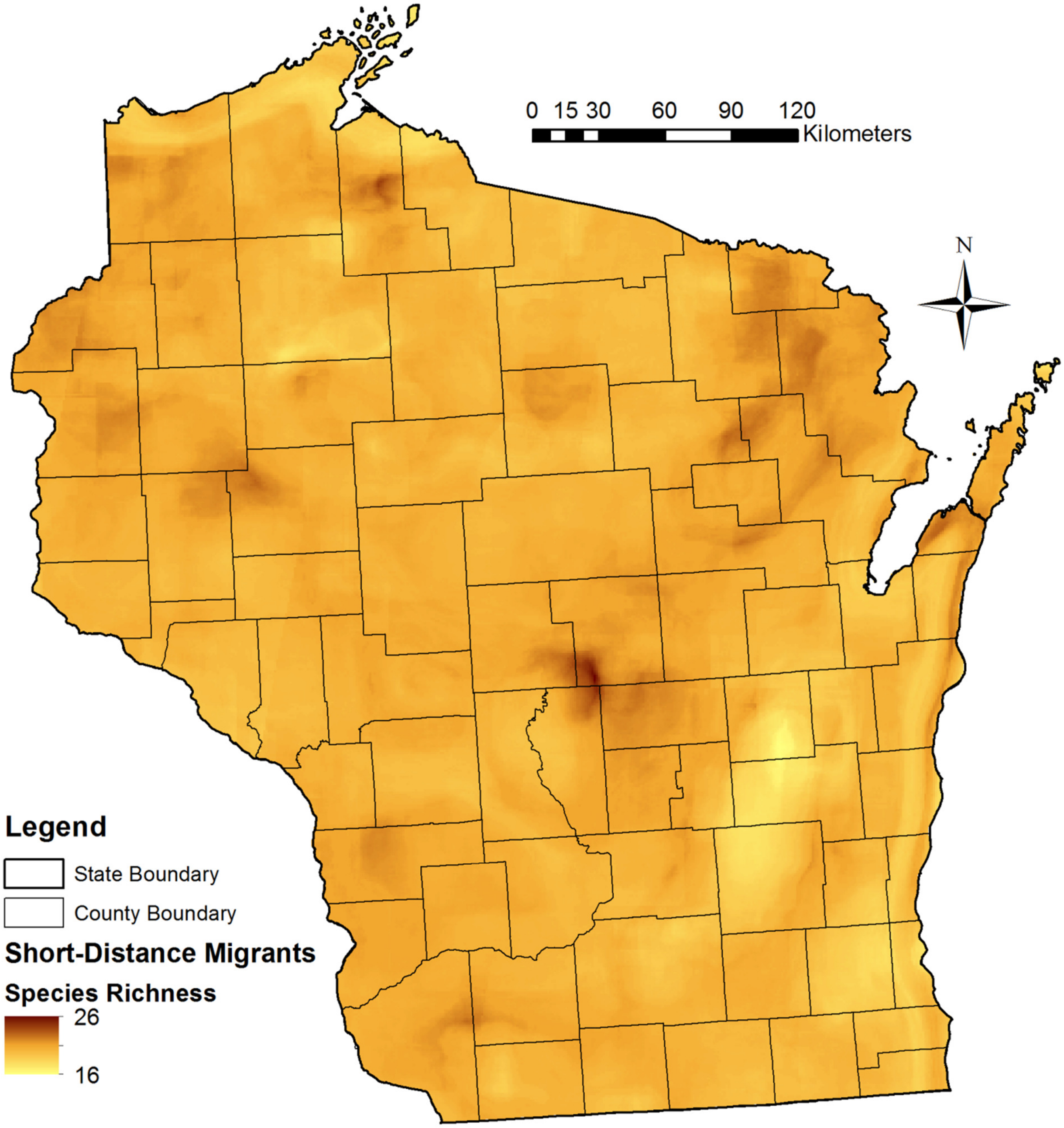

Figure 5-17. Predicted species richness for short-distance migrant birds in the state of Wisconsin. Map indicates the predicted species richness of a hypothetical Breeding Bird Survey centered at a given point. The pseudo-R^2 for this model at the national level is 0.36.

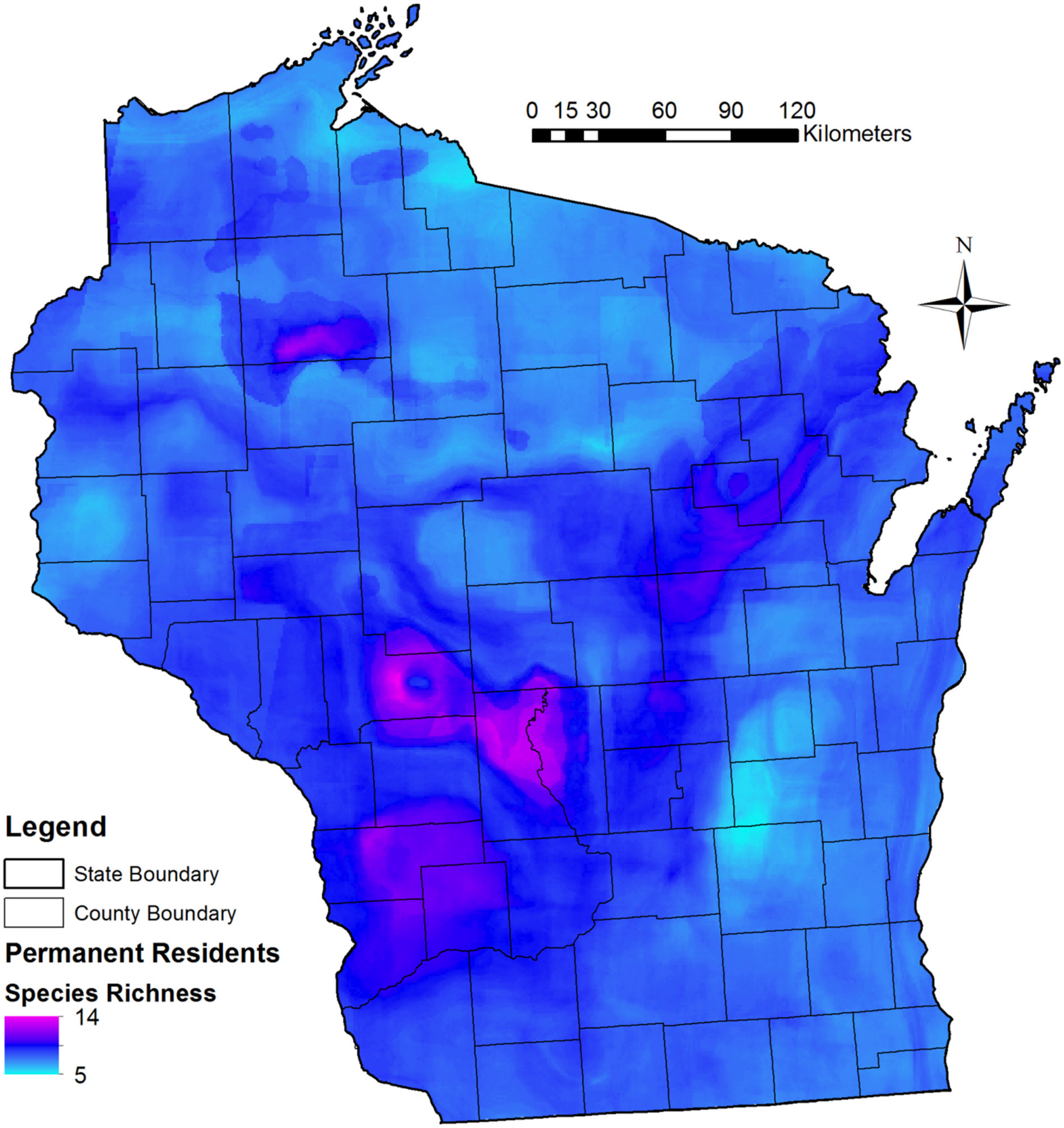

Figure 5-18. Predicted species richness for permanent resident birds in the state of Wisconsin. Map indicates the predicted species richness of a hypothetical Breeding Bird Survey centered at a given point. The pseudo-R^2 for this model at the national level is 0.66.

Appendix A: Avian Guild Definitions

Table A-1. All Birds guild.

American Ornithological Union Code	Common Name
3110	Plain Chachalaca
3000	Ruffed Grouse
3090	Greater Sage-Grouse
3089	Gunnison Sage-Grouse
2980	Spruce Grouse
3010	Willow Ptarmigan
3020	Rock Ptarmigan
3040	White-Tailed Ptarmigan
2970	Blue Grouse
3050	Greater Prairie-Chicken
3070	Lesser Prairie-Chicken
3100	Wild Turkey
2920	Mountain Quail
2930	Scaled Quail
2940	California Quail
2950	Gambel's Quail
2890	Northern Bobwhite
2960	Montezuma Quail
3260	Black Vulture
3250	Turkey Vulture
3240	California Condor
3640	Osprey
3271	Hook-Billed Kite
3270	Swallow-Tailed Kite
3280	White-Tailed Kite
3300	Snail Kite
3290	Mississippi Kite
3520	Bald Eagle
3310	Northern Harrier
3320	Sharp-Shinned Hawk
3330	Cooper's Hawk
3340	Northern Goshawk
3450	Common Black-Hawk
3350	Harris's Hawk
3390	Red-Shouldered Hawk
3430	Broad-Winged Hawk
3460	Gray Hawk
3440	Short-Tailed Hawk

3420	Swainson's Hawk
3410	White-Tailed Hawk
3400	Zone-Tailed Hawk
3370	Red-Tailed Hawk
3480	Ferruginous Hawk
3470	Rough-Legged Hawk
3490	Golden Eagle
3620	Crested Caracara
3600	American Kestrel
3570	Merlin
3590	Aplomado Falcon
3540	Gyrfalcon
3560	Peregrine Falcon
3550	Prairie Falcon
3140	White-Crowned Pigeon
3130	Red-Billed Pigeon
3120	Band-Tailed Pigeon
3190	White-Winged Dove
3160	Mourning Dove
3210	Inca Dove
3200	Common Ground-Dove
3180	White-Tipped Dove
11230	Green Parakeet
3821	Thick-Billed Parrot
3826	Red-Crowned Parrot
3870	Yellow-Billed Cuckoo
3860	Mangrove Cuckoo
3880	Black-Billed Cuckoo
3850	Greater Roadrunner
3830	Smooth-Billed Ani
3840	Groove-Billed Ani
3650	Barn Owl
3740	Flammulated Owl
3732	Western Screech-Owl
3730	Eastern Screech-Owl
3731	Whiskered Screech-Owl
3750	Great Horned Owl
3760	Snowy Owl
3770	Northern Hawk Owl
3790	Northern Pygmy-Owl
3800	Ferruginous Pygmy-Owl
3810	Elf Owl
3780	Burrowing Owl

3690	Spotted Owl
3680	Barred Owl
3700	Great Gray Owl
3660	Long-Eared Owl
3670	Short-Eared Owl
3710	Boreal Owl
3720	Northern Saw-Whet Owl
4210	Lesser Nighthawk
4200	Common Nighthawk
4201	Antillean Nighthawk
4190	Common Pauraque
4180	Common Poorwill
4160	Chuck-Will's-Widow
4161	Buff-Collared Nightjar
4170	Whip-Poor-Will
4220	Black Swift
4230	Chimney Swift
4240	Vaux's Swift
4250	White-Throated Swift
4410	Broad-Billed Hummingbird
4401	White-Eared Hummingbird
4381	Berylline Hummingbird
4390	Buff-Bellied Hummingbird
4391	Violet-Crowned Hummingbird
4270	Blue-Throated Hummingbird
4260	Magnificent Hummingbird
4370	Lucifer Hummingbird
4280	Ruby-Throated Hummingbird
4290	Black-Chinned Hummingbird
4310	Anna's Hummingbird
4300	Costa's Hummingbird
4360	Calliope Hummingbird
4320	Broad-Tailed Hummingbird
4330	Rufous Hummingbird
4340	Allen's Hummingbird
3890	Elegant Trogon
3901	Ringed Kingfisher
3900	Belted Kingfisher
3910	Green Kingfisher
4080	Lewis's Woodpecker
4060	Red-Headed Woodpecker
4070	Acorn Woodpecker
4110	Gila Woodpecker

4100	Golden-Fronted Woodpecker
4090	Red-Bellied Woodpecker
4040	Williamson's Sapsucker
4020	Yellow-Bellied Sapsucker
4021	Red-Naped Sapsucker
4030	Red-Breasted Sapsucker
3960	Ladder-Backed Woodpecker
3970	Nuttall's Woodpecker
3940	Downy Woodpecker
3930	Hairy Woodpecker
3975	Arizona Woodpecker
3950	Red-Cockaded Woodpecker
3990	White-Headed Woodpecker
4010	American Three-Toed Woodpecker
4000	Black-Backed Woodpecker
4123	Northern Flicker
4140	Gilded Flicker
4050	Pileated Woodpecker
4720	Northern Beardless-Tyrannulet
4590	Olive-Sided Flycatcher
4600	Greater Pewee
4620	Western Wood-Pewee
4610	Eastern Wood-Pewee
4630	Yellow-Bellied Flycatcher
4650	Acadian Flycatcher
4661	Alder Flycatcher
4660	Willow Flycatcher
4670	Least Flycatcher
4680	Hammond's Flycatcher
4691	Gray Flycatcher
4690	Dusky Flycatcher
4641	Pacific-Slope Flycatcher
4640	Cordilleran Flycatcher
4700	Buff-Breasted Flycatcher
4580	Black Phoebe
4560	Eastern Phoebe
4570	Say's Phoebe
4710	Vermilion Flycatcher
4550	Dusky-Capped Flycatcher
4540	Ash-Throated Flycatcher
4520	Great Crested Flycatcher
4530	Brown-Crested Flycatcher
4490	Great Kiskadee

4510	Sulphur-Bellied Flycatcher
4460	Tropical Kingbird
4461	Couch's Kingbird
4480	Cassin's Kingbird
4451	Thick-Billed Kingbird
4470	Western Kingbird
4440	Eastern Kingbird
4450	Gray Kingbird
4430	Scissor-Tailed Flycatcher
4411	Rose-Throated Becard
6220	Loggerhead Shrike
6210	Northern Shrike
6310	White-Eyed Vireo
6330	Bell's Vireo
6300	Black-Capped Vireo
6340	Gray Vireo
6280	Yellow-Throated Vireo
6292	Plumbeous Vireo
6291	Cassin's Vireo
6290	Blue-Headed Vireo
6320	Hutton's Vireo
6270	Warbling Vireo
6260	Philadelphia Vireo
6240	Red-Eyed Vireo
6250	Yellow-Green Vireo
6230	Black-Whiskered Vireo
4840	Gray Jay
4780	Steller's Jay
4770	Blue Jay
4830	Green Jay
4832	Brown Jay
4790	Florida Scrub-Jay
4811	Island Scrub-Jay
4810	Western Scrub-Jay
4820	Mexican Jay
4920	Pinyon Jay
4910	Clark's Nutcracker
4750	Black-Billed Magpie
4760	Yellow-Billed Magpie
4880	American Crow
4890	Northwestern Crow
4891	Tamaulipas Crow
4900	Fish Crow

4870	Chihuahuan Raven
4860	Common Raven
4740	Horned Lark
6110	Purple Martin
6140	Tree Swallow
6150	Violet-Green Swallow
6170	Northern Rough-Winged Swallow
6160	Bank Swallow
6120	Cliff Swallow
6121	Cave Swallow
6130	Barn Swallow
7360	Carolina Chickadee
7350	Black-Capped Chickadee
7380	Mountain Chickadee
7370	Mexican Chickadee
7410	Chestnut-Backed Chickadee
7400	Boreal Chickadee
7390	Gray-Headed Chickadee
7340	Bridled Titmouse
7330	Oak Titmouse
7331	Juniper Titmouse
7310	Tufted Titmouse
7320	Black-Crested Titmouse
7460	Verdin
7430	Bushtit
7280	Red-Breasted Nuthatch
7270	White-Breasted Nuthatch
7300	Pygmy Nuthatch
7290	Brown-Headed Nuthatch
7260	Brown Creeper
7130	Cactus Wren
7150	Rock Wren
7170	Canyon Wren
7180	Carolina Wren
7190	Bewick's Wren
7210	House Wren
7220	Winter Wren
7240	Sedge Wren
7250	Marsh Wren
7010	American Dipper
7480	Golden-Crowned Kinglet
7490	Ruby-Crowned Kinglet
7470	Arctic Warbler

7510	Blue-Gray Gnatcatcher
7530	California Gnatcatcher
7520	Black-Tailed Gnatcatcher
7531	Black-Capped Gnatcatcher
7640	Bluethroat
7650	Northern Wheatear
7660	Eastern Bluebird
7670	Western Bluebird
7680	Mountain Bluebird
7540	Townsend's Solitaire
7560	Veery
7570	Gray-Cheeked Thrush
7571	Bicknell's Thrush
7580	Swainson's Thrush
7590	Hermit Thrush
7550	Wood Thrush
7621	Clay-Colored Robin
7610	American Robin
7630	Varied Thrush
7420	Wrentit
7040	Gray Catbird
7030	Northern Mockingbird
7020	Sage Thrasher
7050	Brown Thrasher
7060	Long-Billed Thrasher
7080	Bendire's Thrasher
7070	Curve-Billed Thrasher
7100	California Thrasher
7120	Crissal Thrasher
7110	Le Conte's Thrasher
6940	White Wagtail
6990	Red-Throated Pipit
6970	American Pipit
7000	Sprague's Pipit
6180	Bohemian Waxwing
6190	Cedar Waxwing
6200	Phainopepla
6510	Olive Warbler
6410	Blue-Winged Warbler
6420	Golden-Winged Warbler
6470	Tennessee Warbler
6460	Orange-Crowned Warbler
6450	Nashville Warbler

6440	Virginia's Warbler
6471	Colima Warbler
6430	Lucy's Warbler
6480	Northern Parula
6490	Tropical Parula
6520	Yellow Warbler
6590	Chestnut-Sided Warbler
6570	Magnolia Warbler
6500	Cape May Warbler
6540	Black-Throated Blue Warbler
6556	Yellow-Rumped Warbler
6650	Black-Throated Gray Warbler
6660	Golden-Cheeked Warbler
6670	Black-Throated Green Warbler
6680	Townsend's Warbler
6690	Hermit Warbler
6620	Blackburnian Warbler
6630	Yellow-Throated Warbler
6640	Grace's Warbler
6710	Pine Warbler
6700	Kirtland's Warbler
6730	Prairie Warbler
6720	Palm Warbler
6600	Bay-Breasted Warbler
6610	Blackpoll Warbler
6580	Cerulean Warbler
6360	Black-And-White Warbler
6870	American Redstart
6370	Prothonotary Warbler
6390	Worm-Eating Warbler
6380	Swainson's Warbler
6740	Ovenbird
6750	Northern Waterthrush
6760	Louisiana Waterthrush
6770	Kentucky Warbler
6780	Connecticut Warbler
6790	Mourning Warbler
6800	Macgillivray's Warbler
6810	Common Yellowthroat
6840	Hooded Warbler
6850	Wilson's Warbler
6860	Canada Warbler
6900	Red-Faced Warbler

6880	Painted Redstart
6921	Rufous-Capped Warbler
6830	Yellow-Breasted Chat
6090	Hepatic Tanager
6100	Summer Tanager
6080	Scarlet Tanager
6070	Western Tanager
6071	Flame-Colored Tanager
6020	White-Collared Seedeater
5860	Olive Sparrow
5900	Green-Tailed Towhee
5880	Spotted Towhee
5870	Eastern Towhee
5910	Canyon Towhee
5911	California Towhee
5920	Abert's Towhee
5790	Rufous-Winged Sparrow
5780	Cassin's Sparrow
5750	Bachman's Sparrow
5760	Botteri's Sparrow
5800	Rufous-Crowned Sparrow
5742	Five-Striped Sparrow
5590	American Tree Sparrow
5600	Chipping Sparrow
5610	Clay-Colored Sparrow
5620	Brewer's Sparrow
5630	Field Sparrow
5650	Black-Chinned Sparrow
5400	Vesper Sparrow
5520	Lark Sparrow
5730	Black-Throated Sparrow
5740	Sage Sparrow
6050	Lark Bunting
5420	Savannah Sparrow
5460	Grasshopper Sparrow
5450	Baird's Sparrow
5470	Henslow's Sparrow
5480	Le Conte's Sparrow
5491	Nelson's Sharp-Tailed Sparrow
5490	Saltmarsh Sharp-Tailed Sparrow
5500	Seaside Sparrow
5850	Fox Sparrow
5810	Song Sparrow

5830	Lincoln's Sparrow
5840	Swamp Sparrow
5580	White-Throated Sparrow
5530	Harris's Sparrow
5540	White-Crowned Sparrow
5570	Golden-Crowned Sparrow
5677	Dark-Eyed Junco
5700	Yellow-Eyed Junco
5390	Mccown's Longspur
5360	Lapland Longspur
5370	Smith's Longspur
5380	Chestnut-Collared Longspur
5340	Snow Bunting
5350	Mckay's Bunting
5930	Northern Cardinal
5940	Pyrrhuloxia
5950	Rose-Breasted Grosbeak
5960	Black-Headed Grosbeak
5970	Blue Grosbeak
5990	Lazuli Bunting
5980	Indigo Bunting
6000	Varied Bunting
6010	Painted Bunting
6040	Dickcissel
4940	Bobolink
4980	Red-Winged Blackbird
5000	Tricolored Blackbird
5010	Eastern Meadowlark
5011	Western Meadowlark
4970	Yellow-Headed Blackbird
5090	Rusty Blackbird
5100	Brewer's Blackbird
5110	Common Grackle
5130	Boat-Tailed Grackle
5120	Great-Tailed Grackle
4961	Shiny Cowbird
4960	Bronzed Cowbird
4950	Brown-Headed Cowbird
5060	Orchard Oriole
5050	Hooded Oriole
5051	Streak-Backed Oriole
5080	Bullock's Oriole
5031	Altamira Oriole

5030	Audubon's Oriole
5070	Baltimore Oriole
5040	Scott's Oriole
5241	Unid. Rosy-Finch
5150	Pine Grosbeak
5170	Purple Finch
5180	Cassin's Finch
5190	House Finch
5210	Red Crossbill
5220	White-Winged Crossbill
5280	Common Redpoll
5270	Hoary Redpoll
5330	Pine Siskin
5300	Lesser Goldfinch
5310	Lawrence's Goldfinch
5290	American Goldfinch
5140	Evening Grosbeak

Table A-2. Forest Birds guild.

American Ornithological Union Code	Common Name
3000	Ruffed Grouse
2970	Blue Grouse
3100	Wild Turkey
2920	Mountain Quail
2940	California Quail
2890	Northern Bobwhite
3260	Black Vulture
3250	Turkey Vulture
3640	Osprey
3270	Swallow-Tailed Kite
3290	Mississippi Kite
3520	Bald Eagle
3320	Sharp-Shinned Hawk
3330	Cooper's Hawk
3340	Northern Goshawk
3390	Red-Shouldered Hawk
3430	Broad-Winged Hawk
3370	Red-Tailed Hawk
3600	American Kestrel
3570	Merlin
3120	Band-Tailed Pigeon
3160	Mourning Dove
3870	Yellow-Billed Cuckoo
3880	Black-Billed Cuckoo
3840	Groove-Billed Ani
3732	Western Screech-Owl
3730	Eastern Screech-Owl
3750	Great Horned Owl
3790	Northern Pygmy-Owl
3690	Spotted Owl
3680	Barred Owl
3660	Long-Eared Owl
3720	Northern Saw-Whet Owl
4200	Common Nighthawk
4160	Chuck-Will's-Widow
4170	Whip-Poor-Will
4240	Vaux's Swift
4410	Broad-Billed Hummingbird
4280	Ruby-Throated Hummingbird
4290	Black-Chinned Hummingbird
4310	Anna's Hummingbird
4360	Calliope Hummingbird

4330	Rufous Hummingbird
4340	Allen's Hummingbird
3900	Belted Kingfisher
4080	Lewis's Woodpecker
4060	Red-Headed Woodpecker
4070	Acorn Woodpecker
4110	Gila Woodpecker
4090	Red-Bellied Woodpecker
4040	Williamson's Sapsucker
4020	Yellow-Bellied Sapsucker
4021	Red-Naped Sapsucker
4030	Red-Breasted Sapsucker
3960	Ladder-Backed Woodpecker
3970	Nuttall's Woodpecker
3940	Downy Woodpecker
3930	Hairy Woodpecker
3975	Arizona Woodpecker
3950	Red-Cockaded Woodpecker
3990	White-Headed Woodpecker
4010	American Three-Toed Woodpecker
4000	Black-Backed Woodpecker
4123	Northern Flicker
4050	Pileated Woodpecker
4590	Olive-Sided Flycatcher
4600	Greater Pewee
4620	Western Wood-Pewee
4610	Eastern Wood-Pewee
4630	Yellow-Bellied Flycatcher
4650	Acadian Flycatcher
4661	Alder Flycatcher
4670	Least Flycatcher
4680	Hammond's Flycatcher
4690	Dusky Flycatcher
4641	Pacific-Slope Flycatcher
4640	Cordilleran Flycatcher
4560	Eastern Phoebe
4710	Vermilion Flycatcher
4520	Great Crested Flycatcher
4530	Brown-Crested Flycatcher
4490	Great Kiskadee
4461	Couch's Kingbird
4480	Cassin's Kingbird
4470	Western Kingbird

4440	Eastern Kingbird
4450	Gray Kingbird
4430	Scissor-Tailed Flycatcher
6310	White-Eyed Vireo
6280	Yellow-Throated Vireo
6292	Plumbeous Vireo
6291	Cassin's Vireo
6290	Blue-Headed Vireo
6320	Hutton's Vireo
6270	Warbling Vireo
6260	Philadelphia Vireo
6240	Red-Eyed Vireo
6230	Black-Whiskered Vireo
4840	Gray Jay
4780	Steller's Jay
4770	Blue Jay
4830	Green Jay
4790	Florida Scrub-Jay
4810	Western Scrub-Jay
4820	Mexican Jay
4920	Pinyon Jay
4910	Clark's Nutcracker
4750	Black-Billed Magpie
4760	Yellow-Billed Magpie
4880	American Crow
4890	Northwestern Crow
4900	Fish Crow
4860	Common Raven
6110	Purple Martin
6140	Tree Swallow
6150	Violet-Green Swallow
6170	Northern Rough-Winged Swallow
6160	Bank Swallow
6120	Cliff Swallow
7360	Carolina Chickadee
7350	Black-Capped Chickadee
7380	Mountain Chickadee
7410	Chestnut-Backed Chickadee
7400	Boreal Chickadee
7340	Bridled Titmouse
7330	Oak Titmouse
7331	Juniper Titmouse
7310	Tufted Titmouse

7320	Black-Crested Titmouse
7430	Bushtit
7280	Red-Breasted Nuthatch
7270	White-Breasted Nuthatch
7300	Pygmy Nuthatch
7290	Brown-Headed Nuthatch
7260	Brown Creeper
7150	Rock Wren
7170	Canyon Wren
7180	Carolina Wren
7190	Bewick's Wren
7210	House Wren
7220	Winter Wren
7010	American Dipper
7480	Golden-Crowned Kinglet
7490	Ruby-Crowned Kinglet
7510	Blue-Gray Gnatcatcher
7660	Eastern Bluebird
7670	Western Bluebird
7680	Mountain Bluebird
7540	Townsend's Solitaire
7560	Veery
7580	Swainson's Thrush
7590	Hermit Thrush
7550	Wood Thrush
7610	American Robin
7630	Varied Thrush
7420	Wrentit
7040	Gray Catbird
7030	Northern Mockingbird
7050	Brown Thrasher
6190	Cedar Waxwing
6200	Phainopepla
6510	Olive Warbler
6410	Blue-Winged Warbler
6420	Golden-Winged Warbler
6470	Tennessee Warbler
6460	Orange-Crowned Warbler
6450	Nashville Warbler
6440	Virginia's Warbler
6430	Lucy's Warbler
6480	Northern Parula
6590	Chestnut-Sided Warbler

6570	Magnolia Warbler
6500	Cape May Warbler
6540	Black-Throated Blue Warbler
6650	Black-Throated Gray Warbler
6670	Black-Throated Green Warbler
6680	Townsend's Warbler
6690	Hermit Warbler
6620	Blackburnian Warbler
6630	Yellow-Throated Warbler
6640	Grace's Warbler
6710	Pine Warbler
6730	Prairie Warbler
6720	Palm Warbler
6600	Bay-Breasted Warbler
6610	Blackpoll Warbler
6580	Cerulean Warbler
6360	Black-And-White Warbler
6870	American Redstart
6370	Prothonotary Warbler
6390	Worm-Eating Warbler
6380	Swainson's Warbler
6740	Ovenbird
6750	Northern Waterthrush
6760	Louisiana Waterthrush
6770	Kentucky Warbler
6780	Connecticut Warbler
6790	Mourning Warbler
6800	Macgillivray's Warbler
6810	Common Yellowthroat
6840	Hooded Warbler
6850	Wilson's Warbler
6860	Canada Warbler
6900	Red-Faced Warbler
6830	Yellow-Breasted Chat
6090	Hepatic Tanager
6100	Summer Tanager
6080	Scarlet Tanager
6070	Western Tanager
5880	Spotted Towhee
5870	Eastern Towhee
5750	Bachman's Sparrow
5600	Chipping Sparrow
5650	Black-Chinned Sparrow

5850	Fox Sparrow
5810	Song Sparrow
5830	Lincoln's Sparrow
5580	White-Throated Sparrow
5540	White-Crowned Sparrow
5677	Dark-Eyed Junco
5930	Northern Cardinal
5950	Rose-Breasted Grosbeak
5960	Black-Headed Grosbeak
5970	Blue Grosbeak
5990	Lazuli Bunting
5980	Indigo Bunting
6010	Painted Bunting
5110	Common Grackle
5120	Great-Tailed Grackle
4950	Brown-Headed Cowbird
5060	Orchard Oriole
5030	Audubon's Oriole
5070	Baltimore Oriole
5150	Pine Grosbeak
5170	Purple Finch
5180	Cassin's Finch
5190	House Finch
5210	Red Crossbill
5220	White-Winged Crossbill
5330	Pine Siskin
5310	Lawrence's Goldfinch
5140	Evening Grosbeak

Table A-3. Grassland Birds guild.

American Ornithological Union Code	Common Name
3050	Greater Prairie-Chicken
3070	Lesser Prairie-Chicken
3310	Northern Harrier
3420	Swainson's Hawk
3480	Ferruginous Hawk
3650	Barn Owl
3780	Burrowing Owl
3670	Short-Eared Owl
4200	Common Nighthawk
4180	Common Poorwill
4740	Horned Lark
7240	Sedge Wren
7000	Sprague's Pipit
6810	Common Yellowthroat
5780	Cassin's Sparrow
5760	Botteri's Sparrow
5400	Vesper Sparrow
5520	Lark Sparrow
6050	Lark Bunting
5420	Savannah Sparrow
5460	Grasshopper Sparrow
5450	Baird's Sparrow
5470	Henslow's Sparrow
5480	Le Conte's Sparrow
5390	Mccown's Longspur
5380	Chestnut-Collared Longspur
6040	Dickcissel
4940	Bobolink
5010	Eastern Meadowlark
5011	Western Meadowlark

Table A-4. Shrubland Birds guild.

American Ornithological Union Code	Common Name
3090	Greater Sage-Grouse
3089	Gunnison Sage-Grouse
2920	Mountain Quail
2930	Scaled Quail
2940	California Quail
2950	Gambel's Quail
2890	Northern Bobwhite
3350	Harris's Hawk
3190	White-Winged Dove
3200	Common Ground-Dove
3850	Greater Roadrunner
3830	Smooth-Billed Ani
3840	Groove-Billed Ani
3660	Long-Eared Owl
4210	Lesser Nighthawk
4180	Common Poorwill
4300	Costa's Hummingbird
4661	Alder Flycatcher
4660	Willow Flycatcher
4691	Gray Flycatcher
4540	Ash-Throated Flycatcher
4461	Couch's Kingbird
6310	White-Eyed Vireo
6330	Bell's Vireo
6340	Gray Vireo
4830	Green Jay
4790	Florida Scrub-Jay
4811	Island Scrub-Jay
4810	Western Scrub-Jay
4920	Pinyon Jay
7460	Verdin
7430	Bushtit
7130	Cactus Wren
7180	Carolina Wren
7190	Bewick's Wren
7210	House Wren
7520	Black-Tailed Gnatcatcher
7420	Wrentit
7040	Gray Catbird
7020	Sage Thrasher
7050	Brown Thrasher
7080	Bendire's Thrasher

7070	Curve-Billed Thrasher
7100	California Thrasher
7120	Crissal Thrasher
7110	Le Conte's Thrasher
6200	Phainopepla
6410	Blue-Winged Warbler
6420	Golden-Winged Warbler
6460	Orange-Crowned Warbler
6450	Nashville Warbler
6440	Virginia's Warbler
6430	Lucy's Warbler
6520	Yellow Warbler
6590	Chestnut-Sided Warbler
6650	Black-Throated Gray Warbler
6730	Prairie Warbler
6720	Palm Warbler
6780	Connecticut Warbler
6790	Mourning Warbler
6800	Macgillivray's Warbler
6810	Common Yellowthroat
6850	Wilson's Warbler
6830	Yellow-Breasted Chat
5860	Olive Sparrow
5900	Green-Tailed Towhee
5880	Spotted Towhee
5870	Eastern Towhee
5910	Canyon Towhee
5911	California Towhee
5790	Rufous-Winged Sparrow
5800	Rufous-Crowned Sparrow
5610	Clay-Colored Sparrow
5620	Brewer's Sparrow
5630	Field Sparrow
5650	Black-Chinned Sparrow
5520	Lark Sparrow
5730	Black-Throated Sparrow
5740	Sage Sparrow
5850	Fox Sparrow
5810	Song Sparrow
5830	Lincoln's Sparrow
5580	White-Throated Sparrow
5540	White-Crowned Sparrow
5930	Northern Cardinal

5940	Pyrrhuloxia
5970	Blue Grosbeak
5990	Lazuli Bunting
5980	Indigo Bunting
6000	Varied Bunting
6010	Painted Bunting
5040	Scott's Oriole
5300	Lesser Goldfinch
5290	American Goldfinch

Table A-5. Neotropical Migrants guild

American Ornithological Union Code	Common Name
3270	Swallow-Tailed Kite
3290	Mississippi Kite
3430	Broad-Winged Hawk
3420	Swainson's Hawk
3400	Zone-Tailed Hawk
3570	Merlin
3560	Peregrine Falcon
3120	Band-Tailed Pigeon
3870	Yellow-Billed Cuckoo
3880	Black-Billed Cuckoo
3740	Flammulated Owl
3780	Burrowing Owl
4210	Lesser Nighthawk
4200	Common Nighthawk
4160	Chuck-Will's-Widow
4161	Buff-Collared Nightjar
4170	Whip-Poor-Will
4220	Black Swift
4230	Chimney Swift
4240	Vaux's Swift
4250	White-Throated Swift
4370	Lucifer Hummingbird
4280	Ruby-Throated Hummingbird
4290	Black-Chinned Hummingbird
4300	Costa's Hummingbird
4360	Calliope Hummingbird
4320	Broad-Tailed Hummingbird
4330	Rufous Hummingbird
4340	Allen's Hummingbird
3900	Belted Kingfisher
4020	Yellow-Bellied Sapsucker
4021	Red-Naped Sapsucker
4590	Olive-Sided Flycatcher
4620	Western Wood-Pewee
4610	Eastern Wood-Pewee
4630	Yellow-Bellied Flycatcher
4650	Acadian Flycatcher
4661	Alder Flycatcher
4660	Willow Flycatcher
4670	Least Flycatcher
4680	Hammond's Flycatcher
4691	Gray Flycatcher

4690	Dusky Flycatcher
4641	Pacific-Slope Flycatcher
4640	Cordilleran Flycatcher
4560	Eastern Phoebe
4570	Say's Phoebe
4710	Vermilion Flycatcher
4540	Ash-Throated Flycatcher
4520	Great Crested Flycatcher
4510	Sulphur-Bellied Flycatcher
4480	Cassin's Kingbird
4470	Western Kingbird
4440	Eastern Kingbird
4450	Gray Kingbird
4430	Scissor-Tailed Flycatcher
6220	Loggerhead Shrike
6310	White-Eyed Vireo
6330	Bell's Vireo
6300	Black-Capped Vireo
6340	Gray Vireo
6280	Yellow-Throated Vireo
6292	Plumbeous Vireo
6291	Cassin's Vireo
6290	Blue-Headed Vireo
6270	Warbling Vireo
6260	Philadelphia Vireo
6240	Red-Eyed Vireo
6250	Yellow-Green Vireo
6230	Black-Whiskered Vireo
6110	Purple Martin
6140	Tree Swallow
6150	Violet-Green Swallow
6170	Northern Rough-Winged Swallow
6160	Bank Swallow
6120	Cliff Swallow
6130	Barn Swallow
7210	House Wren
7250	Marsh Wren
7490	Ruby-Crowned Kinglet
7510	Blue-Gray Gnatcatcher
7560	Veery
7570	Gray-Cheeked Thrush
7571	Bicknell's Thrush
7580	Swainson's Thrush

7590	Hermit Thrush
7550	Wood Thrush
7040	Gray Catbird
7020	Sage Thrasher
6970	American Pipit
7000	Sprague's Pipit
6190	Cedar Waxwing
6200	Phainopepla
6410	Blue-Winged Warbler
6420	Golden-Winged Warbler
6470	Tennessee Warbler
6460	Orange-Crowned Warbler
6450	Nashville Warbler
6440	Virginia's Warbler
6471	Colima Warbler
6430	Lucy's Warbler
6480	Northern Parula
6520	Yellow Warbler
6590	Chestnut-Sided Warbler
6570	Magnolia Warbler
6500	Cape May Warbler
6540	Black-Throated Blue Warbler
6556	Yellow-Rumped Warbler
6650	Black-Throated Gray Warbler
6660	Golden-Cheeked Warbler
6670	Black-Throated Green Warbler
6680	Townsend's Warbler
6690	Hermit Warbler
6620	Blackburnian Warbler
6630	Yellow-Throated Warbler
6640	Grace's Warbler
6700	Kirtland's Warbler
6730	Prairie Warbler
6720	Palm Warbler
6600	Bay-Breasted Warbler
6610	Blackpoll Warbler
6580	Cerulean Warbler
6360	Black-And-White Warbler
6870	American Redstart
6370	Prothonotary Warbler
6390	Worm-Eating Warbler
6380	Swainson's Warbler
6740	Ovenbird

6750	Northern Waterthrush
6760	Louisiana Waterthrush
6770	Kentucky Warbler
6780	Connecticut Warbler
6790	Mourning Warbler
6800	Macgillivray's Warbler
6810	Common Yellowthroat
6840	Hooded Warbler
6850	Wilson's Warbler
6860	Canada Warbler
6900	Red-Faced Warbler
6830	Yellow-Breasted Chat
6090	Hepatic Tanager
6100	Summer Tanager
6080	Scarlet Tanager
6070	Western Tanager
5900	Green-Tailed Towhee
5600	Chipping Sparrow
5610	Clay-Colored Sparrow
5620	Brewer's Sparrow
5400	Vesper Sparrow
5520	Lark Sparrow
6050	Lark Bunting
5420	Savannah Sparrow
5460	Grasshopper Sparrow
5450	Baird's Sparrow
5830	Lincoln's Sparrow
5840	Swamp Sparrow
5540	White-Crowned Sparrow
5950	Rose-Breasted Grosbeak
5960	Black-Headed Grosbeak
5970	Blue Grosbeak
5990	Lazuli Bunting
5980	Indigo Bunting
6000	Varied Bunting
6010	Painted Bunting
6040	Dickcissel
4940	Bobolink
4970	Yellow-Headed Blackbird
5100	Brewer's Blackbird
4950	Brown-Headed Cowbird
5060	Orchard Oriole
5050	Hooded Oriole

5080	Bullock's Oriole
5070	Baltimore Oriole
5040	Scott's Oriole

Table A-6. Short-Distance Migrants guild.

American Ornithological Union Code	Common Name
3010	Willow Ptarmigan
3020	Rock Ptarmigan
3250	Turkey Vulture
3640	Osprey
3520	Bald Eagle
3310	Northern Harrier
3320	Sharp-Shinned Hawk
3330	Cooper's Hawk
3450	Common Black-Hawk
3390	Red-Shouldered Hawk
3460	Gray Hawk
3440	Short-Tailed Hawk
3370	Red-Tailed Hawk
3480	Ferruginous Hawk
3470	Rough-Legged Hawk
3490	Golden Eagle
3600	American Kestrel
3540	Gyrfalcon
3550	Prairie Falcon
3140	White-Crowned Pigeon
3130	Red-Billed Pigeon
3190	White-Winged Dove
3160	Mourning Dove
3821	Thick-Billed Parrot
3840	Groove-Billed Ani
3650	Barn Owl
3760	Snowy Owl
3770	Northern Hawk Owl
3810	Elf Owl
3700	Great Gray Owl
3660	Long-Eared Owl
3670	Short-Eared Owl
3720	Northern Saw-Whet Owl
4180	Common Poorwill
4410	Broad-Billed Hummingbird
4390	Buff-Bellied Hummingbird
4391	Violet-Crowned Hummingbird
4270	Blue-Throated Hummingbird
4260	Magnificent Hummingbird
3890	Elegant Trogon
4080	Lewis's Woodpecker
4060	Red-Headed Woodpecker

4040	Williamson's Sapsucker
4030	Red-Breasted Sapsucker
4123	Northern Flicker
4720	Northern Beardless-Tyrannulet
4600	Greater Pewee
4700	Buff-Breasted Flycatcher
4550	Dusky-Capped Flycatcher
4530	Brown-Crested Flycatcher
4460	Tropical Kingbird
4451	Thick-Billed Kingbird
6210	Northern Shrike
4770	Blue Jay
4880	American Crow
4900	Fish Crow
4740	Horned Lark
6121	Cave Swallow
7280	Red-Breasted Nuthatch
7260	Brown Creeper
7150	Rock Wren
7190	Bewick's Wren
7220	Winter Wren
7240	Sedge Wren
7480	Golden-Crowned Kinglet
7660	Eastern Bluebird
7670	Western Bluebird
7680	Mountain Bluebird
7540	Townsend's Solitaire
7610	American Robin
7630	Varied Thrush
7050	Brown Thrasher
7080	Bendire's Thrasher
7070	Curve-Billed Thrasher
6180	Bohemian Waxwing
6510	Olive Warbler
6490	Tropical Parula
6710	Pine Warbler
6880	Painted Redstart
5880	Spotted Towhee
5870	Eastern Towhee
5780	Cassin's Sparrow
5750	Bachman's Sparrow
5590	American Tree Sparrow
5630	Field Sparrow

5650	Black-Chinned Sparrow
5730	Black-Throated Sparrow
5740	Sage Sparrow
5470	Henslow's Sparrow
5480	Le Conte's Sparrow
5491	Nelson's Sharp-Tailed Sparrow
5490	Saltmarsh Sharp-Tailed Sparrow
5500	Seaside Sparrow
5850	Fox Sparrow
5810	Song Sparrow
5580	White-Throated Sparrow
5530	Harris's Sparrow
5570	Golden-Crowned Sparrow
5677	Dark-Eyed Junco
5390	Mccown's Longspur
5360	Lapland Longspur
5370	Smith's Longspur
5380	Chestnut-Collared Longspur
5340	Snow Bunting
5350	Mckay's Bunting
4980	Red-Winged Blackbird
5010	Eastern Meadowlark
5011	Western Meadowlark
5090	Rusty Blackbird
5110	Common Grackle
4960	Bronzed Cowbird
5031	Altamira Oriole
5241	Unid. Rosy-Finch
5150	Pine Grosbeak
5170	Purple Finch
5180	Cassin's Finch
5190	House Finch
5210	Red Crossbill
5220	White-Winged Crossbill
5280	Common Redpoll
5270	Hoary Redpoll
5330	Pine Siskin
5300	Lesser Goldfinch
5290	American Goldfinch
5140	Evening Grosbeak

Table A-7. Permanent Residents Guild

American Ornithological Union Code	Common Name
3110	Plain Chachalaca
3000	Ruffed Grouse
3090	Greater Sage-Grouse
3089	Gunnison Sage-Grouse
2980	Spruce Grouse
3040	White-Tailed Ptarmigan
2970	Blue Grouse
3050	Greater Prairie-Chicken
3070	Lesser Prairie-Chicken
3100	Wild Turkey
2920	Mountain Quail
2930	Scaled Quail
2940	California Quail
2950	Gambel's Quail
2890	Northern Bobwhite
2960	Montezuma Quail
3260	Black Vulture
3240	California Condor
3280	White-Tailed Kite
3300	Snail Kite
3340	Northern Goshawk
3350	Harris's Hawk
3410	White-Tailed Hawk
3620	Crested Caracara
3590	Aplomado Falcon
3210	Inca Dove
3200	Common Ground-Dove
3180	White-Tipped Dove
3826	Red-Crowned Parrot
3860	Mangrove Cuckoo
3850	Greater Roadrunner
3830	Smooth-Billed Ani
3732	Western Screech-Owl
3730	Eastern Screech-Owl
3731	Whiskered Screech-Owl
3750	Great Horned Owl
3800	Ferruginous Pygmy-Owl
3690	Spotted Owl
3680	Barred Owl
3710	Boreal Owl
4190	Common Pauraque
4310	Anna's Hummingbird

3901	Ringed Kingfisher
3910	Green Kingfisher
4070	Acorn Woodpecker
4110	Gila Woodpecker
4100	Golden-Fronted Woodpecker
4090	Red-Bellied Woodpecker
3960	Ladder-Backed Woodpecker
3970	Nuttall's Woodpecker
3940	Downy Woodpecker
3930	Hairy Woodpecker
3975	Arizona Woodpecker
3950	Red-Cockaded Woodpecker
3990	White-Headed Woodpecker
4010	American Three-Toed Woodpecker
4000	Black-Backed Woodpecker
4050	Pileated Woodpecker
4580	Black Phoebe
4490	Great Kiskadee
4461	Couch's Kingbird
6320	Hutton's Vireo
4840	Gray Jay
4780	Steller's Jay
4830	Green Jay
4790	Florida Scrub-Jay
4811	Island Scrub-Jay
4810	Western Scrub-Jay
4820	Mexican Jay
4920	Pinyon Jay
4910	Clark's Nutcracker
4750	Black-Billed Magpie
4760	Yellow-Billed Magpie
4890	Northwestern Crow
4870	Chihuahuan Raven
4860	Common Raven
7360	Carolina Chickadee
7350	Black-Capped Chickadee
7380	Mountain Chickadee
7370	Mexican Chickadee
7410	Chestnut-Backed Chickadee
7400	Boreal Chickadee
7390	Gray-Headed Chickadee
7340	Bridled Titmouse
7330	Oak Titmouse

7331	Juniper Titmouse
7310	Tufted Titmouse
7320	Black-Crested Titmouse
7460	Verdin
7430	Bushtit
7270	White-Breasted Nuthatch
7300	Pygmy Nuthatch
7290	Brown-Headed Nuthatch
7130	Cactus Wren
7170	Canyon Wren
7180	Carolina Wren
7010	American Dipper
7530	California Gnatcatcher
7520	Black-Tailed Gnatcatcher
7420	Wrentit
7030	Northern Mockingbird
7060	Long-Billed Thrasher
7100	California Thrasher
7120	Crissal Thrasher
7110	Le Conte's Thrasher
6020	White-Collared Seedeater
5860	Olive Sparrow
5910	Canyon Towhee
5911	California Towhee
5920	Abert's Towhee
5790	Rufous-Winged Sparrow
5760	Botteri's Sparrow
5800	Rufous-Crowned Sparrow
5742	Five-Striped Sparrow
5700	Yellow-Eyed Junco
5930	Northern Cardinal
5940	Pyrrhuloxia
5000	Tricolored Blackbird
5130	Boat-Tailed Grackle
5120	Great-Tailed Grackle
5030	Audubon's Oriole
5310	Lawrence's Goldfinch

Appendix B: Predicted Avian Species Richness calculated from linear models of the 12 strongest performing variables from hierarchical partitioning analysis.

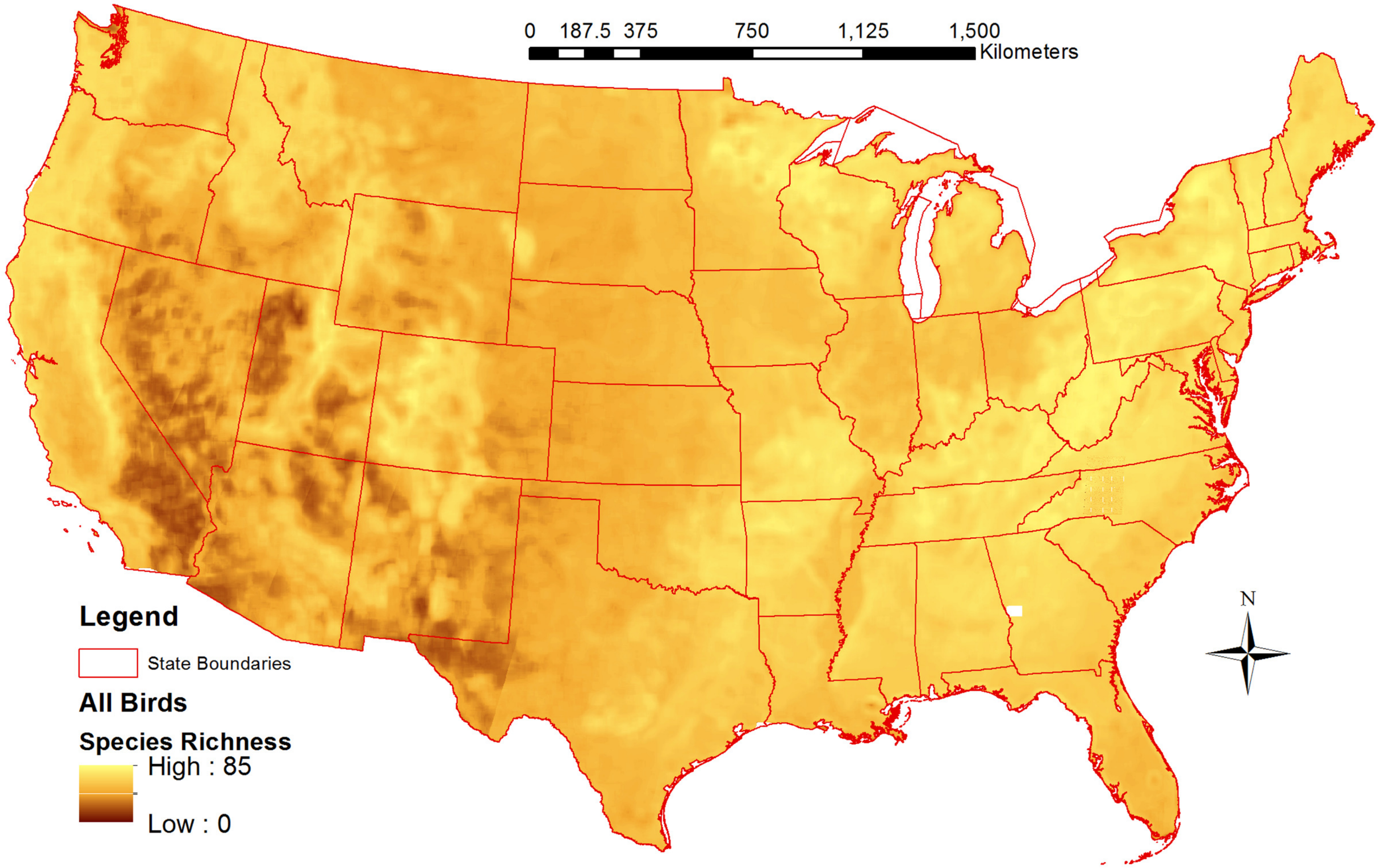

Figure B-1. Predicted species richness of all birds, calculated from a linear model of the 12 strongest performing variables as determined by hierarchical partitioning analysis.

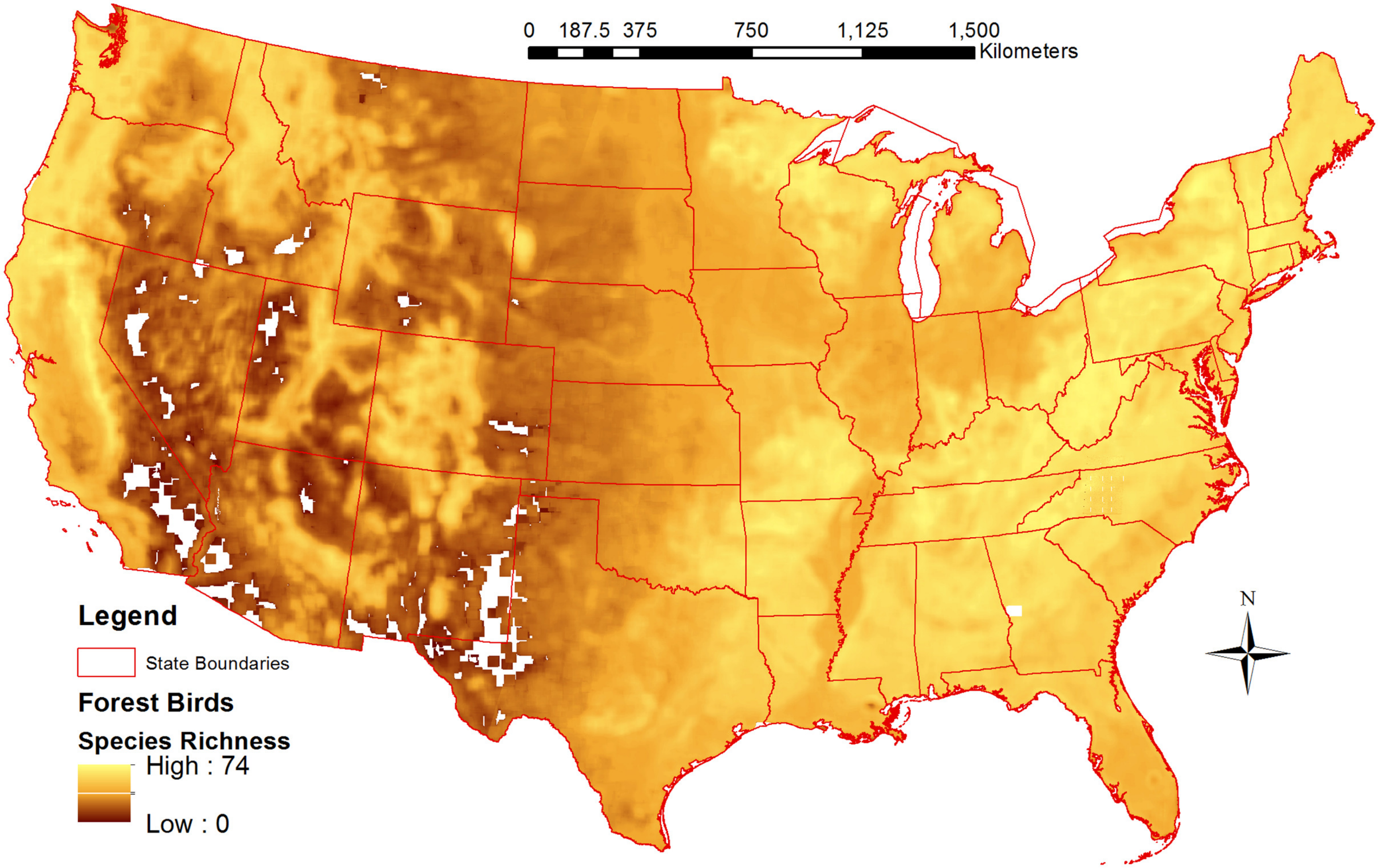

Figure B-19. Predicted species richness of all birds, calculated from a linear model of the 12 strongest performing variables as determined by hierarchical partitioning analysis.

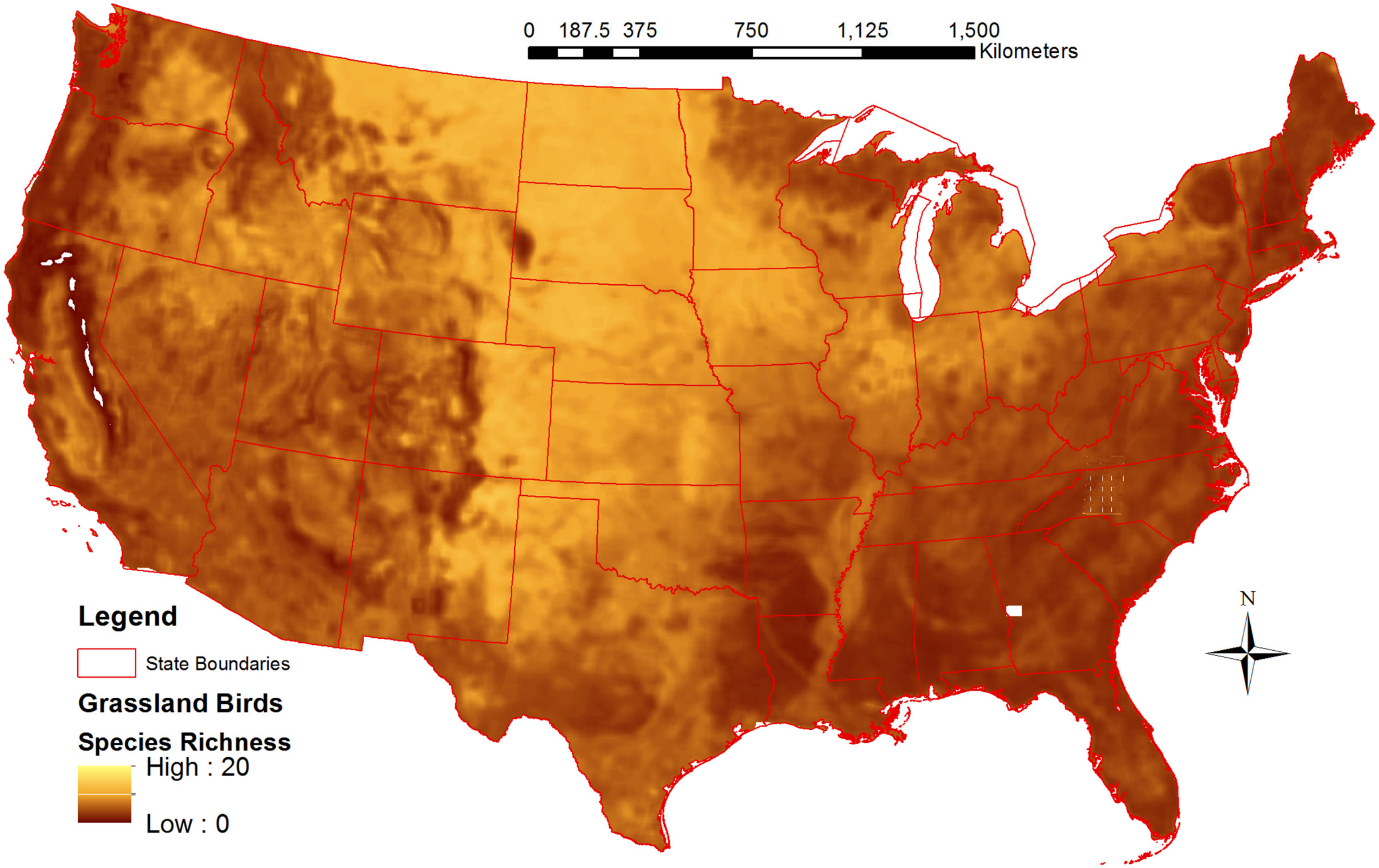

Figure B-20. Predicted species richness of all birds, calculated from a linear model of the 12 strongest performing variables as determined by hierarchical partitioning analysis.

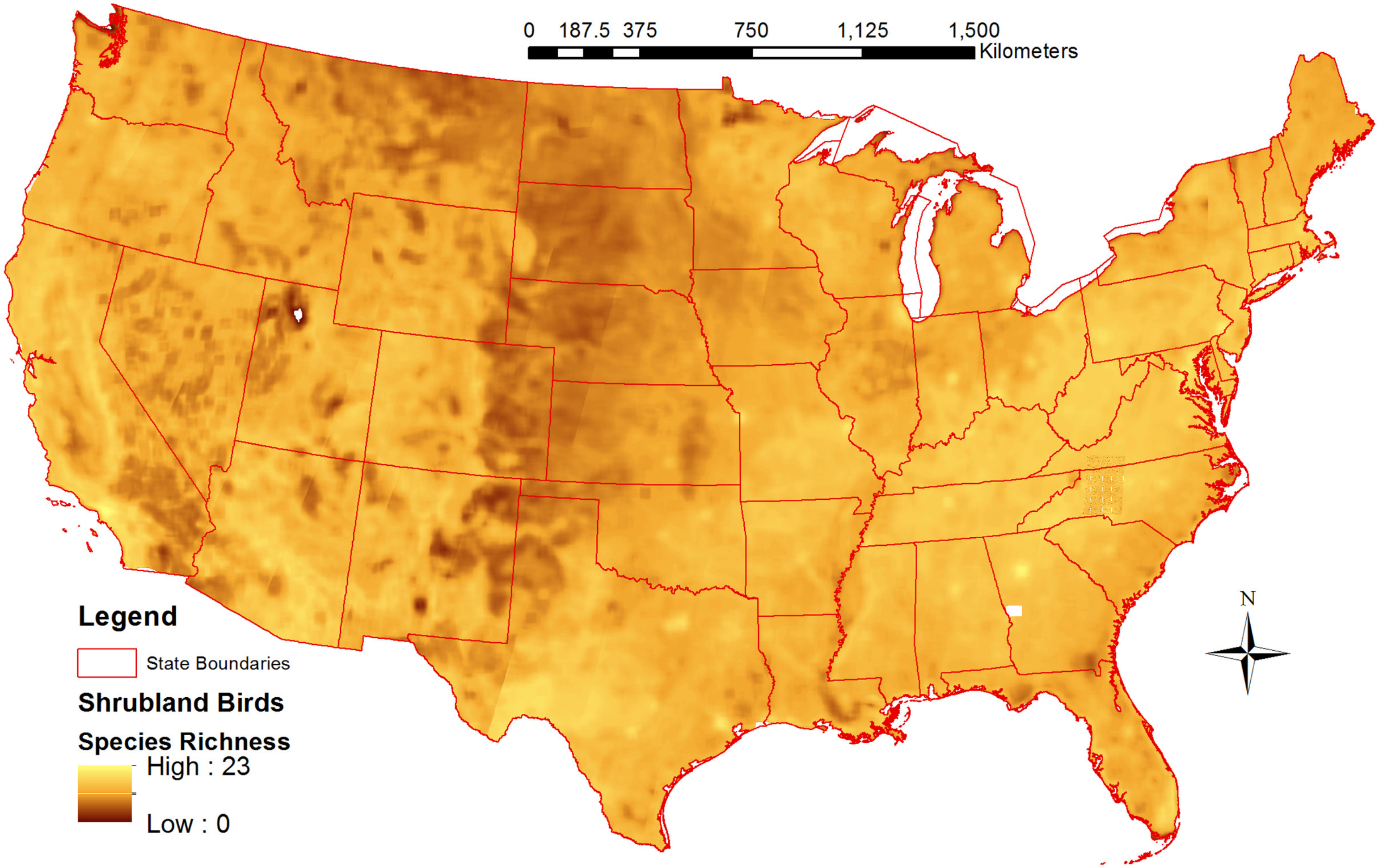

Figure B-21. Predicted species richness of all birds, calculated from a linear model of the 12 strongest performing variables as determined by hierarchical partitioning analysis.

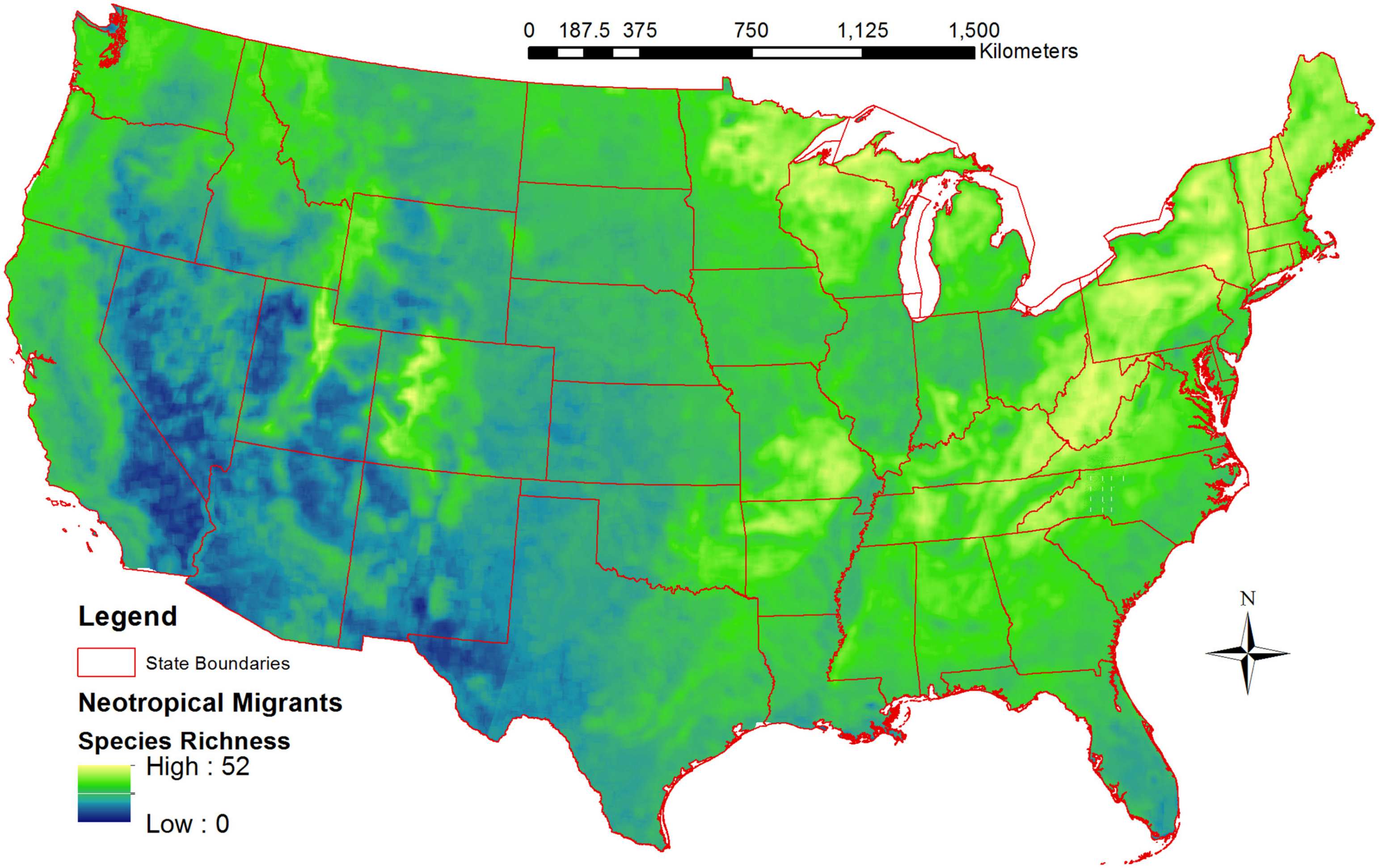

Figure B-22. Predicted species richness of all birds, calculated from a linear model of the 12 strongest performing variables as determined by hierarchical partitioning analysis.

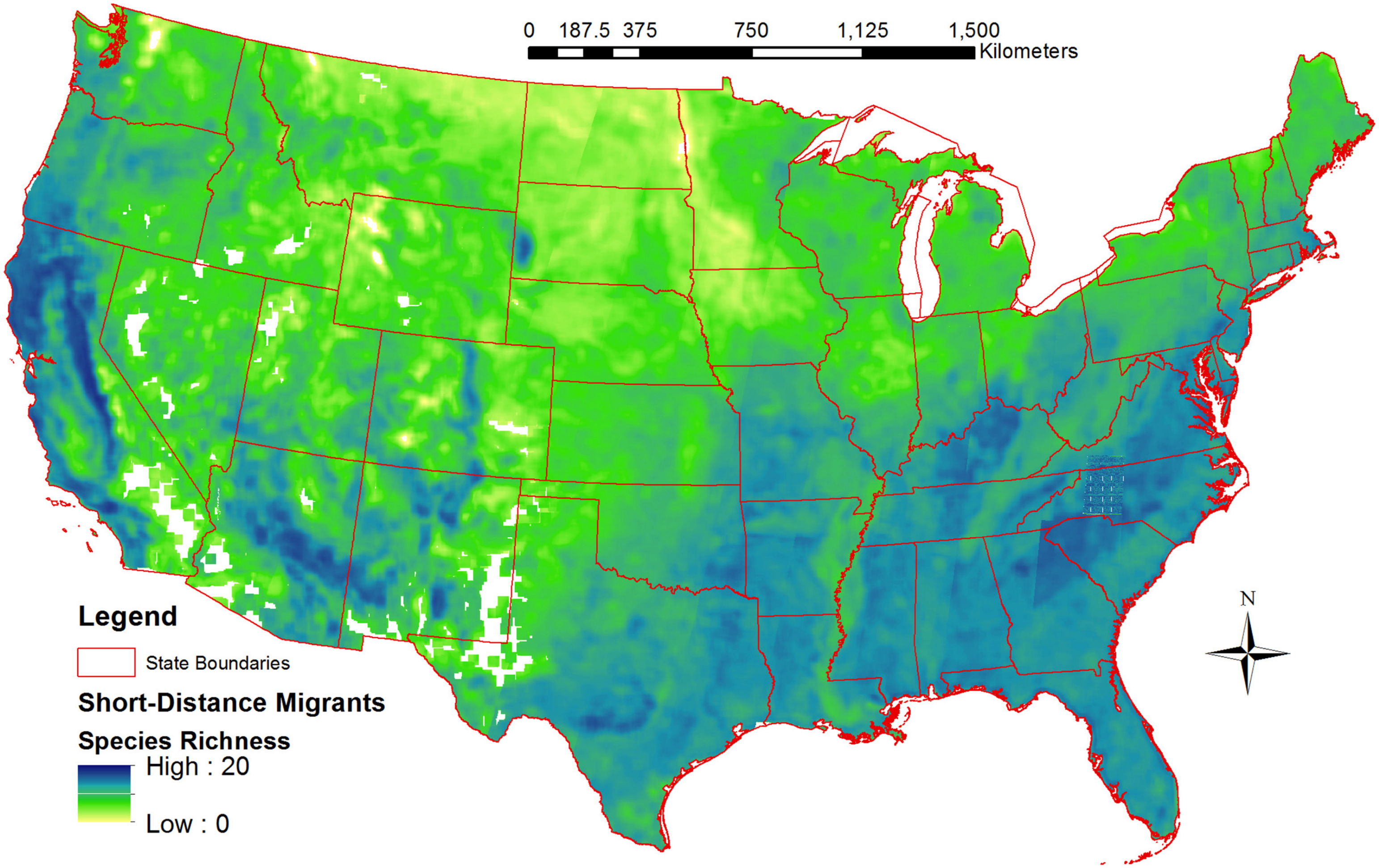

Figure B-23. Predicted species richness of all birds, calculated from a linear model of the 12 strongest performing variables as determined by hierarchical partitioning analysis.

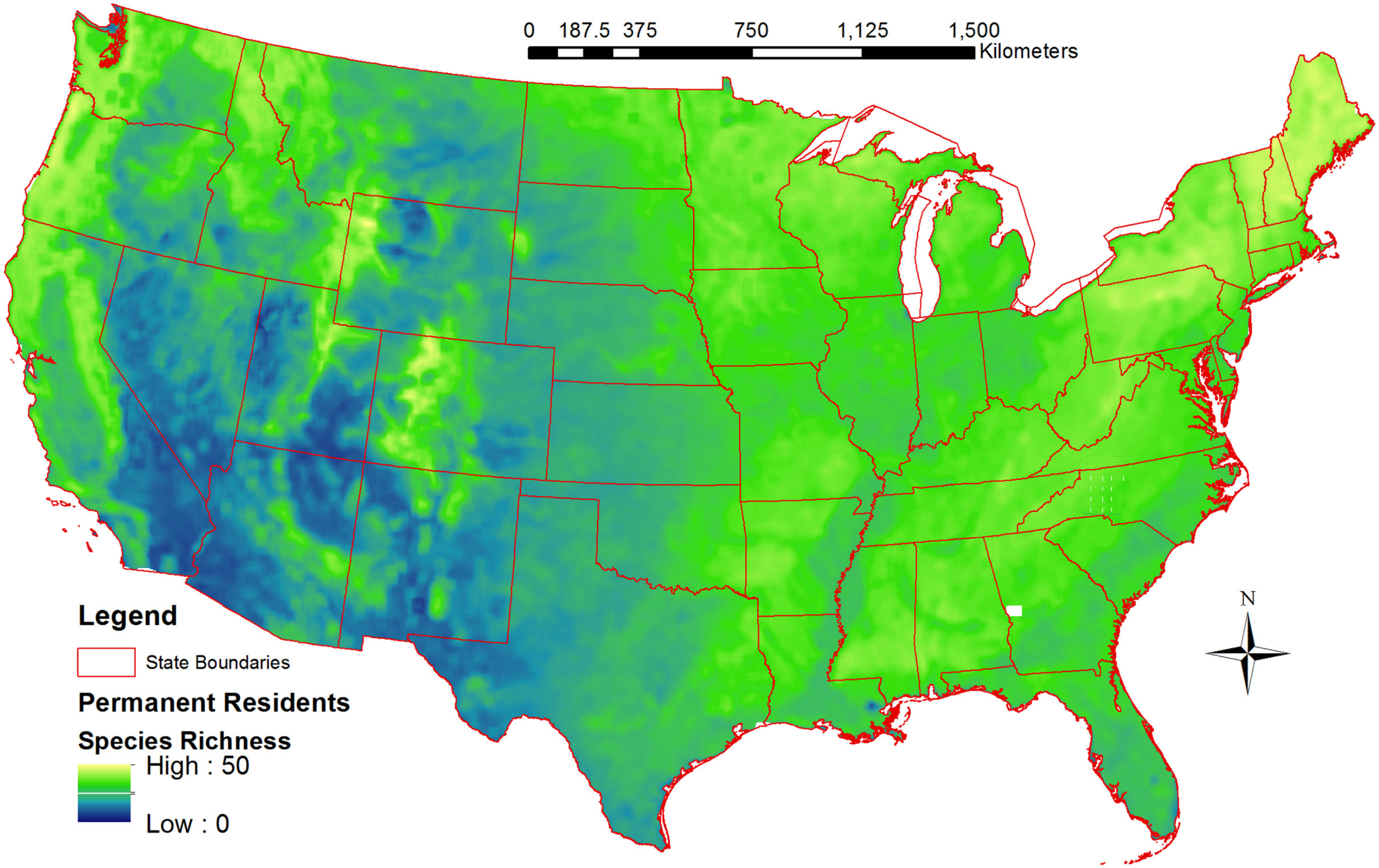

Figure B-24. Predicted species richness of all birds, calculated from a linear model of the 12 strongest performing variables as determined by hierarchical partitioning analysis.

Appendix C: Raw residuals of species richness predictions from random forest models.

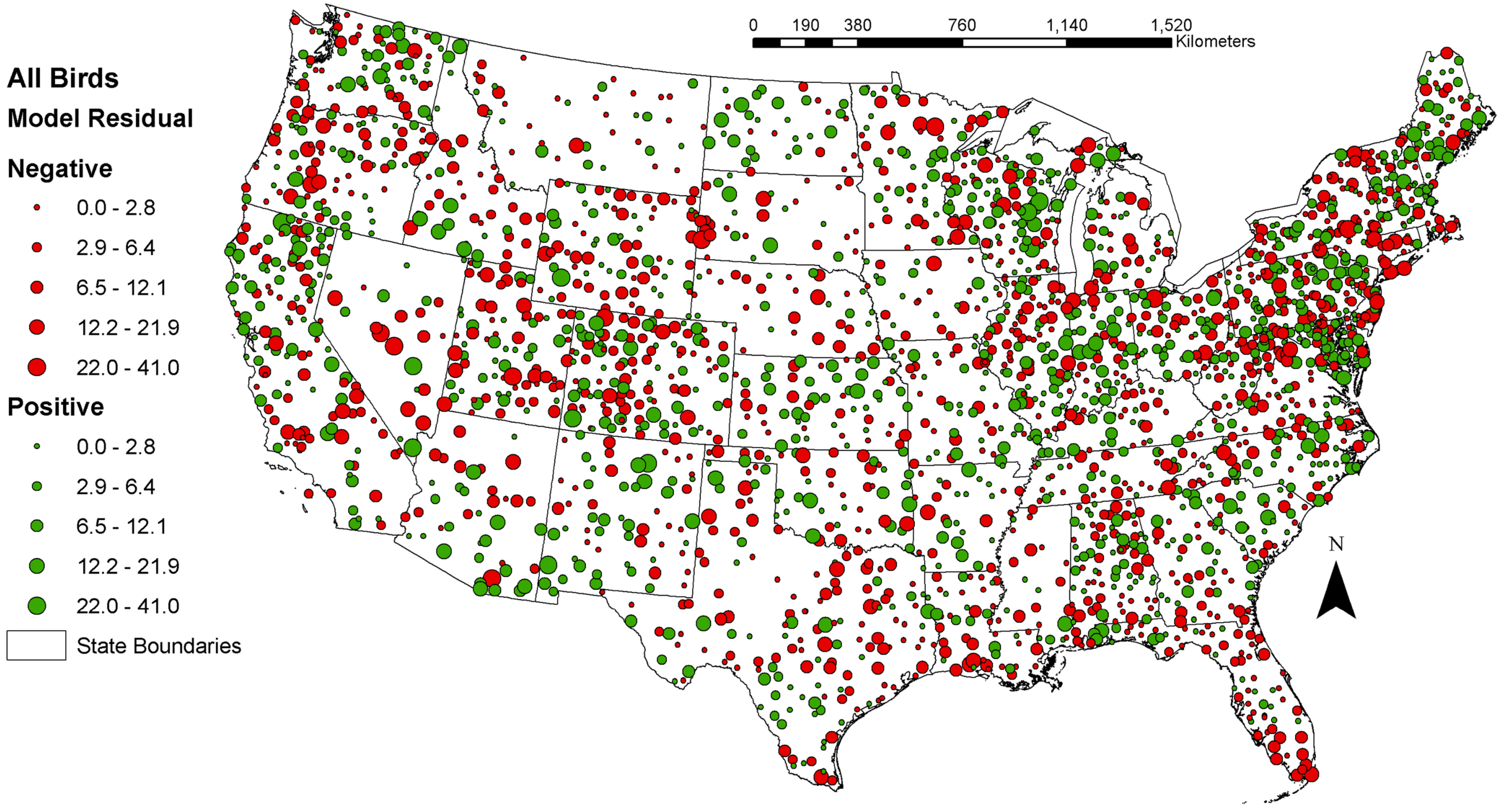

Figure C-1. Raw residuals of predicted species richness of all birds from the final random forest model.

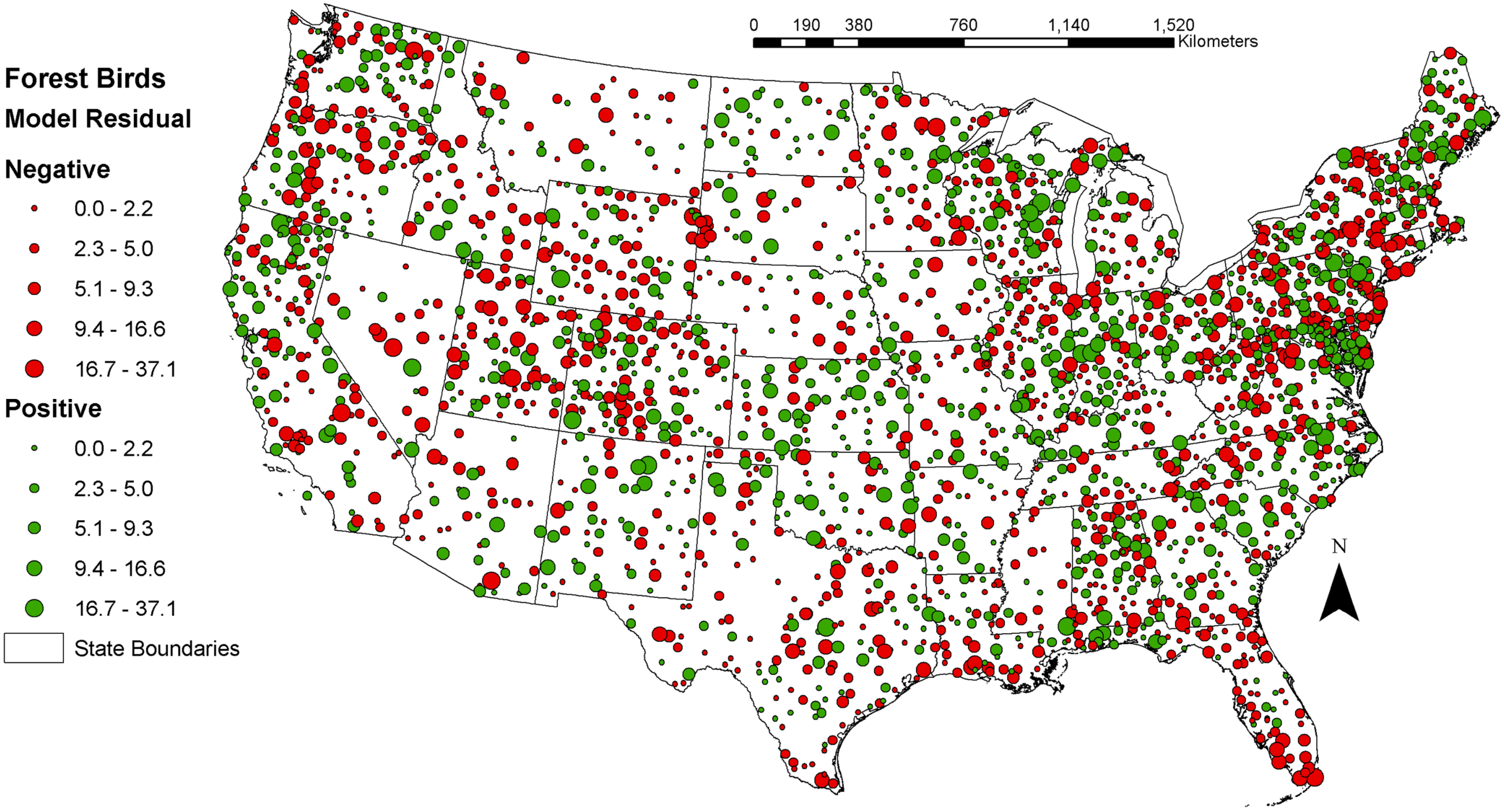

Figure C-2. Raw residuals of predicted species richness of forest birds from the final random forest model

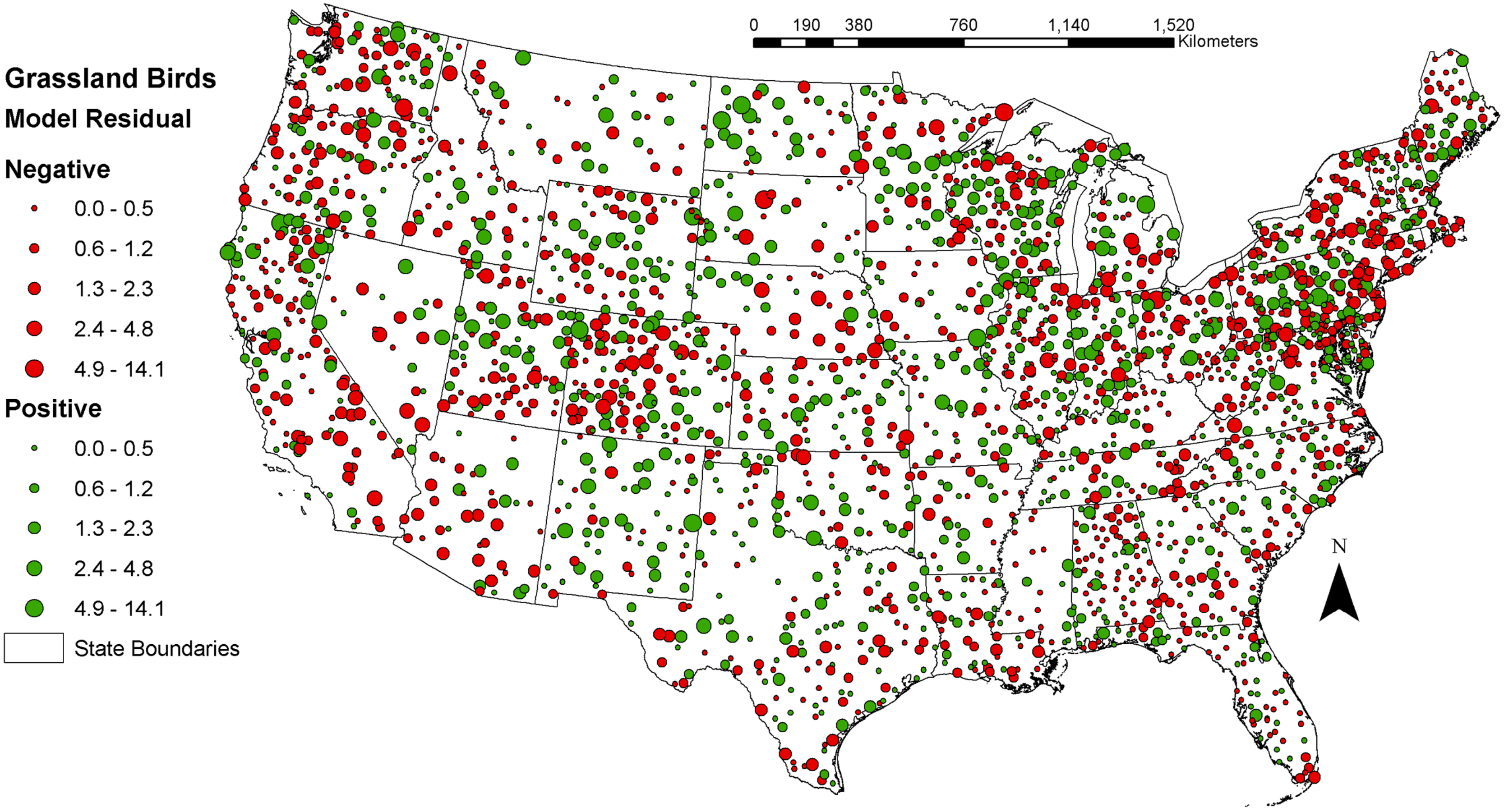

Figure C-25. Raw residuals of predicted species richness of grassland birds from the final random forest model.

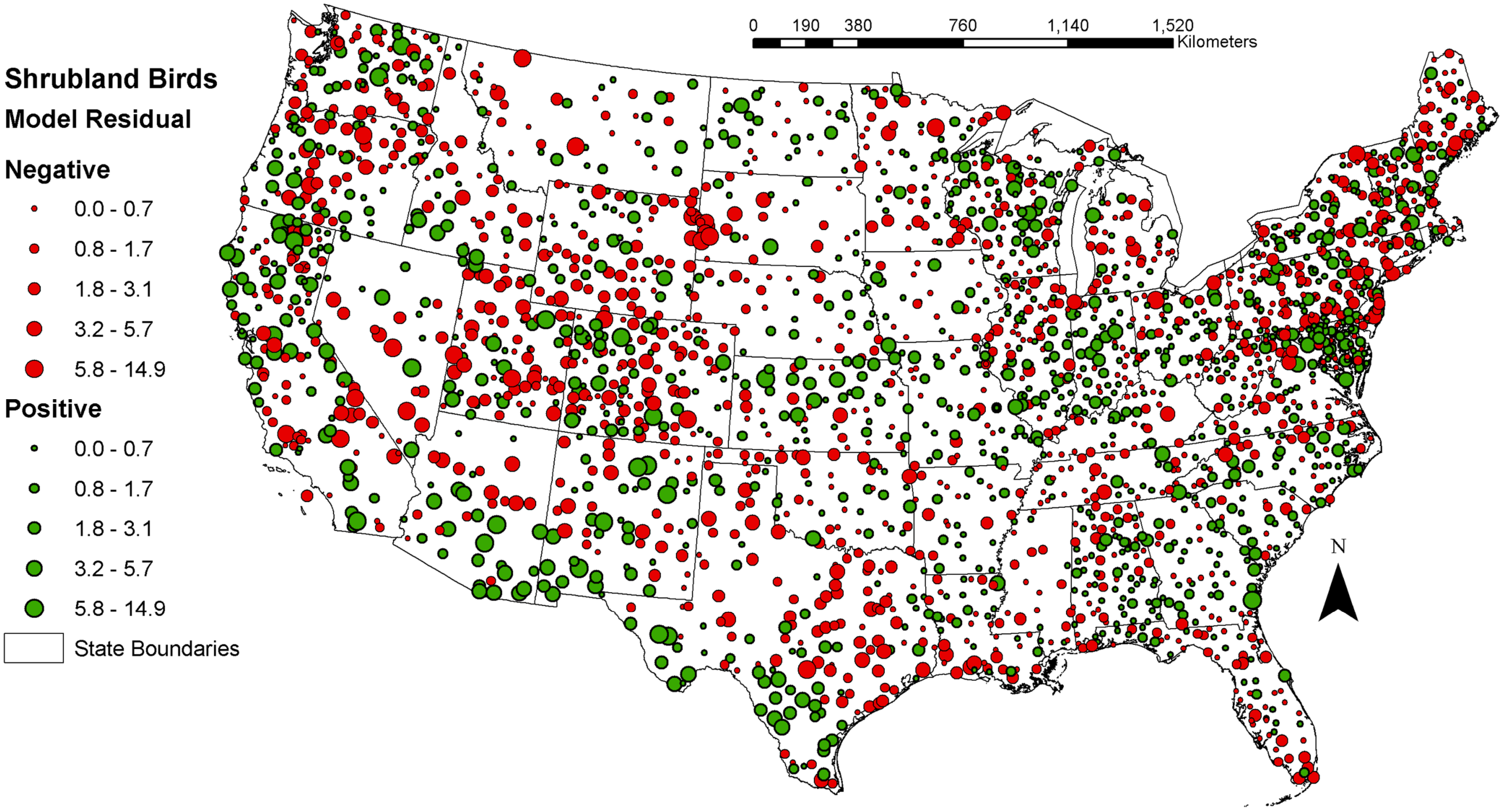

Figure C-26. Raw residuals of predicted species richness of shrubland birds from the final random forest model

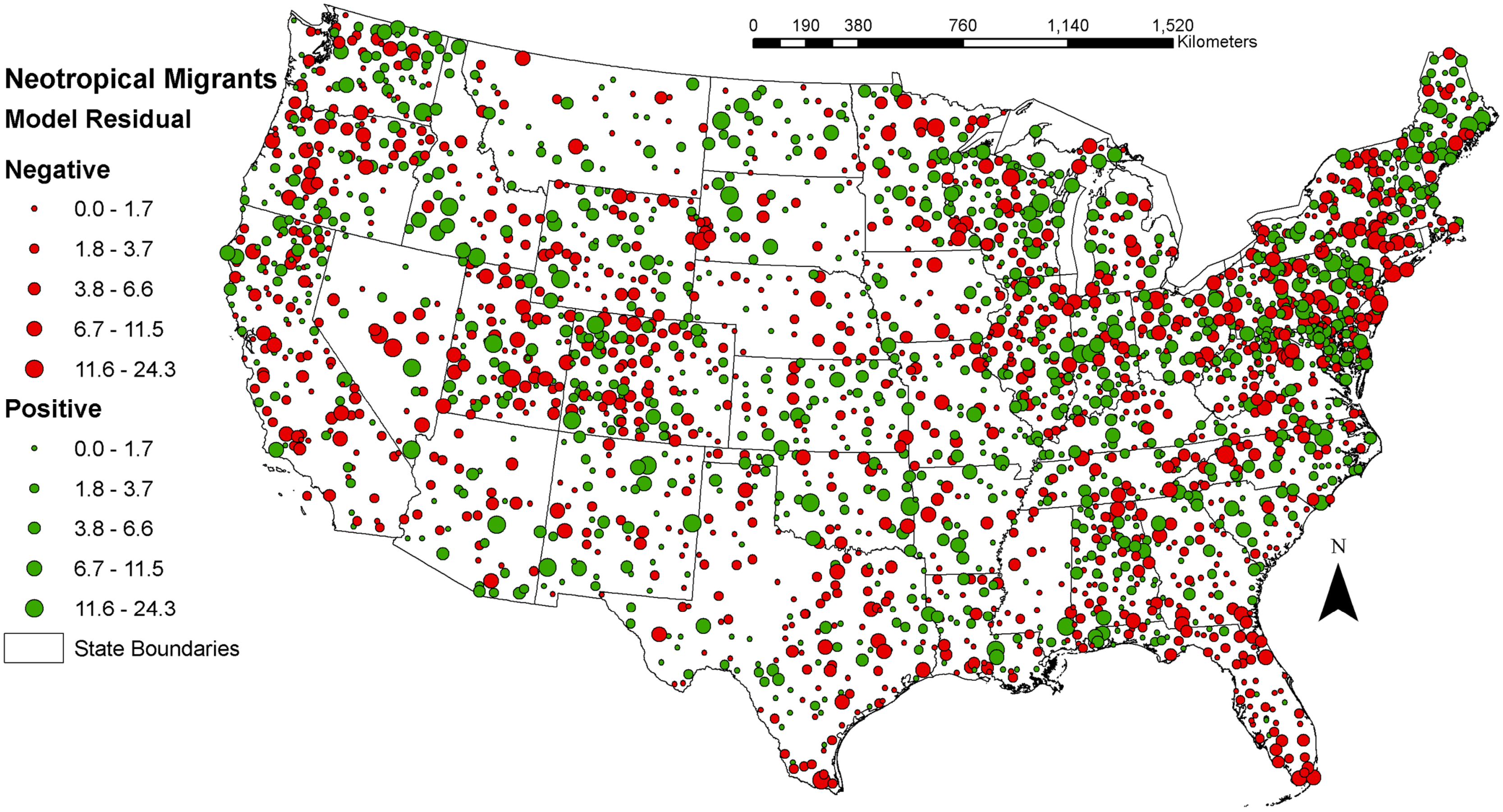

Figure C-27. **Raw residuals of predicted species richness of Neotropical migrants from the final random forest model**

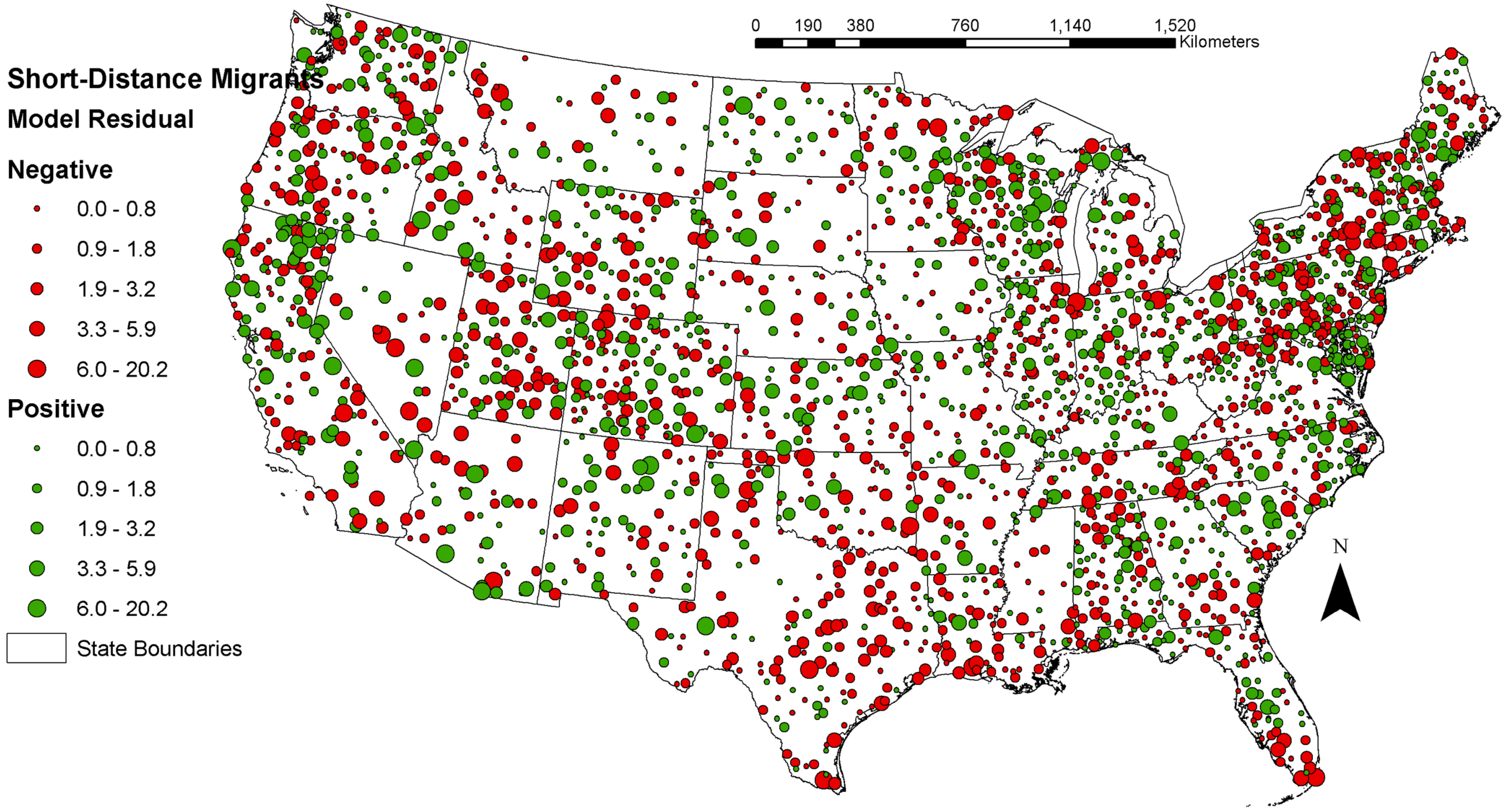

Figure C-28. Raw residuals of predicted species richness of short-distance migrants from the final random forest model

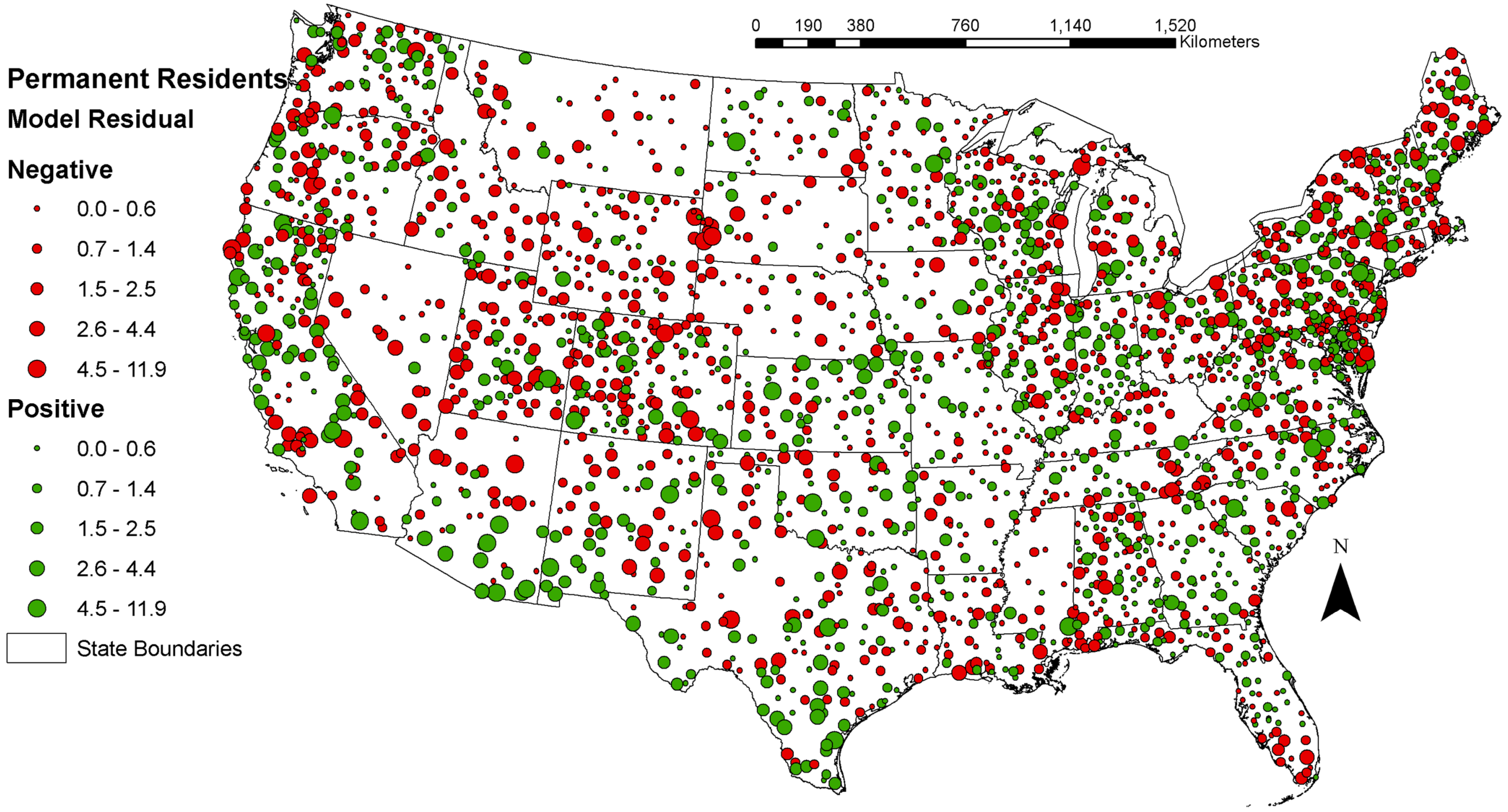

Figure C-29. Raw residuals of predicted species richness of Permanent Residents from the final random forest model